Pathogen-specific antibody response in infective endocarditis and characterization of antibacterial monoclonal antibodies

Inauguraldissertation

zur

Erlangung des akademischen Grades eines

Doktors der Naturwissenschaften
(Dr. rer. nat.)

an der

Mathematisch-Naturwissenschaftlichen Fakultät

der

Universität Greifswald

Vorgelegt von

Jawad Iqbal

Greifswald, den 01.02.2022

Dekan: Prof. Dr. Gerald Kerth

1. Gutachter: Prof. Dr. med. Barbara M. Bröker

2. Gutachter: PD Dr. Knut Ohlsen

Tag der Promotion: 22.06.2022

Diese Inauguraldissertation wurde im Rahmen des Forschungsprojektes „Card-ii-Omics Kardiovaskuläre Implantatentwicklung-Infektionen-Proteomics: Prävention, Diagnostik und Therapie von Implantatinfektionen" angefertigt. Die Förderung des Projektes erfolgte aus Mitteln des Europäischen Sozialfonds (ESF) im Rahmen des Qualifikationsprogrammes „Förderung von Nachwuchswissenschaftlern in exzellenten Forschungsverbünden - Exzellenzforschungsprogramm des Landes Mecklenburg-Vorpommern" (ESF/14 – BMA55 0037/16).

Table of contents

List of abbreviations

Abbreviations	Definitions
%	percentage
°C	celsius
µg	microgram
µl	microliter
µm	micromolar
3DTEE	three-dimensional transesophageal echocardiography
A. baumannii	*Acinetobacter baumannii*
Aap	accumulation associated protein
Ab	antibody
ACE	angiotensin-converting enzyme
Ac-VEID-AMC	acetyl- L- valyl- L- glutamyl- L- isoleucyl- L- aspartic acid α-(4-methyl-coumaryl- 7-amide)
ALAT	alanine transaminase
AMP	ampicillin
APS	ammonium persulfate
ASAT	aspartate transaminase
AVE	aortic valve endocarditis
Bap	biofilm-associated protein
BC	blood culture
BCR	B cell receptor
bpm	beats per minute
BSA	bovine serum albumin
C	control
C. difficile	*Clostridioides difficile*
C. acnes	*Cutibacterium acnes*
C. albicans	*Candida albicans*
C. striatum	*Corynebacterium striatum*
CP	capsular polysaccharide
CA-MRSA	community-associated methicillin-resistant *Staphylococcus aureus*
cDNA	complementary deoxyribonucleic acid
CDRs	complementarity determining regions
CHIPs	chemotaxis inhibitory protein of staphylococci
CI	cerebral infarction
CIP	ciprofloxacin
ClfA	Clumping factor A
CLI	clindamycin
CNIE	blood culture-negative IE
CRP	C-reactive protein
CT	cardiac computed tomography
d0	day of diagnosis
DMSO	dimethyl sulfoxide
DNA	deoxyribonucleic acid
DNABII	DNA-binding proteins
DNAse	deoxyribonuclease
dNTP	deoxynucleoside triphosphate
DTT	dithiothreitol
E	endocarditis
E. cloacae	*Enterobacter cloacae*
E. coli	*Escherichia coli*
E. faecalis	*Enterococcus faecalis*
E. faecium	*Enterococcus faecium*
Eap	extracellular adherence protein
ECM	extracellular polymeric matrix
ECP	extracellular proteins
eDNA	extracellular DNA

EDTA	ethylenediaminetetraacetic acid
ELISA	enzyme-linked immunosorbent assay
Exfoliative toxins	ETs
FCS	fetal calf serum
Fibrinogen	Fg
Fibronectin	Fn
FLX	flucloxacillin
FnBPA and FnBPB	fibronectin-binding proteins A and B
FRs	framework regions
g	gravity
g	gram
GEN	gentamycin
GIES	Greifswald Infective Endocarditis Study
GlpQ	Glycerophosphodiester phosphodiesterase
Glu	Glutamine
h	hour
H. influenzae	*Haemophilus influenzae*
H_2O	Water
H_2SO_4	sulphuric acid
HC	heavy chain
HCl	hydrochloric acid
His-tag	histidine-tag
Hla	alpha-hemolysin
HlB	*S. aureus* beta toxin
HlgAb	alpha-hemolysin AB
HRP	horseradish peroxidase
IDU	intravenous drug users
IE	infective endocarditis
IgA, IgD, IgE, IgG, IgM	immunoglobulins A, D, E, G, and M
IQR	interquartile range
IsdB	Iron-regulated surface determinant protein B
K. aerogenes	*Klebsiella aerogenes*
K. oxytoca	*Klebsiella oxytoca*
K. pneumoniae	*Klebsiella pneumoniae*
K_d	dissociation constant
kDa	kilodaltons
kg	kilogram
L. pneumophila	*Legionella pneumophila*
LA-MRSA	livestock-associated methicillin-resistant *Staphylococcus aureus*
LC	light chain
LTA	lipoteichoic acid
LukA, LukB, LukS, and LukF	Leukocidin A, B, S, and F
LZD	linezolid
M	molar
M. catarrhalis	*Moraxella catarrhalis*
mA	milliampere
mAb	monoclonal antibody
mg	milligram
$MgCl_2$	magnesium chloride
min	minute
ml	milliliter
mM	millimolar
MntC	manganese transporter protein C
MRI	magnetic resonance imaging
MRSA	methicillin-resistant *Staphylococcus aureus*
MSCRAMMs	microbial surface components recognizing adhesive matrix molecules
MST	microscale thermophoresis
MVE	mitral valve endocarditis
N	normal

NaCl	sodium chloride
NaOH	sodium hydroxide
nm	nanometer
nM	nanomolar
P	patient
P. aeruginosa	*Pseudomonas aeruginosa*
P. mirabilis	*Proteus mirabilis*
PAGE	polyacrylamide gel electrophoresis
PBMCs	peripheral blood mononuclear cells
PBS	phosphate buffered saline
PCR	polymerase chain reaction
PE	phycoerythrin
PE	pulmonary embolism
Pen/Step	Penicillin/ Streptomycin
pH	potential of hydrogen
PJI	prosthetic joint infection
Plc	1-phosphatidylinositol phosphodiesterase
PNAG	polymeric N-acetyl-glucosamine
POD	peroxidase
PSMs	phenol-soluble modulins
PVDF membrane	polyvinylidene fluoride membrane
PVL	panton-valentine leukocidin
R10F	RPMI 1640 medium with 10% FCS
R20F	RPMI 1640 medium with 20% FCS
RBC	red blood cells
RIF	rifampicin
RNA	ribonucleic acid
rpm	revolutions per minute
RPMI 1640	Roswell Park Memorial Institute 1640 medium
RT	room temperature
Rt	reverse transcriptase
S. aureus	*Staphylococcus aureus*
S. epidermidis	*Staphylococcus. Epidermidis*
S. gallolyticus	*Streptococcus gallolyticus*
S. haemolyticus	*Staphylococcus haemolyticus*
S. hominis	*Staphylococcus hominis*
S. lugdunsensis	*Staphylococcus lugdunsensis*
S. maltophilia	*Stenotrophomonas maltophilia*
S. marcescens	*Serratia marcescens*
S. mitis	*Streptococcus mitis*
S. oralis	*Streptococcus oralis*
S. pneumoniae	*Streptococcus pneumoniae*
S. sanguinis	*Streptococcus sanguinis*
S. warneri	*Staphylococcus warneri*
SasG	*S. aureus* surface protein
Sbi	second immunoglobulin-binding protein
SCIN	staphylococcal complement inhibitor
SD	standard deviation
SdrD, SdrE, and SdrG	Serine-aspartate repeat-containing protein D, E and G
SDS	sodium dodecyl sulfate
SDS-PAGE	sodium dodecyl sulfate-polyacrylamide gel electrophoresis
SEA and SEB	Staphylococcus Enterotoxin A and B
sec	second
SpA	staphylococcal protein A
SplB	Serine protease–like protein B
SseC	Surface exposed protein C
SSSS	staphylococcal scalded skin syndrome
TAZ	tazobactam
TBE	tris borate EDTA
TBST	tris buffered saline with Tween® 20

TCA	trichloroacetic acid
TEMED	tetramethylethylenediamine
Th2	T helper 2
TOE	transoesophageal echocardiography
TSST-1	toxic shock syndrome toxin 1
TT	tetanus toxoid
TTE	transthoracic echocardiography
TVE	tricuspid valve endocarditis
TZP	piperacillin/tazobactam
V	volt
v/v	volume/volume
VAN	vancomycin
VDJ region	variable, diversity, and joining region
VGS	viridans-group streptococci
w/v	weight/volume
WBC	white blood cells
WTA	wall teichoic acid
κ –chain	kappa chain
λ-chain	lambda chain

Abstract

Infective endocarditis (IE) is a potentially life-threatening infection of the endocardial surfaces of the heart, most frequently the valves. It is typically caused by bacteria, less commonly by fungi. Over the past years, the morbidity and mortality of IE have gradually increased, and it is now the fourth most common life-threatening infection after sepsis, pneumonia, and intra-abdominal abscess. Despite advances in cardiac imaging and diagnostic techniques, the diagnosis of IE remains challenging. The lack of fast and reliable diagnosis of IE can lead to serious complications. Therefore, new diagnostic and therapeutic tools are urgently needed.

This study had two main aims: (i) to investigate whether a pathogen-specific antibody response in IE patients is mounted against different IE pathogens and whether analysis of such a response might be useful for complementing the classical blood culture diagnosis, and (ii) generate and characterize neutralizing monoclonal antibodies (mAbs) against three virulence factors of *Staphylococcus aureus* (*S. aureus*), which is the most common etiological agent in IE.

Our research group has recently established an xMAP® (Luminex®) technology-based serological assay that simultaneously quantifies the antibody response against 30 different pathogens. Within the research consortium Card-ii-Omics, we conducted a prospective, observational clinical discovery study involving 17 IE patients and 20 controls (i.e., patients with non-infectious heart-related conditions). Plasma samples were obtained on the day of IE diagnosis from all patients, while samples at later dates over the course of infection were available for only some patients. Invasive pathogens were identified by blood culture.

The infection array revealed antibodies against a broad range of pathogens in both controls and IE patients, suggesting a broad immune memory. Overall, antibody levels did not significantly differ between both groups, but we observed high antibody titers against those pathogens that were detected by blood culture. Whenever available (in the case of 13/17 IE patients), back-up and follow-up plasma samples (obtained before or after diagnosis, respectively) were included in the analyses that provided valuable information about the kinetics of antibody response during the course of infection. Notably, infection array data confirmed (and extended) the blood culture data in only 2/13 cases. In three cases, serology contradicted the microbiological diagnosis, and in three cases, the infection array was able to identify pathogens, while the microbiological diagnosis failed. In three cases, serology was negative while microbiological diagnosis was positive, and in two cases, both serology and microbiological diagnosis were

negative. In 6 out of 8 cases with increases in antibody levels, this response was directed against gut microbes. This supports the leaky gut hypothesis, which assumes that breaching of the gut barrier causes translocation of gut microbes into the bloodstream, which then infect the heart valves. Moreover, we observed an increase in antibody titers in 4 patients against the yeast *C. albicans*, suggesting a secondary fungal infection. Finally, this study emphasized that the timing of plasma collection is crucial for studying antibody kinetics in IE.

After demonstrating that pathogen-specific antibodies are generated during IE, we aimed to generate mAbs against the prime IE pathogen *S. aureus* and study their functions on a molecular level. Using the hybridoma technology, our research group has recently generated mAbs against two *S. aureus* surface proteins/adhesion factors (clumping factor A (ClfA) and fibronectin-binding protein A (FnBPA)), both involved in biofilm formation, as well as an extracellular enzyme, the staphylococcal serine protease–like protein B (SplB), a virulence factor. In this work, the sequences of the mAbs were determined from hybridoma RNA. Then those mAbs were produced at a larger scale in order to determine their binding and neutralizing capacities using *in vitro* assays such as ELISA, Western blot, Dot blot, microscale thermophoresis, and in a mouse model.

The anti-SplB mAb specifically targeted SplB, with no cross-reactivity to other Spls or extracellular proteins (ECP) of *S. aureus*. Though anti-SplB mAb showed moderate binding to SplB with a K_d value of 2.54 μM and high sequence homology to the germline sequence, it neutralized the enzymatic activity of SplB up to 99% in 5-fold molar excess as showed in an *in vitro* substrate cleavage assay. Previous work showed that SplB facilitates the release of proinflammatory cytokines in endothelial cells and induces endothelial damage in mice. Here, we demonstrated that the anti-SplB mAb efficiently blocked the function of SplB *in vivo*, thus markedly reducing the damage to the endothelial barrier. In conclusion, we identified the strong neutralizing potential of a mAb against SplB, which merits further investigation as a candidate for the immunotherapy of SplB-induced *S. aureus* pathologies, including IE.

High antibody titers against *S. aureus* adhesins, including ClfA and FnBPA, have been reported in IE patients. Besides, ClfA is involved in serious *S. aureus* bloodstream and biofilm-related infections. Similarly, FnBPA facilitates biofilm formation and inhibits macrophage invasion. These important properties make the two bacterial adhesins ideal candidates for a passive vaccination strategy. We generated two murine ClfA-mAbs, ClfA-002 and ClfA-004, which showed strong specificity to ClfA. However, ClfA-004 showed reduced binding strength

compared to ClfA-002 due to a single non-synonymous nucleotide change (Phe→ Tyr) at the CDR3 region. While the ClfA-002 mAb reduced the binding of ClfA to fibrinogen by around 60%, the ClfA-004 had no inhibitory capacity. We also generated two murine and twelve humanized anti-FnBPA mAbs, which showed similar and moderate binding to FnBPA. One murine mAb (anti-FnBPA D4) partially inhibited the binding of FnBPA to fibronectin. FnBPA contains 11 tandem repeats that can all bind to fibronectin. This redundancy could be the reason for the lack of complete inhibition. Hence, in this work, we characterized the properties of neutralizing mAbs against two adhesins of *S. aureus.* These mAbs should be tested in the future, alone and in combination with other mAbs and antibiotics, for their ability to reduce staphylococcal biofilm formation.

In conclusion, we showed that antibody profiling of IE patients can provide valuable insights into the causative agent(s), and can help in guiding the antibiotic therapy. However, sampling is crucial in IE, which often dwells for many weeks before being clinically diagnosed. Because of the severity of IE, which can be life-threatening, I suggest to establish biobanks to store patient samples upon hospital admission that will provide a baseline in case of a later microbial infection. Moreover, our results suggest that *C. albicans* plays an important and so far underestimated role in IE. In the second part of the thesis, we characterized several mAbs against an *S. aureus* protease and two adhesins. Of high interest is a neutralizing mAb against SplB, which shows promising results *in vitro* and *in vivo*. Further *in vitro* and *in vivo* tests need to be conducted to study the anti-biofilm activity of the anti-FnBPA- and anti-ClfA-mAbs and explore their utility as therapeutic agents.

1. Introduction

1.1. Infective endocarditis

Infective endocarditis (IE) is a rare and life-threatening multisystem disease that results from infections, usually bacterial, of the endocardial surface of the heart. It affects 1.5 to 11.6 people out of 100,000 per year in primarily high-income countries, and studies suggest that these numbers are on the rise [1, 2]. The mortality from IE is almost 25%, and this situation has not improved in over two decades, leading to the fact that IE is now the fourth most common life-threatening infection after sepsis, pneumonia, and intra-abdominal abscess [3–5]. More than 50% of the cases are patients over the age of 50, and two-thirds of them are men [3, 6].

Most structural heart diseases can predispose to IE, with rheumatic heart disease as the most frequent cause, while the mitral valve is the most common site. Though IE cases related to rheumatic heart disease have dropped to 5% in developed countries, it still remains an important predisposing condition in less developed countries [3]. Individuals with prosthetic valve replacement and cardiac devices are susceptible to developing IE. Because of the increase in the implantation of these devices, the number of IE cases increases too [7]. Congenital heart disease is another important factor contributing to the increase in IE cases [3]. Other crucial factors predisposing to IE include intravenous drug users (IDU) and nosocomial infections, with the latter being on the rise in the past few decades in developed countries [3, 6].

1.2. Pathogens involved in IE

Historically, the majority of IE infections were caused by streptococci from the oral and gastrointestinal tract. However, in recent times, *Staphylococcus aureus* (*S. aureus*) emerged as the leading cause of IE in developed countries [8]. Staphylococci and streptococci, collectively, have been responsible for 80% of IE cases, but the proportion of these organisms varies by region and has changed over time. The number of healthcare-associated IE caused by *S. aureus* and coagulase-negative staphylococci has increased in the recent past, while the number of IE caused by viridans-group streptococci (VGS) has declined [9, 10]. In addition, the rate of infection due to MRSA in health care and community settings has increased in the past years [6]. In Europe, 28% of the IE infections are caused by *S. aureus*, and while in North America, it is 43% [2]. Enterococci are the third leading cause of IE and are associated with healthcare settings [11].

IE caused by Gram-negative bacteria and fungal pathogens is not common and is mainly healthcare-associated [12, 13]. The opportunistic fungus *Candida albicans (C. albicans)* is one of the most common pathogens among fungal species and accounts for 24-46% of all the cases of fungal IE [13, 14]. It is an emerging disease and a global health concern that mainly affects the elderly population and immunocompromised individuals [15]. Besides the vulnerable populations mentioned, *C. albicans* also infect patients with cardiac devices and targets IDUs (third most common cause of IE in IDUs) [16]. Because of the challenges faced in diagnosing *C. albicans* IE, its epidemiology, prognosis, and therapy is poorly defined [14, 17, 18].

1.3. Diagnosis of IE

Identification of the specific microbial pathogen causing the IE is essential for patient management and appropriate therapy. Delays in diagnosis can lead to late initiation of therapy, leading to severe health complications [19]. Duke criteria, which are a set of clinical criteria set for the diagnosis of IE, rely on detection of the infecting pathogen in addition to clinical findings and echocardiography [5, 20]. To date, various methods are used for IE diagnosis, including blood culture, molecular typing techniques, endocardiography, and serological assays.

Blood cultures (BC) are the standard tests to determine the microbiologic etiology because of the persistent presence of a pathogen in the blood of IE patients. Modern BC techniques enable the detection of most pathogens causing IE and account for 2.5 to 70% of all IE cases depending on the country in which it was diagnosed [21]. However, the rate of positive cultures declines when the patient is taking antibiotics or the infectious agent is a fastidious pathogen [2, 22]. BC should be collected from the patients at different time points and before administering antibiotics [19]. A typical BC takes five days to detect a pathogen, including fungi, making it a time-intensive method.

Molecular methods are routinely utilized for diagnosis in blood culture-negative IE and account for 2.5-31% of etiologic agent detection [23]. They include organism-specific PCR and broad-range bacterial PCR (16S PCR) followed by sequencing. As the name suggests, in organism-specific PCR, designated primers against one pathogen are used, while in broad-range bacterial PCR, primers targeting the bacterial 16s ribosomal RNA are used to detect bacteria in general, which is followed by comparing the DNA sequence to the established databases. The sensitivity of organism-specific PCR is higher than the broad-range bacterial PCR when diagnosing IE [24]. Care should be taken while interpreting PCR-based results because bacterial DNA has

been reported in patients even after resolving tissue lesions and infections and can give false-positive results [25]. Simultaneously, PCR inhibitors and microbial DNA/RNA below the detection level can give false-negative results. Moreover, both blood samples and valve tissues are used in the molecular diagnosis, though blood samples have low sensitivity [2]. For example, the sensitivity of the organism-specific *Bartonella* PCR assay performed on valve tissue was 92% compared to 33% for the blood samples [26].

Endocardiography is the second most common method after BC to diagnose IE in suspected patients though it cannot identify the pathogen [5, 27]. Transthoracic echocardiography (TTE) is used to visualize microbial vegetations in patients, and its sensitivity is highest when used in the right-sided IE due to the proximity of the tricuspid and pulmonic valves to the chest wall [28]. Transoesophageal echocardiography (TOE) performs better in diagnosis than TTE when the vegetation is on prosthetic valves [29]. Both techniques complement each other, and it is recommended to try TOE when TTE is negative. The timing of performing endocardiography is crucial as the test may be negative early in the course of the disease. It is suggested to repeat endocardiography after several days in patients when high suspicion of IE persists [5, 27]. Other imaging techniques have been evaluated for the diagnosis of IE. Some of these methods are three-dimensional transesophageal echocardiography (3D TEE), cardiac computed tomography (CT), and cardiac magnetic resonance imaging (MRI) [30, 31]. The use of these methods may increase in the future depending on their sensitivity and efficacy.

Serological assays are widely used in research and medicine for the determination of antibodies in the blood. These assays have been included as diagnostic criteria for IE in the modified Duke criteria [32]. Serological testing is routinely used to diagnose *Coxiella burnetii*, *Bartonella* spp., *Chlamydia* spp., *Brucella melitensis*, *Mycoplasma pneumoniae*, and *Legionella pneumophila*, which are the most common pathogen involved in culture-negative IE [33–35]. Though *Bartonella* can be diagnosed via blood culture if special culture techniques are used, serological tests might be more effective [2].

Serological tests have shown promising results so far in the case of IE, yet one must be careful relying solely on these tests because of cross-reactions. For instance, the currently available serological test for *Bartonella*-induced IE identification may not reliably distinguish between antibody response to either *B. henselae* and *B. quintana* or between those to *Bartonella* spp. and *Chlamydia* spp [34, 36].

Antimicrobial antibodies can be detected with different approaches. For the serologic diagnosis of *Brucella melitensis,* a tube agglutination test is used, while indirect immunofluorescence is used for *Legionella pneumophilia.* Furthermore, ELISA is performed to diagnose *Mycoplasma pneumoniae,* and ELISA or indirect immunofluorescence to diagnose *Chlymadia* spp [35, 36].

Serological tests are fast and reliable when performed to diagnose a single pathogen. However, if one wants to determine the plasma antibodies against a large number of pathogens, this method can become cost-intensive and time-consuming. The Luminex xMAP® technology has been used successfully in the serological detection of antibodies against multiple antigen targets in a single assay for various viruses (including SARS-CoV-2) and also *Staphylococcus aureus* [37–43]. Therefore, a high-throughput method such as the multiplex approach based on xMAP® technology (Luminex) is a desirable choice in research and the clinical setting.

The multiplex approach was used in our research group by Dr. Nicole Normann [44] and Dr. Dina Raafat to establish the 20-plex infection array. ECP of 16 typical sepsis pathogens were used in this high-throughput screening method to study antibody response to the selected pathogens in sepsis patients. The preliminary work showed promising results and demonstrated that serological assays could provide crucial diagnostic information. Moreover, it has the potential to be used in biofilm-associated infections like IE and prosthetic joint infection (PJI), where the infection is often asymptomatic long before it is clinically diagnosed.

1.4. *Staphylococcus aureus* as a major IE pathogen

S. aureus, a Gram-positive bacterium, is one of the most common opportunistic human pathogens and a leading cause of various diseases ranging from mild infections to severe illnesses such as IE, bacteremia, toxic shock syndrome, and necrotizing pneumonia [45–47]. The bacteria harbor a large set of pore-forming toxins and superantigens, which cause host tissue damage and septic shock, respectively [48]. They are capable of attaching to host tissues (e.g., heart valves and bones) as well as medical devices (e.g., catheters, pacemakers, and prosthetic joints), thereby causing chronic infections such as osteomyelitis and endocarditis [47, 49, 50].

Though a serious pathogen, *S. aureus* is also a human commensal that permanently colonizes the anterior nares of nearly 20% of the healthy adult population while the remaining 80% are intermittent carriers [51, 52]. *S. aureus* nasal colonization increases the risk of infection [52–54]. Nearly 65% of people with *S. aureus* skin lesions are colonized with the infecting strain,

while the percentage increases to 80% in the case of bacteremia [52]. Moreover, *S. aureus* carriers can transmit the colonizing strain to the environment and contact persons, thereby amplifying the spread of *S. aureus* in health care settings [52, 55].

S. aureus is equipped with a wide array of accessory factors to colonize and/or infect their host. Some factors promote bacterial fitness by promoting adherence to epithelial or damaged host tissues, and others support nutrient acquisition and iron uptake [56, 57]. It also produces a range of toxins, most prominently pore-forming toxins and superantigens that lyse immune cells and interfere with a coordinated T cell response, respectively [58, 59]. Moreover, *S. aureus* and other staphylococci form biofilms that shield the pathogens from the immune system of the host and enhance their resistance to antibiotics [60, 61]. Furthermore, these pathogens produce numerous immune-modulatory factors that can evade innate and adaptive defense mechanisms [62]. Many virulence and immune evasion genes are encoded on mobile genetic elements such as pathogenicity islands (e.g., toxic shock syndrome toxin-1 (TSST-1) and enterotoxins) or bacteriophages (e.g., Panton-Valentine leukocidin (PVL)) [63, 64].

The main problem with hospital-associated infections caused by *S. aureus* is that many hospital-acquired strains are resistant to antibiotics [46]. This species has acquired resistance to penicillin and methicillin in a short period [65]. With a prevalence of around 20% among all *S. aureus* isolates in German hospitals and slightly less in the rest of Europe, methicillin-resistant *S. aureus* (MRSA) continues to be a serious threat to the immunocompromised and hospitalized patients [66–68]. Additionally, the so-called community-associated MRSA (CA-MRSA) can also infect healthy individuals without prior contact to healthcare settings because of unique virulence factors, combined with antibiotic resistance [69]. One specific strain, USA300, has become a recurrent source of skin and soft tissue infections in the USA [70–72]. Moreover, livestock-associated MRSA (LA-MRSA) is an emerging problem in various parts of the world due to the high use of antibiotics in farm animals [73, 74]. The continuously high prevalence of MRSA in hospital settings severely limits treatment options [75, 76].

Even though *S. aureus* infections are associated with high morbidity and mortality, none of the *S. aureus* vaccines has made its way into clinical practice to date [65, 77]. On the other hand, alternative therapies like bacteriophages, natural antibacterial compounds, cationic antimicrobial compounds, and photodynamic therapies need further studies as some of them seem to be promising [78, 79].

As IE is characterized by bacterial biofilms, it is important to understand its formation and clinical implications. Biofilms are composed of sessile communities of bacteria embedded in an extracellular matrix, which can attach to biotic and abiotic surfaces [80]. As mentioned before, *S. aureus* is a frequent cause of biofilm-associated infections in humans, which places an enormous strain on healthcare systems worldwide [81]. A big challenge presented by biofilms is their resistance to chemotherapies and host defense mechanisms, allowing *S. aureus* to persist on host tissues. Moreover, *S. aureus* biofilms are responsible for 33% of all medical device-related infections, while the rest are caused by other pathogens [47]. The ability of *S. aureus* to cause biofilm-associated infections has attracted significant interest in studying the complex mechanisms governing the formation of persistent biofilms and different strategies that can be implemented to dismantle them.

The stages involved in biofilm formation are quite complex and have been described comprehensively in many reviews [47, 77, 81, 82]. It is generally divided into at least three major events; attachment, maturation, and dispersal/detachment of biofilm [49]. During the attachment stage, planktonic cells reversibly adhere to biotic and abiotic surfaces and proliferate to form aggregations called microcolonies. During maturation, these microcolonies expand, and bacterial cells produce an extracellular polymeric matrix (ECM). This biofilm matrix varies in composition from one strain to another. In general, it comprises polysaccharides, proteins, host factors, and extracellular DNA (eDNA) [82–84]. Channels are also formed during this phase, facilitating the delivery of nutrients to all the layers of biofilm [45]. Upon reaching a specific cell density, mechanisms to initiate ECM degradation are activated, allowing the cells in the biofilm to disperse and reinitiate biofilm formation at another site.

Numerous proteins and polysaccharides have been implicated as important components in attachment and biofilm formation. For attachment, staphylococcal adhesins, including the "microbial surface components recognizing adhesive matrix molecules" (MSCRAMMs) family, play a significant role [82]. These include proteins such as fibronectin-binding proteins (FnBPA and FnBPb), clumping factor A (ClfA), biofilm-associated protein (Bap), and *S. aureus* surface protein (SasG) [85–90]. The binding property of ClfA makes it an essential player in the colonization of implant material or damaging endothelial surfaces [82, 91]. FnBPs mediate binding to fibrinogen (Fg), fibronectin (Fn), and elastin and are also involved in biofilm development [82]. Moreover, secreted proteins like extracellular adherence protein (Eap) promote biofilm maturation [49].

Another principal constituent of biofilm is the surface-associated exopolysaccharide polymeric N-acetyl-glucosamine (PNAG), also known as polysaccharide intercellular adhesin (PIA) [92]. Although PNAG is not involved in all staphylococcal biofilms, it is a crucial component of *S. aureus* and *S. epidermidis* biofilms and supports cell to cell adhesion [93–95]. The cationic nature of PNAG allows the attachment of bacteria to the cell surface of the host [96].

A more recently identified component of a biofilm matrix is eDNA. With its negative charge, eDNA facilitates binding to the cell surface, host factors, and also to other bacteria in biofilm [49]. Biofilms are sensitive to DNAse treatment in the attachment phase, suggesting that eDNA might be an essential player during this phase [97]. Autolysis of bacterial cells in the biofilms is responsible for the production of eDNA, and this activity is mediated through hydrolases encoded by *atl* and *lytM* genes [98]. Some studies have shown that eDNA interacts with certain proteins within biofilms. One of these proteins is *S. aureus* beta toxin (Hlb) which forms insoluble oligomers after binding to DNA that could help retain the biofilm structure [99]. Another vital protein family, DNABII, is often found associated with eDNA that helps to keep the structural integrity of the biofilms [100].

Biofilms contain channels used for nutrient delivery to different parts of the biofilm. To create these channels, enzymatic digestion of the biofilm matrix molecules, like eDNA and proteins, is carried out by nucleases and proteases, respectively [49]. So far, only one enzyme has been reported in staphylococci that can digest PNAG [101]. Besides forming channels, some factors also aid in the dispersal of microbes. Phenol-soluble modulins (PSMs) are surfactant-like proteins that take part in the dissociation of biofilm by disrupting hydrophobic and hydrophilic bonds between biofilm matrix molecules [45, 102]. Lastly, various proteases, DNnases, hydrolases, and surfactants also contribute to dispersing the biofilm [103, 104].

Numerous studies demonstrated a broad spectrum of antibodies against *S. aureus* antigens in healthy individuals and patients [52, 105–109]. The quality of the immune response depends on the history of encounters with the invading strain. *S. aureus* carriers usually develop an endogenous infection with a rise in IgG antibodies, while non-carriers develop an exogenous infection with a strong but transient IgM response with new IgG antibody production. The rise in antibody titer is mostly specific against the invasive strain [108]. There is a strong variation in the antibody titers reflecting the history of an encounter of a person with *S. aureus,* suggesting that an individual will have a different immunological "starting point" against an infection [110]. Moreover, *S. aureus* carriers tend to have more anti- *S. aureus* antibodies than non-

carriers because the likelihood of carriers developing an infection from the colonizing strain is higher [108, 111]. Our group demonstrated that the antibody response in carriers is highly specific and targets only the SAgs produced by the colonizing strain [58]. A large prospective clinical trial has shown that carriers with *S. aureus* bacteremia have a better prognosis than non-carriers. Additionally, high antibody titers against specific antigens like Hla, SAgs, PSMs, and PVL are correlated with protection against infections in humans [112–114]. In conclusion, these studies suggest that antibodies against *S. aureus* can provide protection, and the use of monoclonal antibodies is a promising approach to tackle infections.

1.5. Clinical trials on anti-*S. aureus* vaccines

Two different immunization strategies could be used to target *S. aureus* via a vaccine. Active immunization refers to the process of exposing the host to an antigen to provoke an adaptive immune response. The response takes days/weeks to develop, but it usually induces long-lasting and robust protective immune memory. Passive immunization refers to transferring antibodies/immune sera/immune cells to a host to protect against infection. It gives immediate and effective protection, but it is short-lived and can last from several weeks to 3 or 4 months at most [77, 115]. Both active and passive immunization techniques have been tried against *S. aureus* infections to obtain an effective vaccine. Here, we will focus on passive vaccination strategies used, the clinical trials already conducted using this strategy, and the prospects.

Passive vaccines have been extensively studied. In 2021, FDA approved the 100th monoclonal antibody (mAb) product for testing in clinical trials. Out of the 100 mAbs, 10 are approved for use in infectious diseases mainly caused by viruses [116]. Passive immunization has also been in the spotlight of the SARS-CoV-2 pandemic. It can be used in regions of high incidence to protect immunocompromised patients whose responses to active vaccination is insufficient [117, 118].

Passive vaccination strategy has also been tested against *S. aureus*. Studies have reported that antibody response against *S. aureus* plays a major role in specific immunity against it [119]. Moreover, passive immunization with antigen-specific antibodies has been shown to provide partial protection in various *S. aureus* infections [87, 120–124]. These studies suggest that passive vaccination could be a promising strategy against *S. aureus*. Passive vaccines could protect against *S. aureus* biofilms by the mechanisms explained in Figure 1.

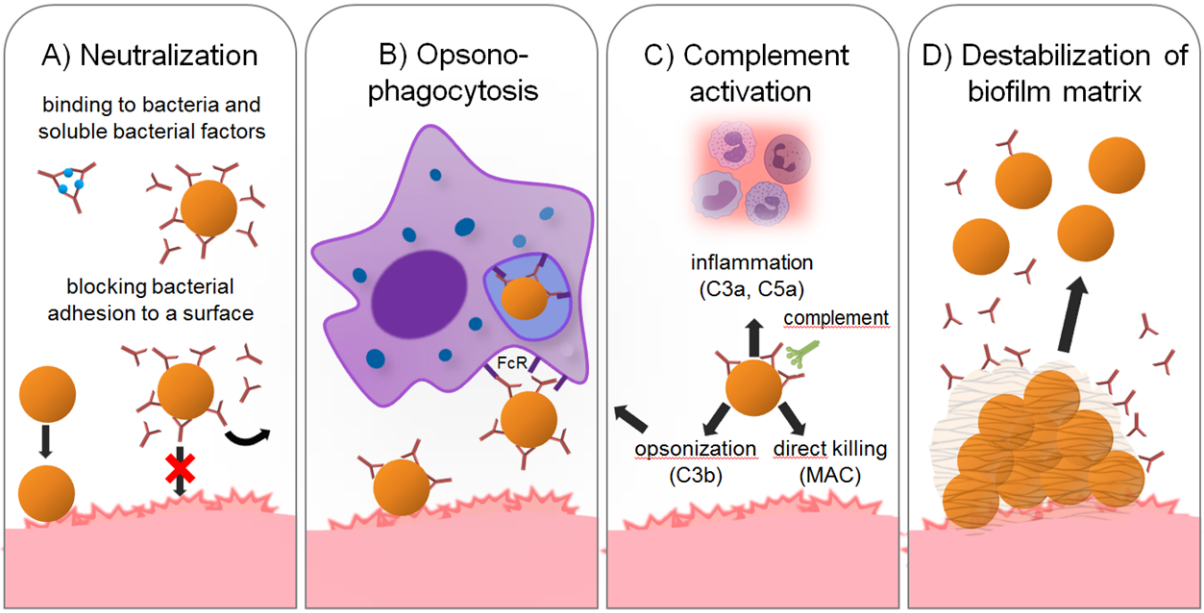

Figure 1. Antibodies against *S. aureus* can penetrate the biofilm and hamper biofilm formation at different stages. It can target the adhesins on the surface of *S. aureus* to prevent its initial attachment to a surface. (a) *S. aureus* can secrete a wide range of proteins (e.g., immune evasion molecules, toxins, exoenzymes) and express surface proteins, which play an important role in biofilm development and can be used as a potential target for vaccine development. Neutralizing IgA and IgG can disrupt the function of bacterial toxins as well as surface proteins. Additionally, high-affinity antibodies can bind to the surface bacterial adhesins (e.g., ClfA, ClfB, FnBPA, FnBPB) and cell wall components (e.g., PNAG) and block the binding to bacteria to biotic and abiotic surfaces to block the initiation of biofilm formation. It can also block the cell-to-cell adhesion by targeting proteins involved in this process and retard biofilm maturation. (b) Surface-bound antibodies (primarily IgG) can enhance opsonophagocytosis carried out by neutrophils and macrophages, which express FC receptors (FcR) on their surfaces. The activation of neutrophils can lead to the release of trigger granules, NETosis, and oxidative burst. (c) Surface-bound antibodies (IgM and IgG) can also lead to the activation of the complement system through the classical pathway. The complement cascade is activated after C1q binds to the surface-bound antibody, leading to the formation of C3 convertase. C3 convertase cleaves the main component of the complement system, C3, into C3a and C3b. C3b can function as an opsonin and enables phagocytes, which express the C3b receptor, to engulf C3b coated bacteria. Besides, the other released factor, C3a functions as a chemoattractant, which recruits immune cells to the infection site, leading to inflammation. Additionally, C3 activation triggers the formation of membrane attack complex (MAC) that causes lytic pore formation in certain microbes. However, Gram-positive pathogens, e.g., *S. aureus*, are not affected by it because of a thick peptidoglycan layer. (d) Antibodies can target certain components of the biofilm matrix, such as DNABII, and destabilize the biofilm matrix leading to bacterial dispersion. The dispersed bacteria can be targeted by immune cells and antibiotics. (adapted from Raafat et al., 2019)

Passive vaccination strategy has been tested against various *S. aureus* antigens, including ClfA, capsular polysaccharide (CP) 5, CP8, lipoteichoic acids (LTA), wall teichoic acid (WTA), PNAG, GrfA (ABC transporter), and pore-forming toxins (Hla, HlgAB, HlgCB, LukED, LukSF, LukAB). They are discussed in detail below.

Staphylococcal cells are covered with surface glycopolymers like WTA, LTA, peptidoglycans, and CP against which antibodies are found in the serum. Antibodies against WTA mediate complement C3 deposition via the classical pathway and facilitate opsonophagocytosis of *S. aureus* isolates by neutrophils [125, 126]. Human mAbs against WTA were ineffective in preventing *S. aureus* infection in a mouse infection model but showed promising results when conjugated to an antibiotic [127]. Furthermore, antibodies against the CPs have yielded

contradictory results so far. Rabbit polyclonal antibodies promoted opsonophagocytosis and provided partial protection, while murine antibodies were not protective [128–130].

Adhesins, including MSCRAMMs, are amongst the most studied targets for passive immunization. For more than a decade, many monoclonal antibodies have been produced against ClfA, blocking biofilm formation *in vitro*. Anti-ClfA mAbs promoted opsonophagocytosis *in vitro* and interfered with biofilm formation (e.g., IE) as well as non-biofilm-associated infections (e.g., sepsis) [131–133]. A humanized mAbs against ClfA, Tefibazumab by Aurexis, gave full protection against IE in rabbits when administered prophylactically but failed to achieve statistically significant results in bacteremia and cystic fibrosis patients even when administered with antibiotics [132, 134]. Another essential MSCRAMM protein is FnBPA, which binds to Fn, Fg, and elastin, and plays an integral part in forming biofilm [82]. Anti-FnBPA mAbs inhibited biofilm formation *in vitro* and protected mice against endocarditis following sepsis [87, 120].

Bacterial DNA-binding proteins (DNABII family) serve as an adapter protein for eDNA and help stabilize the biofilm matrix [135, 136]. Neutralizing antibodies against these scaffolding proteins leads to the dispersal of biofilm, which makes the bacteria more susceptible to be cleared by antibiotics and phagocytes [136, 137]. A human mAb (TRL1068) has been generated against an epitope of DNABII, which is conserved across Gram-positive and -negative bacteria [138]. TRL1068 was effective not only in an *in vitro* biofilm assay but also *in vivo* in murine infectious implant model and the catheter-related rat infection model [135, 138].

Various proteomics studies have shown that some of the pore-forming toxins (e.g., Hla, LukAb, and γ-Hla [HlgAb]), immune evasion molecules (e.g., Chemotaxis inhibitory protein of staphylococci [CHIPs]), and Staphylococcal complement inhibitor [SCIN]) are found in biofilms *in vitro* and *in vivo*. Some of them are produced in higher amounts in biofilms compared to planktonic cultures, whereas others, like the immune evasion protein A, are down-regulated [139–141]. The immune cells, including T cells, monocytes, and neutrophils, are under attack because of the pore-forming abilities of toxins like Hla, LukAB, and HlgAb, thereby crippling the immune response [142].

Human anti-Hla mAbs (MEDI4893) have been generated, which can inhibit the interaction of Hla to its receptor ADAM10, thus effectively reducing its pore-forming ability. It dismantled the *ex vivo* biofilm formation on porcine vaginal mucosa explants and promoted wound healing

as a prophylactic treatment in a mice wound infection model [143, 144]. Because of the neutralizing ability of MEDI4893, it has been extensively studied in biofilm and non-biofilm-related models [143–145]. Aridis pharmaceuticals also tested antibodies against Hla for countering *S. aureus* pneumonia, and the trial is now entering Phase 3 [146, 147]. Another important toxin that facilitates Hla to kill phagocytic cells is LukAB. It also helps in the persistence of staphylococcal biofilm [148]. Neutralizing Human IgG1 mAb, ASN-2, has been produced against LukAB, which binds strongly to the antibody-binding site on LukAB dimer. [149] Human mAbs against LukAB have also shown promising results in reducing bacterial load in a murine sepsis model [150].

Some of the targets, including ClfA, type 5 and 8 CP, Hla, HlgAb, and PNAG, which showed promising results in pre-clinical studies, were tested as passive vaccines in various stages of clinical trials. Unfortunately, none of the vaccines are widely and commercially available so far. Biosynexus developed a mAb against LTA named Pagimaximab, which failed in Phase III clinical trials. Similarly, Nabi generated a vaccine called Altastaph by deriving polyclonal antibodies against CP5 and CP8 from sera obtained from individuals who were treated with Staphvax. Two clinical trials were conducted in different sets of bacteremia patients to investigate the efficiency of Altastaph, and both failed in Phase II [151–154]. Moreover, anti-PNAG mAb did not protect in Phase IIa clinical trials in ventilated intensive care unit patients, and the trial was terminated [77].

1.6. Failure to generate *S. aureus* vaccine to date

As discussed before, various antigens have been tested as vaccine candidates against *S. aureus*, but none of the clinical trials involving those vaccines have been successful so far. One reason single target adhesins vaccines have failed could be the high functional redundancy of these proteins. For example, there are five known Fg-binding proteins in *S. aureus*, and neutralizing the action of one is not sufficient [82]. Another major reason can be the agglutination of bacteria in the blood by antibodies, which may not be cleared by the host's immune cells. These aggregated bodies can stick in various tissues, particularly in the lungs, leading to further complications [155, 156]. Finally, opsonophagocytosis might not be the ideal mechanism for protecting against *S. aureus* because *S. aureus* produces a wide variety of toxins and immune evasion factors that take part in pathogenesis.

Besides focusing on single-component vaccines, multi-component passive vaccines are also being prepared and tested for many *S. aureus* infections [157, 158]. Arsanis Biosciences prepared a combination of human mAbs against Hla, HlgAB, HlgCB, LukED, LukSF, and LukAB (ASN100) and tested it in pneumonia patients [149, 158]. Finally, mAbs have also been used as a means to deliver an antimicrobial to its specific target. For example, an antibody-antibiotic conjugate (AAC), which has specificity for WTA, is currently used in *S. aureus* bacteremia patients in phase 1b clinical trial [159, 160]. Because of the functional redundancy of various *S. aureus* antigens, a multi-component vaccine against different virulence factors might be more effective.

1.7. Monoclonal antibodies against biofilm-relevant targets

Even though biofilms are involved in a majority of bacterial infections, they are frequently not specifically targeted by mAb generated so far. As our research group focuses on *S. aureus* biofilm formation, candidate antigens for the generation of mAbs were chosen based on their roles in the life cycle of a biofilm. Some selected candidates are well known for their role in biofilm formation, while one new candidate was chosen because of its expected role in biofilms and other infections [77, 161].

The two well-known candidates are ClfA and FnBPA. As mentioned above, ClfA and FnBPA are involved in various life-threatening infections and take a crucial part in the life cycle of biofilm formation. Besides, mAbs against serine protease–like protein B (SplB) will be generated, which is part of the Spl family that elicits immune responses in asthmatic patients, cystic fibrosis patients, and healthy individuals colonized with *S. aureus* [162]. Though SplB might not be directly involved in biofilm formation, proteases play an essential and dual role in the biofilm life cycle.

S. aureus is one of the major pathogens in IE alongside other major infections. Antibody response against *S. aureus* in the carriers has shown a better prognosis in bacteremia patients than non-carriers [163]. Interestingly, the *S. aureus* isolated from IE patients exhibits a higher expression of adhesin proteins such as ClfA, ClfB, FnBPA, and FnBPB. IE patients also produced significantly higher IgG antibody titers against these proteins as compared to the healthy controls. More importantly, IgG isolated from the patients moderately inhibited the binding of *S. aureus* to immobilized Fn [164]. Because of these reasons, mice and humanized monoclonal antibodies (mAbs) have been generated against ClfA, which have shown protection in different animal models, including IE. Moreover, anti-FnBPA mAbs also provided protection

in mice IE models. These reasons provide strong support to generate neutralizing mAbs against two adhesins, ClfA and FnBPA, and a protease SplB.

1.7.1. SplB

The staphylococcal serine protease–like proteins (Spls) are encoded on the *v*Sa*β* pathogenicity island in an operon comprising six genes: *splA, splB, splC, splD, splE,* and *splF*. The Spl operon is unique to the species *S. aureus* though some strains do not have the full operon [165–167]. Out of the array of virulence factors, including many proteases, the Spls are not well characterized so far. Recent work from our group has shed some light on the role of Spls during *S. aureus* infection. Interestingly, these proteases induce a type 2 response, characterized by anti-Spl-IgE and -IgG4 as well as a Th2 memory response in healthy individuals [162]. Similarly, Spls induce IgE and IgG4 antibody production in sepsis and asthmatic patients [162, 168–170]. Notably, one of the Spls, SplB, might be involved in biofilm formation [161].

Proteases have been reported to play a role in biofilm remodeling or disruption. Proteases like Esp from *S. epidermidis* and Staphopains from *S. aureus* either inhibit or disrupt the biofilm, thus allowing the increase of antibiotics efficacy [171, 172]. Similarly, proteases like Spls are reported to be involved in the biofilm dispersal by degrading extracellular polymeric substance's ECP, and it may lead to colonization of new sites [104, 173, 174]. Vaccination with SplB, in combination with three other antigens ((LukE, LukS-PV, and SspB), provided modest antibody-independent protection against dermonecrosis in C57BL/6 mice [175]. Collectively, Spls potentially play an important role in *S. aureus*-host interactions and could be a useful target for vaccination.

1.7.2. ClfA

ClfA is an essential member of the MSCRAMMs family. As mentioned, ClfA is an adhesion that promotes bacterial binding to Fg and fibrin and plays a vital role in the colonization of biotic and abiotic surfaces [82, 91]. The Fg binding domain of ClfA is present in a 218-residue segment in the A region [176]. ClfA also mediates binding to human platelets membrane receptors [91, 177]. The *clfA* gene is present in nearly all clinical *S. aureus* strains and is expressed *in vivo* [178, 179]. The biological role of ClfA in various diseases (arthritis, biofilm-related infections, bloodstream infections) has been shown in various studies, which suggest that it is one of the major virulence factors in *S. aureus* [180–182].

Murine, humanized, and human anti-ClfA monoclonal antibodies have been previously generated by several groups [131–133, 183]. These antibodies promote opsonophagocytosis and interfere with biofilm formation [131, 133]. Their protective potential in biofilm settings was studied in a range of assays, from *in vitro* biofilm models to biofilm-related infection models as well as non-biofilm-associated infections [131, 132]. In conclusion, previous research and data suggest that ClfA is a valid and vital target to develop a passive vaccine against *S. aureus* and should be tested in combination with other mAbs as well as antibiotics.

1.7.3. FnBPA

The cell wall-anchored protein FnBPA is a critical member of the MSCRAMMs family. FnBPA binds not only to Fn but also Fg and elastin [82]. The N-terminal A domain of FnBPA is 24% identical to the A domain of ClfA, and each of these binds to the C-terminus of the γ chain of Fg. Moreover, the A domain of FnBPA is structurally and functionally related to *Staphylococcus epidermidis* SdrG protein [184]. While the A domain of FnBPA binds to elastin, ClfA lacks this ability [87]. FnBPA promotes biofilm formation of clinically relevant MRSA strains and facilitates specific cell-cell interactions that involve its A domain and cause microscale cell aggregation [184]. Immunization with FnBPA provides protection against *S. aureus* infection in the immunized mice [185]. Rat antibodies against truncated FnBPA facilitated opsonization of *S. aureus* and promoted neutrophil activity as well as macrophage phagocytosis *in vitro* [120]. Murine antibodies against FnBPA reduced biofilm formation *in vitro* and inhibited the adherence of *S. aureus* to immobilized Fn [87, 186]. As discussed, antibodies against FnBPA have shown protection against IE and protected mice against weight loss due to SAB [120]. Because of these properties, FnBPA seems like a promising candidate for a passive vaccination strategy to protect humans against *S. aureus* biofilm-associated infections.

1.8. Card-ii-Omics - Developing new approaches to prevent, diagnose and treat cardiac implant infections.

The research consortium Card-ii-Omics was funded by the ESC from 2017 - 2021 and brought together expertises from the University Medicines of Greifswald and Rostock in implant development, infections, and proteomics to study cardiovascular implant infections. The consortium aimed at developing new approaches to prevent, diagnose and treat implant infections. I was part of a junior research group comprising a junior group leader, three Ph.D. students, and several master students. Focussing on pathogen-specific antibodies, our research

group had two major aims: (1) Establishing the infection array 33-plex and exploiting it to investigate the pathogen-specific antibody response in a pilot study on IE patients, and (2) Generating and characterizing mAbs against *S. aureus*.

To study the pathogen-specific antibody response, the above-mentioned xMAP®-based infection array was established by co-workers (Dr. Dina Raafat), the principle of which is explained in sections 1.3, 3.1, and Figure 2. The array was subsequently tested and evaluated in a pilot clinical study (GIES) on IE patients. The Greifswald IE study (GIES) is a small pilot study was performed in Greifswald under the direction of Dr. R. Busch (Cardiovascular Cell Research, Clinic and Polyclinic for Internal Medicine B, University Medicine Greifswald) in Greifswald. This study aimed at the analysis of cell mechanical properties of blood cells in endocarditis patients. It included 17 endocarditis patients and 20 cardiac control patients between July 2018 and April 2019. Biomaterials (plasma, PBMCs, blood culture isolates) were collected and stored for subsequent analyses. Detection of antibodies in the blood could provide crucial information about how the immune system responds during an infection caused by Gram-positive, Gram-negative, atypical bacteria and yeast. Furthermore, it can provide information about the infection-causing pathogen(s), which can be used as a potential diagnostic technique in the future. Once the pathogen is diagnosed, antimicrobial therapy can be optimized and directed against the infectious agent.

In addition, several mAbs against *S. aureus* have been generated and extensively characterized by our junior research group within the Card-ii-Omics consortium. We have followed 2 strategies: the production of murine mAbs and the - technically much more demanding - production of human mAbs. Murine and humanized mAbs against adhesion factors (FnBPA, ClfA) and extracellular bacterial enzymes (GlpQ, SplB, Plc) were generated using hybridoma technology. The production and characterization of some of these antibodies were conducted within this Ph.D. thesis.

1.9. Objectives

Upon IE, antibodies are generated that are highly specific for the invading pathogen and mediate clearance of the infection [187–190]. These antibodies could form a basis for a diagnostic strategy as well as the generation of a passive vaccine against *S. aureus*, which is the most prominent pathogen in IE.

This study aimed at utilizing the antibody response directed against IE pathogens to work towards better diagnosis and therapy of IE. In detail, we investigated if a pathogen-specific antibody response can be measured in IE patients and if this can complement the classical blood culture diagnosis. Moreover, we aimed to generate and characterize neutralizing monoclonal antibodies (mAbs) against three virulence factors of *S. aureus*, which is the most common etiological agent in IE.

To study the pathogen-specific antibody response in IE patients, we conducted a prospective clinical observational discovery study on 17 IE patients and 20 controls (patients with non-infectious heart-related conditions). A recently established xMAP® (Luminex®) technology-based serological assay that simultaneously quantifies the antibody response against 30 pathogens (infection array) was used for high-throughput antibody profiling.

Recently, using hybridoma technology, our research group has generated mAbs against two *S. aureus* surface proteins/adhesion factors (clumping factor A (ClfA) and fibronectin-binding protein A (FnBPA)), both involved in biofilm formation, as well as an extracellular enzyme, the staphylococcal serine protease–like protein B (SplB), a virulence factor known to induce Th2 immune response in healthy individuals. In this work, these mAb were produced at a larger scale, and their sequence was determined. Afterwards, their binding and neutralizing capacities were investigated using *in vitro* assays such as ELISA, Western blot, Dot blot, microscale thermophoresis, and in a mouse model.

2. Materials

2.1. Equipment

Equipment	Manufacturer
Air shaker	Sartorius AG, Göttingen, DE
Analytical balance	Sartorius AG, Göttingen, DE
Autoclave	Systec GmbH, Linden, DE
BioPlex® 200 System	Bio-Rad Laboratories, California, US
Mini-Sub Cell DNA Cell	Bio-Rad Laboratories, California, US
Canon CanoScan LiDE 110	Canon Deutschland GmbH, Krefeld, DE
Centrifugation tube 250 ml	ThermoFisher Scientific, Massachusetts, US
ChemoCam Imager	Intas Science, Göttingen, DE
Digital scales	Sartorius AG, Göttingen, DE
DynaMag™ -2 magnet	ThermoFisher Scientific, Massachusetts, US
Electronic pipette E4 XLS +	Mettler-Toledo GmbH, Giesen, DE
Freezer, -20°C	Liebherr-International GmbH, Hamburg, DE
Freezer, -80°C	Heraeus Instruments, Hanau, DE
Fridge, 4°C	Liebherr-International GmbH, Hamburg, DE
GenoPlex gel documentation system/imager	VWR™ International GmbH, Darmstadt, DE
Heidolph Pumpdrive 5001 peristaltic pump	Heidolph Instruments, Schwabach, DE
Heraeus Biofuge Pico	ThermoFisher Scientific, Massachusetts, US
HLC heating block	HLC Biotech, Bovenden, DE
Ice machine	Manitowoc GmbH, Herbron, DE
Incubator	Binder Labortechnik, Tuttlingen, DE
Induction hotplate	Imtron GmbH, Ingolstadt, DE
Magnetic 96-well separator	ThermoFisher Scientific, Massachusetts, US
Microwave	Bosch, Stuttgart, DE
Mini-PROTEAN Tetra	Bio-Rad Laboratories, California, US
Monolith NT.115	NanoTemper Technologies GmbH, Munich, DE
Multichannel pipettes	Eppendorf AG, Hamburg, DE
Multifuge X3R	ThermoFisher Scientific, Massachusetts, US
Olympus Microscope CKX31	Olympus Corporation, Tokyo, JP
pH-meter	Mettler-Toledo GmbH, Gießen, DE
Pipettes	Eppendorf AG, Hamburg, DE
PowerPac™ Basic Power Supply	Bio-Rad Laboratories, California, US
Semi-Dry Transfer Unit (TE77XP)	Hoefer, Inc., Massachusetts, US
Spectrophotometer (DS–11)	DeNovix Inc., Wilmington, US
SpeedVac (Concentrator plus)	Eppendorf AG, Hamburg, DE
Sterile workbench	ThermoFisher Scientific, Massachusetts, US
TECAN Infinite M200	Tecan Group AG, Männedorf, DE
Thermal magnetic stirrer	Phoenix Instrument GmbH, Garbsen, DE
Thermocycler T1	Biometra, Göttingen, DE
Ultrasonic bath	VWR™ International GmbH, Darmstadt, DE

UV-Photometer	Biometra, Göttingen, DE
UV-Transilluminator	Fluo–Link, Marne-la-Vallée, FR
Vortex mixer	Heidolph Instruments GmbH & Co. KG, Schwabach, DE
Water purification system	Merck Millipore, Massachusetts, US
Waterbath	Grant Instruments, Shepreth, UK

2.2. Consumables

Materials	Manufacturer
96-well half area microplates	Greiner Bio-One GmbH, Frickenhausen, DE
Aluminum foil	Carl Roth GmbH & Co. KG, Karlsruhe, DE
Aluminum foil for 96-well plates	Sarstedt AG & Co. KG, Nümbrecht, DE
Bioreclamation IVT Human Serum (Cat: HMSRM Lot: BRH1235375)	Bioivt & Elevating Science, New York, US
C-Chip, disposable hemocytometer	NanoEntek, Seoul, KR
Cryotubes (1.0 ml)	Sarstedt AG & Co. KG, Nümbrecht, DE
Dialysis membrane (14 kDa)	Sigma-Aldrich, Missouri, US
Falcon® Cell Culture Flasks (353028)	Corning Inc., Amsterdam, NL
Falcon® Reaction tube (50 ml) (352070)	Corning Inc., Amsterdam, NL
Surgical gloves (latex free)	Paul Hartmann AG, Heidenheim, DE
MagPlex® - C Microspheres	Luminex® corporation, Texas, US
MagPlex® Beads	Luminex® corporation, Texas, US
Microcentrifuge tubes (0.5 ml, 1.5 ml, 2 ml)	Sarstedt AG & Co. KG, Nümbrecht, DE
Microcentrifuge tubes 1.5 ml (protein low binding)	Eppendorf AG, Hamburg, DE
Microplate, 96-well, black (655077) (ELISA)	Greiner Bio-One GmbH, Frickenhausen, DE
Monolith NT.115 Standard Capillaries	NanoTemper Technologies GmbH, Munich, DE
Nunc-Immuno module (469914) (ELISA)	ThermoFisher, Massachusetts, US
Nunc-Immuno plate, Maxisorp, 96-well (439454) (ELISA)	ThermoFisher, Massachusetts, US
Nunclon Delta Surface, 96-well (167008), 12-well (150628), 6-well (140675) (cell culture)	ThermoFisher, Massachusetts, US
Pipette tips	Eppendorf AG, Hamburg, DE
Polyethylene-10 catheter	Portex, Grasbrunn, DE
PVDF- membrane (Immobilon®- FL)	Merck Millipore, Massachusetts, US
Reaction tube (15 ml) (62.554.502)	Sarstedt AG & Co. KG, Nümbrecht, DE
Serological pipettes (5 ml, 10 ml, 25 ml)	Sarstedt AG & Co. KG, Nümbrecht, DE
Syringe filter (0.2 µm)	Sartorius AG,Göttingen, DE
Syringes (50 ml)	Braun, Melsungen, DE
Whatman®- Paper	Carl Roth GmbH & Co. KG, Karlsruhe, DE

2.3. Chemicals and reagents

Chemicals and reagents	Manufacturer
1-ethyl-3-(3-dimethylaminopropyl) carbodiimide (EDC)	ThermoFisher Scientific, Massachusetts, US
2-(N-morpholino)ethanesulfonic acid (MES)	Sigma-Aldrich, Missouri, US
5× Gel loading buffer	Sigma-Aldrich, Missouri, US
Acetic acid	Sigma-Aldrich, Missouri, US
Acrylamide/bisacrylamide 40% (w/v) (29:1)	AppliChem GmbH, Darmstadt, DE
Ac-VEID-AMC (substrate for SplB neutralization assay)	PeptaNova GmbH, Sandhausen, DE
Agarose	ThermoFisher Scientific, Massachusetts, US
Amido black 10B dye	Sigma-Aldrich, Missouri, US
Ammonium persulfate (APS)	Serva Electrophoresis GmbH, Heidelberg, DE
Ammonium sulfate	Sigma-Aldrich, Missouri, US
Anti-Fibrinogen antibody (HRP) (ab10068)	Abcam, Cambridge, UK
Anti-Fibronectin antibody (HRP) (ab207628)	Abcam, Cambridge, UK
Anti-mouse kappa LC-PE	Merck Millipore, Massachusetts, US
Anti-mouse lambda LC-PE	Merck Millipore, Massachusetts, US
BD opteia TMB Substrate Reagent Set	BD Biosciences, Heidelberg, DE
Binding buffer NT1	Macherey–Nagel, Düren, DE
Boric acid	Sigma-Aldrich, Missouri, US
Bovine serum albumin	Sigma-Aldrich, Missouri, US
Bromophenol blue	Sigma-Aldrich, Missouri, US
CANDOR Low cross buffer	CANDOR Bioscience GmbH, Wangen, DE
Coomassie brilliant blue G250	Merck KGaA, Darmstadt, DE
Dimethylsulfoxid (DMSO)	Sigma-Aldrich, Missouri, US
Dithiothreitol (DTT)	ThermoFisher Scientific, Massachusetts, US
Elution buffer NE	Macherey–Nagel, Düren, DE
Ethanol (ETOH, 96%, v/v)	Carl Roth GmbH & Co. KG, Karlsruhe, DE
Ethylenediaminetetraacetic acid (EDTA)	Sigma-Aldrich, Missouri, US
Fetal calf serum (P30-3306)	PAN Biotech, Aidenbach, DE
Fibrinogen (human plasma) (341576)	Merck KGaA, Darmstadt, DE
Fibronectin (human plasma) (F2006)	Sigma-Aldrich, Missouri, US
FITC-dextran	Sigma-Aldrich, Missouri, US
Gel loading buffer (western blot)	Sigma-Aldrich, Missouri, US
GeneRuler 100 bp DNA ladder	ThermoFisher Scientific, Massachusetts, US
Glycerol (50%, v/v)	Sigma-Aldrich, Missouri, US
Glycine	Sigma-Aldrich, Missouri, US
Goat Anti-Mouse IgG(H+L)-HRP (Cat. No.1036-05)	Southern Biotech, Alabama, US
HRP conjugation kit (ab102890)	Abcam, Cambridge, UK

Hydrochloric acid (HCL)	Sigma-Aldrich, Missouri, US
Igepal CA–630	Sigma-Aldrich, Missouri, US
Isopropanol	Merck KGaA, Darmstadt, DE
Magnesium chloride	Sigma-Aldrich, Missouri, US
Methanol (100%)	Carl Roth GmbH & Co. KG, Karlsruhe, DE
Milk powder	Bio-Rad Laboratories, California, US
Milli-Q H_2O	Merck Millipore, Massachusetts, US
N,N,N′,N′-tetramethylethylendiamine (TEMED)	GE Healthcare GmbH, Solingen, DE
N-hydroxysulfosuccinimide sodium salt (sulfo-NHS)	ThermoFisher Scientific, Massachusetts, US
Pancoll human	PAN Biotech, Aidenbach, DE
Penicillin (10,000 U/ml)/ Streptomycin (10,000 µg/ml) /L-Glutamine (29.2 mg/ml) (10378-016)	ThermoFisher Scientific, Massachusetts, US
Phosphate-buffered saline (DPBS) (P04-36050P)	PAN biotech, Aidenbach, DE
Phosphate-buffered saline (DPBS) (P04-36500)	PAN biotech, Aidenbach, DE
Phosphoric acid	Sigma-Aldrich, Missouri, US
Proclin300	Sigma-Aldrich, Missouri, US
Protein G sepharose® 4 fast flow	GE Healthcare, Illinois, US
Proteinmarker VI (prestained)	AppliChem GmbH, Darmstadt, DE
Redsafe nucleic acid staining solution	JH Science / iNtRON Biotechnology, Washington, US
RNase away	Carl Roth GmbH & Co. KG, Karlsruhe, DE
RNasin® plus ribonuclease inhibitor	Promega, Wisconsin, US
Roti®-Quant solution	Carl Roth GmbH & Co. KG, Karlsruhe, DE
R-Phycoerythrin AffiniPure $F(ab')_2$ Fragment Goat Anti-Human IgG (H+L) (109-116-088)	Jackson ImmunoResearch, Cambridgeshire, GB
RPMI 1640 (w/o: L-Glutamine, w: 2 g/l $NaHCO_3$) (P04-17500)	PAN Biotech, Aidenbach, DE
Sheath fluid	Bio-Rad Laboratories, California, US
Sodium chloride	Carl Roth GmbH & Co. KG, Karlsruhe, DE
Sodium dihydrogen phosphate	Sigma-Aldrich, Missouri, US
Sodium dodecyl sulfate (SDS)	Carl Roth GmbH & Co. KG, Karlsruhe, DE
Sodium hydroxide	Carl Roth GmbH & Co. KG, Karlsruhe, DE
Sodium phosphate	Carl Roth GmbH & Co. KG, Karlsruhe, DE
Sulfuric acid	Sigma-Aldrich, Missouri, US
Superscript™ IV Reverse Transcriptase	ThermoFisher Scientific, Massachusetts, US
Supersignal™ West Femto Maximum Sensitivity Substrate	ThermoFisher Scientific, Massachusetts, US
Tetanus-Toxoid	State Serum Institute, Copenhagen, DK
TiterMax Gold Adjuvant	Sigma-Aldrich, Missouri, US
Trichloroacetic acid (TCA)	Carl Roth GmbH & Co. KG, Karlsruhe, DE
Tris-base	Carl Roth GmbH & Co. KG, Karlsruhe, DE
Tris-Buffered Saline	Sigma-Aldrich, Missouri, US

Tris-Hydrochloride	Sigma-Aldrich, Missouri, US
Trypan blue solution	Dr. K. Hollborn & Söhne GmbH & Co. KG, Leipzig, DE
Tween 20	Bio-Rad Laboratories, California, US
UltraPure™ DNase/RNase-Free Distilled Water (PCR water)	Invitrogen, Massachusetts, US
Wash buffer NT3	Macherey–Nagel, Düren, DE
β-Mercaptoethanol (≥ 99%)	Sigma-Aldrich, Missouri, US

2.4. Softwares and databases

Software / database	Manufacturer
Bio Plex® Manager 5.0	Bio-Rad Laboratories, California, US
Biorender 2021	(https://biorender.com/) BioRender, California, US
ChromasPro 2.1	(http://technelysium.com.au/wp/chromaspro/) Technelysium Pty Ltd. South Brisbane, AU
Citavi 6	(https://www.citavi.com/en) Swiss Academic Software, Wädenswil, CH
GraphPad Prism 7.0	(https://www.graphpad.com/) GraphPad Software Inc., California, US
i–Control 1.10	Tecan, Mannerdorf, CH
IgBlast	(https://www.ncbi.nlm.nih.gov/igblast/) National Institutes of Health, Maryland, US
ImageJ 1.52a [187]	National Institutes of Health, Maryland, US
ImMunoGeneTics [188]	http://www.imgt.org/IMGT_vquest/input
Microsoft Office 2016	Microsoft Corporation, Redmond ,US
MO Affinity Analysis 2.3	NanoTemper Technologies GmbH, Munich, DE
MO Control software 1.6	NanoTemper Technologies GmbH, Munich, DE
MultAlin [189]	http://multalin.toulouse.inra.fr/multalin
SIB ExPASy [190]	SIB Swiss Institute of Bioinformatics, Lausanne, CH
SnapGene Viewer 5.0.7	SnapGene software (from Insightful Science; available at snapgene.com)
UniProt [191]	European Bioinformatics Institute (EBI), the Swiss Institute of Bioinformatics (SIB), and the Protein Information Resource (PIR)
xMAPr	https://michalik.shinyapps.io/xMAPr_app/

2.5. Kits

Kits	Manufacturer
Accuprime Taq DNA Polymerase System (200 reactions)	ThermoFisher Scientific, Massachusetts, US
dNTPs 100 mm Solutions	ThermoFisher Scientific, Massachusetts, US
Mix2seq kit	Eurofins Genomics, Kentucky, US

Mouse Immunoglobulin isotyping Magnetic Bead Panel 96–well Plate Assay	Merck Millipore, Massachusetts, US
NucleoSpin™ Gel and PCR clean up	Macherey-Nagel, Düren, DE
Protein Labeling Kit RED-NHS 2nd Generation (Amine Reactive)	NanoTemper Technologies GmbH, Munich, DE
RNeasy mini kit	Qiagen GmbH, Hilden, DE
Superscript™ IV first-strand synthesis system	ThermoFisher Scientific, Massachusetts, US

2.6. Proteins

Protein	Abbreviation	Cloned gene	Stock conc.	Molecular weight (kDa)	N-Terminus Tag	Expression system
Serine protease–like protein B	SplB	*S. aureus* NCTC8325	1-5	26	HisTag	*E. coli BL21*
Clumping factor A	ClfA	*S. aureus* NCTC8325	0.92	97	HisTag	*E. coli BL21*
Fibronectin binding protein A	FnBPA	*S. aureus* NCTC8325	1.03	105.2	HisTag	*E. coli BL21*

The GMO *E. coli* strains harbouring the vectors encoding the above-listed N-terminal His-tag proteins were kindly provided by Tanja Meyer at the Interfaculty Institute for Genetics and Functional Genome Research, University of Greifswald. All proteins lacked the signal peptide and LPXTG anchor. Recombinant proteins were produced and purified by members of our research group, including Nico Wittmann, Daniel Mrochen, Juan José Izquierdo González, Jawad Iqbal, and Dr. Darisipudi Venkata Murthy. Since the stock concentrations of the proteins were different, the working stocks were prepared by diluting the proteins either in PBS or water and used for the experiments described in the material and methods sections.

2.7. Solutions, media, and buffers

2.7.1. Cell culture and freezing medium

R20F	
RPMI 1640	394.5 ml
Fetal calf serum	100 ml
Penicillin/ Streptomycin/L-Glutamine (ThermoFisher Scientific)	5.5 ml

Freezing medium	
Fetal calf serum	9.25 ml
DMSO	0.75 ml

2.7.2. Buffers used for antibody purification

Washing buffer	
Sodium phosphate (20mM)	2.84 g
Milli-Q H_2O	*ad* 1 l

Elution buffer	
Glycine	3.8 g
Milli-Q H_2O	*ad* 500 ml
Adjust to pH 2.8	

2.7.3. B-cell receptor sequencing

Gel electrophoresis of PCR products

5× TBE	
Tris-base	54 g
Boric acid	27.5 g
EDTA	3.75 g
Milli-Q H_2O	*ad* 1 l

Running buffer	
TBE	1×
Redsafe	20 µl

Agarose gel	
Agarose	1.2 g
TBE (1×)	80 ml
Redsafe	2.3 µl

2.7.4. ELISA

10× PBS	
PBS	191 g
Milli-Q H_2O.	*ad* 2 l

Wash buffer	**Final conc. (FC)**
PBS	2 l (1×)
(v/v) Tween 20	1 ml (FC: 0.05%)

Blocking buffer (1%, w/v)	
Bovine serum albumin (BSA)	0.5 g
Wash buffer	*ad* 50 ml

2.7.5. Inhibition assay

Fibrinogen solution	
Fibrinogen (stock solution: 4.1 mg/ml)	4.87 µl (FC: 20 µg/ml)
Blocking buffer (2.7.4)	1 ml
Fibonectin solution	
Fibronectin (stock concentration: 1 mg/ml)	2.5 µl (FC: 0.25 µg/ml)
Blocking buffer (2.7.4.)	10 ml

2.7.6. Substrate assay (SplB)

Stock solution of the substrate	
Ac-VEID-AMC	5.5 µl
PBS	*ad* 2 ml

Working solution	
Stock solution of Ac-VEID-AMC	10 µl
SplB	0.5 µg
Anti-SplB mAb	(1:1, 1:2, 1:5) (SplB: Anti-SplB mAb)

2.7.7. Microscale thermophoresis (MST)

Assay buffer	
PBS	2 l
(v/v) Tween 20	1 ml (FC: 0.05%)

MST buffer	
Tris-HCl (pH 6.8)	3.02 g (FC: 50 mM)
$MgCl_2$ (10 mM)	0.476 g (FC: 10 mM)
NaCl	4.38 g (FC: 150 mM)

Milli-Q H_2O	*ad* 500 ml

2.7.8. SDS-PAGE

APS (10%, w/v)	
Ammonium persulfate (APS)	1 g
Milli-Q H_2O	*ad* 10 ml

Tris-HCl (0.5 M; pH 6.8; 0.4% SDS)	
Tris-Base	60.57 g
SDS (20% w/v)	20 ml
HCl	adjust pH to 6.8
Milli-Q H_2O	*ad* 1 l

Tris-HCl (1.0 M; pH 6.8; 0.4% SDS)	
Tris-Base	121.1 g
SDS (20%)	20 ml
HCl	adjust pH to 6.8
Milli-Q H_2O	*ad* 1 l

Tris-HCl (1.5 M; pH 8.8; 0.4% SDS)	
Tris-Base	181.7 g
SDS (20%)	20 ml
HCl	adjust pH to 6.8
Milli-Q H_2O	*ad* 1 l

SDS-sample buffer (5×), reducing	
1 M Tris-HCl (pH 6.8)	0.6 ml
SDS (10% w/v)	2 ml
Glycerol (50% v/v)	5 ml
Bromophenol blue (1% w/v)	1 ml
β-Mercaptoethanol	0.5 ml
Milli-Q H_2O	0.9 ml

SDS-PAGE-running buffer (10×)	
Tris-Base	30 g
Glycine	144 g
SDS	10 g
Milli-Q H_2O	*ad* 1 l

Separation gel (12%)	
1.5 M Tris-HCl (pH 8.8)	3 ml
Acrylamide/Bisacrylamide (40% w/v)	3.6 ml
APS (10% w/v)	100 µl

TEMED	10 µl
Milli-Q H_2O	5.4 ml

Stacking gel (4%)

0.5 M Tris-HCl (pH 6.8)	1.25 ml
Acrylamide/Bisacrylamide (40% w/v)	0.5 ml
APS (10% w/v)	30 µl
TEMED	7 µl
Milli-Q H_2O	3.2 ml

Coomassie staining solution

Methanol (100%)	200 ml
Phosphoric acid (80%, w/v)	118 ml
Ammonium sulphate	100 g
Coomassie Brilliant Blue G250	1.2 g
Milli-Q H_2O	*ad* 1 l

2.7.9. Dot blot and western blot

Transfer buffer (pH ≤ 8.5)

Tris-Base	3.025 g
Glycine	15 g
Methanol (100%)	200 ml
HCl	for pH correction
Milli-Q H_2O	*ad* 1 l

TBS (10×), pH 7.6

Tris-Base	24.2 g
NaCl	80 g
HCl	for pH correction
Milli-Q H_2O	*ad* 1 l

TBST

TBS (1×)	1 L
(v/v) Tween 20	1 ml (FC: 0.05%)

Blocking buffer (0.5%, w/v)

TBST	100 ml
Milk powder	5 g

Amido black

Amido Black 10B dye	0.1 g
Methanol	40 ml
Acetic acid	10 ml

Milli-Q H_2O	*ad* 100 ml

2.7.10. Infection array

Block store buffer without ProClin300	
BSA	0.1 g
PBS	10 ml
Bead buffer (with BSA)	
Block store buffer without ProClin300	250 ml
CANDOR Low cross buffer	250 ml
Block store buffer with ProClin300	
BSA	1.2 g
ProClin300	60 µl
PBS	120 ml
Activation buffer	
Sodium dihydrogen phosphate (NaH_2PO_4)	1.2 g (100 mM)
Milli-Q H_2O	100 ml
	adjust pH to 6.2
EDC solution (pro bead region)	
1-ethyl-3-(3-dimethylaminopropyl)carbodiimide (EDC)	2.5 mg
Milli-Q H_2O	50 µl
Coupling buffer	
2-(N-morpholino)ethanesulfonic acid (MES)	1.066 g (FC: 50 mM)
Milli-Q H_2O	100 ml
	adjust pH to 6.2
sulfo-NHS solution (pro bead region)	
N-hydroxysulfosuccinimide sodium salt (sulfo-NHS)	2.5 mg
DMSO	50 µl
Extracellular proteins (ECPs) and tetanus toxoid (TT) coupled to the beads	
ECPs	10 mg/ml (stock sol.)
	0.5 mg/ml (working sol.)
TT	1.96 mg/ml (stock sol.)
	0.25 mg/ ml (working sol.)
Wash buffer	
PBS	2000 ml
(v/v) Tween 20	1 ml (FC: 0.05%)

3. Methods

3.1. Analyzing pathogen-specific antibody responses using the infection array

The main aim of the study was to study the pathogen-specific antibody response and the immune memory against different pathogens in infectious endocarditis (IE) patients.

The Greifswald Infectious Endocarditis Study (GIES) was conducted between 07/2018 and 05/2019. At first, GIES was designed to test the Real-time deformability cytometry (RT-DC) as a tool for diagnosing IE. RT-DC is a microfluidic technique, co-founded by Dr. Oliver Otto (Universität Greifswald, Greifswald), to capture and analyze the morphology and rheology of up to 1000 cells in a microfluidic channel. Through this method, different subpopulations of cells in the whole blood can be studied together [192]. The study was extended at later stages to include the analysis of the antibody response in IE patients, with follow-up samples collected at d14-d200 after diagnosis. Follow-up samples were collected from 7 patients, while plasma (additional biosamples) from 8 patients were provided by the Institute of Clinical Chemistry and Laboratory Medicine. These samples were collected between d-7 to -1 before IE diagnosis and d1 to d21 after diagnosis. GIES comprises 17 IE patients and 20 controls, i.e., patients with non-infectious heart-related conditions. IE in the patients was confirmed by ultrasound, and pathogens isolated after BC were stored for later analysis. After diagnosis (d0), around 25 ml EDTA blood were obtained for PBMC and plasma isolation. PBMCs were used to analyze pathogen-specific B cell response for another study (discussed in section 5.1.3.2), while plasma samples were analyzed in this study.

The tool used to study the pathogen-specific immune response and immune memory is the infection array, which is a multiplex suspension bead array that is based on the xMAP® technology (Luminex®). Antigens are covalently coupled to magnetic particles (MagPlex® Beads) and incubated with patient serum or plasma samples. The bound antibodies can then be detected with a phycoerythrin (PE)-conjugated detection antibody and quantified using the fluorescence signal.

The infection array as a high-throughput screening method was established in our research group by Dr. Nicole Normann [44] and Dr. Dina Raafat. In this work, we used a 33-plex infection array panel containing the extracellular proteins (ECP) of 30 different pathogens (2 different strains of *S. aureus* and *P. aeruginosa* are added), as well as the control tetanus

toxoid (TT) antigen (Table 1). The cultivation of the various pathogens, the purification of their ECP through TCA (trichloroacetic acid) precipitation as well as the ECP quantification using the BCA kit were conducted by Dr. Dina Raafat and Fawaz Al'Sholui. The principle of the infection array is explained in Figure 2.

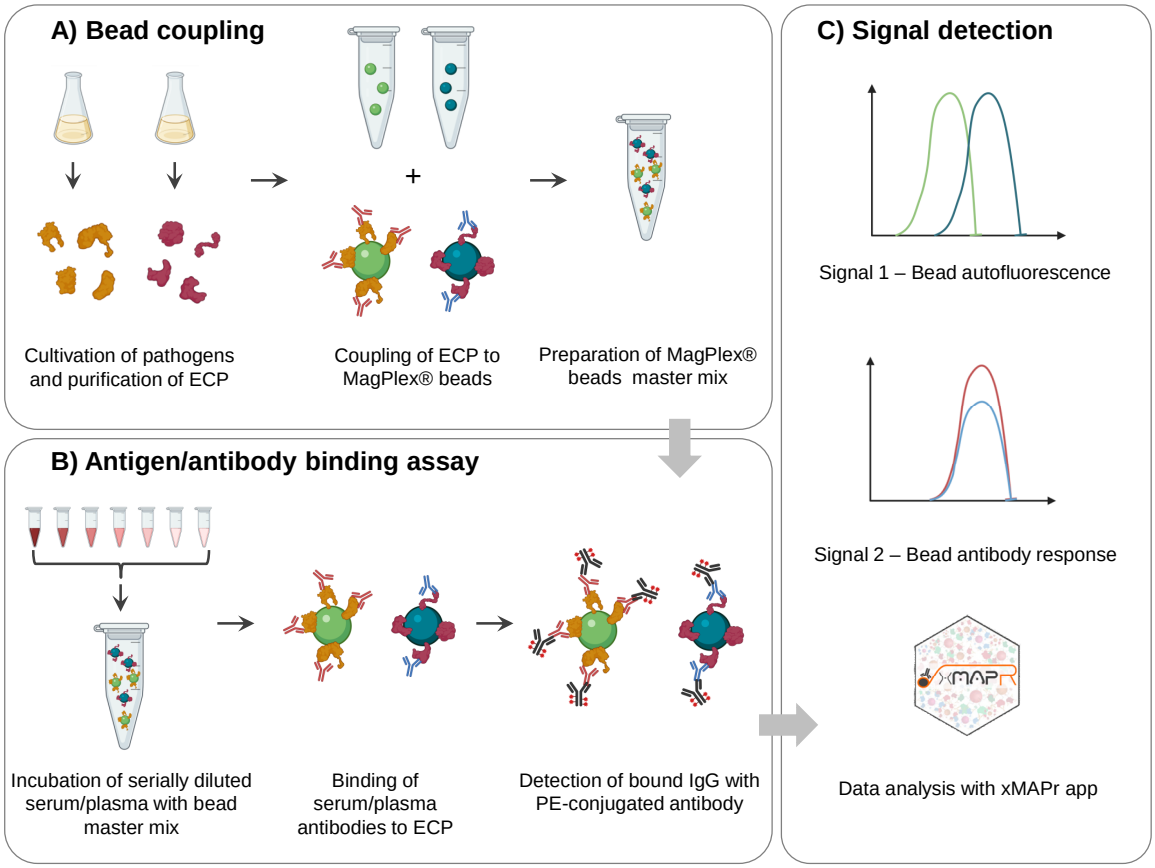

Figure 2. Principle of infection array 33-plex. Infection array 33-plex, which is a bead-based suspension array, was used as a tool to study the pathogen-specific immune response in IE patients sera/plasma samples. (a) The pathogens added to the infection array were cultivated, and the ECP were collected at the stationary phase. Afterwards, the ECP were bound to MagPlex® beads with different autofluorescence. All the beads with ECP from different pathogens were collected in a storage buffer to prepare a bead master mix. (b) For antigen-antibody binding assay, the serum/plasma was serially diluted and incubated with the master mix to allow IgG binding to the respective ECP. Bound IgG was detected using PE-conjugated antibody. (c) The signal detection was performed in two steps by using BioPlex® 200. In the first step, the autofluorescence of the MagPlex® beads was determined, which is characteristic of the pathogens because of its ECP bound to the bead. In the second step, the fluorescence intensity of the bound detection antibody was determined, which would help determine the sera/plasma antibody binding to the ECP (adapted from Normann, 2021). This image is generated by using BioRender.

3.1.1. Coupling of extracellular proteins to magnetic beads

3.1.1.1. Washing the magnetic beads

Coupling ECP and control antigen (TT) to the magnetic beads (MagPlex® beads, Luminex®) by covalent bonds is one of the crucial steps in the infection array, which has previously been described in detail [44]. Briefly, the bead stock solutions (1 ml) were vortexed for 30 seconds (sec) at room temperature (RT), placed in the ultrasonic bath for 3 minutes (min), and then vortexed again for 30 sec. Then, the bead stock solutions (1 ml of each bead region) were

transferred to the respective 1.5 ml protein low binding reaction tube. To discard the bead storage buffer, the reaction tubes were placed onto a magnetic stand (DynaMag™ -2 magnet, Thermo Fisher Scientific) for 3 min to allow the beads to adhere to the wall of the reaction tubes, and the buffer was carefully removed by pipetting. Afterwards, the beads were washed 3× (following the same washing technique and steps as described above) each with 400 µl of activation buffer per reaction tube to adjust the pH value to 6.8, which is required for the subsequent activation reaction.

3.1.1.2. Bead activation

Before coupling the ECPs and TT, the beads were activated by adding 50 µl 1-Eethyl-3-(3-dimethylaminopropyl)carbodiimide (EDC) solution and 50 µl N-hydroxysulfosuccinimide (sulfo-NHS) solution to each bead region, and the reaction tubes were incubated in the dark for 20 min at RT on a shaker at 900 rpm. The addition and subsequent reaction of EDC and sulfo-NHS activate the carboxyl groups of the beads, and a sulfo-NHS ester intermediate is produced. This semi-stable intermediate is replaced with primary amines from the ECP, leading to a covalent amide bond between the beads and ECP, the details of which are explained in the next section.

3.1.1.3. Coupling proteins to the beads

After activating the beads, the next step was to couple the desired proteins to it. For this purpose, the beads were washed 3× each with 500 µl coupling buffer, as explained above. The proteins to be coupled (ECPs and TT), which were dissolved in 5% SDS buffer for rehydration after purification, were diluted in the coupling buffer to the desired concentration (Table 1). Then, the washed beads were mixed with 1 ml protein solution (final conc.: 0.5 mg/ml for ECPs; 0.25 mg/ml for TT) and incubated in the dark at RT for 2 hours (h) at 900 rpm. After incubation, the beads were washed 6× with wash buffer to remove all traces of SDS from the surface of the beads. SDS should be removed because it will reduce the binding of proteins to the beads. Finally, the respective beads were resuspended in 10 ml block store buffer (with ProClin300) and transferred to 15 ml protein low bind centrifugation tubes (2.7.10). Proclin 300 is a biocide used for controlling microbial growth in reagents and products in diagnostic tools. The protein-coupled beads were stored overnight at 4°C. Finally, as the beads were later used in a multiplex assay, all 33 bead regions were pooled into a bead master mix. The bead master mix was adjusted to 1,250 beads/50 µl/bead region and was aliquoted and stored at 4°C until further use.

Table 1. List of microbial species targeted by the infection array 33-plex.

No	Species/Proteins*	Isolate/Batch	Source	Natural habitat	IE	PJI	SE	PN	Bead region (BR)	Lot. No
Gram-positive bacteria (rods)										
1	*Corynebacterium striatum*	DSM 20668	Type strain	Nose	●	●	●	●	35	B67629
2	*Cutibacterium acnes*	DSM 1897	Type strain	Skin	●	●			37	B61756
Gram-positive bacteria (cocci)										
3	*Staphylococcus aureus*	USA300Δ*spa*Δ*hla*	Clinical isolate; laboratory strain	Nose	●	●	●	●	8	B64927
4	*S. aureus subsp. aureus*	NCTC 8325Δ*spa*	IE patient	Nose	●	●	●	●	13	B61351
5	*Staphylococcus epidermidis*	RP62A	Biofilm-producing MRSE strain	Skin	●	●	●	●	15	B64949
6	*Staphylococcus haemolyticus*	DSM 20263	Type strain, human skin	Skin	●	●	●	●	19	B65772
7	*Staphylococcus hominis*	DSM 20328	Human skin	Skin	●	●	●	●	22	B64499
8	*Staphylococcus lugdunsensis*	SL0902	Clinical isolate; pneumonia	Skin	●		●	●	26	B68496
9	*Staphylococcus warneri*	DSM 20316	Type strain	Skin	●		●		28	B63685
10	*Enterococcus faecalis*	ATCC 29212	Urine	Gut	●	●	●	●	30	B62542
11	*Enterococcus faecium*	ATCC 51559	Clinical isolate, Brooklyn, NY	Gut	●	●	●	●	33	B67638
12	*Streptococcus pneumoniae*	TIGR4Δ*cps*	Type strain	Respiratory tract	●	●	●	●	39	B67628
13	*Streptococcus mitis*	DSM 12643	Oral cavity, human	Respiratory tract	●				42	B67367
14	*Streptococcus oralis*	DSM 20627	Human mouth	Respiratory tract	●				44	B65123
15	*Streptococcus sanguinis*	DSS-10	Subacute bacterial endocarditis	Respiratory tract	●		●		46	B69173
16	*Streptococcus gallolyticus*	CCUG 35224T	Koala, feces; Australia	Gut	●		●		48	B70233
17	*Clostridioides difficile*	DSM 27147	Type strain	Gut	●	●	●		51	B70689
Aerobic Gram-negative bacteria (bacilli)										
18	*Haemophilus influenzae*	DSM 24049	Human sputum; pneumonia	Respiratory tract	●		●	●	53	B71686
19	*Klebsiella aerogenes*	DSM 30053	Type strain; sputum	Gut	●	●	●	●	55	B64369
20	*Klebsiella pneumoniae*	ATCC 700721	Sputum	Respiratory tract, Gut, Skin	●	●	●	●	57	B68150
21	*Klebsiella oxytoca*	DSM 5175	Pharyngeal tonsil	Gut	●	●	●	●	59	B75054
22	*Enterobacter cloacae*	DSM 30054	Type strain; spinal fluid	Gut	●	●	●	●	62	B64652
23	*Escherichia coli*	ATCC 47076	Transformation host	Gut	●	●	●	●	66	B65692
24	*Proteus mirabilis*	DSM 4479	Clinical isolate	Environment	●	●	●	●	64	B69678
25	*Serratia marcescens*	DSM 30121	Pond water	Environment	●	●	●	●	68	B78022
Non-lactose fermenting Gram-negative bacteria (bacilli)										
26	*Pseudomonas aeruginosa*	PAO1	Type strain; wound infection	Skin, Environment	●	●	●	●	73	B65125
27	*Pseudomonas aeruginosa*	PA6077	PA6077	Skin, Environment	●	●	●	●	90	B63814
28	*Acinetobacter baumannii*	DSM 105126	CSF, fatal meningitis	Environment (Hospital)	●	●	●	●	75	B61839
29	*Stenotrophomonas maltophilia*	SM1404	Clinical isolate; pneumonia	Environment	●	●	●	●	77	B64776
Atypical bacteria										
30	*Legionella pneumophila*	DSM 25061	Respiratory tract secretions	Environment	●	●		●	82	B68631
Gram-negative bacteria (cocci)										
31	*Moraxella catarrhalis*	DSM 9143	Type strain	Respiratory tract	●	●	●	●	84	B64058
Yeast										
32	*Candida albicans*	SC5314	Human clinical isolate	Gut	●	●	●	●	86	B68485
Tetanus Toxoid										
33	Tetanus Toxoid	SSI							88	B63308

* ECPs of species involved in multiple infections (IE, PJI, SE, PN) were coupled to different bead regions, and then a master mix of the beads was used in the infection array 33-plex.
Abbreviations: IE, Infective Endocarditis; PJI, Prosthetic Joint Infection; PN, Pneumonia; SE, Sepsis; SSI, State Serum Institute, Copenhagen, Denmark
Amount of ECP of each pathogen used: 0.5 µg Protein/1 µl Bead stock solution. Amount of TT used: 0.25 µg Protein/1 µl Bead stock solution. ● Pathogen involved in infection (Table adapted from Dr. Dina Raafat)

3.1.2. Antigen-antibody binding assay

The next step was the antigen-antibody binding assay, for which the bead master mix was first thoroughly resuspended as described above (vortexing, sonication, and vortexing), and then 50 µl aliquots were transferred into each well of an assay plate (96-well half area microplates, Greiner Bio-One).

Seven serial 1:5 dilutions of the serum and plasma samples were prepared in bead buffer (with BSA), starting from a 1:20 dilution. Additionally, a reference serum pool of healthy donors, Bioreclamation IVT Human Serum (Bioivt & Elevating Science), was used for normalization. The assay plate was placed on the magnetic 96-well separator for 3 min to allow the beads to settle, and then the liquid was discarded by inverting the plate while attached to the magnet. After transferring 50 µl each of the serum/plasma dilutions into the assay plate, it was sealed with adhesive aluminum foil to ensure protection from light and then incubated in the dark at 4°C on a shaker at 900 rpm. After 18 h of incubation, the beads were washed 3× with 100 µl wash buffer per well. Then, 50 µl of the detection antibody (R-Phycoerythrin AffiniPure $F(ab')_2$ Fragment Goat Anti-Human IgG (H+L)) (final concentration: 5 µg/ml) were added to each well, and the microtiter plate was incubated for 1 h at RT on a shaker at 900 rpm. Afterwards, the beads were washed 3× each with 100 µl wash buffer and finally resuspended in 100 µl sheath fluid for 1 min, shaking at 900 rpm. The measurement was carried out on the BioPlex® 200 (measurement settings: bead type: MagPlex® beads; beads: 100 per bead region; sample timeout: 60 sec; sample volume: 80 µl; gate settings: 8,000-20,000) and data was retrieved by using Bio Plex® Manager 5.0 software.

3.1.3. Analysis of the infection array data

For analyzing the data generated from the infection array, the xMAPr® app was used, which performs multiple regression modeling on the data of each sample/antigen combination and calculates a Median Fluorescence Intensity (MFI) value at the end. Meyer et al. explained the process of generating MFI values in detail [193]. The xMAPr app was developed by Dr. Stephan Michalik from the Interfaculty Institute for Genetics and Functional Genome Research, University of Greifswald (https://michalik.shinyapps.io/xMAPr_app/) [193].

After generating the MFI, the final antibody response levels were calculated as the product of the dilution factor at the half-maximal MFI and the half-maximal MFI itself, as explained before [44, 193].

$$Antibody\ level = \frac{MFI\ max}{2} \times dilution\ factor \left(\frac{MFI\ max}{2}\right)$$

Finally, the increase in antigen-specific antibodies during the course of infection was measured. For determining the increase, the fold-change was calculated from the antibody level of the latest (follow-up samples) and earliest (d0 or retention samples) available serum/plasma samples.

$$Fold\text{-}change\ in\ antibody\ levels = \frac{Antibody\ level\ (follow\text{-}up\ samples)}{Antibody\ level\ (d0\ or\ retention\ samples)}$$

The infection array includes a wide range of microbes such as commensals, opportunistic and true pathogens. However, for ease in data interpretation and communication, the term "pathogen" was used in the entire thesis.

3.1.4. Statistics

The statistical evaluation of the infection array data was carried out with GraphPad Prism 6. The comparison of age, CRP, ALAT, ASAT, leukocytes, WBC, RBC, and heart frequency between controls and IE patients was analyzed by using an unpaired t-test. $p < 0.05$ was considered statistically significant. A two-sided Chi-square test was used to compare the sex of control and IE patients, and $p < 0.05$ was considered statistically significant. For comparing the basal antibody levels against the pathogens between control and IE patients, a mean value was first calculated for each study participant, and then the Shapiro-Wilk test was used to assess the normality of data distribution with $p < 0.05$ as a threshold for data set not following the normal distribution. In normally distributed data sets, an unpaired t-test was used to compare the antibody increases against each pathogen in controls and IE patients, and $p < 0.05$ was considered significant. The kinetics of the pathogen-specific antibody response was also analyzed. For determining a threshold of increase, the ratios of all the calculated response values from all the patients against the pathogens were taken, and then the median + 3× interquartile range (IQR) was calculated. This led to a threshold value of 2.0, meaning that a more than 2-fold increase in antibody titers was considered to be meaningful.

3.2. Characterization of monoclonal antibodies

For the production of murine and humanized monoclonal antibodies (mAbs), the antibody-producing hybridomas were generated and kindly provided by Nico Wittmann [194], Daniel Mrochen, and Dr. Dina Raafat. In short, intraperitoneal (i.p.) immunization of male C57BL/6 mice was carried out on day 0 (d0), d21, and d42 with 100 µg, 50 µg, and 30 µg, respectively, of the target proteins (SplB, ClfA, and FnBPA) (2.6) in 100 µl isotonic sodium chloride which was supplemented with the same amount (100 µl) of adjuvant (TiterMax Gold Adjuvant, Sigma-Aldrich). Booster immunization was performed on d63 with 10 µg antigen with no adjuvant. After 66 days, the animals were sacrificed, and the spleen was removed in a sterile manner. Then, splenocytes were isolated from the spleen and fused with myeloma cells (P3X63Ag8.653) to generate antibody-producing hybridomas. After cell fusion, the hybridoma cells were selected and tested for IgG production via ELISA. The IgG-producing hybridomas were frozen in the freezing medium (2.7.1) and stored at -80°C for future use.

For the production of the humanized FnBPA mAbs, C57BL/6 mice were used which were provided by Prof. Dr. Hans-Martin Jäck (Friedrich-Alexander-University, Erlangen-Nürnberg). Two strains of humanized C57BL/6 mice were provided: HHKK (human: variable regions of the heavy chain and the kappa light chains; murine: lambda light chain of the variable region and constant regions) and HHKKLL (human: variable region of the heavy chain, variable region of the light chains; murine: constant regions). Immunization and downstream processes were performed as described before. This Ph.D. project aimed at the characterization of the antibodies produced by the hybridomas mentioned above.

3.2.1. Subcloning of the hybridomas producing mAbs against the target proteins

For obtaining a single clone producing the desired mAbs, subcloning of the hybridomas was performed by following a protocol established in our research group. Briefly, the IgG-producing hybridoma cells were harvested, and the number of cells were counted by using a C-Chip disposable hemocytometer (NanoEntek). Cells were diluted (1:10) in Trypan Blue dye (Dr. K. Hollborn & Söhne GmbH) to check their viability and to count them on the hemocytometer. The number of cells were then adjusted to 1×10^2 cells/ml with R20F medium (2.7.1). The resuspended hybridoma cells were inoculated into the first row of a 96-well microtiter plate (Thermo Fisher Scientific) and then serially diluted 1:2 in R20F medium to a final volume of 100 µl/well (12 wells per dilution). This serial dilution is performed in such a manner to ensure that, in the end, each diluted well contains only one cell. The plate was

incubated at 37°C for 4-5 days. Using a microscope (Olympus Microscope CKX31), those wells were identified where single hybridoma cells were starting to divide since those cells would be producing mAbs originating from one and the same cell. The hybridoma cells were fed twice a week (depending on cell divisions) with R20F medium, and the culture supernatant was collected when the R20F medium turned yellow (medium changes color as pH changes due to the metabolites released by the dividing cells). The collected hybridoma culture supernatants were subjected to a rapid primary screening process using ELISA to identify and select only those hybridomas that produce antibodies of appropriate antigen specificity. Once the hybridoma clones were selected, they were further kept in culture (initially in multi-well (96, 12, 6) plates and then in tissue culture flasks) to scale up the culture volume and to collect sufficient supernatant for subsequent investigations. The culture supernatants (Table 2) were stored at -20°C until further use.

3.2.2. Purification of monoclonal antibodies

For the purification of murine mAbs from the culture supernatants, Protein-G-Sepharose resin (GE Healthcare, Munich) were used, which will bind the antibodies in the supernatants and allow their purification. To prepare a Protein G-Sepharose column, a clean glass Econo-Column® was rinsed with 20 ml of 20% (v/v) ethanol, and then the column was sealed at the bottom and filled with 1.5 ml of Protein-G-Sepharose resin (GE Healthcare. Munich). After 1 h, the resin were rinsed first with 2 ml of 20% (v/v) ethanol and then with 10 ml of washing buffer (2.7.2). Now the Econo-Column® with the Protein-G-Sepharose resin is ready to be used.

In parallel, the supernatant, collected from the antibody-producing hybridoma cells, was centrifuged (21,000 rpm, 20 min, 4°C) to remove the living cells and dead cell debris, and the supernatant was sterilized by membrane filtration. Afterwards, about 100 ml of the antibody-containing solution was pumped (Heidolph Pumpdrive 5001) through the Econo-Column® with the Protein-G-Sepharose resin at a rate of 1 ml/min. The slow flow rate allows the binding of antibodies to the sepharose resin. Unbound components were washed with 20 ml of washing buffer. To ensure that all unbound proteins from the supernatants were washed out, a few drops of the flow-through were collected. Aliquots of 10 µl of the washing fractions were mixed with 40 µl of Roti®-Quant solution to perform a Bradford assay and quantify protein concentration. The presence of proteins turns the color of the Coomassie Brilliant Blue Dye-G250 in the Roti®-Quant solution from reddish-purple to blue. The change in color is proportional to the

protein concentration. After thorough washing, the elution of the bound antibodies was carried out with 10 ml of elution buffer (2.7.2). The eluate was collected in 1 ml fractions first, and later the eluate fractions were pooled together. Afterwards, the antibody-containing eluate was transferred into a dialysis membrane (14 kDa) for re-buffering and left for dialysis overnight in 1× PBS. To determine the final concentration of the purified mAbs, the absorbance/extinction of the final antibody solution was measured on the DS-11 spectrophotometer from DeNovix (IgG: extinction coefficient E1% = 14; A280; 1g/100ml). A SpeedVac concentrator was used to concentrate the mAbs for the neutralization assay, to be able to use them in a high molar ratio without exceeding the total reaction volume. The yield of purified antibodies from the different hybridomas of SplB, ClfA, and FnBPA is listed in Table 2.

Table 2. Yield of purified mAbs from the collected supernatants of each hybridoma

Target protein	Hybridoma designation	Volume of supernatant collected [ml]	Yield of purified mAb [mg]
SplB	**G8**	3,000	48
	H7	3,000	54
	H9	3,000	49
ClfA	**001**	500	10
	002	500	19
	003	500	14.8
	004	500	10
	005	500	16.5
	006	500	12
FnBPA	**D4**	400	15.7
	E9	400	5.3

3.2.3. Isotyping of the purified monoclonal antibodies

Antibody isotyping is an essential step in the characterization of mAbs, because the isotype strongly influences the induced biological effector functions of the antibodies. For this reason, MILLIPLEX MAP (Mouse Immunoglobulin Isotyping Magnetic Bead Panel, Merck), which can be used to accurately measure mouse IgG subclasses (1, 2a, 2b, and 3), IgM and IgA, was used to identify the isotype of the purified mAbs. In principle, there are beads with different fluorescent dyes and capture antibodies, which will bind to their respective heavy chains (HC) of the sample mAb depending on its isotype. After the mAb is captured by the bead, a biotinylated detection antibody is introduced, which will bind to the light chain (LC) of the mAb. The reaction mixture is then incubated with a Streptavidin-PE conjugate, a reporter molecule, to complete the reaction on the surface of each bead.

For isotyping, the MILLIPLEX MAP kit was used according to the manufacturer's guidelines. Shortly, the microtiter plates were prepared by incubating the plates with 100 µl assay buffer (provided by the manufacturer) and left shaking in the dark for 10 min, after which the assay buffer was discarded. Then the bead solution was vortexed for 30 sec, sonicated for 15 sec, and then 18.75 µl were added to each well. To allow the binding of mAbs to the capture antibodies on the beads, the purified mAbs were diluted 1:5 in the assay buffer, and 50 µl of diluted mAbs were added to each well containing the beads and incubated at RT in the dark for 15 min on a shaker at 150 rpm. For removing the solution from each well, the plate was placed on a magnetic 96-well separator for 3 min allowing the beads to settle down, and the solution was discarded. Then the beads were washed 2× with 100 µL washing buffer (provided by the manufacturer), and the buffer was discarded, as explained above. Next, 18.75 µL of the biotinylated detection antibody, anti-mouse kappa LC-PE (κ-LC-PE), were added, and the plate was incubated on a shaker at 150 rpm in the dark for 15 min, allowing its binding to the LC of the mAb if the mAB has a kappa (κ) chain. Finally, the plates were washed as described above, and the beads were resuspended in 100 µL of sheath fluid, after which the fluorescent reporter signal was measured using BioPlex® 200 instrument (measurement settings: bead type: MagPlex®-C Microspheres; beads: 50 per bead region; sample timeout: 60 sec; sample volume: 100 µl; bead numbers: 21 (IgG1), 36 (IgG2a), 51 (IgG2b), 54 (IgG3)). The data was recorded and retrieved by using Bio Plex® Manager 5.0 software. In case no signal was detected with the κ-LC-PE antibody, the above procedure was repeated with a λ-LC-PE antibody to check for a lambda (λ) LC.

3.2.4. Sequencing of the variable regions of the heavy and light chain of the purified mAbs

To sequence the variable regions of the heavy and light chains of the generated mAbs, the ribonucleic acid (RNA) was isolated from the respective hybridomas and then reverse-transcribed into complementary DNA (cDNA). Then, a polymerase chain reaction (PCR) was performed to amplify the desired DNA sequence. The protocol used for the above-mentioned step was established in our research laboratory by using in-house techniques as well as by consulting literature [195, 196].

3.2.4.1. RNA isolation from the hybridomas

For isolating RNA from the hybridomas, the RNeasy Kit from QIAGEN was used according to the manufacturer's instructions. Shortly, a total of 1×10^6 cells were pelleted (2,000 rpm; 4 min),

mixed with 350 µL RLT buffer (provided by the manufacturer), and vortexed. The RLT buffer facilitates cell lysis while inactivating RNases, to ensure the purification of intact RNA. The cell mixture was then centrifuged at maximum speed (13,000 rpm; 3 min) to pellet down the cell debris. The RNA-containing supernatant was transferred to a new reaction tube. Then 350 µl of 70% (v/v) ethanol was added and mixed to precipitate the RNA. The RNA-containing supernatant with ethanol (700 µl) was immediately pipetted into the RNeasy mini kit column from Qiagen (collection tube with the membrane), centrifuged (15 sec at 9,000 rpm), and the flow-through was discarded. RNA binds to the membrane of the RNeasy mini spin column. To remove any contaminants, the membrane in the spin column was washed with RW1 buffer (700 µl) and then twice with RPE buffer (500 µl), with a centrifugation step (15 sec at 9,000 rpm) following each washing step, and the flow-through was discarded. For completely drying the spin column, it was centrifuged again (1 min at 9,000 rpm), and the remaining flow-through was discarded. To elute the RNA, the spin column was then placed in a new 1.5 ml RNase-free reaction tube, and 40 µl RNase-free water was pipetted onto the column and centrifuged. Finally, the RNA concentration was measured using a DS-11 spectrophotometer from DeNovix at the wavelengths of 230, 260, and 280 nm.

3.2.4.2. Complementary DNA (cDNA) synthesis

For amplification and analysis of the variable regions of the gene segments encoding the B-cell receptor (BCR), the isolated RNA was first reverse transcribed into cDNA. This was done using a viral reverse transcriptase (Rt), as well as oligo-dT primers, which bind to the poly-A tail of the mRNA and serve as the starting sequence for the process of reverse transcription.

For performing the cDNA synthesis, the Oligo-dT mix (Table 3) was prepared. Then, 3.5 µl oligo-dT Mix and 5 µl isolated RNA (between 10 pg to 5 µg) were added to each PCR reaction tube. Afterwards, the samples were hybridized for 5 min at 65°C by using a thermocycler (Thermocycler T1, Biometra) which allowed the binding of the oligo-dT to the poly-A tail of mRNA, and the samples were taken out of the thermocycler after the first hybridization step.

For the synthesis of cDNA by using dNTPs and the Superscript™ IV first-strand synthesis system, 7 µl Rt mix (Table 4) were added to each sample from the first hybridization step and was returned to the thermocycler (50°C for 20 min, 80°C for 10 min, 4°C for 10 min). RNasin® plus (a ribonuclease inhibitor) was added to both oligo-dT and Rt mixes to inhibit RNAse activity and maintain RNA integrity. Finally, the cDNA samples were stored in the refrigerator at 4°C for one day or were frozen at -20°C for more extended storage.

Table 3. Composition of the oligo-dT mix

Component	Volume/ sample [µl]
PCR water	2.8
Oligo-dT primer	0.05
Igepal CA-630 (10% v/v)	0.5
RNasin® plus (40 U/µl)	0.15
Total	3.5

Table 4. Composition of the Rt mix

Rt mix	Amount used/ sample [µl]
PCR water	2.05
5× Rt buffer	3
DTT (100mM)	1
dNTP	0.5
RNasin® plus (40 U/µl)	3.5
SuperScript™ IV	0.25
Total	10.3

3.2.4.3. Polymerase chain reaction (PCR) used to amplify the cDNA

After cDNA preparation, PCR was used to amplify the DNA. The main steps of PCR consist of denaturation, annealing, and elongation. During denaturation, the double-stranded (ds) DNA is converted into two single strands by heating the DNA. During annealing, the forward and reverse primers attach to the single strands of DNA. Lastly, elongation begins after the primers have attached, leading to the synthesis of ds DNA using the polymerase enzyme. The primers used for the PCR amplification of the cDNA are listed in Table 5.

For the amplification of the cDNA of BCR, a master mix was prepared (Table 6) by using the Accuprime Taq DNA Polymerase System kit, primers, and the cDNA. Afterwards, 45 µl of the master mix and 5 µl of the cDNA sample were mixed into each PCR reaction tube, and the samples were placed in the thermocycler (Thermocycler T1, Biometra) for the amplification reaction. The settings of the thermocycler used for amplification are mentioned in Table 7. Finally, the amplified cDNA samples were stored in the refrigerator at 4°C, or at -20°C for extended storage.

Table 5. List of primers used for the amplification of the variable region of the heavy and light chains of B-cell receptor (BCR)

Area amplified	Number	Name	Specifics	Sequence
Forward primer in the variable region				
Heavy chain	O839	VH deg	mouse and human universal VH degenerate primer, FR1	AGGTSMARCTGCAGSAGTCWGG
		msVHE	mouse and human universal VH degenerate primer, FR1	GGGAATTCGAGGTGCAGCTGCAGGAGTCTGG
Light chain	p647	mouse VK deg 2	universal primer for mouse Vκ amplification, FR1	GACATTCTGATGACCCAGTCT
	p648	mouse VK deg 1	universal primer for mouse Vλ amplification, FR1	CAGGCTGTTGTGACTCAGGAATCT
Reverse primer in the constant region				
Heavy chain	p348	IgM-inner-as	beginning of mouse constant region μ	GAAGACATTTGGGAAGGACTGACT
	p350	IgG1-inner-as	beginning of mouse constant region γ1	ATGGAGTTAGTTTGGGCAGCAGAT
	p354	IgG2b-inner-as	beginning of mouse constant region γ2b	AGGAACCAGTTGTATCTCCACACC
	p616	IgG2c-inner-as	beginning of mouse constant region γ2c	GAGCCAGTTGTACCTCCACACAC
	p614	IgG3-inner-as	beginning of mouse constant region γ3	AGGGACCAAGGGATAGACAGATG
		IgG1 reverse	beginning of mouse constant region γ1	GATCCAGGGGCCAGTGGATAG
		IgG2b reverse	beginning of mouse constant region γ2b	CACCCAGGGGCCAGTGGATAG
		IgG2a	beginning of mouse constant region γ2a	CACGCAGGGGCC AGTGGATAG
		IgG2c inner	beginning of mouse constant region γ2c	GCTCAGGGAAATAACCCTTGAC
		IgG3 inner		GCTCAGGGAAGTAGCCTTTGAC
Light chain	p355	Kappa-outer	beginning of mouse constant region κ	CTCCAGATGTTAACTGCTCATGG
	p357	mlC1-outer	beginning of mouse constant region λ1	ATCTACCTTCCAGTCCACTGTCAC
	p358	mlC23-outer	beginning of mouse constant region λ2, 3	ATTTGCCTTCCAGGCCACTGTCAC

Abbreviations: Gamma, γ; Kappa, κ, Lambda, λ

Table 6. Composition of the PCR master mix

Component	Amount used / sample [µl]
Accu PCR buffer 1	5
Forward primer	1 (for each primer)
Reverse primer	1 (for each primer)
Accu-Taq polymerase	1
PCR water	*ad* 45
Total	45

Table 7. Thermocycler settings

Cycle	Temperature [°C]	Time
Activation	95	5 min
Denaturation*	95	20 sec
Annealing*	56	30 sec
Elongation*	68	60 sec
Final elongation	68	10 min
Cooling	4	∞
**** steps repeated during 35 cycles of PCR***		

3.2.4.4. PCR product purification for sequencing

For the purification of the PCR product, agarose gel electrophoresis was performed to separate the DNA product on a gel (2.7.3). 30 µl of the PCR product were loaded on an agarose gel (1.5%) and ran in a Mini Sub DNA cell (Bio-Rad) at 100 V for 1 h. Image of the gel was taken by using GenoPlex (VWR). Next, the DNA was visualized by using UV-transilluminator (Fluo–Link). The DNA fragments of the size corresponding to the light and heavy chains (400 bp) were cut out and purified from the gel by using NucleoSpin™ Gel and PCR clean kit according to the manufacturer's manual. Shortly, the 100 mg agarose gel cut-out was mixed with 200 µl binding buffer NT1 (provided by the manufacturer) and was heated at 50°C for 10-15 min to melt and dissolve the gel. The mixture was transferred to a NucleoSpin Gel and PCR clean-up column and centrifuged (30 sec at 11,000 × *g*), allowing the DNA to bind to the silica membrane of the NucleoSpin Gel. Contaminations were removed by washing the gel twice with 700 µl ethanolic wash buffer NT3 (30 sec at 11,000 × *g*) (provided by the manufacturer). Afterwards, the pure DNA, bound to the silica membrane, was eluted under a low salt condition with 30 µl elution buffer (1 min at 11,000 × *g*) (provided by the manufacturer). Finally, the DNA concentration was measured using DS-11 spectrophotometer, and 15 µl (5 ng/µl) of the DNA sample and 2 µl (10 pmol/µl) of primer were added to the Mix2seq kit and sent to Eurofins for sequencing.

To analyze the DNA sequence, ChromasPro 2.1 was used. Comparison to the germline sequence as well as identification of different regions of the antibody and mutations were detected by using IgBlast and ImMunoGeneTics (2.4). Moreover, the comparison of DNA sequences amongst the clones was analyzed by using MultAlin. Finally, the SnapGene viewer was used to generate figures showing the DNA and amino acid sequences, as well as the different regions of the antibody (Figure 9).

3.2.5. ELISA used to analyze the binding of mAbs to the target proteins

The supernatants from the antibody-producing hybridomas as well as purified antibodies were tested for their ability to bind to the respective target proteins (SplB, ClfA, and FnBPA) by using an ELISA. High-binding 96-well microtiter plates (Nunc-Immuno plate, Maxisorp, ThermoFisher Scientific) were coated with 2 µg/ml of target protein (SplB, ClfA, or FnBPA) in 1× PBS, pH 7.4, and incubated overnight at 4°C. Eighteen hours later, the plates were washed and blocked with a 1% (w/v) bovine serum albumin (BSA) solution for 1 h (2.7.4). Purified anti-SplB, anti-ClfA, and anti-FnBPA mAbs were 10-fold serially diluted in 1× PBS–0.05 tween (w/v) 20–1% (w/v) BSA. Plates were incubated with the supernatants (undiluted) or purified mAbs (serially diluted) for 1 h at RT, allowing the antibodies to bind to their target proteins. Then the plates were washed 3× with wash buffer to remove the unbound mAbs and incubated with the POD-conjugated detection antibody (Goat–anti–mouse–IgG–POD, Southern Biotech) (1:30,000) in 1× PBS–0.05% (v/v) Tween 20–1% (w/v) BSA. Following incubation for 1 h at RT, plates were washed to remove the unbound detection antibodies, and the substrate (BD OptEIA) was added. Plates were incubated for 10 min at RT, to ensure that the peroxidase activated the substrate. Finally, the reaction was stopped by the addition of H_2SO_4 (2N) solution. The absorbance was read at 450 nm with a TECAN Infinite M200 instrument, and values were retrieved by using i–Control 1.10 software.

3.2.6. Analysis of the binding affinity of mAbs to their target using Microscale thermophoresis (MST)

To assess the binding affinity of anti-SplB mAb to SplB, SplB was labeled using the Protein Labeling Kit RED-NHS 2nd Generation (Amine Reactive) (NanoTemper Technologies) by following the methods explained before with certain modifications [197]. Briefly, 2 µM SplB (in 100 µl volume) was mixed with RED-NHS dye (molar dye: protein ratio ≈ 3:1) and incubated at RT for 30 min in the dark. The dye carries a reactive NHS-ester group that binds with lysine residues in the target protein. Excessive dye was removed using the supplied dye

removal column, which was previously equilibrated with MST buffer (2.7.7). The degree of labeling was determined using UV/VIS spectrophotometry at 650 nm and 280 nm. Typically, a degree of labeling (DOL) of 0.8 was achieved. The degree of labeling shows the number of dye molecules bound to the target protein, and labeling between 0.5 and 1.0 is considered optimum. DOL of 1.0 means that 1 dye is bound to 1 target protein (dye:protein, 1:1), while above 1.0 suggests that more than 1 dye is attached to the target protein, which is not recommended. The labeled SplB protein was adjusted to 120 nM with MST buffer supplemented with 0.05% (w/v) Tween-20. Anti-SplB mAb G8, as a ligand, was dissolved in MST buffer supplemented with 0.05% (w/v) Tween-20, and a series of 16 dilutions (2-fold) were prepared using the same buffer, producing ligand concentrations ranging from 0.000244 µM to 7.32 µM. For the measurement, each ligand dilution was mixed with one volume of labeled SplB (25 µl + 25 µl), which led to a final concentration of 60 nM SplB and final anti-SplB mAb G8 concentrations ranging from 0.000122 µM to 3.66 µM. Samples were loaded into Monolith NT.115 Standard Capillaries (NanoTemper Technologies). MST was measured using a Monolith NT.115 instrument (NanoTemper Technologies) at an ambient temperature of 25°C. Instrument parameters were adjusted to 80% LED power and medium MST power, and the data was generated by using MO Control software 1.6. Data of three independently pipetted experiments performed on the same day were analyzed (MO Affinity Analysis software, NanoTemper Technologies) using the signal from an MST at a time of 15 sec. The software measures the normalized fluorescence (Fnorm (‰)), which is calculated by using the equation described before [198].

$$F_{norm} = (1 - FB)\, F_{norm,unbound} + (FB)\, F_{norm,bound})$$

FB: fraction bound

F_{norm}, unbound: normalized fluorescence of the unbound state

F_{norm}, bound: normalized fluorescence of the bound state

3.2.7. Visualization of mAbs binding to native and denatured proteins by using dot blot

Dot blot was performed to demonstrate and visualize the binding of antibodies to native and/or denatured proteins. 1 µg of the recombinant protein (SplB, ClfA, or FnBPA) was pipetted onto a polyvinylidene fluoride (PVDF) membrane (Immobilon-P PVDF Membrane, Merck) and left for a few seconds to dry. The membrane was incubated in amido black dye (2.7.9) for 10 min to stain the proteins, and images were taken by using a Canon CanoScan LiDE 110 scanner.

Later, the membrane was washed for 5 min with Tris Buffered Saline with 0.05% (w/v) Tween-20 (TBST) to decolorize it and then incubated for 60 min at RT in a blocking buffer to block the free binding sites and avoid non-specific binding of the mAbs in the subsequent step (2.7.9). The membrane was then incubated for 1 h at RT (or overnight at 4°C) on a shaker with antigen-specific mAbs (1:10,000 in blocking buffer), facilitating its binding to the target protein. After incubation, the membrane was washed three times for 10 min with a washing buffer to remove the unbound mAbs, and incubated with the peroxidase (POD)-conjugated detection antibody (Goat–anti–mouse–IgG–POD, Southern Biotech) (1:100,000 in blocking buffer) for 1 h at RT. The membrane was then rewashed with washing buffer for 10 min (3×), to remove the unbound detection antibodies, and finally, chemiluminescent western blotting substrate was added (3 ml of luminol reagent A and peroxide reagent (1:1) (Supersignal™ West Femto Maximum, ThermoFisher Scientific)) for 3 min. The signal strength of the reaction was detected on the chemiluminescence measuring device (ChemoCam Imager, Intas Science) with an exposure time of 15-30 sec. Signal intensities of bands were quantified by using ImageJ 1.52a.

3.2.8. Separation of extracellular proteins and target proteins on SDS-PAGE

Sodium Dodecyl Sulfate-Polyacrylamide Gel Electrophoresis (SDS-PAGE) is an analytical technique to separate proteins according to their molecular mass. Shortly, SDS-PAGE gel was prepared by first preparing the separation gel, and after polymerization, the stacking gel was added on top and left for 30 min till the stacking gel was also completely polymerized (2.7.8.). After preparing the gel, 10 µg/ml of ECP were mixed with 5× Gel Loading Buffer (Sigma), which contains SDS and denatures and linearizes the proteins, conveying them with a negative charge. Similarly, 1 µg/ml of the protein candidate (SplB, ClfA, or FnBPA) were also mixed with 5× Gel Loading Buffer (Sigma). The samples were heat-denatured at 95°C for 10 min. A total of 10 µl sample was loaded in each lane, and the gel was run at 100 volts (V) for 120 min using Mini-PROTEAN Tetra (Bio-Rad). For visualizing the proteins, the gel was stained overnight with Coomassie Brilliant Blue G250 with shaking at RT, and the next day it was washed for 10 min (3×) with water to remove the extra unbound stain and finally, images were taken by using a Canon CanoScan LiDE 110 scanner.

3.2.9. Western blot used to analyze the binding specificity of mAbs

Western blot was employed to analyze if the generated mAbs bind specifically to the target proteins and do not cross-react with other ECPs of *S. aureus*. For western blot, SDS-PAGE was run the same way and with the same protein concentration as explained before (3.2.8). The

proteins were then transferred to a PVDF membrane (Immobilon-P PVDF Membrane, Merck) by using a Semi-Dry Transfer Unit (Hoefer) (80 milliamperes (mA)/gel, 100 min). The membrane was stained with Amido black dye for 10 min to visualize the proteins, and images were taken via a Canon CanoScan LiDE 110 scanner. Afterwards, the membrane was washed for 5 min with TBST to decolorize it and then incubated for 60 min at RT in a blocking buffer (2.7.9). Blocking will prevent the non-specific binding of primary antibodies (mAbs) to the membrane. Next, the membrane was incubated with antigen-specific mAbs (1:10,000 in blocking buffer) for 1 h at RT (or overnight at 4°C) on a shaker. After incubation, the membrane was washed for 10 min (3×) with a washing buffer to remove the excess and unbound mAbs. The membrane was then incubated with the POD-conjugated detection antibody (Goat–anti–mouse–IgG–POD, Southern Biotech) (1:100,000 in blocking buffer) for 1 hr at RT, which will bind to the mAbs. The membrane was rewashed with washing buffer for 10 min (3×) to remove the unbound antibodies, chemiluminescent western blotting substrate (luminol reagent A and peroxide reagent (1:1) (Supersignal™ West Femto Maximum, ThermoFisher Scientific)) was added for 3 min, and reaction signal was detected as explained in 3.2.7.

3.2.10. ELISA-based inhibition assay (ClfA)

An inhibition assay was performed to test the ability of the anti-ClfA mAbs to inhibit the binding of ClfA to human fibrinogen (Fg) as described before but with certain modifications [183]. For performing the assay, high-binding 96-well microtiter plates (Nunc-Immuno plate, Maxisorp, ThermoFisher Scientific) were coated with ClfA (2 µg/ml in 1× PBS, pH 7.4) overnight at 4°C. Eighteen hours later, the plates were washed to remove the unbound ClfA and blocked with a 1% BSA solution for 1 h (2.7.4). Next, purified anti-ClfA mAbs were diluted in 1× PBS–0.05% (w/v) Tween-20–1% (w/v) BSA ranging from 0.01 to 1000 µg/ml. Plates were incubated with purified mAb for 1 h at RT with shaking at 150 rpm to allow the blocking of Fg-binding sites of ClfA by the mAbs. To allow the binding of Fg to ClfA, 20 µg/ml Fg was added, and the plates were incubated for 2 h at 37°C with shaking. Afterwards, the plates were washing 3× to remove the unbound Fg. A 1:4,000 dilution of the detection antibody (anti-fibrinogen antibody (HRP)) in 1× PBS–0.05% Tween (w/v) 20–1% (w/v) BSA) was then added to the plate and incubated for 1 h at RT with shaking. Following incubation, plates were washed 3×, and the 3,3',5,5' tetramethylbenzidine (TMB) substrate (BD OptEIA, BD Biosciences) was added. In the presence of peroxide-labeled conjugates, the solution develops a vivid blue color. After incubating the plates for 10 min at RT, the reaction was stopped by the addition of H_2SO_4 (2N) solution, which will change the color from blue to yellow. Finally, the

absorbance was read at 450 nm with a TECAN Infinite M200 instrument and i–Control 1.10 software.

3.2.11. ELISA-based inhibition assay (FnBPA)

A similar inhibition assay, as explained above (3.2.10), was carried out to test the ability of anti-FnBPA mAbs to inhibit the binding of Fg and human fibronectin (Fn). As FnBPA has different binding sites to interact with Fg and Fn [87], both the binding protein partners were tested in the inhibition assay. Anti-FnBPA mAbs were used in the range of 1 to 1000 µg/ml, and the rest of the steps were followed as mentioned in 3.2.10.

3.2.12. SplB-specific substrate cleavage assay

To test if the anti-SplB mAb G8 neutralizes the enzymatic activity of SplB, a substrate-specific neutralization assay was performed. The substrate peptidyl-AMC substrate, Ac-VEID-AMC (Peptanova), was used, which has a cleavage site for SplB [199]. This substrate is covalently linked to an α-(4-methyl-coumaryl-7-amide (MCA)). Upon proteolytic cleavage, MCA is converted into the fluorescent amino-methyl-cumarin (AMC), which can be quantified in a fluorescence reader. Recombinantly produced and purified SplB (0.5 µg) was incubated with different molar ratios (1:1, 1:2, and 1:5) of anti-SplB mAb at 37°C for 1 h. Anti-SplB mAb will bind to the target protein and inhibit the enzymatic activity in a concentration-dependent manner. Native-SplB served as a positive control, while heat-inactivated SplB (90°C for 30 min) was used as a negative control. For preparing the working solution of the substrate (5 mg/ml stock), 5.5 µl of the substrate was taken, and it was diluted with 1× PBS, and the final volume was raised to 2 ml to reach the final concentration of 13.75 µg/ml. 10 µl of the SplB in one well and SplB + anti-SplB mAb mix in another well were taken, and 90 µl of the diluted substrate were added, allowing SplB to cleave the substrate (2.7.6). After the addition of the substrate, AMC generation was quantified over 75 min on a TECAN Infinite M200 (excitation= 360 nm, emission= 460 nm).

3.2.13. Intravital microscopy of cremaster muscles to test anti-SplB mAb neutralizing capacity

For testing the neutralizing capacity of anti-SplB mAbs *in vivo,* a mouse cremaster muscle microvascular leakage model was used. The surgical preparation of the mouse cremaster muscle was executed as described before [200]. Briefly, 6-8 weeks old male C57BL/6 WT mice were sedated with ketamine/xylazine (100 mg/kg ketamine and 10 mg/kg xylazine; intraperitoneal

(*i.p*) injection). The left femoral artery was then cannulated in a retrograde manner using a polyethylene-10 catheter (inner diameter 0.28 mm, Portex) to ease the administration of SplB ± anti-SplB mAb. Afterwards, through a ventral incision of the scrotum, the right cremaster muscle was uncovered. The muscle was exposed ventrally in a fairly avascular zone, and then it was spread over the glass (see-through) pedestal of a custom-made microscopy stage. Next, the epididymis and testicle were separated from the cremaster muscle and placed in the abdominal cavity. The muscle was super-fused with buffered saline (at 37°C) throughout the procedure to maintain the metabolic and physiological activity. After intrascrotal stimulation with 10 µg SpIB, leakage of intravenously applied FITC-dextran (Sigma-Aldrich) to the perivascular adipose tissue was analyzed in the mice. In similar experiments, mice also received mAbs directed against SpIB before SplB administration to observe if the mAb could neutralize the effect of SplB. Each animal experiment that was carried out complied with the German animal protection laws and was approved by the local animal protection authority (AZ ROB-55.2Vet-2532.Vet_02-17-68; Regierung von Oberbayern, Munich, Germany). The signal was quantified using fluorescence microscopy (excitation 488 nm and emission >515 nm), and the images were recorded by a CCD camera (Sensicam, PCO, Kelheim, Germany). Mean Fluorescence Intensity (MFI) values in six randomly selected regions of interest (ROIs, 50×50 μm^2) localized ~50 µm apart from the postcapillary venule under observation were measured by using the Image J software. Data were calculated as the mean MFI ± SD of 4-5 animals per group. A t-test was utilized to determine the statistical significance (*p <0.05 SplB vs. SplB+anti-SplB mAb).

4. Results

4.1. Pathogen-specific antibody response in infective endocarditis

4.1.1. Greifswald Infective Endocarditis Study (GIES)

Infective endocarditis is a life-threatening condition that, despite advances in cardiac imaging, is difficult to diagnose. Diagnosis of IE can be delayed for up to 35 days due to inadequate diagnosis methods leading to clinical complications [50]. Blood cultures (BC) are standard tests for diagnosing IE, but the rate of positive cultures drops if the patient is undergoing antibiotics treatment [2, 22]. Our research group has recently established xMAP® (Luminex®) technology-based serological assay that simultaneously quantifies the antibody response against 30 pathogens. Within Card-ii-Omics, we conducted a prospective clinical trial on IE patients to analyze if a pathogen-specific antibody response can be determined in IE patients and if it complements the classical blood culture (BC) diagnosis.

The Greifswald Infective Endocarditis Study (GIES) is a pilot study conducted by the Clinic for Internal Medicine B at the University Medicine Greifswald between 07/2018 and 05/2019. GIES aimed at identifying biomarkers for IE using plasma proteomics (Department of Functional Genomics, Greifswald) and real-time deformability cytometry (ZIK HIKE, Greifswald) as well as identifying the causative agent(s) by antibody profiling (Institute of Immunology, Greifswald). GIES comprised 17 IE patients and 20 controls, i.e., patients with non-infectious heart-related conditions (Figure 3). The type of IE was confirmed by ultrasound. Furthermore, the BC isolates were stored for later analyses. On day 0, ~25 ml EDTA blood was obtained for PBMC and plasma isolation. PBMCs were stored for later analysis of the pathogen-specific B cell response while plasma samples were used in this study. From 7 patients, another biosample (check-up) was obtained during a control visit in the hospital (between d14 to 200 after diagnosis). In addition, back-up and follow-up plasma samples from eight patients, collected between d-7 to -1 before IE diagnosis and d1-d21 after diagnosis, respectively, were provided by the Institute of Clinical Chemistry and Laboratory Medicine (IKCL). The important point to note here is that the back-up and follow-up samples from patients collected at IKCL were for routine analysis and were stored at 4°C for nearly a week before they were handed over to us and stored at -80°C. On the other hand, the check-up samples were collected from patients who visited the hospital for a control visit, and fresh plasma and cells were obtained from their blood, which were immediately stored at -80°C. The logistics and documentation of the samples were coordinated by Dr. Silva Holtfreter and Jawad Iqbal. The

complex sample processing and storage (collection and storage of immune cells and plasma from whole blood) was performed by Mr. Iqbal. Information about the number of back-up, follow-up, and check-up samples is provided in Table 8.

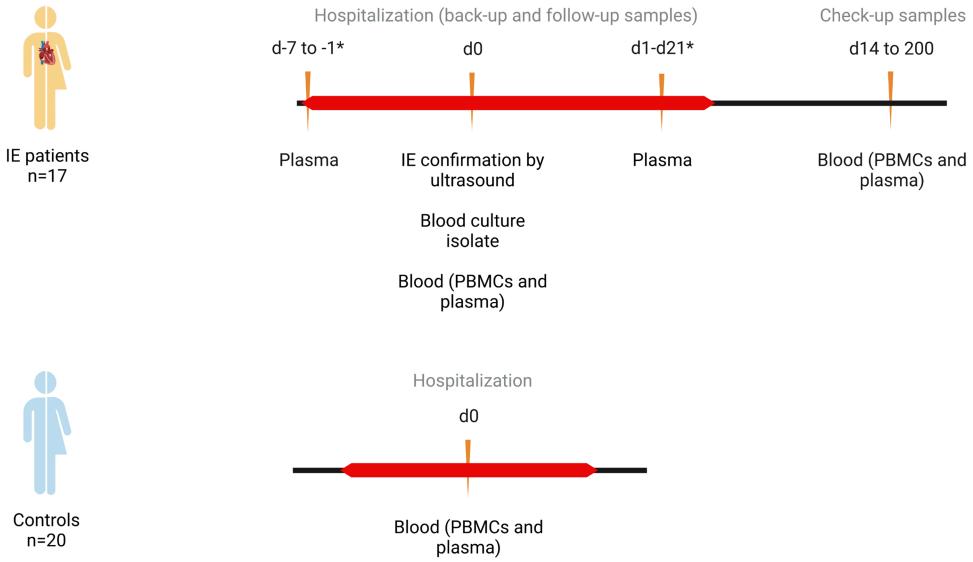

Figure 3. A graphical representation of the timeline at which clinical samples were collected in GIES. Greifswald Infective Endocarditis Study (GIES) comprised of 17 patients and 20 control (patients with non-infectious heart-related conditions). Biological samples were collected from patients at different time points. Blood was collected at day 0 (d0) to isolate PBMCs and EDTA plasma. Plasma of back-up and follow-up samples (*) were provided by the Institute of Clinical Chemistry and Laboratory Medicine, which were collected between d-7 to -1 and d1 to 21, respectively. Back-up and follow-up samples were stored at 4°C for nearly a week before they were handed over to the Institute of Immunology and stored at -80°C. Check-up samples were collected during a control visit to the hospital (between d14 to 200 after diagnosis). Fresh PBMCs and plasma were obtained, and the samples were immediately stored at -80°C

The control cohort comprised continuously recruited patients in the Clinic for Internal Medicine B with non-infectious heart-related diseases, mostly atrial fibrillation (N=11), but also thrombosis (N=2), and others (Table 8). The IE study cohort comprised of controls and patients of mean age 61.6 (± 12.4) and 69.9 (± 8.9), respectively, and the difference was statistically significant. The number of males was higher than females in both the control cohort (65% and 35%) and in the IE cohort (70.6% and 29.4%). Further information about the health status of the patients, infection status, medication, and biomarkers is provided in Table 8 and Table 9.

Pathogens were isolated from the blood culture (BC) (n=13), wound swabs (decubitus, n=2), urine (n=3), and tracheal secretions (n=1). In our data analysis, we clearly distinguished the pathogens isolated from the BC and other colonization/infection sites. A list of pathogens isolated from the BC and other colonization/infection sites is provided in Table 8.

Table 8. Patient characteristics in GIES (age, sex, clinical diagnosis, microbiological findings, antibiotics, and immunosuppressive drugs).

Patient ID	Age	Sex	Check-up (days)	Back-up and follow-up (days)	CRP [mg/l] <5.0	Main diagnosis	Blood culture (BC)	Other colonization/infection sites	Antibiotics	Immunosuppresive drugs*
1-1 C	81	f			4.4	Secondary glaucoma				
2-1 C	48	m			<3.1	CI due to cerebral artery thrombosis				-
3-1 C	65	f			<3.1	A-Fib, persistent				-
4-1 C	40	m			<3.1	CI due to thrombosis of precerebral arteries				-
5-1 C	62	f			11.5	A-Fib, paroxysmal				-
6-1 C	35	m			<3.1	Internal carotid artery syndrome (unilateral)				-
7-1 C	57	m			4.9	Infections of the optic nerve				-
18-1 C	66	m			29.9	A-Fib, paroxysmal				-
20-1 C	84	f			3.7	PE				-
21-1 C	51	m			<3.1	Ischemic optic nerve neuropathy				(+)
23-1 C	50	m			5.4	A-Fib, persistent				-
26-1 C	59	m			11.7	A-Fib, paroxysmal				(+)
27-1 C	61	m			8.5	A-Fib, persistent				(+)
28-1 C	69	m			<3.1	Retinal artery occlusion				-
30-1 C	69	f			10.8	A-Fib, persistent				(+)
31-1 C	72	f			<3.1	A-Fib, paroxysmal				-
32-1 C	69	f			18.3	A-Fib, persistent				-
33-1 C	78	m			<3.1	A-Fib, persistent				-
39-1 C	58	m			12.0	Secondary right heart failure				-
41-1 C	59	m			<3.1	A-Fib, persistent				-
8-1 P	57	m	100		41.4	Tube E with pocket infection	*S. epidermidis, S. aureus*	**Nasal swab**: *S. aureus*	CLI	-
9-1 P †	63	m			49	TVE with transit thrombus	*S. saccharolyticus*	**Nasal swab**: MRSA-PCR positive **Rectal smear**: *K. pneumoniae,*	TZP, FLX, VAN	(+)
10-1 P	81	f			4.3	Tube E with TVE	*S. epidermidis*		FLX	(+)
11-1 P †	78	m			21.8	Tube E with tricuspid and AVE	*S. epidermidis*	**From decubitus at Sacrum:** *K. pneumoniae*, *A. baumannii* complex, *E. coli*, *S. epidermidis* **Urine**: *E. coli*, *K. oxytoca*	RIF/LZD	+
12-1 P	67	m	54		46.5	AVE after biological AV replacement	VRE *Enterococcus faecium*		RIF/LZD/GEN	+
13-1 P	69	f			110	TAVI-E	*S. epidermidis*	**Urine**: *P. aeruginosa*, *S. aureus*	VAN/TAZ	+
14-1 P	54	m	193		59.2	AVE / Dressler syndrome	sterile		AMP/FLX/GEN	+
16-1 P	75	f	94		146	TVE acute infection	*S. aureus*		FLX	+
17-1 P	75	m	16		55.0	Tube E	sterile		CIP, GEN, VAN	-
24-1 P	72	m	63	d-3, d-1, d30	71.0	MVE	*S. capitis*		FLX/TAZ	+
25-1 P †	81	f		d-7, d-5	81.2	AVE	*S. gallolyticus*	**From decubitus at Sacrum:** *E. faecium*, *C. amycolatum*, *C. xerosis*	TAZ	+
34-1 P	77	m		d-4	31.4	Abscess around the prosthetic AVE	sterile		FLX/GEN/VAN	-
36-1 P	55	m		d-6, d+11, d+21	157	AVE DD Lenta	sterile	**Tracheal secretions**: *C. albicans*, streptococci, **bronchial secretions**: Enterococcus species, *S. dysgalactiae*. **Rectal swab**: *E. faecium*	AMP/GEN/FLX	-
37-1 P	84	f		d-3, d-2	143	AVE	*S. oralis/mitis*	**Urine**: *E. cloacae* complex	Unacid	-
38-1 P †	65	m	14	d-4, d-5, d-6, d+13	61.5	MVE (MitraClip)	*S. aureus*		FLX,GEN/RIF	+
40-1 P	68	m		d-5, d+9	38.8	AVE and MVE	*S. warneri*		GEN/FLX	-
42-1 P	68	m		d-2	152	AVE and early E abscess	*E. faecalis*		GEN/RIF/VAN	+

† deceased patients, Abbreviations: A-Fib, atrial fibrillation; AMP, ampicillin; AVE, aortic valve endocarditis; CI, cerebral infarction; CIP, ciprofloxacin; CLI, clindamycin; C, control; E, endocarditis; f, female; FLX, flucloxacillin; GEN, gentamycin; LZD, linezolid; m, male; MVE, mitral valve endocarditis; P, patient; TZP, piperacillin/tazobactam; PE, pulmonary embolism; RIF, rifampicin; TAZ, tazobactam; TVE, tricuspid valve endocarditis; VAN, vancomycin; +, taking immunosuppressive drugs, e.g. (Desloratadin, Amitryptilin, Buprenorphin, Ibuprofen, Ranitidin, Targin, Metamizol); -, not taking immunosuppressive drugs; (+), potential immunosuppressive drugs, e.g. (Clexane, Diclofenac, Noscapin)

Table 9. Cohort description of the IE study Greifswald (GIES).

	Control (n=20)	IE patients (n=17)	*p* - value
Age (Years, mean ± SD) [Min.-Max.]	61.6 ± 12.4 [35-84]	69.9 ± 8.9 [54-84]	0.0324*
Sex (m/f, absolute No.(%))	13/7 (65%/35%)	12/5 (70.6%/29.4%)	0.9139 n.s.
Diabetes mellitus (absolute No. (%))	1 (5%)	10 (59%)	<0.0001***
Medication			
Heart			
Beta blockers	12 (60%)	12 (71%)	n.s.
Loop diuretics / diuretics	5 (25%)	10 (59%)	0.0375*
I_f-Inhibitors	1 (5%)	1 (6%)	n.s.
Angiotensin-converting enzyme (ACE)-Inhibitors	2 (10%)	5 (29%)	n.s.
Aldosteron blockers	1 (5%)	2 (12%)	n.s.
Calcium channel blockers	3 (15%)	4 (24%)	n.s.
Angiotensin (AT)1-Receptor antagonists	5 (25%)	4 (24%)	n.s.
Statins	6 (30%)	10 (59%)	n.s.
Thrombosis prophylaxis			
Anticoagulants	10 (50%)	8 (47%)	n.s.
Acetylsalicylic acid	8 (40%)	3 (16%)	n.s.
Others			
Glucocorticoids	1 (5%)	1 (6%)	n.s.
Opioids	0	4 (24%)	0.0212*
Analgesics	1 (5%)	3 (16%)	n.s.
Antihistamines	1 (5%)	0	
Antidepressants	0	4 (24%)	0.0212*
Antiepileptics	0	4 (24%)	0.0212*
Biomarkers			
CRP [mg/l] (mean ± SD)	7.25 ± 6.7	74.7 ± 48.7	<0.0001****
Alanine transaminase (ALAT) [µkatal/L]	0.60 ± 0.32	3.12 ± 9.4	0.2860 n.s.
Aspartate transaminase (ASAT)[µkatal/L]	0.61 ± 0.27	3.62 ± 11.3	0.2867 n.s.
Others			
Leukocytes [Gpt/L]	7.8 ± 2.2	9.4 ± 4.6	
White blood cells × 10^9 (WBC)	5.99 ± 1.79	17.75 ± 32.4	0.0657 n.s.
Red blood cells × 10^{12} (RBC)	4.2 ± 0.81	3.9 ± 1.47	0.5213 n.s.
Heart frequency [bpm 70-90]	72.15 ± 18.4	81.2 ± 17.8	0.1457 n.s.

*An unpaired t-test was used for the comparison between age, CRP, ALAT, ASAT, leukocytes, WBC, RBC, and heart frequency of controls and IE patients. *p* values for each parameter indicate the difference between the controls and IE patients, and **p* <0.05 was considered statistically significant. For comparing sexes of control and IE patients, A two-sided Chi-square test was used, and *p* <0.05 was considered statistically significant.

4.1.2. High level of C-reactive protein detected in IE patients

In all GIES patients, several blood and serum parameters were assessed during routine diagnostics. C-reactive protein (CRP) was significantly elevated in the IE cohort as compared

to the control group (74.7 vs. 7.25 mg/l, p <0.0001) (Figure 4). CRP is an acute-phase protein, and its serum concentration increases in response to tissue injury, infection, or inflammation [201]. Normal CRP levels in a healthy individual are between 0 and 8 mg/l, and >40 mg/l is associated with adverse outcomes [202]. All the IE patients were taking antibiotics at the time of collecting the samples (Table 8), which has been reported to reduce the CRP levels rapidly [203]. However, in this study, the CRP levels in IE patients were significantly higher than controls.

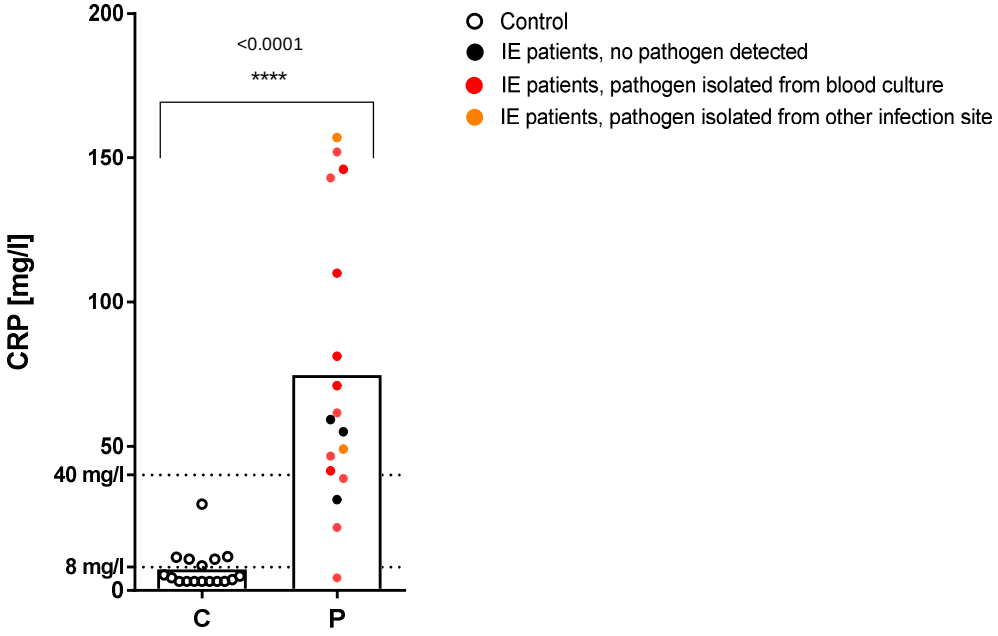

Figure 4. High CRP levels in IE patients. CRP levels (mg/l) of 20 controls and 17 patients were measured for each control (C) and patients (P) at baseline (d0). The blank circles represent the controls, while the filled circles represent the patients. The IE patients with positive BC are represented by a red circle, while an orange circle represents patients from whom pathogens were isolated from swabs. Bars indicate the mean values for both controls and IE patients. Dashed lines indicate the CRP levels in a healthy state (between 0 and 8 mg/l) and the CRP level associated with adverse outcomes (>40 mg/l). Groups were compared with an unpaired t-test "****", p < 0.0001. p <0.05 was considered statistically significant.

4.1.3. Infection array - an xMAP®-based assay for antibody profiling of bacterial infections

During the past 2 years, Dr. Dina Raafat from our Department has established an xMAP® (Luminex®) technology-based array, called the infection array, to simultaneously analyze the antibody response against numerous clinically relevant pathogens. Antigens from different pathogens are covalently coupled to magnetic particles (MagPlex® Beads) and incubated with diluted serum/plasma, similar to an ELISA. Later, the bound antibodies can then be detected with a PE-conjugated detection antibody and quantified using the fluorescence signal.

Initially, our group established a 20-plex to examine the antibody response against different pathogens in sepsis patients. It provided valuable insight into the immune response and showed that serological assays could provide important information about the infectious agent(s). These promising results prompted Dr. Raafat to establish a 33-plex array.

The pathogens included in the 33-plex cover the main causative agents of several severe bacterial infections: IE, prosthetic joint infections (PJI), sepsis, and pneumonia [2, 204–206]. A comprehensive literature survey and clinical data from several studies facilitated shortlisting the pathogens. The selected 30 pathogens include 16 Gram-positive bacteria, 12 Gram-negative bacteria, one atypical bacterium, and a yeast (Table 1). Tetanus toxoid (TT) served as an internal control. Out of the 30 pathogens, 20 are common infectious agents in all 4 clinical conditions (Table 1). Although many pathogens can cause IE, the most common pathogens involved are *S. aureus, S. epidermidis,* and streptococci. For each species, one isolate was selected based on the following criteria: (i) it is a clinical isolate, (ii) it is a representative strain, (iii) the whole genome sequence is available, and (iv) it is commercially available. The established assay is a highly informative tool and is currently employed to unravel the pathogen-specific antibody response in various clinical studies with a focus on infectious diseases, including infective endocarditis (Card-ii-Omics), joint infections, pneumonia, and sepsis.

4.1.4. IE patients show high antibody titers against pathogens detected in blood culture

Using the infection array, we compared pathogen-specific serum IgG antibody profiles in 20 controls and 17 IE patients at baseline (d0). Baseline (d0) is the day on which IE was diagnosed in the patients. The vaccine antigen TT served as a positive control. To ease data interpretation, pathogens were stratified on the basis of their natural habitat (gut, skin, nose, throat, and environment) and their status as Gram-positive or Gram-negative pathogen (Figure 5 a and b). As explained in section 3.1.3, for ease in communication, the term “pathogen” is used for all microbes in the entire thesis while explaining and discussing the results, although the microbes in the infection array also include commensals, opportunistic and true pathogens.

The antibody response at d0 provided interesting information. First, antibodies were detected against a broad range of pathogens in controls and IE patients, and the level of antibodies did not differ significantly except for *E. faecalis* and *S. lugdunensis*. The detection of antibodies against the range of pathogens in both controls and IE patients could be explained by their periodic exposure to the pathogens in their lifetime, and the difference in antibody response

could be a latest exposure, thus leading to a high antibody titer. Second, in most cases, higher antibody titers were detected against microbes residing on the skin and nose than against microbes residing in the gut, throat, or the environment. Third, antibodies titer against opportunistic pathogens (*E. faecalis, E. faecium, C. albicans, S. haemolyticus, S. sanguinis, S. aureus,* and *S. epidermidis*) was high as compared to commensals (e.g., *K. aerogenes, K. oxytoca, K. pneumoniae, S. hominis*). Fourth, high antibody titers were detected against the pathogens (*S. epidermidis, E. faecium,* and *S. aureus*) isolated from the BCs or wound swabs of the IE patients even though the samples were collected at d0 (Figure 5 c). In the case of *S. epidermidis,* the antibody titers detected against the isolated pathogen cross the mean value in one patient, while in *E. faecium* and *S. aureus,* the mean value was crossed in two and three patients, respectively (Figure 5 c). This could mean that the immune system already mounted an antibody response, and the infection might have started before the day of IE diagnosis. This phenomenon is explained in detail in a later section (4.1.5.4).

Interestingly, the highest antibody titers were detected against an opportunistic fungus, *C. albicans*. The antibody titer was significantly higher than the titer against pathogens habitating the skin and nose in both patients and controls. This suggests that frequent, probably unnoticed, (micro-)invasions with this fungus trigger a strong B cell memory.

Finally, higher antibody titers against the gut commensal *E. faecalis* were observed in IE patients than in control patients. A similar trend was observed for *E. faecium*. This trend could support the leaky gut hypothesis. The integrity of the intestinal barrier can be disturbed by changes in the epithelial mucosa of the change in gut microbiota. This can be triggered by various factors, including age, diet, and antibiotics. Certain dietary habits and medications have also been reported to cause the episodic breach of microbes from the gut and induce the production of IgG antibodies [207, 208]. The factors causing the disturbance of the gut barrier could lead to the breach of gut microbes, like *E. faecalis and E. faecium,* leading to the IgG antibody response.

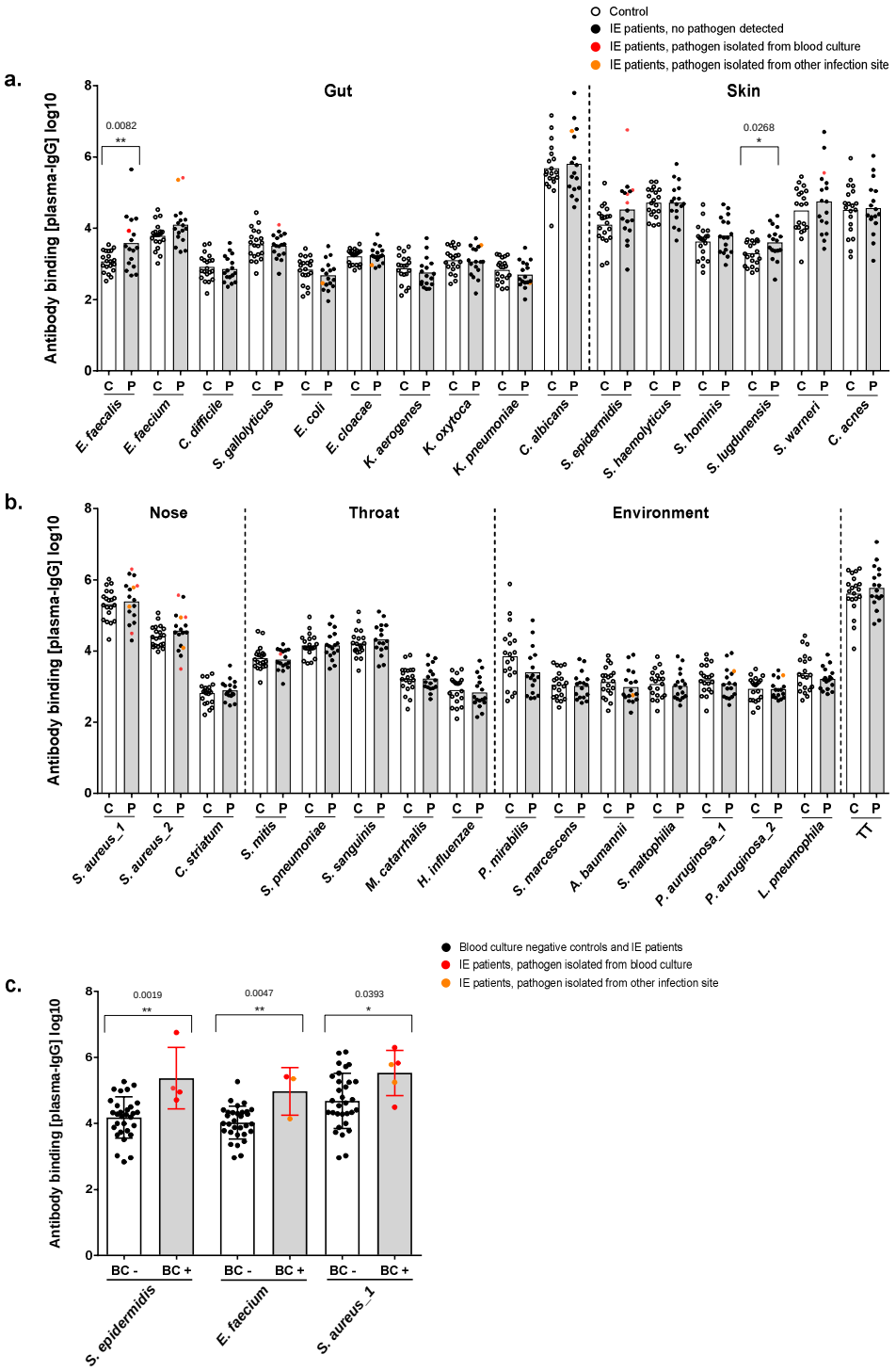

Figure 5. Basal antibody levels of controls and IE patients against the pathogens included in the infection array. The antibody response against extracellular proteins of common IE pathogens and TT was quantified with the infection array. The basal IgG levels were determined from plasma of 20 controls (C) and 17 IE patients (P), which were taken at the time of clinical diagnosis. The plasma samples were measured in 7 dilution steps, and the IgG levels were calculated using the xMAPr app. The mean values for both controls and IE patients are marked and shown on a logarithmic scale. Pathogens were stratified into 5 groups depending on their natural habitat (gut, skin, nose, throat, and environment). The blank circle represents the controls, and a black-filled circle represents the patients. The patients from whom the pathogens were isolated via BC are represented by a red circle, and the patients from whom the pathogens were isolated from decubitus at sacrum wound swabs, tracheal secretions, and urine are represented by an orange circle. Figure (a) shows the IgG response against gut and skin pathogens, while Figure (b) shows IgG response against nose, throat, and environmental pathogens. Figure (c) compares the antibody titers against the pathogens isolated from the BC or swabs of patients compared to antibodies titers against the same pathogen in BC-negative (against the respective pathogens) patients and controls at d0. The Shapiro-Wilk test evaluated the normality of the data distribution. A threshold of $p < 0.05$ was set for data not following the normal distribution. For each pathogen, the IE patients and control samples were compared with an unpaired t-test. $p < 0.05$ was considered statistically significant.

4.1.5. Kinetics of pathogen-specific antibody responses in IE patients

4.1.5.1. Moderate concordance of antibody signatures with the microbiological diagnosis

Besides analyzing the IgG antibody response against the pathogens in the infection array at the baseline level, available back-up (d-7 to d-1; n=8), follow-up (d1-d21; n=7), and check-up samples (d14-d200; n=7) from the IE patients were also analyzed and compared to baseline levels. This approach provided valuable information about the kinetics of the pathogen-specific IgG response during infection and helped identify putative causative pathogen(s). To compare the IgG profile of patients from different time points, a fold-change was calculated from the IgG level of the latest and earliest available plasma samples. A threshold of 2.0 was calculated as explained before (3.1.4), and a value above that was considered biologically significant. The patients were divided into five groups according to the concordance of their antibodies signatures with the microbiological diagnosis (BC) diagnosis (Table 10).

Table 10. Patients were classified into groups according to the concordance of the antibodies signature with the microbiological diagnosis (BC).

Group	Classification	No. of patients (in group/total)	Patient's ID
1	Serology = blood culture	2/13	P16, P38
2	Serology ≠ blood culture	3/13	P8, P12, P40
3	Serology +; blood culture -	3/13	P24, P34, P36
4	Serology -, blood culture +	3/13	P25, P37, P42
5	Serology -, blood culture -	2/13	P14, P17

Group 1: Serology confirms (and extends) microbiological diagnosis: Group 1 consists of 2 IE patients where serology confirmed the BC. Interestingly, the serological assay also provided indications of additional pathogens. In P38, *S. aureus* was detected in blood culture. In line with this, we observed a 4.7-fold increase in IgG antibodies against *S. aureus* at day 14 as compared to d-6. Additionally, a more than 2-fold increase in antibody titers was observed for *E. cloacae,* and *S. lugdunensis* (Figure 6, a). In P16, we saw a similar phenomenon where antibodies titers against the BC diagnosed *S. aureus* increased alongside *S. hominis, S. mitis,* and *L. pneumophila* (Table 11).

Group 2: Serology contradicts microbiological diagnosis: In 3/13 cases, high antibody titers were detected against pathogens that were not detected in the BC. In P40, *S. warneri* was isolated from the blood culture, but we observed no increase in antibody titers against this pathogen. In contrast, antibody titers were increased against two other pathogens (*K. oxytoca*

and *S. haemolyticus*), which were not detected in the BC (Figure 6, b). Similarly, in P8, *S. aureus* and *S. epidermidis* were isolated from the BC, but high antibody titers were observed against *C. albicans*. It could mean that multiple pathogens were involved in infection, and BC tests were negative for those pathogens. However, we cannot rule out the possibility of contamination in the BC tests, leading to a false BC diagnosis.

Group 3: Serology identifies pathogens while microbiological diagnosis is negative: In 3/13 cases, high antibody titers were detected against different pathogens while the BC was negative. In P24, BC results were negative, while serology showed an increase in antibody titers against *C. albicans* and *C. acnes* (Figure 6, c). Similarly, in P36, serology identified *C. striatum* and *C. albicans*, while BC diagnosis is negative (Table 11). *C. albicans* was isolated from the tracheal secretions though suggesting a parallel *Candida* pneumonia and possibly a reason for the increase in anti-*C. albicans* antibodies. Moreover, in P34, BC diagnosis was negative while an increase in antibody titer was detected against *S. sanguinis*.

Group 4: Serology does not identify pathogens while microbiological diagnosis is positive: In 3/13 cases, microbiological diagnosis was positive, but the serology did not detect an increase in antibody titers. In P37, BC diagnosed *S. mitis* while *E. cloacae* was detected in urine, but antibody titers did not show an increase against any pathogen (Table 11). Similarly, in P25, *S. gallolyticus* was isolated from the BC, and *E. faecium* was isolated from an infection site, while no increase in antibody titers was detected against any pathogen. Additionally, in P42, *E. faecalis* was isolated from BC without any increase in antibody titers (Figure 6, d, Table 11).

Group 5: Both serology and microbiological diagnosis are negative. In 2/13 cases, BCs, as well as a serological diagnosis, were negative (P14 and P17, Figure 6, e, Table 11). This phenomenon could be attributed to several reasons. The infecting pathogen might not be included in the infection array panel, or the patient may not generate a robust immune response. Moreover, in 11/17 cases, patients were taking immunosuppressive drugs (e.g., Desloratadin, Ibuprofen, Ranitidin, Targin, Metamizol), which could compromise the immune system. The BC diagnosis could be negative if the infectious agent is a fastidious pathogen.

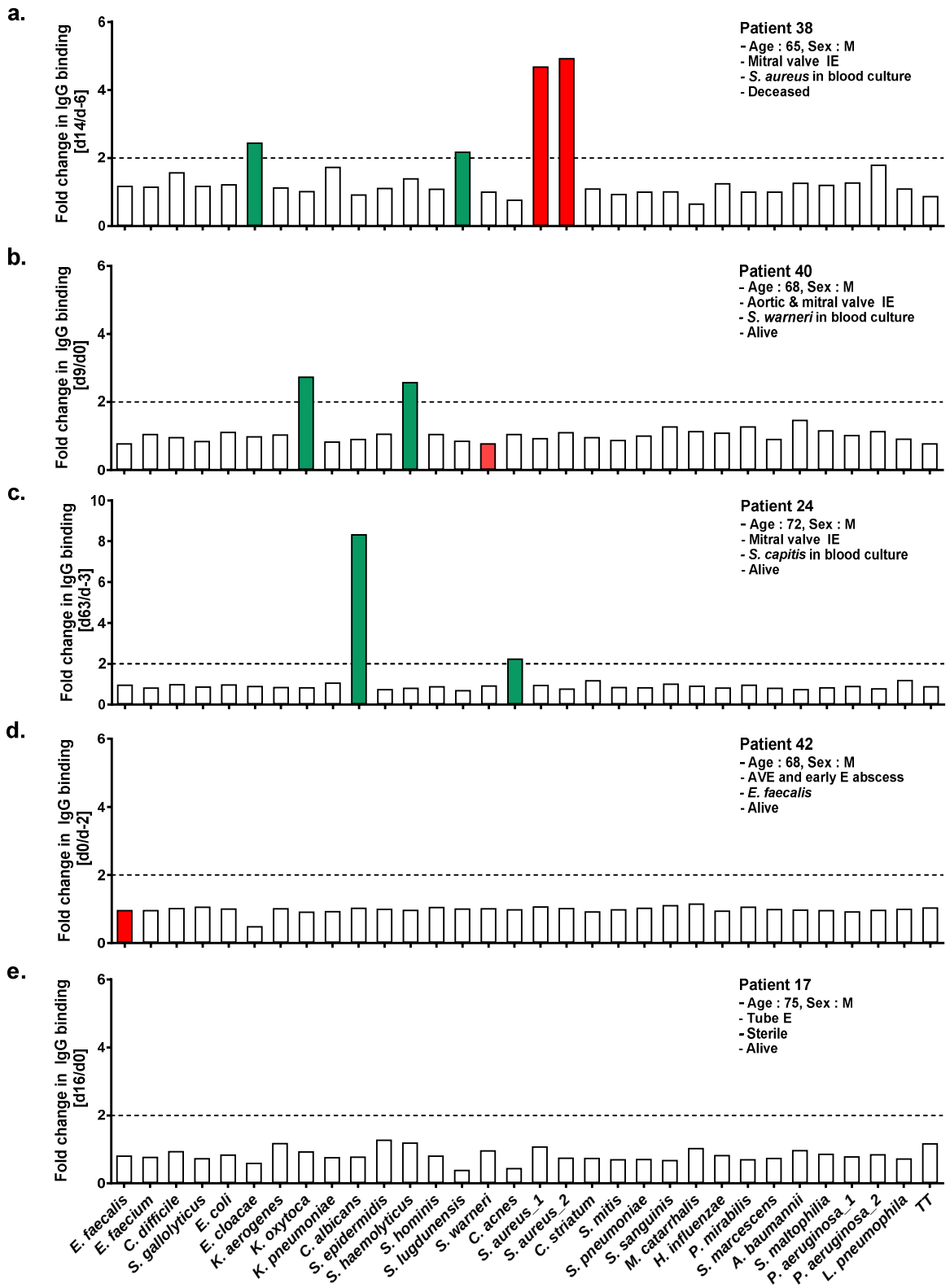

Figure 6. Kinetics of pathogen-specific antibody responses in IE patients. The fold-change in pathogen-specific antibody titers during the course of infection was determined by calculating by dividing the IgG binding values for the latest time point by the earliest time point. Black dotted lines mark the significance threshold of 2.0, and an antibody response above this threshold is represented by green bars. Antibody profiles were compared to the microbiological diagnosis. Fold-change against the BC- and swab-detected pathogens are depicted as red and orange bars, respectively. The patients were divided into five groups according to the concordance of their antibodies signatures with the microbiological diagnosis: (a) Serology confirms (and extends) the microbiological diagnosis. (b) Serology contradicts microbiological diagnosis. (c) Serology identifies pathogens while microbiological diagnosis is negative. (d) Serology does not identify pathogens, while microbiological diagnosis is positive. (e) Both serology and microbiological diagnosis are negative. The significance threshold of 2.0 was determined as median + 3 interquartile range (IQR) of the ratios of the antibodies response values from all patients against all 30pathogens. Abbreviations: AVE, aortic valve endocarditis; E, endocarditis; IE, infective endocarditis; M, male

4.1.5.2. Serology frequently detects an antibody response against *C. albicans*

Notably, we observed increased serum IgG against *C. albicans* in 4/13 IE patients. Three of them (P8, P24, and P36) showed a > 5-fold increase in antibody binding, corresponding to the strongest antibody increases observed in the whole study (Table 11). None of these patients were BC-diagnosed with *C. albicans* infection. However, in P36, it was detected in tracheal secretions. Of the 4 patients, 1 patient (P36) had an artificial valve, and none of the 4 patients died till the end of the IE study (Table 8).

In 2/4 cases, the increase in antibody titers against *C. albicans* coincided with the increase in antibody titers against *C. acnes* (P12, P24). In both the patients, the microbiological diagnosis was negative (Table 11). One of them had an infection on the aortic valve, which was replaced, while the other one had an infection on the mitral valve. None of the 2 patients died until the end of the IE study (Table 8). Patients showed a 2.3 - (P24) and 3.5-fold (P12) increase against *C. acnes* (Table 11).

4.1.5.3. IE patients present with high antibody titers against some gut microbes

As mentioned above, IE patients represented with higher antibody titers against some gut microbes (*E. faecium, E. faecalis*) than control patients. In line with this, the analysis of consecutive plasma samples revealed that 6/13 (46.1%) patients (P8, P12, P24, P36, P38, and P40) showed an increase in the IgG antibody titer against some gut microbes during the course of infection (Table 11). These microbes include *C. albicans*, *K. oxytoca*, *E. cloacae*, and *C. difficile*. The increase of Ab levels in consecutive plasma samples may suggest the leakage of gut microbes because of the antibiotics treatment or other factors mentioned before. Interestingly, P25 showed a marked reduction in anti-*S. gallolyticus* antibodies, which was isolated from BC, suggesting infection-induced antibody consumption (Table 11, Figure S 2).

4.1.5.4. Time matters - insights from back-up samples

For a total of 8 patients, we had access to back-up plasma samples obtained before the diagnosis of IE (d0). These samples provided valuable insights into the kinetics of the antibody response. For instance, antibodies titer did not rise against any of the pathogens in P36 between d0 and d21, but the difference in titers became apparent when the d21 sample was compared to a back-up sample obtained 6 days before IE diagnosis (d-6) (Figure 7). Now the rise in antibody titers against *C. albicans* and *C. striatum* was clearly visible. Similarly, in P38, antibodies titers did

not increase at all between d0 and d14. However, a comparison with a d-6 back-up sample revealed a more than 4-fold increase in antibody titers against *S. aureus* (Figure 7, Figure S 1).

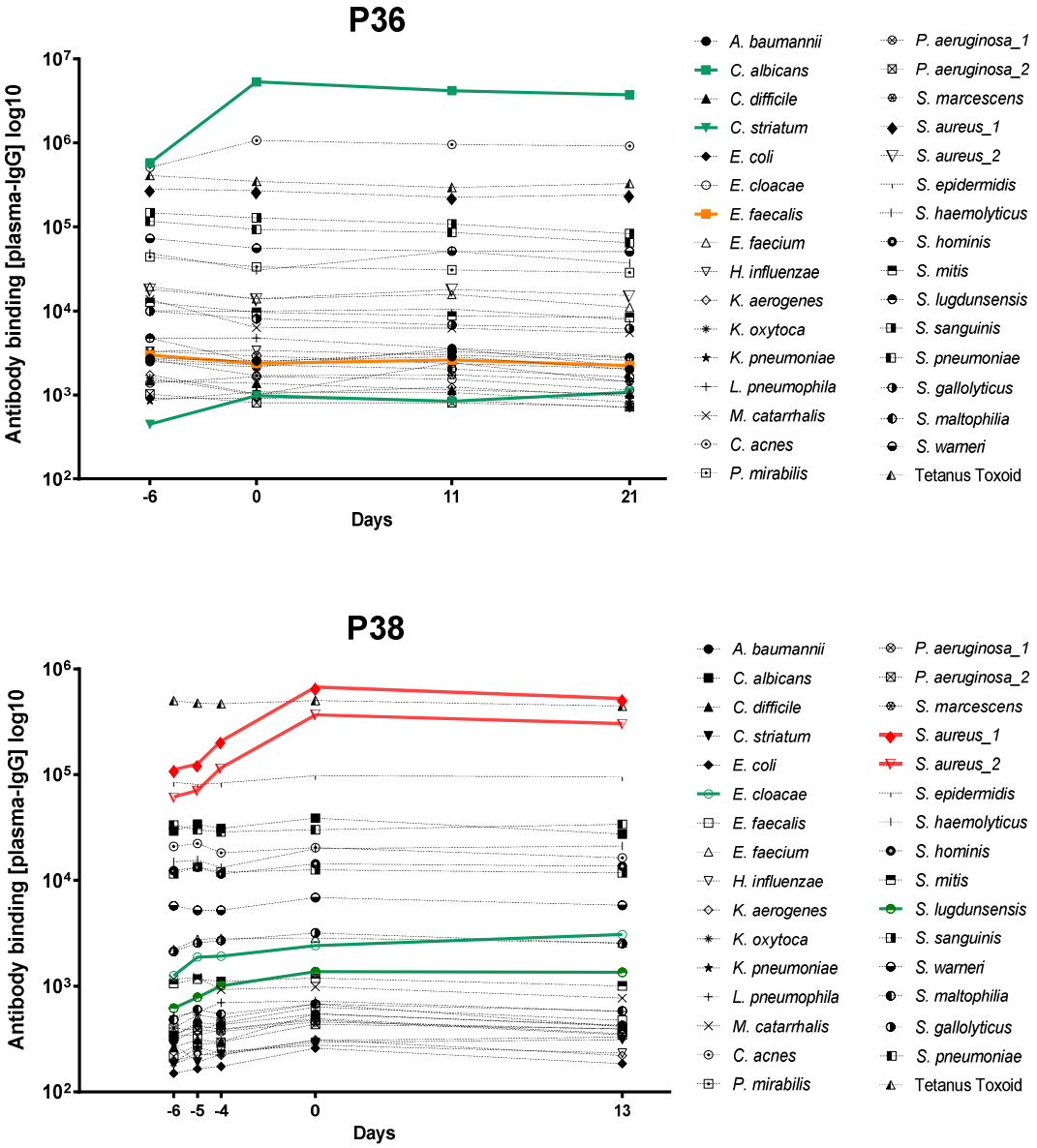

Figure 7. For studying the antibody response to IE, the timing of sample collection is crucial. Antibody response values against the extracellular proteins of pathogens included in infection array 33-plex were quantified in consecutive plasma samples. The response values reflecting IgG binding against the pathogens are depicted on a logarithmic scale on the y-axis and are plotted against the time point of sample collection. Fold-changes in antibody binding were determined by calculating the ratio of the time of point of interest vs. the earliest sampling time point. The red lines show the BC-diagnosed pathogens, against which we observed a more than 2-fold rise in antibody titers during the course of infection. The green lines show the pathogens which were detected by the infection array but not isolated from the BC. The orange lines depict the pathogens isolated from other infection sites, which did not cross the threshold of significance.

This suggests that the infection developed days or even weeks before the clinical diagnosis, and hence we observed the rise in antibodies a few days before the clinical diagnosis. Timing is therefore essential in antibody profiling in chronic infectious diseases. Moreover, in this study,

the samples were collected over a large span of time, as shown in Table 8. During such an extended period, the patient could have developed further infections in the meantime, which might not be directly related to IE. Therefore, the data should be interpreted while considering these critical points.

In summary, antibody titers were detected against a broad range of pathogens in both the controls and IE patients. High antibody titers were observed against pathogens that were BC-diagnosed, suggesting that the infection array can complement BC diagnosis and offers diagnostic potential. While analyzing the kinetics of antimicrobial antibody titers, it was observed that in some cases, serology not only confirms but extends the BC diagnosis. This shows that crucial information is missed by only analyzing the BC results. In some cases, serology contradicted microbiological diagnosis, while in others, the serological assay identified pathogens while the microbiological diagnosis failed. Interestingly, antibodies against intestinal microbes increased during the course of infection in a total of six patients supporting the leaky gut hypothesis. Moreover, we also observed antibody formation against the fungus *C. albicans* in 4/13 patients. This clearly shows that fungi play a more important role in infectious endocarditis than previously thought. The finding is clinically highly relevant, as fungi are hard to detect via microbiological diagnosis and are not covered by standard antibiotic regimens. Furthermore, an increase in antibodies against *C. acnes* was detected in the patients with native valve infection, suggesting that it may play an essential part in native valve IE. Finally, the timing of collecting the plasma sample is crucial, and biobanks should be established to collect and store patient samples before, on the day of surgery, and after surgery.

Table 11. Comparison of the infection array-based increase in pathogen-specific antibody responses with the BC-diagnosed pathogen(s).

		Gut										Skin						Nose			Throat					Environment							
Patient ID	**Latest/earliest time point**	***E. faecalis***	***E. faecium***	***C. difficile***	***S. gallolyticus***	***E. coli***	***E. cloacae***	***K. aerogenes***	***K. oxytoca***	***K. pneumoniae***	***C. albicans***	***S. epidermidis***	***S. haemolyticus***	***S. hominis***	***S. lugdunensis***	***S. warneri***	***C. acnes***	***S. aureus_1***	***S. aureus_2***	***C. striatum***	***S. mitis***	***S. pneumoniae***	***S. sanguinis***	***M. catarrhalis***	***H. influenzae***	***P. mirabilis***	***S. marcescens***	***A. baumannii***	***S. maltophilia***	***P. aeruginosa_1***	***P. aeruginosa_2***	***L. pneumophila***	**Tetanus Toxoid**
8	100/0	0.3	1.0	1.4	1.2	1.4	1.1	1.3	1.8	1.2	5.5	0.5	0.6	0.3	0.8	0.5	1.3	0.6	0.7	0.7	1.0	0.8	0.9	1.2	1.7	1.1	1.5	1.6	1.6	1.5	1.0	1.1	0.8
12	54/0	1.1	1.0	2.2	1.2	1.5	1.1	1.4	1.0	1.2	3.7	1.4	2.0	2.1	2.5	1.2	3.5	1.5	1.3	2.0	1.4	1.8	1.3	1.1	1.3	1.5	1.3	1.5	1.1	1.3	1.3	1.8	1.8
14	193/0	0.5	0.4	0.4	0.4	0.5	0.5	0.3	0.4	0.4	0.6	0.4	0.5	0.3	0.3	0.1	1.0	1.3	0.2	0.8	0.4	0.6	0.4	0.4	0.4	0.5	0.4	0.4	0.4	0.3	1.1	0.5	1.5
16	94/0	1.3	1.3	1.0	1.8	0.9	1.0	0.8	0.9	1.0	1.8	1.7	1.9	2.7	1.3	0.7	1.3	2.3	1.7	0.8	2.0	1.3	1.5	0.8	0.7	1.1	0.8	0.8	1.0	0.8	0.8	3.4	2.5
17	16/0	0.8	0.8	1.0	0.8	0.9	0.6	1.2	1.0	0.8	0.8	1.3	1.2	0.8	0.4	1.0	0.5	1.1	0.8	0.8	0.7	0.7	0.7	1.0	0.8	0.7	0.8	1.0	0.9	0.8	0.9	0.7	1.2
24	63/0	0.8	0.6	1.1	0.7	0.8	0.7	0.6	0.7	0.9	5.8	0.6	0.8	0.6	0.6	0.9	1.6	0.7	0.7	0.8	0.7	0.7	0.7	0.8	0.7	0.8	0.7	0.6	0.7	0.8	0.7	1.1	0.6
	63/-3	1.0	0.9	1.0	0.9	1.0	0.9	0.9	0.9	1.1	8.3	0.8	0.8	0.9	0.7	1.0	2.3	1.0	0.8	1.2	0.9	0.9	1.0	0.9	0.9	1.0	0.8	0.8	0.9	0.9	0.8	1.2	0.9
25	0/-7	0.6	0.8	0.9	0.3	1.3	0.9	1.0	0.8	0.9	0.8	0.8	0.8	0.9	0.8	1.1	1.2	1.0	1.0	0.7	0.6	0.8	0.5	1.0	0.9	0.9	1.1	1.1	1.0	1.1	1.0	0.9	1.0
34	0/-4	0.9	1.3	1.0	1.0	0.9	1.0	0.9	1.0	1.0	1.0	0.8	1.9	0.8	0.8	1.2	1.1	1.0	1.0	1.1	0.9	1.1	2.0	1.0	1.0	0.8	0.8	0.9	0.9	1.1	0.9	1.0	0.9
36	21/0	0.9	0.8	0.7	0.8	0.8	0.7	0.9	1.4	0.8	0.7	0.8	1.2	1.0	1.1	0.9	0.9	0.9	1.1	1.1	0.9	0.7	0.6	0.9	0.8	0.9	0.9	0.8	0.7	0.7	0.9	0.6	0.9
	21/-6	0.8	0.6	0.7	0.6	0.8	0.8	0.6	0.9	1.0	6.5	0.8	0.8	0.9	0.6	0.7	1.8	0.9	0.8	2.4	0.7	0.6	0.6	0.4	0.8	0.7	0.6	0.7	0.6	0.6	0.7	0.6	0.8
37	0/-2	1.2	1.2	0.9	1.1	1.2	1.0	1.2	1.0	1.0	1.1	1.0	0.9	1.0	1.0	1.0	1.0	1.1	1.0	1.4	1.2	1.0	1.1	1.1	1.2	1.0	1.0	0.9	1.2	1.1	1.2	1.0	1.1
38	14/0	0.7	0.9	0.8	0.8	0.7	1.3	0.7	0.6	1.1	0.7	1.0	1.1	1.0	1.0	0.8	0.8	0.8	0.8	1.1	0.8	1.1	0.9	0.8	0.8	0.7	0.7	0.8	0.9	0.9	0.9	0.8	0.9
	14/-6	1.2	1.2	1.6	1.2	1.2	2.5	1.1	1.0	1.7	0.9	1.1	1.4	1.1	2.2	1.0	0.8	4.7	4.9	1.1	0.9	1.0	1.0	0.7	1.3	1.0	1.0	1.3	1.2	1.3	1.8	1.1	0.9
40	9/0	0.8	1.1	1.0	0.9	1.1	1.0	1.0	2.7	0.8	0.9	1.1	2.6	1.1	0.9	0.8	1.1	0.9	1.1	1.0	0.9	1.0	1.3	1.1	1.1	1.3	0.9	1.5	1.2	1.0	1.2	0.9	0.8
	9/-5	0.8	1.2	1.0	0.9	1.2	1.1	1.0	3.1	0.8	0.9	1.1	1.2	0.9	0.9	1.0	1.0	1.2	1.0	1.2	1.0	0.9	1.0	1.1	1.0	1.5	0.9	1.5	1.1	1.2	1.2	1.0	0.9
42	0/-2	1.0	1.0	1.0	1.1	1.0	0.5	1.0	0.9	0.9	1.0	1.0	1.0	1.1	1.0	1.0	1.0	1.1	1.0	0.9	1.0	1.0	1.1	1.2	1.0	1.1	1.0	1.0	1.0	0.9	1.0	1.0	1.1

Pathogen isolated from blood culture

Pathogen isolated from other infection sites

Pathogen isolated from blood culture + increase in anti-microbial IgG levels

Pathogen isolated from other infection sites + increase in anti-microbial IgG levels

No pathogen isolated from blood culture + increase in anti-microbial IgG levels

This table shows the fold-change of the antibody response against the pathogens for all 13 patients with consecutive serum/plasma samples. The fold-change was calculated by dividing the latest time point by d0 or - if applicable - by an earlier time point. Pathogens were stratified into 5 groups depending on their natural habitat (gut, skin, nose, throat, and environment). The BC-diagnosed pathogens are depicted in blue, while the pathogens isolated via swabs are depicted in orange. The fold-changes of IgG levels against the pathogens isolated from the BC that crossed the significance threshold are depicted in red, the IgG fold-change against the swab-isolated pathogens that crosses the significance threshold are depicted in violet, while the green color depicts the pathogens with increased IgG levels, but without any BC or swab diagnosis. The threshold of 2.0 was measured as median + 3 interquartile range (IQR) of the ratios of the antibodies response values from all IE patients against all the pathogens in infection array.

4.2. Characterization of antibacterial monoclonal antibodies

4.2.1. Purification and characterization of murine anti-SplB mAbs

4.2.1.1. Purification of anti-SplB mAbs

Our group has previously generated three murine mAbs against SplB (anti-SplB G8, H7, and H9) using hybridoma technology. This work aimed at purifying these mAbs at a large scale and characterizing them in depth. First, the frozen hybridomas were thawed, subcloned, and tested for anti-SplB mAb production. Second, ELISA-positive clones were expanded in 24-well tissue culture plates, followed by 750 ml cell culture flasks. The cell-free culture supernatants were collected, and finally, the mAbs in the supernatants were purified by affinity-based chromatography using Protein-G columns (Figure S 3). A total of 50 mg highly pure mAbs was obtained for each anti-SplB mAb from 3 liters of hybridoma culture supernatant.

Next, we performed an ELISA to confirm that all three anti-SplB mAbs bind to SplB. All three clones (anti-SplB G8, H7, and H9) showed similar strong binding to the recombinant SplB protein, with a mean half-maximal (EC-50) binding at 0.18, 0.17, 0.19 µg/ml, respectively (Figure 8).

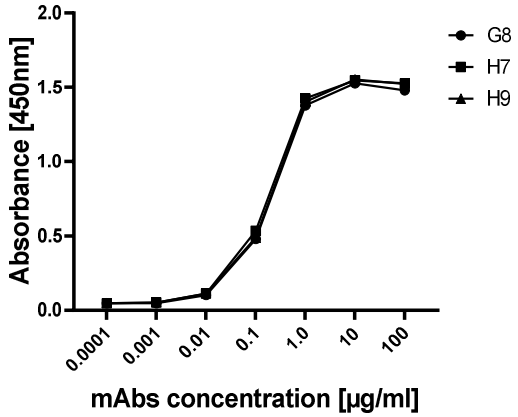

Figure 8. Murine anti-SplB mAbs bind to recombinant SplB in a concentration-dependent manner. The purified anti-SplB mAbs were tested for their ability to bind to recombinant SplB. ELISA plates were coated with 1 µg/ml SplB, blocked, and subsequently incubated with serially diluted anti-SplB mAbs. The signal was detected using a goat-anti-mouse-IgG conjugated to POD and TMB as a substrate (BD OptEIA™). The data from 1 of 3 similar experiments is shown.

4.2.1.2. Isotyping of anti-SplB mAbs

Constant region of antibodies determines the isotype and mediates the biological effector functions, including complement activation and antibody-dependent cytotoxicity. Since antibody isotypes differ strongly in their induced effector functions and this information is also relevant for BCR sequencing, we next determined the isotype of the three anti-SplB mAbs.

SplB hybridomas were initially selected for producing IgG antibodies. Moreover, the immunized C57Bl/6 mice do not form antibodies of the subclass IgG2a [209]. Hence, the produced mAbs were only tested for the subclasses IgG1, IgG2b, IgG2c, and IgG3 using the MILLIPLEX® Mouse Immunoglobulin Isotyping Magnetic Bead Panel. The LC types kappa (κ) and lambda (λ) were also determined. All 3 anti-SplB mAbs belonged to the IgG1 subclass and had κ LCs (Table 12). Based on the isotyping results, suitable primers were selected for the subsequent BCR sequencing.

Table 12. Isotyping of the 3 murine anti-SplB mAbs, 6 murine anti-ClfA mAbs and 2 murine anti-FnBPA mAbs

Antigen	mAbs	IgG Subclass				Light chain type	
		IgG1	IgG2b	IgG2c	IgG3	κ	λ
SplB	G8	●				●	
	H7	●				●	
	H9	●				●	
ClfA	001		●			●	
	002		●			●	
	003		●			●	
	004		●			●	
	005		●			●	
	006		●			●	
FnBPA	D4		●			●	
	E9		●			●	

4.2.1.3. Sequencing revealed that the three anti-SplB mAbs are identical

All three mAbs were derived from a single immunized mouse, showed similar binding affinities and an identical isotype. To test whether the mAbs were identical, we sequenced the gene segments encoding the variable regions of HC and LCs. RNA was isolated from anti-SplB G8, H7, and H9 hybridoma cultures, and cDNA was generated via reverse transcription. Afterwards, the gene regions encoding variable regions of the LCs and HCs of each clone were amplified by PCR and sequenced.

Notably, all three anti-SplB mAbs were identical (Figure S 5, a – b). Different regions of the mAb, like framework regions (FRs) and complementarity determining regions (CDRs), were identified using IgBLAST and were graphically represented using SnapGene Viewer (Figure 9 a – b). The variable region of the HC of G8 was 94.9 % identical to the germline sequence. There were 4 silent and 16 non-silent mutations in the DNA sequence (some mutations in the

same codons); the latter led to 12 amino acid (AA) changes as compared to germline sequence. Similarly, the variable region of the LC was 98.6 % identical to the germline sequence with 2 silent and 2 non-silent mutations leading to 2 AA changes (Table S 1). In consequence, all subsequent experiments were performed only with the anti-SplB G8 clone.

a. Light chain_G8

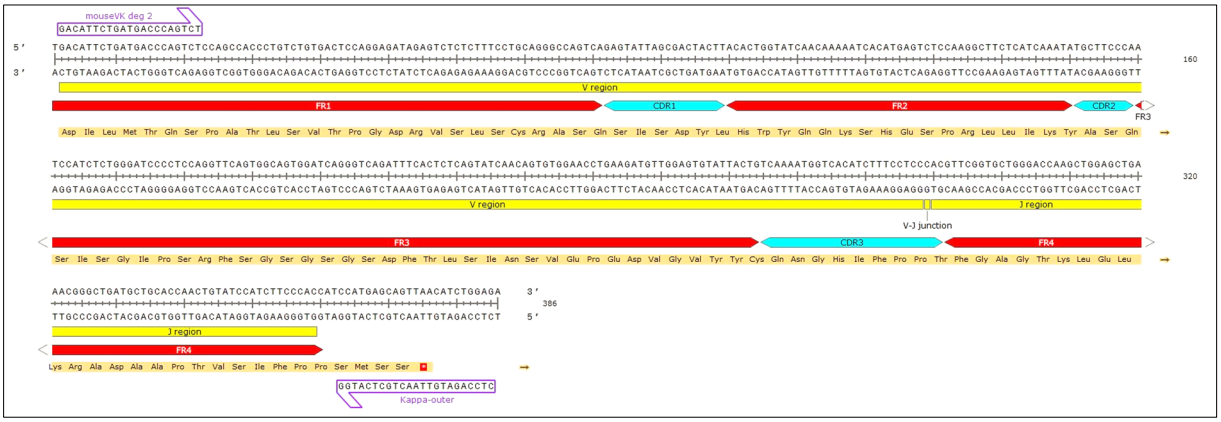

b. Heavy chain_G8

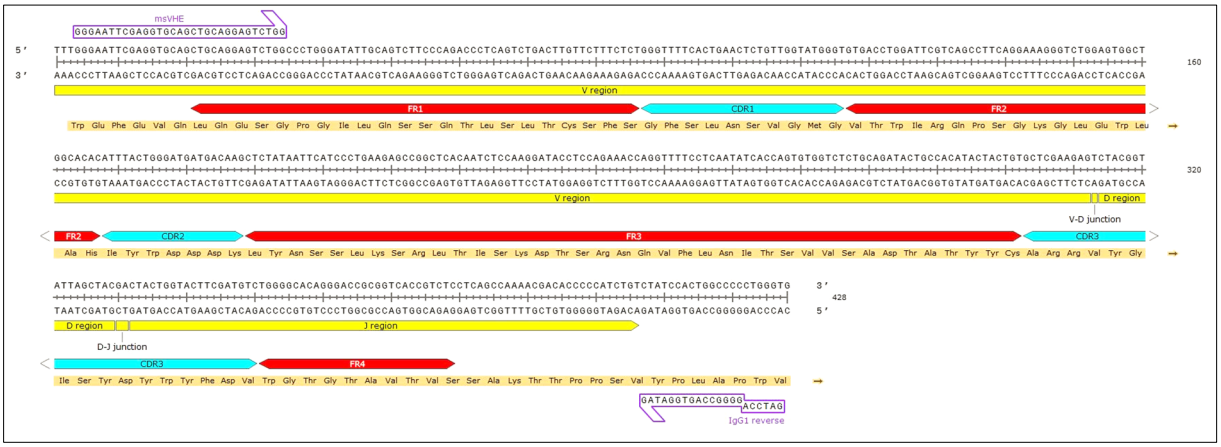

Figure 9. Annotated variable regions of LC and HC of SplB G8. RNA was isolated from anti-SplB G8 hybridoma culture and reverse transcribed into cDNA. Afterwards, the gene regions encoding the variable regions of the LCs and HCs of each clone were amplified by PCR and sequenced. (a – b) The DNA sequence of the anti-SplB G8 mAb was analyzed by using Ig-BLAST software to annotate the variable/diversity/joining (VDJ) or variable/joining region of the HC or LC along with framework regions (FRs, red) and complementarity-determining regions (CDRs, light blue). The final image was generated by using SnapGene Viewer. The translated amino acid sequence is also shown underneath the DNA sequence. Primers used for amplification of variable regions of HC and LC are framed in purple.

4.2.1.4. Anti-SplB mAb shows a moderate binding affinity to SplB

The next step was to analyze the binding affinity of anti-SplB G8 mAb to SplB using Microscale Thermophoresis (MST) analysis. This method quantifies biomolecular interactions in the liquid phase. SplB was labeled using the Monolith Protein Labeling Kit RED-NHS, which contains a dye that carries a reactive NHS ester group that covalently reacts with random lysine residues of the target. Labeled SplB protein (60 nM) was incubated with different dilutions of anti-SplB G8 mAb (0.000112 µM - 3.66 µM), and binding was recorded at 25 ^{0}C.

The anti-SplB G8 mAb bound to SplB in a concentration-dependent manner (Figure 10). The calculated dissociation constant (K_d) value for anti-SplB G8 and SplB interaction was 2.54 µM. Since the K_d value for antigen-antibody interaction is frequently in the nM range [210, 211], this represents a moderate binding affinity between SplB and anti-SplB G8 mAb.

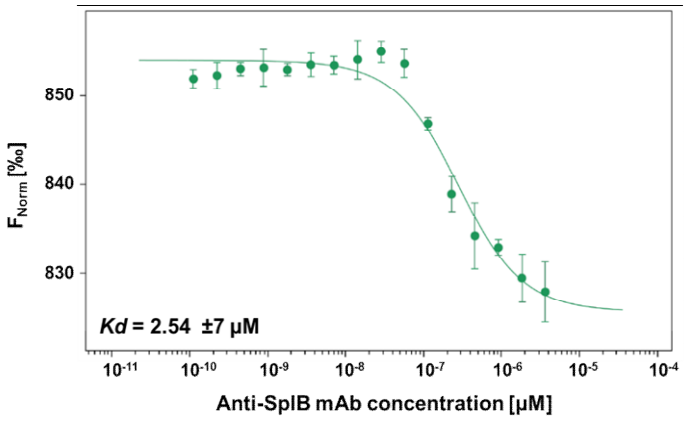

Figure 10. Anti-SplB mAb shows a moderate binding affinity to SplB. The binding affinity of anti-SplB G8 mAb to SplB was determined by MST. The concentration of NHS-RED -labeled SplB was kept constant (60 nM), while the concentration of the non-labeled anti-SplB G8 mAb ranged between 0.000112 µM - 3.66 µM. The samples were loaded into capillaries and analyzed using the Monolith NT.115 (NanoTemper Technologies). Normalized fluorescence (F_{norm} (‰)) is shown on the y-axis. F_{norm} is the function of the concentration of the titrated anti-SplB G8. The value of the fraction bound molecules is derived from measuring the change in normalized fluorescence of the unbound and bound state of the binding partners (SplB and anti-SplB G8). Mean ± standard deviation (SD) of three independent measurements are depicted.

4.2.1.5. Anti-SplB mAb binds to native and denatured SplB

To test if the anti-SplB G8 mAb binds to a three-dimensional or linear epitope on SplB, dot blots were performed using native and heat-denatured SplB as the target antigen. Both proteins were pipetted onto a PVDF membrane, and two different concentrations of anti-SplB G8 mAb (10 ng/ml and 50 ng/ml) were used as a primary antibody. The anti-SplB G8 mAb bound to both native and denatured SplB with similar strength (Figure 11 a – b), suggesting that the mAb recognizes a linear, surface-exposed epitope.

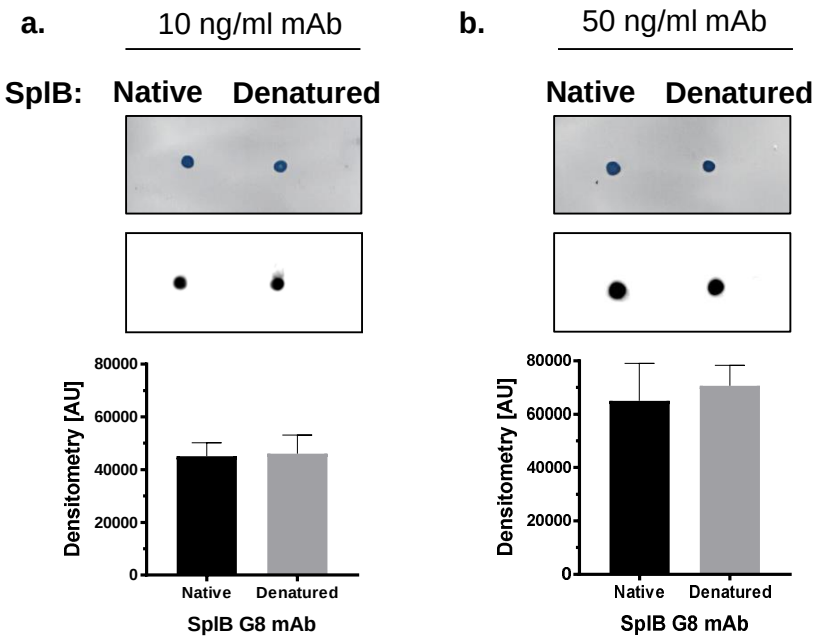

Figure 11. Anti-SplB mAb binds to native and denatured SplB. (a – b) 1 µg of recombinant SplB was pipetted on the PVDF membrane in its native and denatured (heated at 95 ^{0}C for 30 mins) form. Proteins were visualized with amido black 10B (upper panel). Anti-SplB antibody binding to native and denatured SplB was afterwards determined by western blotting using 10 ng/ml or 50 ng/ml of the mAb (middle panel). For quantification of the signal derived from the protein bands, densitometry was performed for each blot by using ImageJ 1.52a, and figures were generated by using GraphPad Prism 7.0 (bottom panel). A representative blot from three independent experiments is shown. Mean +SD of densitometry data of the representative experiments are shown.

4.2.1.6. Anti-SplB mAb does not cross-react with other *S. aureus* proteins

To determine whether the anti-SplB G8 mAb cross-reacts with other *S. aureus* proteins, western blots were performed. The ECP of *S. aureus* strain USA300*Δspa* were obtained from a stationary phase of a TSB culture. As SplB is a secreted protein, it was expected that anti-SplB mAb binds to SplB present in the ECP. First, 10 µg of ECP, 1 µg of SplB, and a mixture of both were run on an SDS-PAGE and stained with Coomassie Brilliant Blue R-250 Dye (Figure 12 a). Another gel, which was run parallel, was used for western blot and incubated with 300 ng/ml of anti-SplB G8 mAb as a primary antibody. The anti-SplB G8 mAb specifically bound to recombinant SplB and did not cross-react with any other protein in the ECP (Figure 12 b, right panel). However, we could not detect a SplB in the ECP preparation. This could be attributed to the relatively moderate amount of SplB expressed by USA300*Δspa* under the used culture conditions (personal communication with Dr. Leif Steil). Overall, the western blot showed that this mAb did not cross-react with any other abundant ECP of *S. aureus* and is specific for SplB.

SplB shows 47.7 - 56.2% AA sequence homology to the other Spl proteins. Hence, we additionally tested whether the anti-SplB mAb cross-reacts with other Spl proteins by ELISA.

Anti-SplB G8 did not bind to SplA, SplD, SplE, and SplF (Figure S 4, a – d), indicating that the produced mAb binds specifically to SplB.

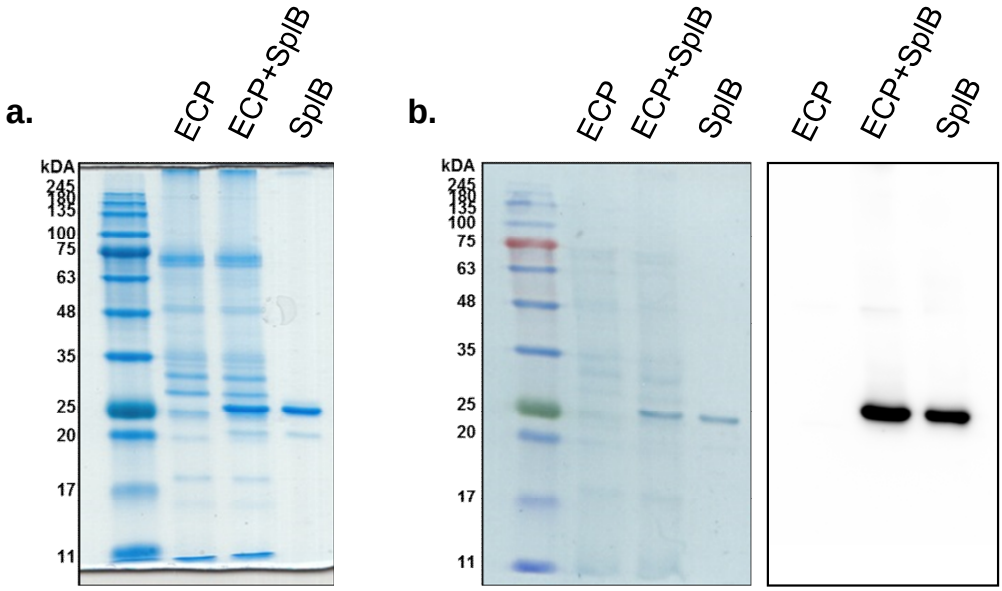

Figure 12. Anti-SplB does not cross-react with other *S. aureus* proteins. (a) 10 µg of ECP, 1 µg of SplB, or a mixture of both were analyzed by SDS-PAGE. Another SDS gel, which was run in parallel, was blotted onto a PVDF membrane. (b, left panel) The membrane was stained with amido black 10B for 10 mins to visualize the transferred proteins. (b, right panel) Afterwards, a western blot was performed using 300 ng/ml of the anti-SplB antibody, an α-mouse-IgG-POD detection antibody (1:100,000), and a luminol substrate. One out of 2 similar experiments is depicted.

4.2.1.7. Anti-SplB mAb neutralizes the enzymatic activity of SplB

Since we demonstrated that anti-SplB G8 mAb specifically and moderately binds to SplB, the next step was to test if anti-SplB G8 mAb neutralizes the enzymatic activity of SplB. Dubin G. et al. previously identified a synthetic substrate, Ac-VEID-MCA, which was preferentially cleaved by SplB [199]. This substrate, Acetyl-L-valyl-L-glutamyl-L-isoleucyl-L-aspartic acid (Ac-VEID), is covalently linked to a α-(4-methyl-coumaryl-7-amide (MCA). Upon proteolytic cleavage, MCA is converted into the fluorescent AMC (7-amino-4-methyl-cumarin), which can be quantified with a fluorescence reader. 2.8 µg SplB was incubated with increasing molar ratios of anti-SplB G8 mAb, i.e., 1:1, 1:2, and 1:5, at 37 °C for 1 h. Native SplB served as a positive control, while heat-inactivated SplB (90 °C for 30 mins) was used as a negative control. After addition of the substrate, AMC generation was quantified over 75 mins. SplB efficiently cleaved the Ac-VEID-MCA substrate in a time-dependent manner (Figure 13). The activity of SplB was neutralized by up to 50% when anti-SplB mAb was used in a molar ratio of 1:2, while the activity of SplB was completely neutralized with a 1:5 molar ratio. In conclusion, our anti-SplB G8 mAb not only binds to SplB but also efficiently neutralizes its enzymatic activity.

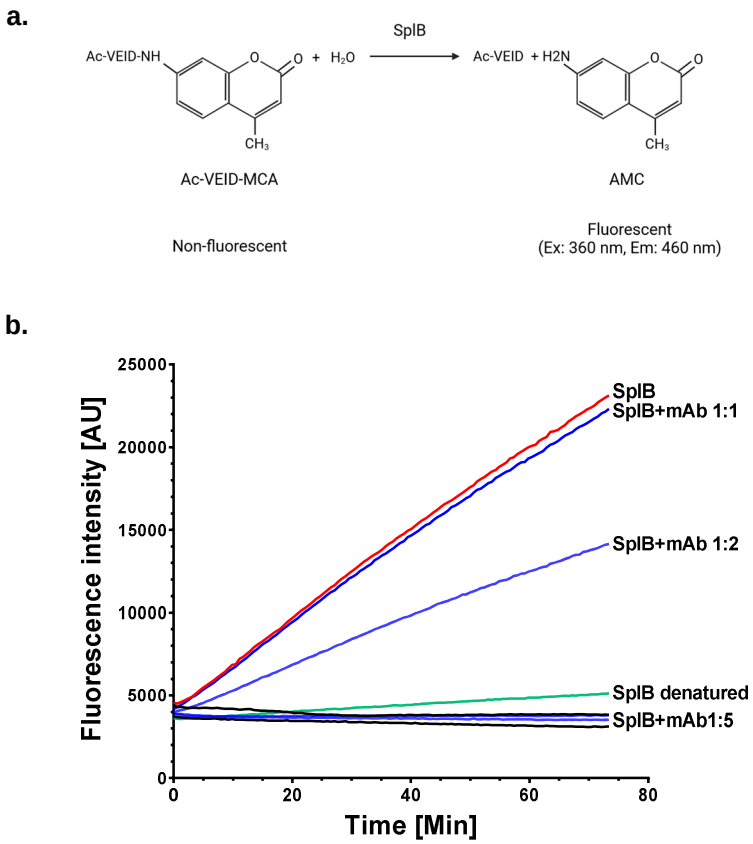

Figure 13. Anti-SplB mAb neutralizes the enzymatic activity of SplB. The enzymatic activity of SplB was quantified using the synthetic substrate Ac-VEID-MCA. (a) Proteolytic cleavage converts MCA into fluorescent AMC, which can be quantified using a fluorescent reader. (b) 0.5 µg recombinant SplB was incubated with different molar ratios (1:1, 1:2, and 1:5) of anti-SplB G8 mAb at 37 °C for 1 h. For positive control, native SplB was employed, whereas heat-inactivated SplB (90 °C for 30 mins) served as a negative control. After the addition of the Ac-VEID-MCA substrate, AMC generation was quantified over 75 mins. Native SplB efficiently cleaved the substrate in a time-dependent manner. The protease activity of SplB was neutralized by up to 50% when anti-SplB mAb was used in a 1:2 molar ratio, while complete neutralization was reached at a 1:5 molar ratio. The black lines show the substrate and anti-SplB mAb alone. One out of 3 similar experiments is depicted. Figure a was generated by using BioRender.

4.2.1.8. Anti-SplB mAb blocks SplB-induced vascular leakage

Several proteases, cytokines, and bacterial toxins are known to promote endothelial barrier damage. Various studies have demonstrated that endothelial barrier disruption can be induced by proteases that can activate PAR2. Our research group has shown that SplB activates PAR2, which leads to the induction of proinflammatory cytokines in endothelial cells [212]. Therefore, we hypothesized that SplB disrupts the endothelial barrier. To test this hypothesis, we carried out intravital microscopy to observe the integrity of the endothelial barrier *in vivo* in a mouse model of microvascular leakage. This work was initiated by a colleague Dr. Darisipudi Venkata Murthy and all experiments were performed in the laboratory of Prof. Christoph Reichel at the Walter-Brendel-Zentrum für Experimentelle Medizin, LMU München.

The cremaster mouse model is a commonly used model to visualize microcirculation and vascular injury in mice [213]. After sedating the mice and exposing the cremaster muscles,

intrascrotal stimulation with 10 µg SplB was carried out to observe the effect of SplB on the endothelial barrier. FITC dextran was intravenously applied, followed by administration of SplB. Administration of SplB led to massive leakage of FITC dextran across the vasculature into the perivascular space in the murine cremaster muscle. Treatment of animals with an anti-SplB G8 mAb 1 h prior to SplB administration almost abolished the SplB effect (Figure 14 a and b). These results demonstrate that SplB induces endothelial dysfunction and that anti-SplB mAb blocks SplB activities *in vivo*.

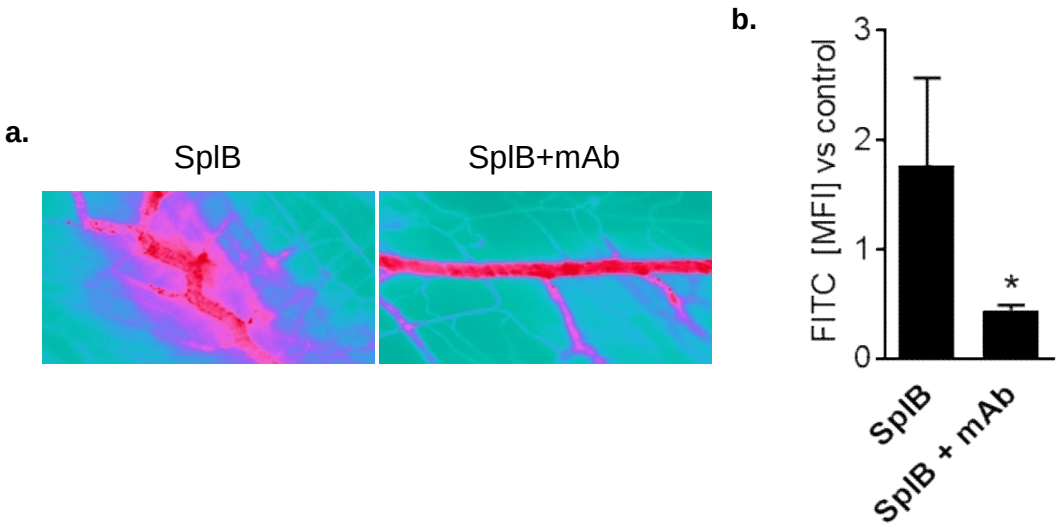

Figure 14. Anti-SplB mAb blocks SplB-induced vascular leakage. (a) Leakage of intravenously applied FITC-dextran to the perivascular tissue was analyzed in 6-8 weeks old male C57BL/6 WT mice after intrascrotal stimulation with SplB with or without pre-treatment with anti-SplB G8 mAb. The leakage of FITC-dextran was analyzed using fluorescence microscopy (excitation 488 nm, emission >515 nm), and a CCD camera was used to record the images. (b) The quantified FITC signal is shown in the graph. Mean Fluorescence Intensity (MFI) values in multiple (6) randomly selected regions of interest (ROIs, 50×50 µm^2), which are localized nearly 50 µm distant from the postcapillary venule under investigation, were measured with the use of Image J software. Data are mean MFI ± SD of 4-5 mice per group. T-test was utilized to determine statistical significance, *p <0.05.

In conclusion, we successfully generated a neutralizing SplB-mAb, which shows specific binding to the target protein. Though it shows moderate binding to SplB and has high sequence homology to the germline antibody sequence, it can efficiently neutralize the enzymatic activity of SplB up to 99% *in vitro* in a substrate-specific assay and *in vivo* in a mouse model of microvascular leakage.

4.2.2. Purification and characterization of murine anti-ClfA monoclonal antibodies

4.2.2.1. Purification of anti-ClfA murine mAbs

Along with the SplB hybridomas, our group has also generated six hybridomas that produce anti-ClfA mAbs from a single ClfA-immunized C57Bl/6 mouse: ClfA-001 - ClfA-006. As explained before (4.2.1.1), these hybridomas were expanded and the secreted mAbs purified by affinity chromatography (Figure S 6). An average of 13.7 mg of mAb was obtained for each anti-ClfA mAb from 1 liter of hybridoma culture supernatant (Table 2).

4.2.2.2. Anti-ClfA mAbs bind to the target ClfA

Out of 6 ClfA clones, 5 showed an identical strong binding to the recombinant ClfA in an ELISA, with a mean EC-50 of 0.067 µg/ml (range: 0.06-0.08). In contrast, ClfA-004 mAb did not show strong binding with an EC-50 of 2.16 µg/ml (Figure 15). The difference in the binding capacity of the ClfA-004 was intriguing. Therefore, we performed isotyping and BCR gene sequencing of all hybridomas to see if the 5 clones were identical and to which degree the ClfA-004 clone differed from them.

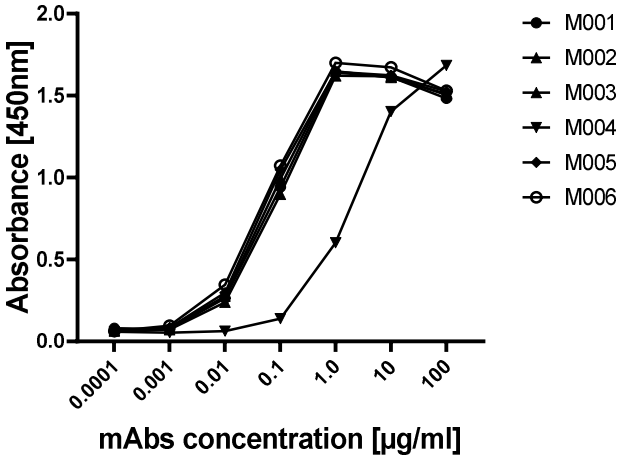

Figure 15. Murine anti-ClfA mAbs binds ClfA in a concentration-dependent manner. The ability of six purified murine anti-ClfA mAbs to bind to recombinant ClfA was determined by ELISA. Plates were coated with 1 µg/ml ClfA, blocked, and consequently incubated with serially diluted anti-ClfA mAbs. The binding of mAbs was visualized using a goat anti-mouse IgG conjugated to POD and TMB substrate. One of 3 similar experiments is depicted.

All six mAbs were subjected to isotyping as described before (4.2.1.2). The 6 ClfA mAbs (001-006) all belonged to the IgG2b subclass and had κ LCs (Table 12). Based on the isotype determination, suitable primers were selected for the BCR sequencing.

4.2.2.3. Sequencing revealed that 5 out of 6 anti-ClfA mAbs were identical

All 6 mAbs were derived from a single immunized mouse and showed comparable binding affinities except for ClfA-004 mAb. Sequencing of the DNA of mAbs was performed to analyze if the mAbs showing comparable binding have similar or identical sequences. Interestingly, the HCs of all 6 ClfA 001-006 mAbs were identical (Figure S 7). The LC of ClfA-004, however, differed in a single nucleotide from the other five sequences, resulting in an AA exchange from phenylalanine to tyrosine at the CDR3 region (Figure 16 a and b). Phenylalanine is a hydrophobic AA, while tyrosine is a polar AA that contains a hydroxyl group attached to the aromatic ring, making it hydrophilic, whereas its aromatic ring itself gives it hydrophobic characteristics. Fascinatingly, this single non-synonymous mutation greatly affected the binding property of the ClfA-004 mAb.

Finally, FRs and CDRs of the mAbs ClfA-002 (as a representative for the 5 identical mAbs) and ClfA-004 were identified by using IgBLAST and were graphically represented by using SnapGene Viewer (Figure 16). The HCs of ClfA-002 and ClfA-004 showed 97.4% similarity with the germline sequence. There were 4 silent and non-silent mutations each, and the non-silent mutations led to 2 AA changes compared to the germline sequence. The LC of ClfA-002 showed 100% similarity to the germline sequence, while LC of ClfA-004 has 99.6% similarity with the germline sequence with 2 non-silent mutations leading to 1 AA change (Table S 1). Since 5 mAbs were identical, ClfA-002 and ClfA-004 mAbs were chosen for the subsequent experiments.

4.2.2.4. Anti-ClfA mAbs bind the native and denatured ClfA to a varying degree

To test if the ClfA-002 and ClfA-004 mAbs bind to a three-dimensional or linear epitope on ClfA, dot blots were performed using native and denatured ClfA protein as the target antigen. As before, both preparations were pipetted on PVDF membrane, and 50 ng/ml of ClfA-002 and 300 ng/ml of ClfA-004 mAb was used as a primary antibody. The dot blot images revealed that both the mAbs bound much stronger to native than denatured ClfA (Figure 17, a – b), indicating that ClfA-002 mAb binds to a three-dimensional epitope that is destroyed upon heating. However, a partial refolding of the denatured protein during the experimental procedure and hence a recognition of a three-dimensional epitope cannot be fully excluded [214].

a. Light chain_ClfA-002

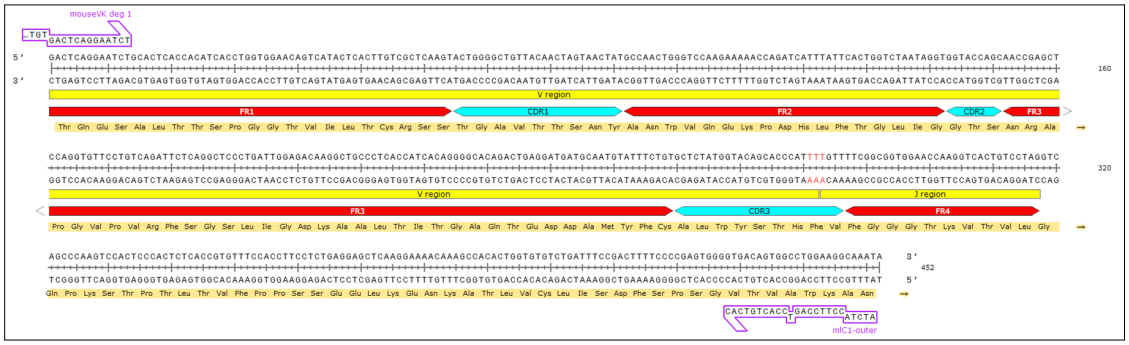

b. Light chain_ClfA-004

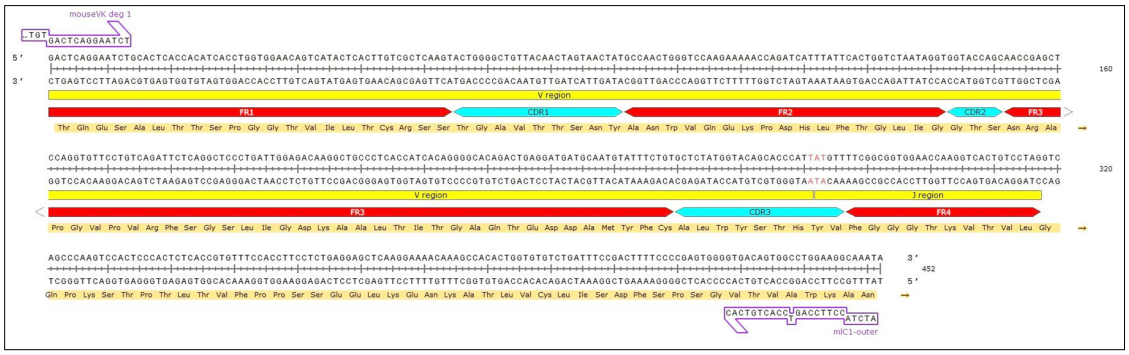

c. Heavy chain_ClfA-002 and ClfA-004

Figure 16. ClfA-002 and ClfA-004 mAbs differ in only a single amino acid in the LC. Hybridomas were lysed, and mRNA was extracted, transcribed into cDNA, and amplified via PCR. (a – c) The DNA sequence of the ClfA-002 and ClfA-004 mAbs were analyzed by using Ig-BLAST software to annotate the VDJ regions along with FRs (red) and CDRs (light blue) of LCs and HC, and the final image was generated by using SnapGene Viewer. The LCs differed in a single nucleotide, resulting in an AA exchange from thyrosine (Tyr) to phenylalanine (Phe) (shown in red), while the HC was identical for ClfA-002 and ClfA-004. The translated amino acid sequence is shown underneath the DNA sequence. Primers used for amplification are framed in purple.

4.2.2.5. Anti-ClfA mAbs shows no cross-reactivity with ECP of *S. aureus*

To determine whether the ClfA-002 and ClfA-004 mAbs cross-react with other *S. aureus* proteins, western blots were performed with *S. aureus* ECP. The ClfA-002 and ClfA-004 mAbs specifically bound to the recombinant ClfA and did not cross-react with any other protein in the

ECP extract, except for a weak band at ca. 35 kDa (Figure 18). Again, the strength of binding of ClfA-004 mAb was weaker as compared to ClfA-002 mAb.

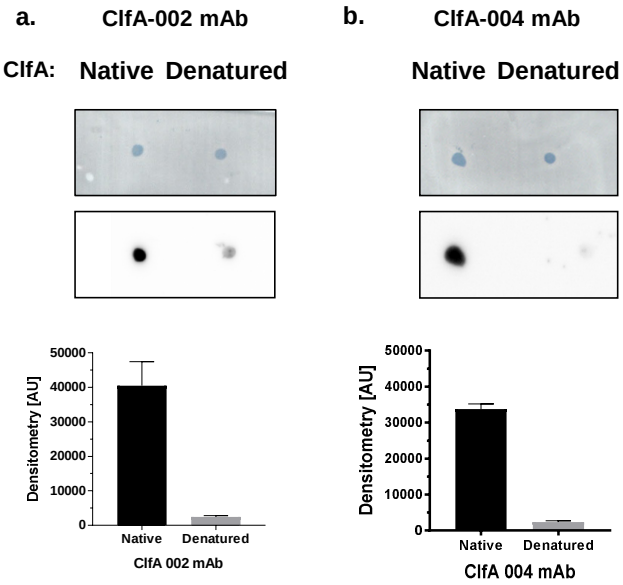

Figure 17. Anti-ClfA mAbs bind the native and denatured ClfA to varying degrees. (a – b) Native and denatured (heated at 95 ^{0}C for 5 mins) recombinant ClfA (1 µg**)** was pipetted on the PVDF membrane. Amido black 10B (upper panel) was used to visualize the proteins. ClfA-002 and ClfA-004 mAbs binding to native and denatured ClfA was subsequently established by western blotting using 50 ng/ml of ClfA-002 and 300 ng/ml of ClfA-004 (middle panel). To quantify the intensity of the band signal, densitometry was carried out by using ImageJ 1.52a (bottom panel)**.** A representative blot from three experiments, as well as mean +SD of densitometry data is shown.

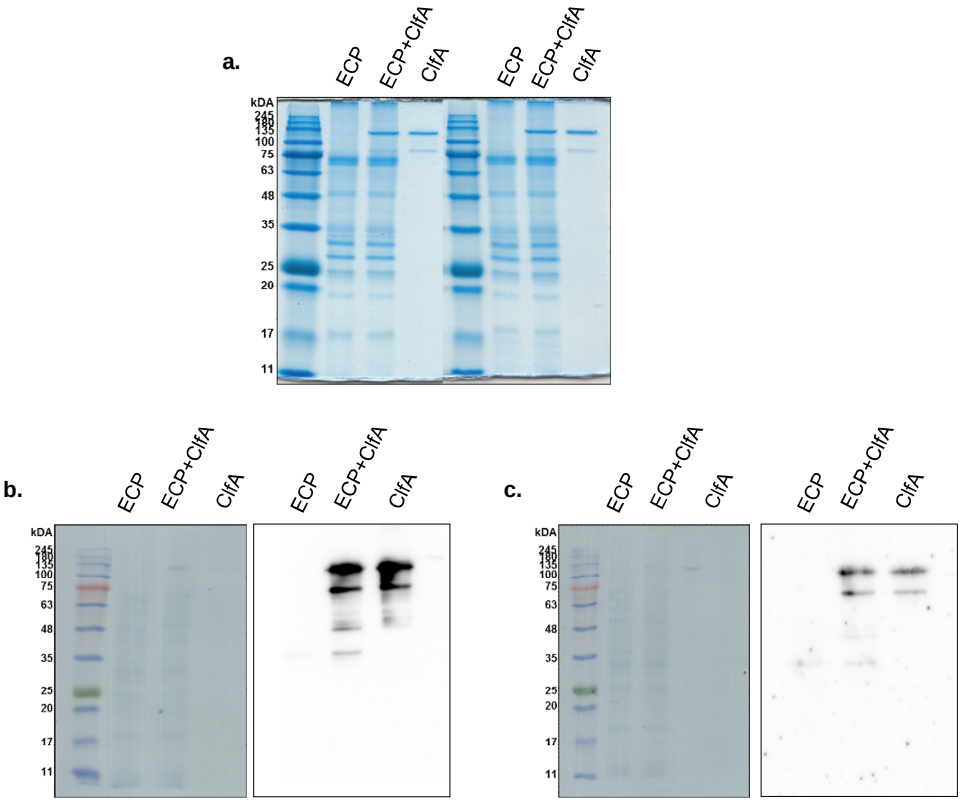

Figure 18. No cross-reactivity of anti-ClfA mAbs with other *S. aureus* proteins. (a) 10 µg of ECP, 1 µg of ClfA, and a mixture of both were analyzed by SDS-PAGE. (b and c, left panel) Two other SDS gels, which were run in parallel, were blotted onto PVDF membranes. Protein transfer was visualized with amido black 10B. (b and c, right panel) After that, a western blot was performed using 300 ng/ml of the ClfA-002 and ClfA-004 mAbs, α-mouse-IgG-POD detection antibody (1:100,000), and luminol substrate. One out of 2 similar experiments is depicted.

4.2.2.6. Anti-ClfA mAbs inhibits binding of fibrinogen (Fg) to ClfA

The binding of ClfA to Fg facilitates *S. aureus* attachment to surfaces coated with Fg during bloodstream infections. Besides that, this interaction also promotes bacterial agglutination in plasma, which plays a critical role in bloodstream infections. Therefore, the next step was to analyze if the ClfA-002 and ClfA-004 mAbs inhibit the interaction between ClfA and Fg. To perform that, ClfA was coated onto an ELISA plate and incubated with ClfA-002 and ClfA-004 mAbs. Then, human Fg was added, and its binding ability to ClfA was measured, which was detected by anti-Fg antibodies.

ClfA-002 mAb inhibited the binding of ClfA to human Fg in a concentration-dependent manner (Figure 19). This mAb inhibited ClfA binding to Fg by ~60% when 100 µg/µl mAb was used. Inhibition increased to ~ 70% when 1,000 µg/µl mAb was used. In contrast, ClfA-004 showed an inhibitory effect only at the highest tested concentration. Since both mAbs differ in only a single AA, these findings point to a lower binding strength and faster dissociation of ClfA-004.

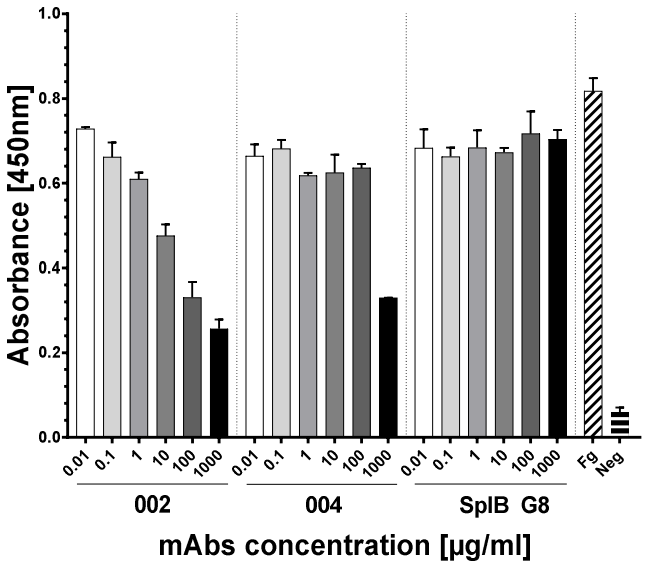

Figure 19. ClfA-002 mAb inhibits binding of Fg to ClfA. 2 µg/ml ClfA was coated on a plate and incubated overnight at 4°C. Following incubation with different concentrations of the mAbs, human Fg (20 µg/ml) was added, and Fg binding to ClfA was quantified using an anti-Fg-HRP detection antibody. ClfA-002 inhibited the binding of ClfA to Fg in a concentration-dependent manner, while ClfA-004 showed an inhibitory effect only at 1,000 µg/ml. Concentrations are depicted as µg/ml. Data from 3 replicates are shown here.

Overall, both ClfA-002 and ClfA-004 mAbs bind to ClfA with different strengths because of the single AA change. Besides, both the mAbs showed stronger binding to the native ClfA rather than the heat-denatured. Moreover, ClfA-002 mAb can inhibit Fg binding to ClfA while ClfA-004 did not show the same inhibitory effect.

4.2.3. Purification and characterization of murine and humanized anti-FnbpA mAbs

4.2.3.1. Purification of anti-FnBPA mAbs

Using hybridoma technology, two murine and twelve humanized hybridomas producing anti-FnBPA mAbs were recently generated. The two murine mAbs E9 and D4 were generated by immunizing C57Bl/6 mouse. Moreover, twelve humanized mAbs (5F12/D2/F8, 5F12/D3/D1, 6E1/C1, 6E1/B4, 6A10/A1, 5F12/D2/D11, 5F12/E4, 6H10/H1/B11, 6G1/H1, 6H10/A1/B8, 5F12/D2/E9 and D3/D7) were generated by immunizing C57Bl/6 (HHKK and HHKKLL) with FnbpA. All the mAbs were purified as mentioned before (4.2.1.1) (Figure S 8). A total of 10-15 mg of mAbs were obtained for each anti-FnBPA mAb from 1 liter of hybridoma supernatant.

4.2.3.2. Murine and humanized anti-FnBPA mAbs bind to FnBPA

The two murine mAbs showed strong binding to FnBPA with an EC-50 of 0.11 (D4) and 0.019 µg/ml (E9) in an indirect ELISA (Figure 20, a). Notably, the twelve humanized FnBPA mAbs showed a similar, moderate binding to the recombinant FnBPA, with an EC-50 between 2.54 – 5.4 for 5F12/E4, 6A10/A1, D3/D7, 6E1/C1, 5F12/D2/F8, 5F12/D2/D11, 5F12/D3/D1, 6H10/H1/B11, an EC-50 between 8.2 – 11.97 for 6E1/B4, 5F12/D2/E), 6G1/H1 and an EC-50 of 59.75 µg/ml for 6H10/A1/B8 (Figure 20, b).

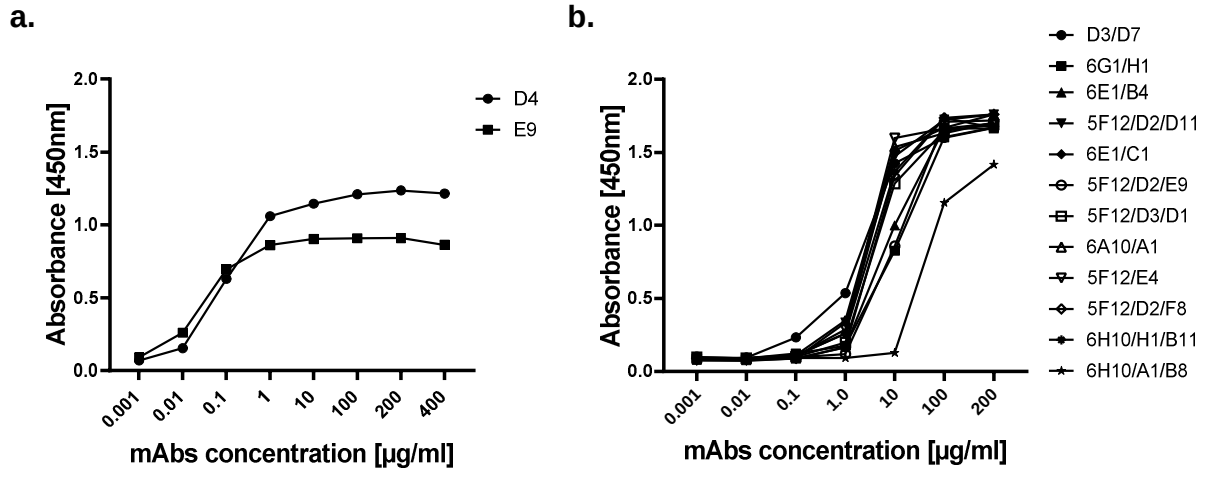

Figure 20. Murine anti-FnBPA mAbs bind with higher affinity to the recombinant FnBPA than the humanized anti-FnBPA mAbs. (a – b) The capacity of the purified murine and humanized anti-FnBPA mAbs to bind to recombinant FnBPA was tested by ELISA. The 96-well microtiter plates were coated with 1 µg/ml FnBPA, blocked, and afterwards incubated with serially diluted anti-FnBPA mAbs. The binding of mAbs was visualized using a goat α-mouse IgG-POD secondary antibody and TMB substrate. One of 3 similar experiments is depicted.

4.2.3.3. Anti-FnBPA mAb inhibits binding of fibronectin to FnBPA

Next, the ability of anti-FnBPA mAbs to inhibit binding of FnBPA to Fg and Fibronectin (Fn) was tested to shortlist the candidate mAbs for further downstream analysis (Figure 21). FnBPA binding to Fg and Fn facilitates *S. aureus* biofilm formation and invasion. The A domain of FnBPA, which binds to Fg and elastin, is involved in biofilm formation and helps in forming cell aggregates, while the Fn-binding R domain is used by *S. aureus* to bind to the N-terminus of Fn (Figure 21, a).

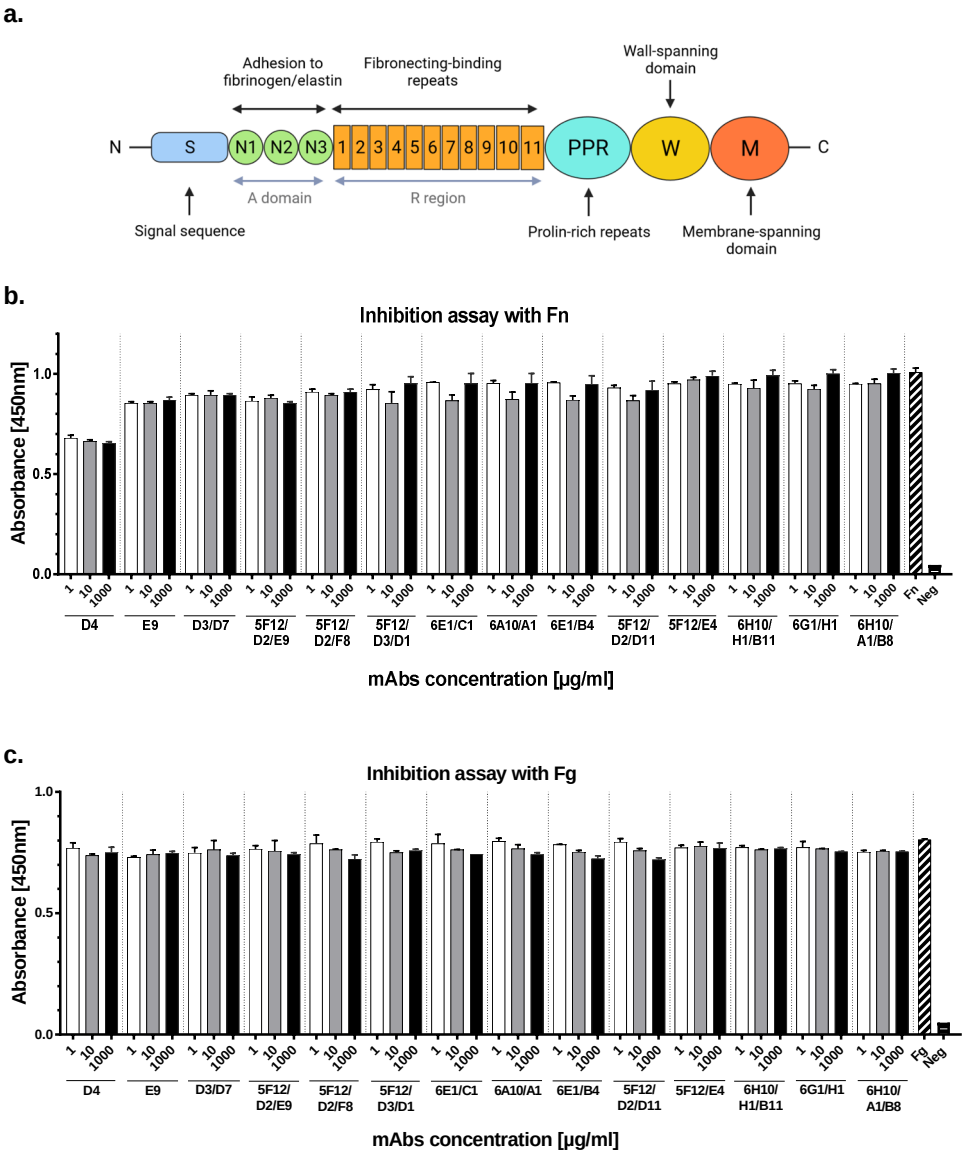

Figure 21. One murine anti-FnBPA mAb moderately inhibits binding of Fn to FnBPA. (a) Schematic representation of the *S. aureus* FnBPA protein. The primary translation product of FnBPA contains a secretory signal sequence (S), the A region comprising N1, N2, and N3 subdomains that are involved in Fg and elastin binding as well as cell-cell aggregation during biofilm formation, 11 tandem repeats of Fn-binding domains (R region), proline-rich repeats (PRR), the cell wall-spanning region (W), the membrane-spanning domain (M), and the positively charged tail (adapted from O'Neill et al. 2008). (b – c) 96-well ELISA plates were coated with 2 µg/ml recombinant FnBPA. After washing and blocking, purified murine and humanized anti-FnBPA mAbs, in different concentrations (1, 10, 1000 µg/ml), were incubated for 1 h at room temperature. Afterwards, 20 µg/ml human Fn or 20 µg/ml human Fg was added to the respective plates. Fn or Fg binding to FnBPA was quantified using anti-Fn, and anti-Fg HRP labeled antibodies. D4 and E9 are murine mAb, and all other clones are humanized mAb. Figure a is generated by using BioRender.

FnBPA-coated ELISA plates were incubated with murine and humanized anti-FnBPA mAbs in different concentrations, followed by the addition of human Fn or human Fg. Ligand binding was quantified using anti-Fn and anti-Fg antibodies. Out of the two murine and twelve humanized mAbs, only the murine mAb D4 slightly inhibited (21%) the binding of FnBPA to Fn when 1µg/ml of the D4 mAb was used. None of the other mAbs inhibited Fn or Fg binding to FnBPA (Figure 21, b – c). FnBPA has eleven Fn-binding repeat motifs, and each motif can bind the N-terminus of Fn. To focus further analysis on the most interesting mAbs, the two murine mAbs (D4 and E9) were chosen for downstream analyses.

The immunoglobulin subclass determination (isotyping) showed that the two murine anti-FnBPA mAbs (D4 and E9) belonged to the IgG2b subclass and had κ LCs (Table 12).

4.2.3.4. Sequencing revealed that the two murine mAbs are not identical

The two murine mAbs D4 and E9 were derived from the same immunized mouse but showed different functional properties. To correlate mAb function with its underlying sequence, the gene segments encoding the variable regions of LCs and HCs were analyzed as mentioned before (

Figure 22). Notably, the LCs and HCs of D4 and E9 showed multiple nucleotide differences in FR1, CDR1, FR2, CDR2, FR3, and CDR3 regions (Figure S 9). The LC of D4 had 97% similarity with the germline sequence with 2 silent and 7 non-silent mutations, which resulted in 6 AA changes. The HC of D4 has 95.3% similarity with the germline sequence. It has 3 silent mutations and 12 non-silent mutations leading to 11 AA changes. Similarly, the E9 LC has 82.8% similarity with 11 silent mutations and 41 non-silent mutations. The non-silent mutations, in this case, led to 31 AA changes. The HC of E9 has 80.1% similarity with the germline sequence with 15 silent and 44 non-silent mutations, which translated to 25 AA changes (Table S 1).

a. Light chain D4

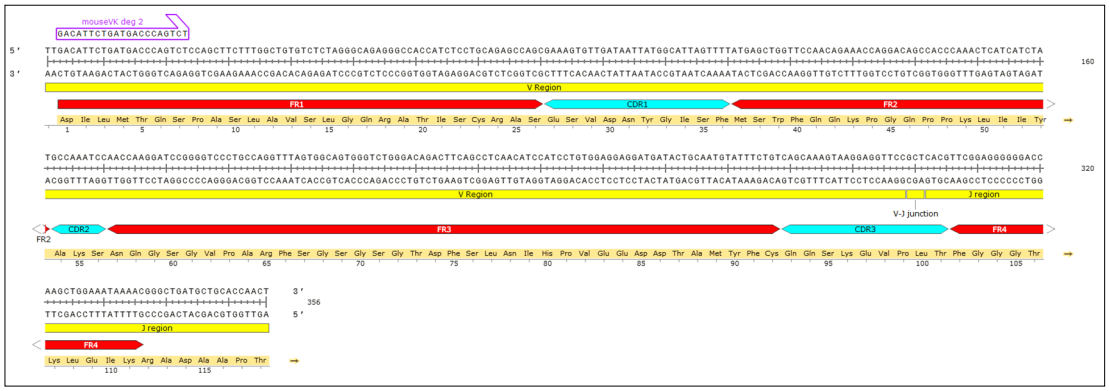

b. Heavy chain D4

c. Light chain E9

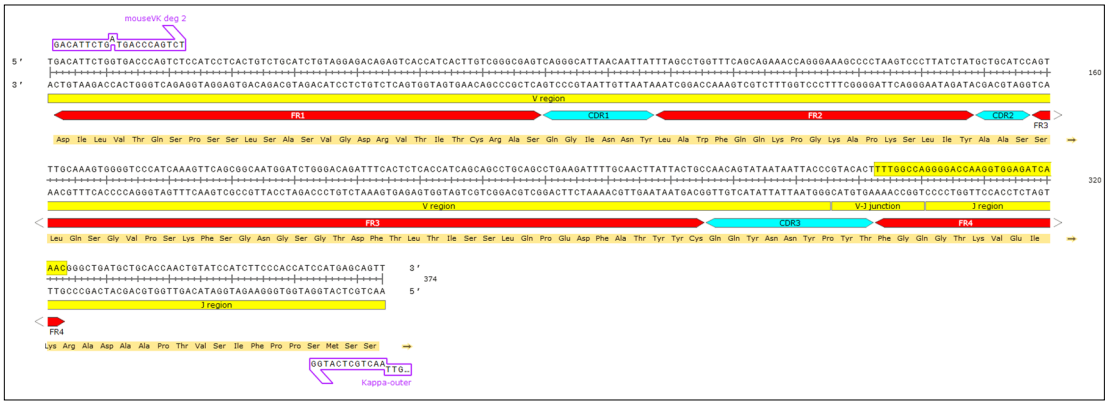

d. Heavy chain E9

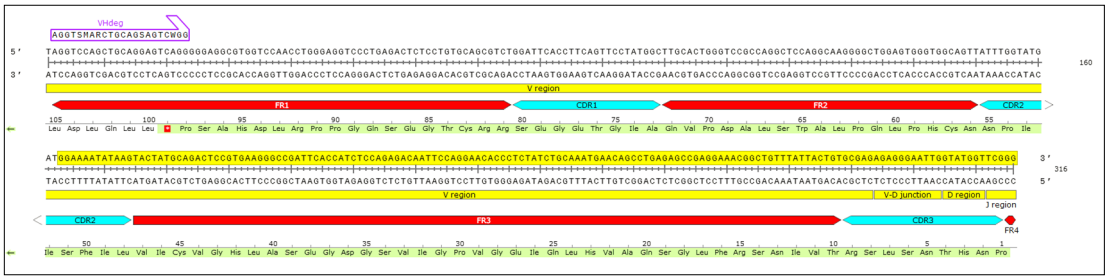

Figure 22. Major differences in the sequenced variable regions of the HCs and LCs of the murine anti-FnBPA mAbs. RNA was isolated from anti-FnBPA D4 and E9 hybridomas, followed by cDNA generation, PCR amplification, and sequencing. (a – d) The DNA sequence of the two murine mAbs was analyzed by using Ig-BLAST software to annotate the VDJ regions along with FRs (red) and CDRs (light blue) of LCs and HC. The final image shown here was generated by using SnapGene Viewer. The LCs and HCs of FnBPA D4 and E9 have differences in the nucleotide sequence in FR and CDR regions. The translated sequence of the amino acids is shown underneath the DNA sequence. Primers used to amplify the DNA sequences are framed in purple.

4.2.3.5. Murine anti-FnBPA mAbs bind both the native and denatured FnBPA

To test if the murine FnBPA mAbs bind to a three-dimensional or linear epitope on FnBPA, dot blots were performed using native and heat-denatured FnBPA as the target antigen. The murine anti-FnBPA mAbs (D4 and E9) bound to both native and denatured FnBPA with similar strengths, suggesting that mAbs recognize the linear, surface-exposed epitope (Figure 23).

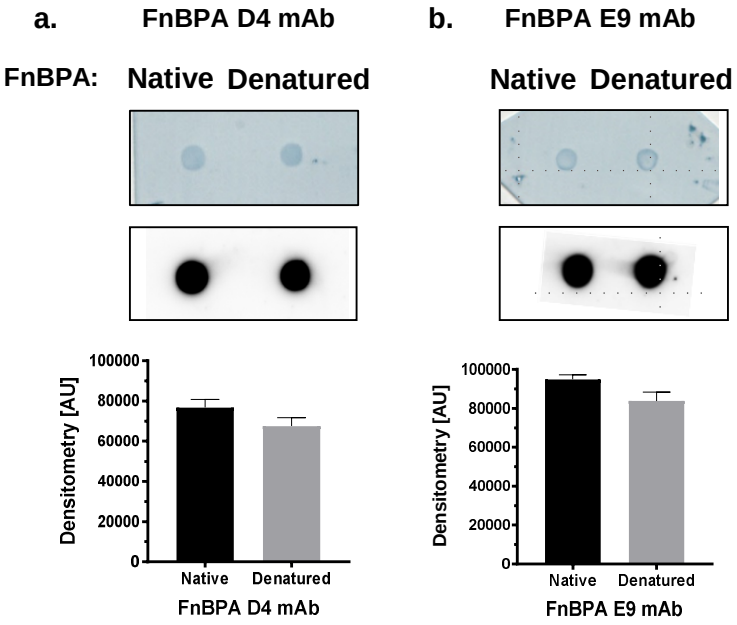

Figure 23. Murine anti-FnBPA mAbs bind the native and denatured FnBPA. (a – b) Recombinantly produced native and denatured (heated at 95 °C for 5 mins) FnBPA (1 µg) was pipetted on the PVDF membrane. The proteins were visualized with amido black 10B (upper panel). Anti-FnBPA mAb binding to native and denatured FnBPA was afterwards determined by western blotting using 50 ng/ml of the murine mAbs D4 and E9 (middle panel). Densitometry was performed using ImageJ 1.52a to analyze the signal intensity of the blot (bottom panel). A representative blot from three experiments is shown, and mean +SD of densitometry data is shown

4.2.3.6. Anti-FnBPA mAbs do not cross-react with other *S. aureus* ECPs

To check if the anti-FnBPA mAbs cross-reacts with other *S. aureus* proteins, western blots were performed, as explained before. The murine mAbs specifically bound to the recombinant protein and showed a slight cross-reactivity with ECP preparation which could be a protein with sequence homology to FnBPA (Figure 24 a and b).

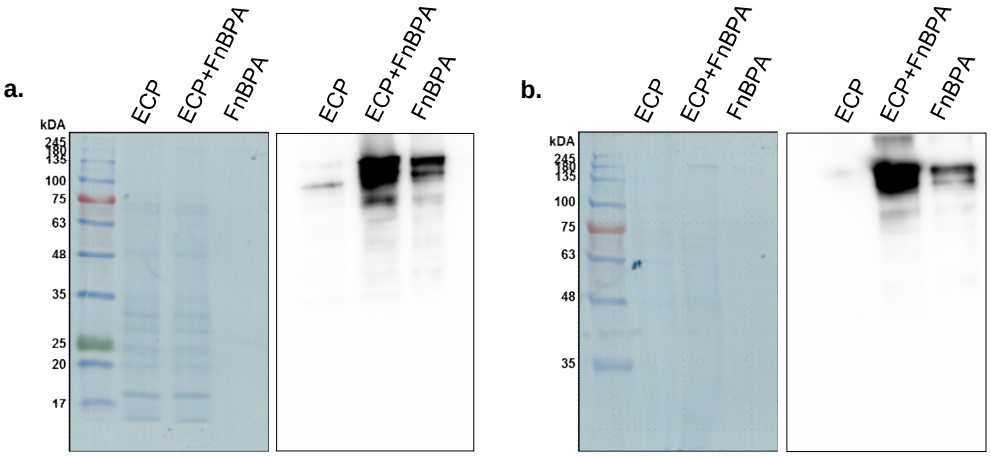

Figure 24. Anti-FnBPA mAbs do not cross-react with *S. aureus* ECP. (a – b) For analyzing the cross-reactivity of the anti-FnBPA mAbs to *S. aureus* ECP, 10 µg of ECP, 1 µg of FnBPA, and a mixture of both were run on an SDS-PAGE, and then, they were blotted onto PVDF membranes. Protein transfer was visualized using amido black 10B. (a – b, right panel) Western blotting was performed using 300 ng/ml of anti-FnBPA mAbs (D4 and E9), α-mouse IgG-POD antibody, and luminol substrate. One of two similar experiments is depicted.

Overall, the dot blot confirms that the mAbs recognized a linear epitope. Furthermore, both of the murine mAbs showed slight cross-reactivity with ECP of *S. aureus*. Besides, both the DNA sequences of D4 and E9 are not identical. Moreover, only anti-FnBPA D4 slightly inhibited the binding of Fn to FnBPA.

5. Discussion

5.1. Pathogen-specific antibody response in IE

5.1.1. GIES - a pilot study aiming at identifying novel biomarkers for IE

IE is a potentially lethal multisystem disease with highly variable clinical signs that make its diagnosis challenging [5, 215]. The difficulty in diagnosis can be attributed to the lack of fast and reliable diagnostic procedures, which can lead to the diagnostic latency of 29 to 35 days, further complicating the infection [50, 216]. The consortium Card-ii-Omics aimed at identifying biomarkers for IE by analyzing plasma proteomics (Department of Functional Genomics, Greifswald), as well as identifying the causative agent(s) by using antibody profiling (Institute of Immunology, Greifswald).

The GIES cohort comprised of 17 IE patients and 20 controls with a mean age of 69.9 and 61.6, respectively. The majority of the IE patients were males (70.6%). This observation confirms previous studies reporting that IE is more prevalent in older male adults [2, 217–219].

In our pilot study, pathogens were isolated from BC in 13/17 (76.5%) IE cases. This rate is similar to other studies where 30-80% of IE cases could be diagnosed via microbiological assays. The variation of successful BC diagnosis depends on the usage of antibiotics by the patients and the country of study [2, 19, 21, 220]. Moreover, in our study, *S. aureus* and *S. epidermidis* were isolated from BC in 3/17 (17.6%) and 4/17 (23.5%) of the cases, which are also reported to be the most prevalent pathogens in IE [2, 19, 219, 221–223]. The gut pathogens *E. faecalis* and *E. faecium* were isolated from two patients. These pathogens are the third leading cause of IE [5, 222, 224]. Hence, despite our small sampling size, our GIES data reflect the previously reported ranking of causative pathogens.

In our pilot study, we observed strongly elevated CRP levels in IE patients as compared to controls (74.7 vs. 7.25 mg/l, $p < 0.0001$). Moreover, WBC counts tended to be higher in patients than controls (17.8 vs. 6.0 × 10^9/l, $p < 0.05$). CRP and WBC counts have been previously evaluated for their prognostic values in IE patients [225]. 13/17 IE patients had a CRP value above 40 mg/l, which is considered a threshold for serious clinical outcomes [202]. CRP values of 93 mg/l or above and WBC of 11.6 × 10^9/l or above have been associated with severe complications or death in IE patients [225, 226].

Various methods are used in research and clinical settings to diagnose IE and identify the causing pathogen. An early and accurate diagnosis will help initiate effective antimicrobial therapy and influence morbidity and mortality. The modified Duke criteria require a combination of clinical, microbiological, and endocardiography results [19]. BC is the standard and most important diagnostic approach, upon failure of which molecular techniques are employed [2, 4, 23]. More recently, serological assays moved into focus for diagnosing pathogens, especially in the case of BC-negative IE. Serological assays may aid in diagnosing fastidious pathogens or those bacterial agents that are hard to culture [19]. Moreover, they are not affected by antibiotic treatment.

In this work, we used the infection array to determine the pathogen-specific antibody response on the day of diagnosis in IE patients. As plasma samples were collected at different time points for some patients, we were also able to analyze the kinetics of the humoral immune response. Since IgG is the most common antibody class in normal human serum (70-85%) and the most important for defense against various pathogens, only IgG was measured in the infection array [227]. The infection array allowed us to study the antibody response in IE patients against 30 different pathogens, making it the first study to use a comprehensive IE-related pathogen panel using xMAP technology. It also allowed us to study the antibody response and the immune memory generated against commensals and opportunistic pathogens.

5.1.2. Antibody profiling at day 0 provides insights into the pathogen-specific antibody repertoire

Initially, pathogen-specific IgG antibodies were determined in plasma samples of controls and patients at the time of diagnosis. Antibodies against a broad range of pathogens were detected in both controls and IE patients, corroborating previous studies [44, 228]. There was no significant difference in the antibodies titers between controls and IE patients, except for *E. faecalis* and *S. lugdunensis*. In line with our data, antibodies against pathogens such as *S. aureus*, *E. faecalis*, *C. albicans*, and *E. coli* were previously reported in healthy individuals [105, 108, 205, 229–231]. This suggests that over time the immune system comes in contact with these pathogens, and under steady-state conditions, memory B cells and plasma cells maintain a basal level of IgG antibodies.

Higher antibody titers were detected against microbes residing on the skin than against microbes residing in the gut, throat, or the environment. Human skin is densely populated by microbes ranging from commensal bacteria, fungi, and viruses which interact with our immune

system and promote homeostasis [232]. Though intact skin is a formidable barrier to both the commensals and pathogens, a disruption of this barrier could be harmful [232]. Additionally, human skin epithelial surface area is nearly 30 m^2 [233, 234], thus providing a large ground for skin microbes to trigger an immune response in the case of breach of the skin barrier. Under steady-state conditions, the human epidermis harbors billions of T cells composed mainly of resident cells and recirculating memory T cells. In the case of skin breach, microbes trigger a localized immune response [235]. Skin homing T cells carry the memory of the antigens which enter through the skin and play an important role in host defense [236]. Upon reexposure of the antigens, it can activate other immune cells (e.g., B cells) or cells in the local environment (e.g., keratinocytes). If the infection is more invasive, then a systemic response is triggered, leading to B cells activation and IgG response [235, 237]. The adaptive immune system takes almost a week to mount a response against an antigen that is encountered for the first time. In our study, skin breaches and repeated minor exposure could lead to high antibody titers against skin microbes and could explain our observation.

Serum IgG titers against gut microbes were detectable but comparably low in both IE patients and controls, except for *C. albicans*. Gut microbes do not pose a threat unless the gut epithelium is compromised. Immunosuppression, damage to the mucosal barrier integrity, or disturbance of the bacterial microbiota can lead to local or disseminated infections [238, 239]. Usually, the gut-associated immune system protects the mucous membrane from penetrating microbes by stimulating mucus production and secreting antimicrobial peptides and IgA. This prevents the transfer of gut microbes from the gut to the bloodstream [240]. Upon the damage of the gut epithelium, the microbes can cross the mucosa into the bloodstream and cause systemic infection, which will lead to IgG response [237, 241]. Previous studies have revealed through antibody profiling with a protein microarray that robust IgG response against gut microbes is common in healthy individuals [230] as well as patients (Crohn's disease, ulcerative colitis) [242]. Similarly, IgG antibodies were present against purified microbiota in healthy individuals when they were tested by flow cytometry assay. About 1% of the gut microbes were bound by the serum IgG of healthy individuals [231]. Serum IgG levels against the gut microbes belong to bacteroidia, and clostridia class develop between 6 and 12 months of age, peak around 2 years of age, and become stable in adulthood [230, 231]. These reports support our observation of the IgG response against gut microbes on the day of diagnosis (d0).

Moreover, higher antibodies titers were detected in controls and patients against opportunistic pathogens (*E. faecalis, E. faecium, C. albicans, S. haemolyticus, S. sanguinis, S. aureus,* and

S. epidermidis) than commensals (*K. aerogenes, K. oxytoca, K. pneumoniae, S. hominis*). This phenomenon illustrates the differential ability of microbes to mount corresponding antibody responses [44, 229]. A huge fraction of commensal microbes (75%) on the mucosal surfaces (nasal and gut) are covered by IgA antibodies during homeostatic conditions, which may contribute to the immune exclusion of its target [52, 237]. Besides, toll-like receptors (TLRs) can differentiate between commensal microbes and pathogens and trigger immune responses accordingly [243]. However, commensals can become pathogens, and thus no microbe can be considered exclusively beneficial [244]. In some conditions, commensals can cause infections if their growth is not kept in check or when the host is immunocompromised [237]. Nevertheless, it is suggested that the opportunistic pathogens cause more damage and harbour more virulence factors which activate the immune response in a stronger way leading to a higher antibody response [245, 246]. This could explain the higher antibody titers against opportunistic pathogens in our study.

Interestingly, the highest antibody titers in both IE patients and controls were detected against an opportunistic fungus, *C. albicans.* It is well documented that IgG antibodies are readily generated against *C. albicans* upon systemic infection, and serological assays have been suggested for diagnosing candidiasis [247–250]. Antibodies inhibit the adhesion of *C. albicans* to the host surfaces to different degrees. They may also contribute to controlling its multiplication and can be immunoprotective during infections [251]. The high antibody titers against *C. albicans* could be explained by the arguments provided in detail in section 5.1.3.4.

Extraordinary high antibody titers were detected against *S. aureus* in both controls and IE patients. Similarly, our group recently observed very high anti-*S. aureus* antibody titers in healthy controls and sepsis patients using the 20-plex infection array [44]. Our observations corroborate other studies that have shown that anti-*S. aureus* antibodies occur in almost all carriers and non-carriers and get triggered and boosted by *S. aureus* infections [52, 105–108]. In the event of an endogenous *S. aureus* infection, the strong, strain-specific antibody response is thought to provide protection from severe disease courses [52, 107, 252]. The factors determining the difference between *S. aureus* as a commensal and as a pathogen are still not clear. Feil et al. reported no significant differences between strains isolated from carriers and strains isolated from patients with invasive pathogens [253]. On the contrary, certain strains belonging to a certain clonal complex (e.g., CC30) are more invasive [52]. Similarly, Jenkins et al. reported that upregulation of virulence factors like *sdrC, fnbA, fhuD, sstD,* and *hla* (adhesins and toxins) in invasive pathogenic strains [246, 254]. These might explain the duality

of interaction between *S. aureus* and the host and might explain why some strains present more vigorous challenges to the host.

Already at the day of IE diagnosis, high antibodies titers were detected against those pathogens that we also diagnosed through BC, e.g., *E. faecium, S. aureus, and S. epidermidis*. This shows that the serological assay is consistent with the microbiological diagnosis. Interestingly, it suggests that the onset of infection was several days before the day of diagnosis (d0), because in the case of the primary response, it would take 7-10 days to mount an antibody (IgM > IgG) response while in secondary response, it will take 3-5 days (predominantly IgG) [237]. Detecting higher IgG antibodies at d0 against the pathogens isolated from the BC suggests that the infection started before d0. This is supported by the analysis of consecutive IE biosamples as outlined below. Hence, the timing of sample collection is crucial in serological assays, especially in chronic infectious diseases such as IE, and strongly impacts data interpretation.

5.1.3. Kinetics of pathogen-specific IgG responses in IE patients

To gain insights into the kinetics of the pathogen-specific IgG responses in IE patients, we also analyzed antibody levels in the back-up (before d0) and follow-up (after d0) samples from the IE patients. Since the production of pathogen-specific IgG takes time during primary and secondary infections, the inclusion of back-up and follow-up samples could give us a clue about the causative pathogen. As GIES was originally designed to study the plasticity of immune cells in whole blood on the day of IE diagnosis using RT-DC, only d0 samples were collected. Later on, the scope of the study was extended to analyze the antibody response in IE patients. Back-up and follow-up samples were collected at ZIK HIKE, Greifswald, as well as the Institute of Immunology, Greifswald. Moreover, only a few patients visited the hospital for a check-up, and hence follow-up samples were only collected from those patients. Furthermore, the time distance between the sample collections was not uniform. In some cases, the follow-up and check-up sample was collected a couple of weeks after diagnosis (14 days, P38), while in some cases, it took months (6.5 months, P14). Therefore, these limitations must be considered when interpreting the obtained antibody profiles.

In 8/13 cases, we observed a > 2-fold increase in IgG antibody titers against one or more pathogens. Based on the comparison of the antibody profiles with BC results, the patients were divided into 5 groups: (1) serology confirms (and extends) microbiological diagnosis (2 cases), (2) serology contradicts microbiological diagnosis (3 cases), (3) serology identifies pathogens while microbiological diagnosis is negative (3 cases), (4) serology does not identify pathogens

while microbiological diagnosis is positive (3 cases), and (5) both serology and microbiological diagnosis are negative (2 cases).

The reasons for the observed discrepancies fall into two categories. (1) BC was negative or detected a different pathogen than the infection array, and (2) the infection array was negative.

Negative BCs are a major hurdle in IE diagnosis and can have several reasons. BC can be negative in 60-65% of cases when a patient is using antibiotics, which could obfuscate diagnosis [19, 35]. Another reason for the serological assay being positive and BC being negative could be an unrelated infection at another body site. For instance, in P36, *C. albicans* was not detected in the BC but was isolated from the tracheal secretions, and the infection array indeed detected an increase in antibody titers against it. *C. albicans*, though rarely, is involved in causing pneumonia and accounts for 0.7% of the cases in primarily immunocompromised patients [255]. Similarly, in P38, BC was negative, but *E. cloacae* was detected in urine, and high antibody titers were detected against it in the infection array. *E. cloacae* is involved in urinary tract infections and could possibly be involved in causing infection, thus explaining our findings [256]. This suggests that a concurrent and unrelated infection at other body sites could lead to positive serology while the BC is negative.

In 3/13 cases (P8, P12, P40), high antibody titers were detected against pathogens that did not correspond to the pathogens detected by BC. This could be attributed to contamination of the BC during sampling by skin commensals. Indeed, 15-30% of the isolated organisms in the hospitals are contaminants, and the majority of them are coagulase-negative staphylococci (CoNS) [257]. Interestingly, these findings corroborate our study, where 2/3 cases (P12 and P40) showed an increase in antibody titers against CoNS.

Conversely, a negative infection array can also have several reasons, e.g., timing, immunosuppression, and pathogen coverage. In our pilot study, in 3/13 cases BC was positive while the infection array was negative. This could be attributed to the timing at which samples were collected, and it is explained in detail later (5.1.3.1). Shortly, if the onset of infection was before d0 then the antibody titers might have reached the plateau, and the increase in titers would not be detected unless a series of samples are taken before and after the onset of infection. Moreover, the patients might not generate a robust immune response because of various factors, including immunosenescence and the usage of immunosuppressive drugs [258–261]. The mean age of IE patients is approximately 70, which could strongly impact the generation of a robust immune response and contribute to the disproportionate rate of IE infections in the elderly. For

instance, in P17, P25, and P37 (all above 75 years of age), an increase in IgG titer was not observed, suggesting that age could be an important factor. Furthermore, the majority (11/17) of the patients were on immunosuppressive drugs (e.g., Desloratadin, Ibuprofen, Ranitidin, Targin, Metamizol); yet, a strong correlation could not be observed between drugs usage and antibody response. Besides, IE prevalence in immunocompromised patients is not well documented [2, 262].

Another reason for negative serology could be that the infecting species or strain type is not included in the infection array. For instance, pathogens like *Coxiella burnetii*, *Bartonella* spp., and *Brucella* spp., are not added to our infection array panel, which might be causing IE. Moreover, most of the *S. aureus* species are genetically highly variable, and the chosen strain might not represent the clinical isolate very well. In fact, no bacterial strain can truly represent its species [263]. Genetic variation in species like *P. aeruginosa* and *S. aureus* can correlate with disease severity [264, 265]. Furthermore, *S. aureus* isolates encoding *tst* show a significantly higher IgG and IgA response against TSST-1 as compared to *tst*-negative isolate [41, 58], thus supporting the argument that strain-specific antibody response could be a limiting factor in a serological assay. Nevertheless, a similar increase was observed in our study against both the *S. aureus* strains. Overall, more species and, if necessary, also strain types should be added to the infection array to broaden its coverage.

Fastidious microbes are hard to culture and could lead to false-negative results in routine BCs [2, 19]. Therefore, alternative assays such as serological assays and PCR are used to suggest a causative pathogen in 60% of the IE cases [266]. In another study, serology assay provided a diagnosis in 77% of the BC-negative IE [267]. Serological assays have been successfully used against IE-causing pathogens such as *Coxiella burnetii*, *Bartonella* spp., *Brucella* spp., and *Tropheryma whipplei*, and because of this reason, it has been added to the major clinical criteria for IE diagnosis [2, 266, 267]. Because of the success of serological assay in the diagnosis of BC-negative IE, it could be used to detect fastidious pathogens, which could reduce the chances of false-negative BC diagnosis. Besides serology, 16 and 18S rRNA sequencing is employed to diagnose the IE causing pathogen from the blood and valvular biopsies.

5.1.3.1. Timing of sample collection is crucial

As discussed before, initiating or amplifying an antibody response takes time: 7-10 days for primary infections and 3-5 days for secondary infections [237]. In consequence, the timing of sample collection is an important factor for antibody profiling [106, 237, 268].

As discussed in section (5.1.3), the samples in GIES were not collected in a uniform manner. On the one hand, in some cases, the time distance between samplings is too short (2 to 3 days in the case of P42 and P37), and further follow-up samples of the later time points were not available. In both of these cases, an increase in antibody titer was not observed. On the other hand, the follow-up samples were collected after more than 30 days in the case of 5 patients. Samples collected at such a late time point could complicate the interpretation of data because the patients could suffer from further IE-unrelated infections in the meantime.

Interestingly, in P36 and P38, no significant change in antibodies titers was observed against any pathogen from d0 to d21 and d14, respectively, but a significant increase against multiple pathogens was recorded from d-6 to d21 and d14 (Table 11). This observation suggests that the time point at which diagnosis was confirmed (d0) was not the actual day of the start of infection. At d0 the antibody titer might have already reached a plateau, and because of this reason, the fold change in the follow-up samples was not significant.

In conclusion, the timing of sample collection is very crucial to detect a change in antibody titers. Therefore, samples should be collected during routine check-ups from patients who are more susceptible to diseases such as IE. Having a biobank of back-up samples from patients at regular check-ups as well as regular follow-up samples after diagnosis might solve this issue and help detect an antibody response against pathogens causing the infection.

5.1.3.2. Infection array data support the leaky gut hypothesis

In our pilot study, we observed an increase in antibody titers against different gut microbes in 6/13 (46.1%) cases. In detail, an increase in antibody titers was detected against *C. albicans*, *K. oxytoca*, *E. cloacae,* and *C. difficile*. Increasing antibody titers against gut microbes support the leaky gut hypothesis. They suggest that in IE the gut barrier becomes more permeable and allows the translocation of gut microbes into the bloodstream. This could trigger a systemic immune response against gut microbes [269]. As discussed in section 5.1.2, in health, intestinal integrity prevents the transfer of microbes and other factors from the gut to the bloodstream. It can be disturbed by changes in the epithelial mucosa or in the gut microbiota composition because of various factors, including age, diet, and antibiotics [208]. Besides, episodic systemic exposure to gut microbes due to the breach of the intestinal barrier has been observed in humans after high-fat meals, excessive alcohol consumption, the use of proton pump inhibitors, antibiotics, and nonsteroidal anti-inflammatory drugs [270–272]. Initially, high IgG titers against gut microbes were thought to be associated with leaky gut epithelium in patients with

inflammatory bowel disease [242]. Today, it is well documented that every individual develops robust IgG response against most gut microbes (e.g., *E. faecalis* , *E. coli*, *C. albicans*) over time, likely due to short episodes of a gut leakage [208, 230, 273]. In case of inflammation or serious disturbance of the intestinal barrier, the gut microbes could invade the bloodstream and lead to serious infection, including a heart valve infection. Because of this infection, the patient would receive antibiotics and other drugs, which could further damage the intestinal barrier, leading to a vicious cycle of gut microbes leaking and causing infection. However, there are some pitfalls that need to be considered before attributing clinical relevance to gut leakage. Any inflammatory process can disturb the gut barrier besides the independent influence of the factors discussed above. Moreover, it is unclear how gut barrier permeability leads to infections and whether it is necessarily a deleterious process [269, 274].

Other studies also support an increase in antibody titers against gut microbes during the course of infection. Normann et al. reported an increase in antibody titers in sepsis patients in the follow-up samples against gut microbes like *E. faecium*, *E. coli*, and *K. pneumoniae* [205]. This is supported by another study conducted by our research group by using patient samples from the same study cohort (GIES). The serum contains antibodies produced by recently activated antibody-secreting cells as well as long-lived plasma cells. For investigating a recently induced antibody response, a medium-enriched for newly synthesized antibodies (MENSA) approach was used. MENSA from the unstimulated PBMCs were used to analyze the acute response (plasmablasts), while supernatants from the stimulated PBMCs provided information about the acute as well as memory response (B memory cells). It was observed in this study that in two cases, plasmablasts produce high antibody titers against *C. albicans* and *E. cloacae*, both of which are gut microbes.

5.1.3.3. Cross-reactivity and/or polymicrobial infection?

In 6/13 patients, we observed increases in IgG levels against several microbial species. This could be explained by three non-exclusive scenarios: (1) several consecutive or concurrent infections, (2) true polymicrobial infections, and (3) antibody cross-reactivity.

Several consecutive or concurrent infections are a plausible explanation for an increase in IgG levels against several pathogens. As discussed before (5.1.3), follow-up samples were collected at irregular time intervals, and in the case of 5 patients, it was collected after more than 30 days. During such a long time, the patients could have developed consecutive infections, followed by increases in antibody titers against multiple pathogens. For instance, in P36, *C. albicans* was

isolated from the tracheal secretions, and high IgG levels were also observed in this patient, which could mean a possible *C. albicans* co-infection. Though in P12, P16, and P38, no other infections were diagnosed, neither a pathogen was isolated from other sites than BC, the possibility of an undiagnosed infection cannot be ruled out.

Another reason for an increase in IgG levels against several pathogens is true polymicrobial infections. Indeed, in 3 cases (P8, P25, and P37), polymicrobial infection was detected through BC and swabs from other infection sites but not confirmed via infection array. The serological assay, on the other hand, suggests that 6/13 patients might have polymicrobial infections. Polymicrobial infections are not uncommon in IE, and comprise 5.9% of IE infections [275]. This phenomenon could be explained by the low sensitivity of BC diagnosis, leading to the underdiagnosis of polymicrobial infections. It appears more frequently (70%) in IE patients with underlying diseases such as diabetes mellitus and chronic renal failures [221, 275, 276]. There is no consensus on the effects of polymicrobial infections on mortality. Some reports have suggested a positive relationship between polymicrobial infection and mortality [277, 278], while other studies suggest that the clinical outcome of polymicrobial infection is not different from single pathogen infection [275, 279, 280]. A possible explanation for polymicrobial infection could be a leaky gut which is discussed in detail above and/or a secondary infection. Nevertheless, due to the limited resolution of the kinetics and a limited number of follow-up samples, we are unable to distinguish a polymicrobial infection from a consecutive or concurrent infection.

Another factor that could play an important role in the detection of an antibody response against multiple species could be antibody cross-reactivity. In 3 patients, there was an increase in IgG levels against several staphylococcal species. In the case of P16, the IgG titers increased against *S. aureus* and the CoNS *S. hominis*. Similarly, in P38, elevated antibody titers were observed against *S. aureus* and *S. lugdunensis*. Cross-reactivity has been reported for closely related species sharing identical or closely related proteins, as well as for conserved bacterial structures, such as capsular polysaccharides and LPS [281, 282]. Bacterial pathogens like *S. aureus* and *S. epidermidis* can exchange virulence factors via horizontal gene transfer [283]. A shared capsular protein, capsule type 8, present in both *S. aureus* and *S. epidermidis*, has been reported to be responsible for a false-positive reaction in a commercial agglutination test for *S. aureus* [284]. Type 5 and 8 capsular polysaccharides (CP) are also present in *S. haemolyticus*, and *S. hominis* [284, 285], which could lead to cross-reactivity, and this might be the case in P16.

Our lab has also reported cross-reactivities of the antibodies between *S. aureus* and CoNS [44]. In addition, human mAbs directed against conserved antigens can trigger cross-reactions. For instance, antibodies against LPS O-antigen of an opportunistic pathogen, *Klebsiella pneumoniae,* cross-react with diverse commensal and non-commensal microbes, including Gram-negative and Gram-positive bacteria and *S. cerevisiae* [286]. These reasons could lead to antibody cross-reactivity and should be considered while interpreting the results.

5.1.3.4. *C. albicans* - an important player in IE?

As discussed in section 5.1.2, high antibody titers were detected against an opportunistic fungal pathogen *C. albicans* in controls and IE patients at the time of diagnosis (d0), which were similar to the antibody titers against *S. aureus*. Moreover, frequent increases in antibody titer were also detected against *C. albicans* during IE. In our study, 4/13 (30.7%) IE patients generated significant antibody titers against *C. albicans*, and out of those, 3/4 patients had >5 fold increases in IgG titers, suggesting either a translocation of *C. albicans* from the gut and/or secondary infection [287]. *C. albicans* has important clinical implications, as it is hard to diagnose and not cleared by routinely used broad-spectrum antibiotics.

C. albicans is carried by 2/3 people on the mucous membrane, mostly the oral cavity, gastrointestinal tract (GIT), and the urogenital tract, without causing infection [239]. We suggest a leakage of *C. albicans* from the gut (explained in sections 5.1.2 and 5.1.3.2) and/or secondary infection as suggested in P36 (explained in section 5.1.3.3), which explains the observed increases in specific antibody titers. However, antibody cross-reactivity can not be completely ruled out. Immunological cross-reactivity between *C. albicans* and human tissues has been reported in the past. Clinical sera specimens positive for thyroid, ovary, and adrenal antibodies have shown cross-reactivity with *C. albicans* suggesting its possible role in autoimmune diseases [288]. Thus, the higher antibody titer we observed in the infection array for IE patients and controls might be observed because of one of the reasons with strong indication towards secondary infections.

Our results suggest that *C. albicans* may play an important role in IE and underline the need for a reliable diagnosis. Nearly 50% of candidiasis cases are diagnosed via BC [289], 33% of those are IE cases [13]. The sensitivity of BC varies from 21-71% in candidiasis, making a case for other diagnostic techniques to be used. For instance, PCR is used for diagnosis with nearly 75% sensitivity. Serological tests and commercially available diagnostic kits for *C. albicans* are discussed in detail in section 5.1.4.

Interestingly, 2/4 patients with an increase in anti-*C. albicans* IgG, also showed an antibody increase against *C. acnes*. *C. acnes*, also known as *Propionibacterium acnes*, is a skin commensal and has only rarely been associated with IE (0.3 % of all cases), which is usually diagnosed through BC [290]. The predominant predisposing conditions include previous surgical intervention and the presence of prosthetic valves [290–293]. Native valve IE is uncommon and involves abnormal native valves, which account for 67% of the cases [294]. In our study, one patient suffered from an IE after a biological AV replacement, while the other represented an infection of the native valves.

Excitingly, *C. albicans* and *C. acnes* have a synergistic relationship. *C. albicans* can enhance the biofilm growth of *C. acnes*, while *C. acnes* can protect *C. albicans* from micafungin (antifungal medication) [295, 296]. *C. albicans* can also have synergistic relation with *S. aureus* and other bacterial pathogens, which can have significant clinical implications [297]. Although data is promising here, yet the sample size is limited. Further studies should be conducted to study the connection between these two pathogens in the context of IE.

5.1.4. Infection array: an efficient and reliable diagnostic strategy

Serological assays have shown promising results and can not only be used in diagnostics but also in understanding the immune response, which could help develop a better therapeutic strategy. Over the course of infection, a strong and highly specific antibody response is generated against the invasive pathogen and its antigens [41, 108, 205, 298, 299]. This highly specific antibody response forms the basis for the utilization of serological assays for diagnostic purposes. Some serological tests are already used in clinical routine, while others are so far only used for basic research.

Rapid antigen and antibody diagnostic tests have been established for some pathogens involved in IE. For instance, the mannan antigen test, which allows detection of circulating mannan *Candida* antigen in human serum or plasma, have been established with a moderate sensitivity and specificity of 58% and 65%, respectively. Besides an antigen test, anti-mannan antibody tests have also been employed with increased sensitivity and specificity of 59% and 83% [300]. Later on, a combination of mannan antigen test and anti-mannan antibody test was developed, showing improved results with a combined sensitivity and specificity of 83% and 86% in invasive candidiasis [250, 289]. In addition, commercially available *C. albicans* germ-tube antibody (IFA IgG) tests provide a faster and easier diagnosis [301]. Nevertheless, better strategies are required to further improve the sensitivity and specificity of *Candida* diagnosis.

Besides *Candida* antibody diagnostic tests, Harro et al. developed a rapid antibody diagnostic test for chronic *S. aureus* infections based on biofilm antigens with 90% sensitivity and 100% specificity [299]. The antigens were recombinantly produced and used in an ELISA-based assay. Similarly, Marmor et al. have developed a multiplex assay using recombinant proteins in an ELISA-based assay to diagnose PJI caused by Staphylococci with 72.3% sensitivity and 80.7 % specificity [302]. Thus, multiplex assays, including the infection array, could complement the microbiological identification of the causative agent in IE, especially when BCs remain negative.

To reliably infer the causative agent, it is important to have a baseline antibody titer, reflecting the antibody levels before the onset of infection. This holds especially true for *S. aureus* and *C. albicans* for which baseline antibody levels are on average very high and differ strongly between individuals. This variability in the IgG titers makes it very difficult or even impossible to determine a threshold for the diagnosis of infection [106–108]. In this case, an increase in antibodies against specific pathogens during the course of infection can help identify the causative agent. In the case of P36 and P38, we observed that serological assays performed with consecutive samples showed a pathogen-specific response. Equally important, it can identify pathogens that are usually underestimated in IE. After identification of the pathogen, appropriate and targeted therapy could be started.

5.1.5. Limitations of the study

The present study also has some limitations. First, the number of healthy individuals and patients was limited. Second, the subjects were not strictly matched based on age and sex. Third, back-up and follow-up samples were restricted in terms of collection points and were not available for 4/17 patients. Fourth, the basal time point might have been the time point where the disease had already advanced to see a change in antibody titer. Finally, the infection array might not contain the pathogen or a strain/subclone closely related to the invasive strain resulting in a false-negative result. The above points should be considered while interpreting the results.

In conclusion, the infection array determines the increase in antibodies against invading pathogens and can thus complement and even extend the microbiological diagnosis of IE. The increase in antibody titer(s) was observed during the course of infection against the pathogens that were diagnosed by BC as well as pathogens that were not diagnosed. It provided significant insight into IE infection and highlighted gut microbiota which might play a crucial role during

IE or as a secondary infection [287]. Our results also show that most of the tested pathogens come in contact with the immune system and generate a memory immune response. Upon re-exposure, plasma cells generate new IgG, resulting in an increase in IgG titers which can be detected by infection array and help diagnose the infection [303]. Furthermore, it pointed out the importance of the timing of sample collection. Lastly, serological assays could highlight the potential role of pathogens like *C. albicans* and *C. acnes*, which are mostly overlooked in BC and which should be explored further.

5.1.6. Prospects of using infection array as a diagnostic tool

In order to improve the diagnostic potential of the infection array, more pathogens should be added to the panel, especially the usual BC-negative pathogens such as *Bartonella* and *Brucella* spp. There are variations in the virulence factors being produced by pathogens like *S. aureus*. Mobile genetic elements like bacteriophages, which carriers PVL, exfoliative toxin A and immune evasion cluster, contribute to strain-to-strain variation [304]. Therefore, besides using ECP, recombinant proteins should also be used to cover the missing virulence factors. Moreover, recombinant proteins will increase the specificity and reproducibility of the assay. Finally, recombinant proteins enable us to expand the infection array panel by adding non-cultivable pathogens. The recombinant proteins should be selected based on their conservation in the species, specificity for the pathogen, and ability to trigger an immune response. Recombinant proteins may help to clearly distinguish between immune responses against closely related pathogens and reduce cross-reactivity.

5.2. Characterization of monoclonal antibodies against *S. aureus*

5.2.1. Fighting *S. aureus* infections with monoclonal antibodies

After demonstrating that pathogen-specific antibodies are generated during IE and presumably contribute to pathogen clearance, we aimed to generate mAb against the prime IE pathogen *Staphylococcus aureus* to study antibody functions on a molecular level. The rationale to generate mAbs against the selected *S. aureus* proteins candidates (ClfA, FnBPA, and SplB) in relation to IE is discussed in detail in section 1.7.

S. aureus infections are a leading cause of morbidity and mortality in hospital settings, with diseases ranging from wound infections to life-threatening infections such as pneumonia, sepsis, and IE [46, 305]. For countering *S. aureus* infections, both active and passive vaccines have been generated against *S. aureus,* but none of them has made their way into clinical practice to date [77, 305, 306]. There is compelling evidence that antibodies against extracellular and surface-bound proteins play an important role in *S. aureus* infection and provide at least partial protection from a severe outcome [41, 105, 110]. Pre-clinical data suggest that antibodies specific for *S. aureus* virulence factors, including SpA, ClfA, and α-Toxin, can contribute to the prevention and clearance of biofilms and provide protection from abscess, sepsis, and IE [133–135, 183, 305, 306]. Given the importance of antibodies in *S. aureus* infections, producing neutralizing mAbs against critical *S. aureus* virulence factors is a promising prophylactic and therapeutic strategy.

Besides their therapeutic potential, mAbs have important applications in the research field. They can be utilized in sensitive detection assays such as ELISA and western blotting to determine the presence and concentration of the targeted antigen [307]. Furthermore, they can also be used in affinity purification techniques to isolate and purify their targets in a single step [308].

Within the research consortium Card-ii-Omics, our group has generated murine, humanized, and human mAbs against *S. aureus* surface proteins (ClfA, FnBPA, SpA), a cell wall-anchored protein (IsdB), and extracellular enzymes (SplB, GlpQ, Plc). Within this Ph.D. project, I characterized murine mAbs against SplB and ClfA as well as murine and humanized mAbs against FnBPA. We aimed to generate antibodies with neutralizing capacity, i.e., the ability to inhibit the enzymatic activity of proteases or block the interaction of adhesins with their human ligands.

5.2.2. Monoclonal antibody against the *S. aureus* serine protease SplB

S. aureus proteases are a promising target for passive immunization as they contribute to *S. aureus* pathogenicity and, in some cases, even cause toxinosis. A prominent example is exfoliative toxins (ETs), the causative agents of bullous impetigo and its generalized form, the staphylococcal scalded skin syndrome (SSSS) [309]. Notably, a lack of maternal anti-ET antibodies renders infants highly susceptible to SSSS, showing the importance of antibodies in counteracting toxin-mediated pathology [310]. Recent work from our department has identified SplB as an exciting target for mAbs. SplB has allergenic properties in humans and mice [169, 311]. It can also activate PAR2 and trigger the release of proinflammatory cytokines in endothelial cells [212]. PAR2 has been reported to have roles in inflammation, pain, cancer, and metabolic diseases [312]. Moreover, SplB is reported to be involved in biofilm formation, though its exact function is not yet elucidated [161]. This makes SplB a promising candidate for a passive vaccination strategy.

In this work, we produced a neutralizing murine monoclonal antibody against SplB. The anti-SplB mAb specifically targeted SplB and did not show cross-reactivity to other Spls and other ECPs of *S. aureus*. In an affinity-based MST assay, the anti-SplB mAb showed moderate binding to SplB with a K_d value of 2.54 µM compared to reported binding affinities for other monoclonal antibodies which are in the nM range [210, 211]. Besides, there is a significant variation in antibody affinity to its antigens ranging from 10 mM to 0.1 nM and even 48 fM [313–315]. Nevertheless, anti-SplB mAb neutralized the enzymatic activity of SplB by up to 99 % in 5-fold molar excess and 50 % in 2-fold molar excess as demonstrated in an *in vitro* substrate cleavage assay.

The moderate K_d value could be strongly influenced by the MST protocol. Buffer composition and pH dictate the ability to detect ligand-protein interactions, influence the thermophoretic movement of the molecules and dramatically change the MST binding characteristics [316, 317]. This could be the reason that we calculated a K_d in a µM range, suggesting moderate binding. Different buffer compositions and pH should be tried in the future to analyze the anti-SplB mAb and SplB interaction in more detail. Moreover, an alternate method, surface plasmon resonance (SPR), could be employed to determine the K_d value.

In addition, affinity maturation during germinal center reaction strongly impacts on the affinity of antibodies to their antigens. In this process, cycles of rapid somatic mutations and selection for antigen binding lead to improved binding and eliminate auto-reactive antibodies [286, 318].

The rate of somatic mutation is approximately 10^{-3} per base-pair per cell division [319]. In our study, the variable regions of the heavy and light chains of the anti-SplB mAb have 94.9 % and 98.6 % sequence similarity, respectively, to the germline sequence (Table S 1). As reported in previous studies, variable region sequence variation of around 2% is considered a low, while 35-55 % is considered as a high mutation rate [320–323]. Hence, the anti-SplB mAb is highly similar to germline sequence.

The affinity, avidity, and anti-pathogen activity of antibodies increase via affinity maturation [318]. However, in some cases, the process of affinity maturation might not be necessary or even redundant for antibody action [324]. Germline-like mAbs with high therapeutic potential have recently been generated in animal models [325]. Although germline-like mAbs retain a degree of structural plasticity in their backbone to bind to several different antigens (a phenomenon known as conformational flexibility hypothesis) [326], our mAb does not bind to the ECP of *S. aureus* and shows high specificity along with a strong neutralizing effect despite having high similarity to germline sequence.

The next step was to test the anti-SplB mAb *in vivo.* Proteases and toxins are known to disrupt the endothelial barrier, and hence promote bacterial spread within the body [327–329]. This process can be mediated by PAR2 activation [330]. Our research group has recently shown that SplB can activate PAR2 and facilitate the release of proinflammatory cytokines in endothelial cells [212]. Therefore, it was interesting to test whether SplB disrupts the endothelial barrier *in vivo,* and if it does, whether anti-SplB mAb can prevent this effect. Interestingly, our results revealed that SplB induced pronounced endothelial damage in the mouse model, supporting the previous observations that proteases can cause endothelial dysfunction. Furthermore, the neutralizing anti-SplB mAb efficiently blocked the function of SplB *in vivo* and significantly reduced the damage to the endothelial barrier.

SplB-induced endothelial dysfunction could potentially contribute to several diseases, including sepsis, endocarditis, and allergy. Kolar et al. reported that proteases, including Spls, promote the dissemination of *S. aureus* in the rabbit model of pneumonia [331]. Similarly, Paharik et al. demonstrated that Spls modulates *S. aureus* virulence in the mouse sepsis model [332]. Furthermore, the endothelial damage caused by proteases could provide a base for forming a characteristic infective endocarditis lesion, termed “the vegetation”, which is composed of bacteria surrounded by platelet and fibrin binding to the endothelium [333–335]. Moreover, SplB cleaves PAR2, the activation of which participates in the sensitization to a wide

variety of allergens and induction of allergic asthma [336]. Blockage of PAR2 function in the airways during allergen challenge prevents allergen-induced airway hyperresponsiveness [337]. Interestingly, vascular endothelial cells, on which PAR2 are expressed, have been reported to play their part in allergic inflammation [338, 339], and our research group has recently shown that SplB mediated inflammation in the endothelial cells is dependent on PAR2 [212]. In addition, SplB has already been shown to have type 2 polarizing potential in a mouse model, suggesting its role in allergy [340].

Taken together, the produced mAb can neutralize the function of SplB both *in vitro* and *in vivo*. If applied prophylactically, the mAb interferes with SplB-induced activation of PAR2 on endothelial cells and preserves the barrier integrity. Neutralizing SplB could also indirectly prevent triggering allergic inflammation by blocking PAR2 cleavage. Additionally, as SplB induces a type 2 response, we would test the mAb in an allergic asthma mouse model in the future. Thus, our anti-SplB mAb has some potential as a therapeutic agent in allergy and infective endocarditis.

5.2.3. Monoclonal antibodies against *S. aureus* adhesins

5.2.3.1. ClfA remains a viable antigen candidate for mAb

S. aureus harbours a wide range of adhesins involved in various infections. ClfA is one of these adhesins which has been linked to the bloodstream and biofilm-related infections [82, 183]. ClfA has the ability to bind to Fg and fibrin, which facilitates bacterial adherence to these extracellular matrix proteins as well as enables bacterial clumping. Both processes contribute to the development of *S. aureus* infections [82, 341, 342]. Additionally, ClfA impairs complement deposition required for opsonophagocytosis and impairs neutrophil and macrophage phagocytosis [343–345]. This makes ClfA a significant virulence factor and an interesting target for active and passive immunization strategies.

In this work, we generated 2 murine mAbs against ClfA. While previous studies often focused on the promotion of opsonophagocytosis by anti-ClfA antibodies, we also wanted to test the neutralizing capacity of the anti-ClfA mAbs *in vitro*. Our ClfA-002 mAb inhibited the binding of ClfA to Fg up to ~ 60% (1:1, protein:mAb molar ratio), while the ClfA-004 mAb showed inhibition of 5.5% in the same molar ratio. The inhibitory effect of ClfA-002 is similar to the inhibition reported by Tkaczyk et al. for their murine mAb (11H10), where it showed ~ 70% inhibition (1:1 molar ratio) [133]. Anti-ClfA mAb, combined with anti-alpha toxin

(MEDI4893) mAb, provided protection in lethal bacteremia, pneumonia, and implant-related infections in mice models when applied prophylactically [145, 183]. Tkaczyk et al. also produced a multimechanistic bispecific antibody (BiSAb), containing anti-alpha-toxin and anti-ClfA activities, which showed promising results *in vitro* but showed reduced activity *in vivo* as compared to the combination of individual anti-alpha-toxin and anti-ClfA mAbs [183]. These data indicate that neutralizing ClfA could inhibit the binding of ClfA to its partner protein, which can reduce the pathogenesis associated with it in animal models.

In our work, a single nucleotide exchange in the LC of ClfA-004, compared to ClfA-002, led to an AA exchange from phenylalanine to tyrosine in the CDR3 region. Interestingly, this single mutation drastically changed the binding and functional properties of ClfA-004 mAb. For instance, the EC-50 for anti-ClfA 004 was 2.16 µg/ml, while ClfA-002 showed strong binding with an EC-50 at 0.07 µg/ml. This observation was also confirmed by western blot and dot blot and notably also the neutralization assay as described above.

The LCs of both the mAbs are identical to the germline IgG genes, which suggests that the respective antibody-coding sequences have not undergone affinity maturation. The HCs of the mAbs are 97.4% identical to the germline IgG genes, indicating an lower degree of affinity maturation. It again supports the observation mentioned in the previous section (5.2.2) that even without affinity maturation, mAbs could neutralize the function of their target proteins.

Minor variations in DNA sequence can be of great importance. Unintended changes in AA sequences resulting from mutation or the lack of translation regulation have been reported in recombinant human mAbs [346–348]. These changes can occur at constant regions as well as CDRs [348]. One to four point mutations in the CDRs can already reduce the ability of the antibody to bind to its target protein [349]. Besides, a point mutation identified via computer simulations suggested that the mutation led to destabilization of the antibody [350]. On the contrary, Wen et al. reported that a single mutation in the first CDR of the LC of a mAb resulted in a minor decrease in its binding affinity to the antigen [351]. Similarly, a point mutation in humanized immunoglobulin G1 mAb, that binds to vascular endothelial growth factor-A, outside the CDRs did not perturb the structure of the antibody [352]. Though sequence variations in the constant regions do not affect the binding property of the mAb, they have the potential to change the allotype provoking antibody responses due to alloimmunization [353, 354]. Antibody sequence variation is a complex trade-off among antibody affinity, stability, specificity, and solubility, and all of the four factors can be influenced by mutations and can be

exploited for antibody engineering [355]. Besides the sequence variation in the mAbs, variation in ClfA sequence can also reduce the binding of a mAb for up to a 1000 fold which lead to loss of functional activity of the mAbs (Tkaczyk et al. 2017).

Active immunization with ClfA showed a varied level of protection in different mice models, despite generating functional polyclonal opsonic antibodies [63, 356]. The variability in antibody titer and protection by active vaccination highlighted the potential benefit of passive vaccination, providing reliable and consistent antibody titers. As described, passive vaccination strategies involving ClfA have been successfully tried in IE rabbit model as well as sepsis, dermonecrosis, pneumonia, bacteremia, and hematogenous implant infection model mice models [131–133, 183]. Despite the promising results demonstrated in pre-clinical models and early clinical settings, the humanized anti-ClfA mAb Tefibazumab failed to protect in the later clinical trials. The mAb failed in phase II of the clinical trial in bacteremia and cystic fibrosis patients [134]. Moreover, INH-A21, which is a human intravenous immune globulin and contains elevated levels of anti-ClfA and anti-SdrG (Serine-aspartate repeat-containing protein G precursor), was tested in sepsis infants, but the trial failed in phase III despite showing promising results in early stages in low birth weight infants with sepsis [157, 357]. This might be attributed to the different levels of expressions of ClfA among clinical isolates, variation in ClfA sequence, or targeting a single or bicomponent virulence factor [358, 359].

Taken together, these results support the advantage of using ClfA as a target, and its neutralization might lead to the inhibition of *S. aureus* binding to Fg. Previous experiments in which multi-component and bispecific antibodies (BiSAb) were effectively used in animal models indicate the importance of ClfA in passive vaccination strategies. Our results also shed light on the influence of the sequence of mAbs on its functional properties. To further characterize the anti-ClfA mAbs, cross-reactivity against *S. aureus* surface proteins should be tested, for instance, by using a 79-plex Luminex panel of *S. aureus* proteins established at the Department of Functional Genomics, University of Greifswald. Moreover, inhibition assays should be performed with anti-ClfA mAbs from Tkaczyk et al. as a control to compare the efficacy of our mAbs. If the results are promising, anti-ClfA mAbs could be tested *in vivo* in the IE animal model, combined with other neutralizing mAbs as a multicomponent vaccine, to further show the efficacy of these mAbs.

5.2.3.2. FnBPA - a promiscuous adhesin and potential vaccine candidate

Another important and broadly expressed adhesin in the MSCRAMMs family is FnBPA. Its binding to Fg, Fn, and elastin facilitates *S. aureus* attachment to biotic and abiotic surfaces leading to biofilm formation [82, 87, 360]. Moreover, FnBPA-dependent biofilms also inhibit macrophage invasion [361].

Studies have shown that FnBPA is highly immunogenic and can trigger an effective immune response. Truncated FnBPA, $F1_{30\text{-}500}$, was strongly immunogenic in mice, and the survival rate of mice upon systemic MRSA infection significantly increased after vaccination [362]. Rat antibodies against truncated FnBPA also triggered opsonophagocytic killing of *S. aureus* via macrophages *in vitro* and promoted neutrophil activity [120]. Additionally, murine antibodies generated against FnBPA hindered biofilm formation, inhibited *S. aureus* binding to Fn, and protected mice against IE [87, 186]. All the studies mentioned support the protective role of anti-FnBPA antibodies and their use as a vaccine candidate against *S. aureus*.

In this study, we generated murine and humanized mAbs against FnBPA and tested its neutralizing capacity *in vitro*. Two murine anti-FnBPA mAbs bound effectively to the target FnBPA. One murine mAb (anti-FnBPA D4) inhibited (20%) the binding of FnBPA to Fn *in vitro*, suggesting that the anti-FnBPA D4 binds to the Fn-binding domains of FnBPA and partially blocks its activity.

The reason for this partial neutralization likely lies in the multiple tandem repeats of FnBPA that mediate Fn binding. The Fn-binding moiety is a collection of 11 tandem repeats, each of which can bind to the N-terminus of Fn, and six of those repeats bind the N-terminus with a K_d in nM range, suggesting a very strong binding [87, 363]. Indeed, it has been reported that antibodies reactive to FnBPA isolated from the plasma of patients did not inhibit the binding of recombinant FnBPA to Fn [363, 364]. However, immunizing mice with the truncated repetitive region of FnBPB triggered the production of a neutralizing mAb (15E11), which showed inhibition of up to 70% [186]. Similarly, Ma et al. produced a mAb against truncated FnBPA and observed a 40% reduction of *S. aureus* binding to Fg [365]. This suggests that even in the presence of the mAb, some of the Fn-binding repeats are not neutralized. Structural analyses by Provenza et al. suggest that repeats 9 and 10 of FnBPA are important for their binding to Fn and that a mAb against these repeats inhibits this interaction [186]. The mechanism by which it inhibits is not merely competition with Fn but also a conformational change in the repeats to which it attaches. Provenza et al. referred to this phenomenon as “the mAb-promoted

conformational change mechanism," which means that antibody binding shifts adhesin repeats from a high-affinity state to a low-affinity state. Another mechanism by which inhibition could work would be the sterical hindrance of the interaction of FnBPA and Fn.

Overall, the tandem repeat structure of FnBPA renders this adhesin a difficult target for neutralizing antibodies. Future studies should focus on using small truncated epitopes of FnBPA proteins as a vaccine candidate, which would trigger the generation of specific antibodies and avoid the production of a myriad of non-specific and non-protective antibodies.

5.2.4. The dilemma of targeting adhesins

Adhesins have been studied for a long time to be used in active and passive immunization strategies, but in the case of *S. aureus* it has not been successful so far. In contrast, *Neisseria* adhesin A is used as a component of a licensed vaccine against *N. meningitidis*. Similarly, adhesins of *H. influenzae*, *A. baumannii*, and *E. coli* have also shown a high potential for a vaccine target [366]. In the case of *S. aureus*, a fair number of adhesins have been tested as vaccine candidates in pre-clinical and clinical trials [65, 77]. Out of those, ClfA is generally chosen as a vaccine candidate because it plays vital functions in various infections, ranging from arthritis to the bloodstream and biofilm-related infections [82, 87, 181, 182, 184]. Additionally, ClfA has the ability to confer virulence independent of other surface antigens [367]. Moreover, previous passive vaccination strategies against ClfA showed promising results in various animal models [131–133, 145, 183]. Similarly, antibodies against FnBPA provided protection against IE in the mice model [120].

However, the successful transition from animal models to human trials has failed, and there could be several reasons. First, the production of a broad spectrum of functionally redundant adhesins like MSCRAMMs by *S. aureus* could be an important factor. Second, naïve animals, mostly mice, are used during the animal trials, whereas humans are immunologically primed against *S. aureus*, which may explain the discrepancies in the effects in animals as compared to humans. Besides, rabbits and non-human primates have been suggested to be more relevant *in vivo* models than mice [156, 368, 369]. Third, different levels of expressions of ClfA among clinical isolates might be an important factor [358, 359]. Besides expression level, variation in ClfA sequence can also reduce the binding of a mAb for up to a 1000 fold and lead to loss of functional activity [183]. Lastly, *S. aureus* has the capacity to inhibit antibody-mediated opsonization by producing protein A which can scavenge antibodies as well as deplete B cells [370, 371].

Currently, there are at least five vaccines against *S. aureus* enrolled in clinical trials [369]. Pfizer has been working on a multivalent SA4Ag vaccine containing type 5 and 8 CP, ClfA, and manganese transporter protein C (MntC) [372]. Unfortunately, it failed in phase IIb in patients undergoing spinal surgery [369]. The focus has recently shifted from opsonizing antibodies to developing neutralizing mAbs against toxins and immune evasion proteins. Opsonizing antibodies have the risk of skewing the immune response, for instance, inducing cytokine response, while antibodies against secreted toxins can directly block toxicity [369, 373]. High natural antibodies against α-toxin have shown protection against *S. aureus* skin infection [114], while lower titers were associated with poor prognosis in bacteremia patients [374]. Similarly, high titers of serum antibodies against pore-forming toxins and SAgs are associated with better clinical outcomes [305]. Because of these reasons, focus has shifted towards using toxins as vaccine candidates against *S. aureus*.

5.2.5. Multi-component vaccines have shown promising results

Although single target vaccines have been a very effective strategy against other bacterial pathogens such as *Streptococcus pneumoniae, Neisseria meningitidis,* and *Haemophilus influenzae*, it has not been effective against *S. aureus* [367, 375–377]. It can be attributed to multitude and redundancy of virulence factors which optimizes its chances of survival at different infection sites. Therefore, a combination of mAbs, in the form of a multivalent vaccine, might provide better protection, as it has been shown in various studies [149, 157, 158, 305, 378]. Within Card-ii-Omics our group aimed to generate neutralizing mAbs against *S. aureus* surface proteins (ClfA, FnBPA, Spa), a cell wall-anchored protein (IsdB), and extracellular enzymes (SplB, GlpQ, Plc). Three of them were characterized in-depth in this Ph.D. work. Future work will aim at testing these mAbs in a multi-component vaccine in pre-clinical *S. aureus* infection models.

Another promising approach is combining mAbs with traditional antibiotic therapy, which has been reported to increase mAb's efficacy [305, 379, 380]. We would test the produced mAbs along with antibiotics *in vitro* and *in vivo* to analyze the combined effect of these therapeutic agents. Besides, the stability of the produced mAbs should be tested as it has been reported that mAbs with a long half-life have better efficacy [146]. In conclusion, a multivalent vaccine could be effective and provide a better therapeutic approach to combat invasive *S. aureus* infections [118].

5.2.6. Selecting future targets for mAb

An important point that should be addressed here is the careful selection of antigens for the purpose of vaccination. A few crucial factors should be considered during the selection process; (i) prevalence of antigens in *S. aureus* clinical isolates [381], (ii) genetic variability in the antigen of interest [133, 382, 383], (iii) expression of the proteins during the course of infection [139, 384] (iv) the direct role of the antigen in various staphylococcal infections, (v) immunologically relevant targets so antibodies and immune cells can access it, (vi) it should trigger a strong as well as the correct type of immune response [77, 385].

In the future, it would be crucial to study and confirm specific antibodies against the antigens of interest that correlate with better outcomes in *S. aureus* infections. Recent studies show that neutralizing antibodies against *S. aureus* toxins have shown promising results in pre-clinical and clinical trials [305]. Moreover, instead of using a full-length antigen, focusing the antibody response against a specific epitope of antigens can provide better protection [365, 373]. It also reduces the production of non-protective antibodies, which bear the potential risk of cross-reactivity with human tissues and sterical hindrance of the binding of protective antibodies [373]. Ultimately, a passive vaccine consisting of neutralizing mAbs against several short epitopes of different *S. aureus* virulence factors combined into a multivalent preparation may provide protection and should be tested in the future.

6. References

1. Bin Abdulhak AA, Baddour LM, Erwin PJ, Hoen B, Chu VH, Mensah GA, Tleyjeh IM. Global and Regional Burden of Infective Endocarditis, 1990–2010: A Systematic Review of the Literature. Global Heart. 2014;9:131–43. doi:10.1016/j.gheart.2014.01.002.

2. Holland TL, Baddour LM, Bayer AS, Hoen B, Miro JM, Fowler VG. Infective endocarditis. Nat Rev Dis Primers. 2016;2:16059. doi:10.1038/nrdp.2016.59.

3. Murdoch DR, Corey GR, Hoen B, Miró JM, Fowler VG, Bayer AS, et al. Clinical Presentation, Etiology and Outcome of Infective Endocarditis in the 21st Century: The International Collaboration on Endocarditis-Prospective Cohort Study. Arch Intern Med. 2009;169:463–73. doi:10.1001/archinternmed.2008.603.

4. Cahill TJ, Baddour LM, Habib G, Hoen B, Salaun E, Pettersson GB, et al. Challenges in Infective Endocarditis. J Am Coll Cardiol. 2017;69:325–44. doi:10.1016/j.jacc.2016.10.066.

5. Baddour LM, Wilson WR, Bayer AS, Fowler VG, Tleyjeh IM, Rybak MJ, et al. Infective Endocarditis in Adults: Diagnosis, Antimicrobial Therapy, and Management of Complications: A Scientific Statement for Healthcare Professionals From the American Heart Association. Circulation. 2015;132:1435–86. doi:10.1161/CIR.0000000000000296.

6. Fowler VG, Miro JM, Hoen B, Cabell CH, Abrutyn E, Rubinstein E, et al. *Staphylococcus aureus* endocarditis: a consequence of medical progress. JAMA. 2005;293:3012–21. doi:10.1001/jama.293.24.3012.

7. Greenspon AJ, Patel JD, Lau E, Ochoa JA, Frisch DR, Ho RT, et al. 16-year trends in the infection burden for pacemakers and implantable cardioverter-defibrillators in the United States 1993 to 2008. J Am Coll Cardiol. 2011;58:1001–6. doi:10.1016/j.jacc.2011.04.033.

8. Esquer Garrigos Z, Sohail MR. Attachment is the source of all suffering: delineating mechanisms of adhesion in *Staphylococcus aureus* endocarditis. Eur Heart J. 2019;40:3260–2. doi:10.1093/eurheartj/ehz353.

9. Benito N, Miró JM, Lazzari E de, Cabell CH, del Río A, Altclas J, et al. Health care-associated native valve endocarditis: importance of non-nosocomial acquisition. Ann Intern Med. 2009;150:586–94. doi:10.7326/0003-4819-150-9-200905050-00004.

10. Duval X, Delahaye F, Alla F, Tattevin P, Obadia J-F, Le Moing V, et al. Temporal trends in infective endocarditis in the context of prophylaxis guideline modifications: three successive population-based surveys. J Am Coll Cardiol. 2012;59:1968–76. doi:10.1016/j.jacc.2012.02.029.

11. Pericás JM, Zboromyrska Y, Cervera C, Castañeda X, Almela M, Garcia-de-la-Maria C, et al. Enterococcal endocarditis revisited. Future Microbiol. 2015;10:1215–40. doi:10.2217/fmb.15.46.

12. Morpeth S, Murdoch D, Cabell CH, Karchmer AW, Pappas P, Levine D, et al. Non-HACEK gram-negative bacillus endocarditis. Ann Intern Med. 2007;147:829–35. doi:10.7326/0003-4819-147-12-200712180-00002.

13. Baddley JW, Benjamin DK, Patel M, Miró J, Athan E, Barsic B, et al. *Candida* Infective Endocarditis. Eur J Clin Microbiol Infect Dis. 2008;27:519–29. doi:10.1007/s10096-008-0466-x.

14. Yuan S-M. Fungal Endocarditis. Braz J Cardiovasc Surg. 2016;31:252–5. doi:10.5935/1678-9741.20160026.

15. Barchiesi F, Orsetti E, Mazzanti S, Trave F, Salvi A, Nitti C, Manso E. Candidemia in the elderly: What does it change? PLoS ONE 2017. doi:10.1371/journal.pone.0176576.

16. Poowanawittayakom N, Dutta A, Stock S, Touray S, Ellison RT, Levitz SM. Reemergence of Intravenous Drug Use as Risk Factor for Candidemia, Massachusetts, USA. Emerging Infect Dis. 2018;24:631–7. doi:10.3201/eid2404.171807.

17. Ellis ME, Al-Abdely H, Sandridge A, Greer W, Ventura W. Fungal endocarditis: evidence in the world literature, 1965-1995. Clin Infect Dis. 2001;32:50–62. doi:10.1086/317550.

18. Pappas PG, Rex JH, Sobel JD, Filler SG, Dismukes WE, Walsh TJ, Edwards JE. Guidelines for treatment of candidiasis. Clin Infect Dis. 2004;38:161–89. doi:10.1086/380796.

19. Liesman RM, Pritt BS, Maleszewski JJ, Patel R. Laboratory Diagnosis of Infective Endocarditis. J Clin Microbiol. 2017;55:2599–608. doi:10.1128/JCM.00635-17.

20. Hoen B, Béguinot I, Rabaud C, Jaussaud R, Selton-Suty C, May T, Canton P. The Duke criteria for diagnosing infective endocarditis are specific: analysis of 100 patients with acute fever or fever of unknown origin. Clin Infect Dis. 1996;23:298–302. doi:10.1093/clinids/23.2.298.

21. Fournier P-E, Gouriet F, Casalta J-P, Lepidi H, Chaudet H, Thuny F, et al. Blood culture-negative endocarditis: Improving the diagnostic yield using new diagnostic tools. Medicine (Baltimore) 2017. doi:10.1097/MD.0000000000008392.

22. Pazin GJ, Saul S, Thompson ME. Blood culture positivity: suppression by outpatient antibiotic therapy in patients with bacterial endocarditis. Arch Intern Med. 1982;142:263–8.

23. Sadaka SM, El-Ghazzawy IF, Hassanen MM, Abu El Kasem AS, Nour El Din AM, Meheissen MA. Molecular and serological techniques for the diagnosis of culture negative infective endocarditis in Alexandria Main University Hospital. The Egyptian Heart Journal. 2013;65:145–52. doi:10.1016/j.ehj.2012.08.001.

24. Morel A-S, Dubourg G, Prudent E, Edouard S, Gouriet F, Casalta J-P, et al. Complementarity between targeted real-time specific PCR and conventional broad-range

16S rDNA PCR in the syndrome-driven diagnosis of infectious diseases. Eur J Clin Microbiol Infect Dis. 2015;34:561–70. doi:10.1007/s10096-014-2263-z.

25. Rovery C, Greub G, Lepidi H, Casalta J-P, Habib G, Collart F, Raoult D. PCR detection of bacteria on cardiac valves of patients with treated bacterial endocarditis. J Clin Microbiol. 2005;43:163–7. doi:10.1128/JCM.43.1.163-167.2005.

26. Edouard S, Nabet C, Lepidi H, Fournier P-E, Raoult D. *Bartonella*, a Common Cause of Endocarditis: a Report on 106 Cases and Review. J Clin Microbiol. 2015;53:824–9. doi:10.1128/JCM.02827-14.

27. Habib G, Lancellotti P, Antunes MJ, Bongiorni MG, Casalta J-P, Del Zotti F, et al. 2015 ESC Guidelines for the management of infective endocarditis: The Task Force for the Management of Infective Endocarditis of the European Society of Cardiology (ESC). Endorsed by: European Association for Cardio-Thoracic Surgery (EACTS), the European Association of Nuclear Medicine (EANM). Eur Heart J. 2015;36:3075–128. doi:10.1093/eurheartj/ehv319.

28. Popp RL. Echocardiography (1). N Engl J Med. 1990;323:101–9. doi:10.1056/NEJM199007123230206.

29. Erbel R, Rohmann S, Drexler M, Mohr-Kahaly S, Gerharz CD, Iversen S, et al. Improved diagnostic value of echocardiography in patients with infective endocarditis by transoesophageal approach. A prospective study. Eur Heart J. 1988;9:43–53.

30. Bruun NE, Habib G, Thuny F, Sogaard P. Cardiac imaging in infectious endocarditis. Eur Heart J. 2014;35:624–32. doi:10.1093/eurheartj/eht274.

31. Pizzi MN, Roque A, Fernández-Hidalgo N, Cuéllar-Calabria H, Ferreira-González I, Gonzàlez-Alujas MT, et al. Improving the Diagnosis of Infective Endocarditis in Prosthetic Valves and Intracardiac Devices With 18F-Fluordeoxyglucose Positron Emission Tomography/Computed Tomography Angiography: Initial Results at an Infective Endocarditis Referral Center. Circulation. 2015;132:1113–26. doi:10.1161/CIRCULATIONAHA.115.015316.

32. Li JS, Sexton DJ, Mick N, Nettles R, Fowler VG, Ryan T, et al. Proposed modifications to the Duke criteria for the diagnosis of infective endocarditis. Clin Infect Dis. 2000;30:633–8. doi:10.1086/313753.

33. Austin SM, Smith SM, Co B, Coppel IG, Johnson JE. Serologic evidence of acute murine typhus infection in a patient with culture-negative endocarditis. Am J Med Sci. 1987;293:320–3. doi:10.1097/00000441-198705000-00007.

34. Raoult D, Fournier PE, Drancourt M, Marrie TJ, Etienne J, Cosserat J, et al. Diagnosis of 22 new cases of *Bartonella* endocarditis. Ann Intern Med. 1996;125:646–52. doi:10.7326/0003-4819-125-8-199610150-00004.

35. Brouqui P, Raoult D. Endocarditis due to rare and fastidious bacteria. Clin Microbiol Rev. 2001;14:177–207. doi:10.1128/CMR.14.1.177-207.2001.

36. Maurin M, Eb F, Etienne J, Raoult D. Serological cross-reactions between *Bartonella* and *Chlamydia* species: implications for diagnosis. J Clin Microbiol. 1997;35:2283–7.

37. Martins TB. Development of Internal Controls for the Luminex Instrument as Part of a Multiplex Seven-Analyte Viral Respiratory Antibody Profile. Clin Diagn Lab Immunol. 2002;9:41–5. doi:10.1128/CDLI.9.1.41-45.2002.

38. Dias D, van Doren J, Schlottmann S, Kelly S, Puchalski D, Ruiz W, et al. Optimization and Validation of a Multiplexed Luminex Assay To Quantify Antibodies to Neutralizing Epitopes on Human Papillomaviruses 6, 11, 16, and 18. Clin Diagn Lab Immunol. 2005;12:959–69. doi:10.1128/CDLI.12.8.959-969.2005.

39. Clavijo A, Hole K, Li M, Collignon B. Simultaneous detection of antibodies to foot-and-mouth disease non-structural proteins 3ABC, 3D, 3A and 3B by a multiplexed Luminex assay to differentiate infected from vaccinated cattle. Vaccine. 2006;24:1693–704. doi:10.1016/j.vaccine.2005.09.057.

40. Khan IH, Mendoza S, Yee J, Deane M, Venkateswaran K, Zhou SS, et al. Simultaneous detection of antibodies to six nonhuman-primate viruses by multiplex microbead immunoassay. Clin Vaccine Immunol. 2006;13:45–52. doi:10.1128/CVI.13.1.45-52.2006.

41. Meyer TC, Michalik S, Holtfreter S, Weiss S, Friedrich N, Völzke H, et al. A Comprehensive View on the Human Antibody Repertoire Against *Staphylococcus aureus* Antigens in the General Population. Front. Immunol. 2021. doi:10.3389/fimmu.2021.651619.

42. Dobaño C, Vidal M, Santano R, Jiménez A, Chi J, Barrios D, et al. Highly Sensitive and Specific Multiplex Antibody Assays To Quantify Immunoglobulins M, A, and G against SARS-CoV-2 Antigens. J Clin Microbiol 2021. doi:10.1128/JCM.01731-20.

43. Mariën J, Ceulemans A, Michiels J, Heyndrickx L, Kerkhof K, Foque N, et al. Evaluating SARS-CoV-2 spike and nucleocapsid proteins as targets for antibody detection in severe and mild COVID-19 cases using a Luminex bead-based assay. J Virol Methods. 2021;288:114025. doi:10.1016/j.jviromet.2020.114025.

44. Normann N. Erreger-spezifische Antikörpersignaturen bei Patienten mit bakterieller Sepsis [Ph.D.]: University Medicine Greifswald; 2021.

45. Otto M. Staphylococcal infections: mechanisms of biofilm maturation and detachment as critical determinants of pathogenicity. Annu Rev Med. 2013;64:175–88. doi:10.1146/annurev-med-042711-140023.

46. Tong SYC, Davis JS, Eichenberger E, Holland TL, Fowler VG. *Staphylococcus aureus* infections: epidemiology, pathophysiology, clinical manifestations, and management. Clin Microbiol Rev. 2015;28:603–61. doi:10.1128/CMR.00134-14.

47. Arciola CR, Campoccia D, Montanaro L. Implant infections: adhesion, biofilm formation and immune evasion. Nat Rev Microbiol. 2018;16:397–409. doi:10.1038/s41579-018-0019-y.

48. Speziale P, Rindi S, Pietrocola G. Antibody-Based Agents in the Management of Antibiotic-Resistant *Staphylococcus aureus* Diseases. Microorganisms 2018. doi:10.3390/microorganisms6010025.

49. Lister JL, Horswill AR. *Staphylococcus aureus* biofilms: recent developments in biofilm dispersal. Front Cell Infect Microbiol. 2014;4:178. doi:10.3389/fcimb.2014.00178.

50. Hoerr V, Franz M, Pletz MW, Diab M, Niemann S, Faber C, et al. *S. aureus* endocarditis: Clinical aspects and experimental approaches. Int J Med Microbiol. 2018;308:640–52. doi:10.1016/j.ijmm.2018.02.004.

51. VandenBergh MFQ, Yzerman EPF, van Belkum A, Boelens HAM, Sijmons M, Verbrugh HA. Follow-Up of *Staphylococcus aureus* Nasal Carriage after 8 Years: Redefining the Persistent Carrier State. J Clin Microbiol. 1999;37:3133–40.

52. Wertheim HFL, Melles DC, Vos MC, van Leeuwen W, van Belkum A, Verbrugh HA, Nouwen JL. The role of nasal carriage in *Staphylococcus aureus* infections. The Lancet Infectious Diseases. 2005;5:751–62. doi:10.1016/S1473-3099(05)70295-4.

53. Dall'Antonia M, Coen PG, Wilks M, Whiley A, Millar M. Competition between methicillin-sensitive and -resistant *Staphylococcus aureus* in the anterior nares. J Hosp Infect. 2005;61:62–7. doi:10.1016/j.jhin.2005.01.008.

54. Ellis MW, Schlett CD, Millar EV, Crawford KB, Cui T, Lanier JB, Tribble DR. Prevalence of Nasal Colonization and Strain Concordance in Patients with Community-Associated *Staphylococcus aureus* Skin and Soft-Tissue Infections. Infect Control Hosp Epidemiol. 2014;35:1251–6. doi:10.1086/678060.

55. Eiff C von, Becker K, Machka K, Stammer H, Peters G. Nasal carriage as a source of *Staphylococcus aureus* bacteremia. Study Group. N Engl J Med. 2001;344:11–6. doi:10.1056/NEJM200101043440102.

56. Foster T. Surface protein adhesins of *Staphylococcus aureus*. Trends Microbiol. 1998;6:484–8. doi:10.1016/S0966-842X(98)01400-0.

57. Mazmanian SK, Skaar EP, Gaspar AH, Humayun M, Gornicki P, Jelenska J, et al. Passage of heme-iron across the envelope of *Staphylococcus aureus*. Science. 2003;299:906–9. doi:10.1126/science.1081147.

58. Holtfreter S, Roschack K, Eichler P, Eske K, Holtfreter B, Kohler C, et al. *Staphylococcus aureus* carriers neutralize superantigens by antibodies specific for their colonizing strain: a potential explanation for their improved prognosis in severe sepsis. J Infect Dis. 2006;193:1275–8. doi:10.1086/503048.

59. DuMont AL, Torres VJ. Cell targeting by the *Staphylococcus aureus* pore-forming toxins: it's not just about lipids. Trends Microbiol. 2014;22:21–7. doi:10.1016/j.tim.2013.10.004.

60. Resch A, Rosenstein R, Nerz C, Götz F. Differential gene expression profiling of *Staphylococcus aureus* cultivated under biofilm and planktonic conditions. Appl Environ Microbiol. 2005;71:2663–76. doi:10.1128/AEM.71.5.2663-2676.2005.

61. Yao Y, Sturdevant DE, Otto M. Genomewide analysis of gene expression in *Staphylococcus epidermidis* biofilms: insights into the pathophysiology of *S. epidermidis* biofilms and the role of phenol-soluble modulins in formation of biofilms. J Infect Dis. 2005;191:289–98. doi:10.1086/426945.

62. Novick RP, Geisinger E. Quorum sensing in staphylococci. Annu Rev Genet. 2008;42:541–64. doi:10.1146/annurev.genet.42.110807.091640.

63. Narita S, Kaneko J, Chiba J-i, Piémont Y, Jarraud S, Etienne J, Kamio Y. Phage conversion of Panton-Valentine leukocidin in *Staphylococcus aureus* : molecular analysis of a PVL-converting phage, φSLT. Gene. 2001;268:195–206. doi:10.1016/S0378-1119(01)00390-0.

64. Novick R. Mobile genetic elements and bacterial toxinoses: the superantigen-encoding pathogenicity islands of *Staphylococcus aureus*. Plasmid. 2003;49:93–105. doi:10.1016/S0147-619X(02)00157-9.

65. Otto M. Novel targeted immunotherapy approaches for staphylococcal infection. Expert Opin Biol Ther. 2010;10:1049–59. doi:10.1517/14712598.2010.495115.

66. European Centre for Disease Prevention and Control. Point prevalence survey of healthcare-associated infections and antimicrobial use in European acute care hospitals :2011 2012: Publications Office; 2013.

67. Behnke M, Aghdassi SJ, Hansen S, Diaz LAP, Gastmeier P, Piening B. The Prevalence of Nosocomial Infection and Antibiotic Use in German Hospitals. Dtsch Arztebl Int. 2017;114:851–7. doi:10.3238/arztebl.2017.0851.

68. S. Donkor E. Nosocomial Pathogens: An In-Depth Analysis of the Vectorial Potential of Cockroaches. Trop Med Infect Dis 2019. doi:10.3390/tropicalmed4010014.

69. Chambers HF, DeLeo FR. Waves of Resistance: *Staphylococcus aureus* in the Antibiotic Era. Nat Rev Microbiol. 2009;7:629–41. doi:10.1038/nrmicro2200.

70. Moran GJ, Krishnadasan A, Gorwitz RJ, Fosheim GE, McDougal LK, Carey RB, Talan DA. Methicillin-resistant *S. aureus* infections among patients in the emergency department. N Engl J Med. 2006;355:666–74. doi:10.1056/NEJMoa055356.

71. DeLeo FR, Chambers HF. Reemergence of antibiotic-resistant *Staphylococcus aureus* in the genomics era. J Clin Invest. 2009;119:2464–74. doi:10.1172/JCI38226.

72. Henderson A, Nimmo GR. Control of healthcare- and community-associated MRSA: recent progress and persisting challenges. Br Med Bull. 2018;125:25–41. doi:10.1093/bmb/ldx046.

73. Voss A, Loeffen F, Bakker J, Klaassen C, Wulf M. Methicillin-resistant *Staphylococcus aureus* in pig farming. Emerging Infect Dis. 2005;11:1965–6. doi:10.3201/eid1112.050428.

74. Anjum MF, Marco-Jimenez F, Duncan D, Marín C, Smith RP, Evans SJ. Livestock-Associated Methicillin-Resistant *Staphylococcus aureus* From Animals and Animal Products in the UK. Front Microbiol. 2019;10:2136. doi:10.3389/fmicb.2019.02136.

75. Lee AS, Lencastre H de, Garau J, Kluytmans J, Malhotra-Kumar S, Peschel A, Harbarth S. Methicillin-resistant *Staphylococcus aureus*. Nat Rev Dis Primers. 2018;4:18033. doi:10.1038/nrdp.2018.33.

76. Layer F. et al. Häufigkeit, Eigenschaften und Verbreitung von MRSA in Deutschland – Zur Situation 2017/2018. Epid Bull. 2019:427–42.

77. Raafat D, Otto M, Reppschläger K, Iqbal J, Holtfreter S. Fighting *Staphylococcus aureus* Biofilms with Monoclonal Antibodies. Trends Microbiol. 2019;27:303–22. doi:10.1016/j.tim.2018.12.009.

78. Kurlenda J, Grinholc M. Alternative therapies in *Staphylococcus aureus* diseases. Acta Biochim Pol. 2012;59:171–84.

79. Vestergaard M, Frees D, Ingmer H. Antibiotic Resistance and the MRSA Problem. Microbiol Spectr 2019. doi:10.1128/microbiolspec.GPP3-0057-2018.

80. Mathur H, Des Field, Rea MC, Cotter PD, Hill C, Ross RP. Fighting biofilms with lantibiotics and other groups of bacteriocins. NPJ Biofilms Microbiomes. 2018;4:9. doi:10.1038/s41522-018-0053-6.

81. Boles BR, Horswill AR. Staphylococcal biofilm disassembly. Trends Microbiol. 2011;19:449–55. doi:10.1016/j.tim.2011.06.004.

82. Foster TJ, Geoghegan JA, Ganesh VK, Höök M. Adhesion, invasion and evasion: the many functions of the surface proteins of *Staphylococcus aureus*. Nat Rev Microbiol. 2014;12:49–62. doi:10.1038/nrmicro3161.

83. Montanaro L, Poggi A, Visai L, Ravaioli S, Campoccia D, Speziale P, Arciola CR. Extracellular DNA in biofilms. Int J Artif Organs. 2011;34:824–31. doi:10.5301/ijao.5000051.

84. Cue D, Lei MG, Lee CY. Genetic regulation of the intercellular adhesion locus in staphylococci. Front Cell Infect Microbiol. 2012;2:38. doi:10.3389/fcimb.2012.00038.

85. Cucarella C, Solano C, Valle J, Amorena B, Lasa Í, Penadés JR. Bap, a *Staphylococcus aureus* Surface Protein Involved in Biofilm Formation. J Bacteriol. 2001;183:2888–96. doi:10.1128/JB.183.9.2888-2896.2001.

86. Corrigan RM, Rigby D, Handley P, Foster TJ. The role of *Staphylococcus aureus* surface protein SasG in adherence and biofilm formation. Microbiology (Reading, Engl). 2007;153:2435–46. doi:10.1099/mic.0.2007/006676-0.

87. O'Neill E, Pozzi C, Houston P, Humphreys H, Robinson DA, Loughman A, et al. A novel *Staphylococcus aureus* biofilm phenotype mediated by the fibronectin-binding proteins, FnBPA and FnBPB. J Bacteriol. 2008;190:3835–50. doi:10.1128/JB.00167-08.

88. Merino N, Toledo-Arana A, Vergara-Irigaray M, Valle J, Solano C, Calvo E, et al. Protein A-mediated multicellular behavior in *Staphylococcus aureus*. J Bacteriol. 2009;191:832–43. doi:10.1128/JB.01222-08.

89. Geoghegan JA, Corrigan RM, Gruszka DT, Speziale P, O'Gara JP, Potts JR, Foster TJ. Role of surface protein SasG in biofilm formation by *Staphylococcus aureus*. J Bacteriol. 2010;192:5663–73. doi:10.1128/JB.00628-10.

90. Abraham NM, Jefferson KK. *Staphylococcus aureus* clumping factor B mediates biofilm formation in the absence of calcium. Microbiology (Reading, Engl). 2012;158:1504–12. doi:10.1099/mic.0.057018-0.

91. Siboo IR, Cheung AL, Bayer AS, Sullam PM. Clumping Factor A Mediates Binding of *Staphylococcus aureus* to Human Platelets. Infect Immun. 2001;69:3120–7. doi:10.1128/IAI.69.5.3120-3127.2001.

92. O'Gara JP. ica and beyond: biofilm mechanisms and regulation in *Staphylococcus epidermidis* and *Staphylococcus aureus*. FEMS Microbiol Lett. 2007;270:179–88. doi:10.1111/j.1574-6968.2007.00688.x.

93. Cerca N, Jefferson KK, Maira-Litrán T, Pier DB, Kelly-Quintos C, Goldmann DA, et al. Molecular basis for preferential protective efficacy of antibodies directed to the poorly acetylated form of staphylococcal poly-N-acetyl-beta-(1-6)-glucosamine. Infect Immun. 2007;75:3406–13. doi:10.1128/IAI.00078-07.

94. Rohde H, Burandt EC, Siemssen N, Frommelt L, Burdelski C, Wurster S, et al. Polysaccharide intercellular adhesin or protein factors in biofilm accumulation of *Staphylococcus epidermidis* and *Staphylococcus aureus* isolated from prosthetic hip and knee joint infections. Biomaterials. 2007;28:1711–20. doi:10.1016/j.biomaterials.2006.11.046.

95. Schommer NN, Christner M, Hentschke M, Ruckdeschel K, Aepfelbacher M, Rohde H. *Staphylococcus epidermidis* Uses Distinct Mechanisms of Biofilm Formation To Interfere with Phagocytosis and Activation of Mouse Macrophage-Like Cells 774A.1 ▿. Infect Immun. 2011;79:2267–76. doi:10.1128/IAI.01142-10.

96. Vuong C, Kocianova S, Voyich JM, Yao Y, Fischer ER, DeLeo FR, Otto M. A crucial role for exopolysaccharide modification in bacterial biofilm formation, immune evasion, and virulence. J Biol Chem. 2004;279:54881–6. doi:10.1074/jbc.M411374200.

97. Mann EE, Rice KC, Boles BR, Endres JL, Ranjit D, Chandramohan L, et al. Modulation of eDNA release and degradation affects *Staphylococcus aureus* biofilm maturation. PLoS ONE. 2009;4:e5822. doi:10.1371/journal.pone.0005822.

98. Thomas VC, Hancock LE. Suicide and fratricide in bacterial biofilms. Int J Artif Organs. 2009;32:537–44. doi:10.1177/039139880903200902.

99. Huseby MJ, Kruse AC, Digre J, Kohler PL, Vocke JA, Mann EE, et al. Beta toxin catalyzes formation of nucleoprotein matrix in staphylococcal biofilms. Proc Natl Acad Sci U S A. 2010;107:14407–12. doi:10.1073/pnas.0911032107.

100. Devaraj A, Buzzo J, Rocco CJ, Bakaletz LO, Goodman SD. The DNABII family of proteins is comprised of the only nucleoid associated proteins required for nontypeable *Haemophilus influenzae* biofilm structure. Microbiologyopen. 2018;7:e00563. doi:10.1002/mbo3.563.

101. Wang S, Breslawec AP, Alvarez E, Tyrlik M, Li C, Poulin MB. Differential Recognition of Deacetylated PNAG Oligosaccharides by a Biofilm Degrading Glycosidase. ACS Chem Biol. 2019;14:1998–2005. doi:10.1021/acschembio.9b00467.

102. Le KY, Dastgheyb S, Ho TV, Otto M. Molecular determinants of staphylococcal biofilm dispersal and structuring. Front Cell Infect Microbiol 2014. doi:10.3389/fcimb.2014.00167.

103. Kiedrowski MR, Horswill AR. New approaches for treating staphylococcal biofilm infections. Ann N Y Acad Sci. 2011;1241:104–21. doi:10.1111/j.1749-6632.2011.06281.x.

104. Jiang Y, Geng M, Bai L. Targeting Biofilms Therapy: Current Research Strategies and Development Hurdles. Microorganisms 2020. doi:10.3390/microorganisms8081222.

105. Kumar A, Ray P, Kanwar M, Sharma M, Varma S. A comparative analysis of antibody repertoire against *Staphylococcus aureus* antigens in patients with deep-seated versus superficial staphylococcal infections. Int J Med Sci. 2005;2:129–36. doi:10.7150/ijms.2.129.

106. Dryla A, Prustomersky S, Gelbmann D, Hanner M, Bettinger E, Kocsis B, et al. Comparison of Antibody Repertoires against *Staphylococcus aureus* in Healthy Individuals and in Acutely Infected Patients. Clin Diagn Lab Immunol. 2005;12:387–98. doi:10.1128/CDLI.12.3.387-398.2005.

107. Verkaik NJ, Vogel CP de, Boelens HA, Grumann D, Hoogenboezem T, Vink C, et al. Anti-staphylococcal humoral immune response in persistent nasal carriers and noncarriers of *Staphylococcus aureus*. J Infect Dis. 2009;199:625–32. doi:10.1086/596743.

108. Kolata J, Bode LGM, Holtfreter S, Steil L, Kusch H, Holtfreter B, et al. Distinctive patterns in the human antibody response to *Staphylococcus aureus* bacteremia in carriers and non-carriers. Proteomics. 2011;11:3914–27. doi:10.1002/pmic.201000760.

109. Karauzum H, Datta SK. Adaptive Immunity Against *Staphylococcus aureus*. Curr Top Microbiol Immunol. 2017;409:419–39. doi:10.1007/82_2016_1.

110. Holtfreter S, Kolata J, Bröker BM. Towards the immune proteome of *Staphylococcus aureus* - The anti-*S. aureus* antibody response. Int J Med Microbiol. 2010;300:176–92. doi:10.1016/j.ijmm.2009.10.002.

111. Selle M, Hertlein T, Oesterreich B, Klemm T, Kloppot P, Müller E, et al. Global antibody response to *Staphylococcus aureus* live-cell vaccination. Sci Rep. 2016;6:24754. doi:10.1038/srep24754.

112. Goss CH, Muhlebach MS. Review: *Staphylococcus aureus* and MRSA in cystic fibrosis. J Cyst Fibros. 2011;10:298–306. doi:10.1016/j.jcf.2011.06.002.

113. Adhikari RP, Ajao AO, Aman MJ, Karauzum H, Sarwar J, Lydecker AD, et al. Lower antibody levels to *Staphylococcus aureus* exotoxins are associated with sepsis in hospitalized adults with invasive *S. aureus* infections. J Infect Dis. 2012;206:915–23. doi:10.1093/infdis/jis462.

114. Fritz SA, Tiemann KM, Hogan PG, Epplin EK, Rodriguez M, Al-Zubeidi DN, et al. A Serologic Correlate of Protective Immunity Against Community-Onset *Staphylococcus aureus* Infection. Clin Infect Dis. 2013;56:1554–61. doi:10.1093/cid/cit123.

115. Baxter D. Active and passive immunity, vaccine types, excipients and licensing. Occup Med (Lond). 2007;57:552–6. doi:10.1093/occmed/kqm110.

116. Mullard A. FDA approves 100th monoclonal antibody product. Nat Rev Drug Discov. 2021;20:491–5. doi:10.1038/d41573-021-00079-7.

117. Marcotte H, Hammarström L. Passive Immunization. In: Mestecky J, editor. Mucosal immunology. Volume 2. Amsterdam: Academic Press; 2015. p. 1403–1434. doi:10.1016/B978-0-12-415847-4.00071-9.

118. Giersing BK, Dastgheyb SS, Modjarrad K, Moorthy V. Status of vaccine research and development of vaccines for *Staphylococcus aureus*. Vaccine. 2016;34:2962–6. doi:10.1016/j.vaccine.2016.03.110.

119. Zhang J, Yang F, Zhang X, Jing H, Ren C, Cai C, et al. Protective Efficacy and Mechanism of Passive Immunization with Polyclonal Antibodies in a Sepsis Model of *Staphylococcus aureus* Infection. Sci Rep. 2015;5:15553. doi:10.1038/srep15553.

120. Rennermalm A, Li Y-H, Bohaufs L, Jarstrand C, Brauner A, Brennan FR, Flock J-I. Antibodies against a truncated *Staphylococcus aureus* fibronectin-binding protein protect

against dissemination of infection in the rat. Vaccine. 2001;19:3376–83. doi:10.1016/S0264-410X(01)00080-9.

121. Anderson AS, Scully IL, Timofeyeva Y, Murphy E, McNeil LK, Mininni T, et al. *Staphylococcus aureus* Manganese Transport Protein C Is a Highly Conserved Cell Surface Protein That Elicits Protective Immunity Against *S. aureus* and *Staphylococcus epidermidis*. J Infect Dis. 2012;205:1688–96. doi:10.1093/infdis/jis272.

122. Karauzum H, Chen G, Abaandou L, Mahmoudieh M, Boroun AR, Shulenin S, et al. Synthetic human monoclonal antibodies toward staphylococcal enterotoxin B (SEB) protective against toxic shock syndrome. J Biol Chem. 2012;287:25203–15. doi:10.1074/jbc.M112.364075.

123. Pastar I, Nusbaum AG, Gil J, Patel SB, Chen J, Valdes J, et al. Interactions of methicillin resistant *Staphylococcus aureus* USA300 and *Pseudomonas aeruginosa* in polymicrobial wound infection. PLoS ONE. 2013;8:e56846. doi:10.1371/journal.pone.0056846.

124. Varshney AK, Wang X, MacIntyre J, Zollner RS, Kelleher K, Kovalenko OV, et al. Humanized staphylococcal enterotoxin B (SEB)-specific monoclonal antibodies protect from SEB intoxication and *Staphylococcus aureus* infections alone or as adjunctive therapy with vancomycin. J Infect Dis. 2014;210:973–81. doi:10.1093/infdis/jiu198.

125. Jung D-J, An J-H, Kurokawa K, Jung Y-C, Kim M-J, Aoyagi Y, et al. Specific serum Ig recognizing staphylococcal wall teichoic acid induces complement-mediated opsonophagocytosis against *Staphylococcus aureus*. J Immunol. 2012;189:4951–9. doi:10.4049/jimmunol.1201294.

126. Lee J-H, Kim N-H, Winstel V, Kurokawa K, Larsen J, An J-H, et al. Surface Glycopolymers Are Crucial for *In vitro* Anti-Wall Teichoic Acid IgG-Mediated Complement Activation and Opsonophagocytosis of *Staphylococcus aureus*. Infect Immun. 2015;83:4247–55. doi:10.1128/IAI.00767-15.

127. Lehar SM, Pillow T, Xu M, Staben L, Kajihara KK, Vandlen R, et al. Novel antibody-antibiotic conjugate eliminates intracellular *S. aureus*. Nature. 2015;527:323–8. doi:10.1038/nature16057.

128. Nemeth J, Lee JC. Antibodies to capsular polysaccharides are not protective against experimental *Staphylococcus aureus* endocarditis. Infect Immun. 1995;63:375–80.

129. Lee JC, Park JS, Shepherd SE, Carey V, Fattom A. Protective efficacy of antibodies to the *Staphylococcus aureus* type 5 capsular polysaccharide in a modified model of endocarditis in rats. Infect Immun. 1997;65:4146–51.

130. Liu B, Park S, Thompson CD, Li X, Lee JC. Antibodies to *Staphylococcus aureus* capsular polysaccharides 5 and 8 perform similarly *in vitro* but are functionally distinct *in vivo*. Virulence. 2016;8:859–74. doi:10.1080/21505594.2016.1270494.

131. Hall AE, Domanski PJ, Patel PR, Vernachio JH, Syribeys PJ, Gorovits EL, et al. Characterization of a protective monoclonal antibody recognizing *Staphylococcus aureus* MSCRAMM protein clumping factor A. Infect Immun. 2003;71:6864–70. doi:10.1128/iai.71.12.6864-6870.2003.

132. Domanski PJ, Patel PR, Bayer AS, Zhang L, Hall AE, Syribeys PJ, et al. Characterization of a humanized monoclonal antibody recognizing clumping factor A expressed by *Staphylococcus aureus*. Infect Immun. 2005;73:5229–32. doi:10.1128/IAI.73.8.5229-5232.2005.

133. Tkaczyk C, Hamilton MM, Sadowska A, Shi Y, Chang CS, Chowdhury P, et al. Targeting Alpha Toxin and ClfA with a Multimechanistic Monoclonal-Antibody-Based Approach for Prophylaxis of Serious *Staphylococcus aureus* Disease. mBio 2016. doi:10.1128/mBio.00528-16.

134. Weems JJ, Steinberg JP, Filler S, Baddley JW, Corey GR, Sampathkumar P, et al. Phase II, Randomized, Double-Blind, Multicenter Study Comparing the Safety and Pharmacokinetics of Tefibazumab to Placebo for Treatment of *Staphylococcus aureus* Bacteremia. Antimicrob Agents Chemother. 2006;50:2751–5. doi:10.1128/AAC.00096-06.

135. Xiong YQ, Estellés A, Li L, Abdelhady W, Gonzales R, Bayer AS, et al. A Human Biofilm-Disrupting Monoclonal Antibody Potentiates Antibiotic Efficacy in Rodent Models of both *Staphylococcus aureus* and Acinetobacter baumannii Infections. Antimicrob Agents Chemother 2017. doi:10.1128/AAC.00904-17.

136. Goodman SD, Obergfell KP, Jurcisek JA, Novotny LA, Downey JS, Ayala EA, et al. Biofilms can be dispersed by focusing the immune system on a common family of bacterial nucleoid-associated proteins. Mucosal Immunol. 2011;4:625–37. doi:10.1038/mi.2011.27.

137. Brockson ME, Novotny LA, Mokrzan EM, Malhotra S, Jurcisek JA, Akbar R, et al. Evaluation of the kinetics and mechanism of action of anti-integration host factor mediated disruption of bacterial biofilms. Mol Microbiol. 2014;93:1246–58. doi:10.1111/mmi.12735.

138. Estellés A, Woischnig A-K, Liu K, Stephenson R, Lomongsod E, Nguyen D, et al. A High-Affinity Native Human Antibody Disrupts Biofilm from *Staphylococcus aureus* Bacteria and Potentiates Antibiotic Efficacy in a Mouse Implant Infection Model. Antimicrob Agents Chemother. 2016;60:2292–301. doi:10.1128/AAC.02588-15.

139. Brady RA, Leid JG, Camper AK, Costerton JW, Shirtliff ME. Identification of *Staphylococcus aureus* proteins recognized by the antibody-mediated immune response to a biofilm infection. Infect Immun. 2006;74:3415–26. doi:10.1128/IAI.00392-06.

140. Xu Y, Maltesen RG, Larsen LH, Schønheyder HC, Le VQ, Nielsen JL, et al. *In vivo* gene expression in a *Staphylococcus aureus* prosthetic joint infection characterized by

RNA sequencing and metabolomics: a pilot study. BMC Microbiol. 2016;16:80. doi:10.1186/s12866-016-0695-6.

141. Lei MG, Gupta RK, Lee CY. Proteomics of *Staphylococcus aureus* biofilm matrix in a rat model of orthopedic implant-associated infection. PLoS ONE. 2017;12:e0187981. doi:10.1371/journal.pone.0187981.

142. Seilie ES, Bubeck Wardenburg J. *Staphylococcus aureus* pore-forming toxins: The interface of pathogen and host complexity. Semin Cell Dev Biol. 2017;72:101–16. doi:10.1016/j.semcdb.2017.04.003.

143. Anderson MJ, Schaaf E, Breshears LM, Wallis HW, Johnson JR, Tkaczyk C, et al. Alpha-Toxin Contributes to Biofilm Formation among *Staphylococcus aureus* Wound Isolates. Toxins (Basel) 2018. doi:10.3390/toxins10040157.

144. Ortines RV, Liu H, Cheng LI, Cohen TS, Lawlor H, Gami A, et al. Neutralizing Alpha-Toxin Accelerates Healing of *Staphylococcus aureus*-Infected Wounds in Nondiabetic and Diabetic Mice. Antimicrob Agents Chemother 2018. doi:10.1128/AAC.02288-17.

145. Wang Y, Cheng LI, Helfer DR, Ashbaugh AG, Miller RJ, Tzomides AJ, et al. Mouse model of hematogenous implant-related *Staphylococcus aureus* biofilm infection reveals therapeutic targets. Proc Natl Acad Sci U S A. 2017;114:E5094-E5102. doi:10.1073/pnas.1703427114.

146. Yu X-Q, Robbie GJ, Wu Y, Esser MT, Jensen K, Schwartz HI, et al. Safety, Tolerability, and Pharmacokinetics of MEDI4893, an Investigational, Extended-Half-Life, Anti-*Staphylococcus aureus* Alpha-Toxin Human Monoclonal Antibody, in Healthy Adults. Antimicrob Agents Chemother 2017. doi:10.1128/AAC.01020-16.

147. François B, Jafri HS, Chastre J, Sánchez-García M, Eggimann P, Dequin P-F, et al. Efficacy and safety of suvratoxumab for prevention of *Staphylococcus aureus* ventilator-associated pneumonia (SAATELLITE): a multicentre, randomised, double-blind, placebo-controlled, parallel-group, phase 2 pilot trial. The Lancet Infectious Diseases. 2021;21:1313–23. doi:10.1016/S1473-3099(20)30995-6.

148. Scherr TD, Hanke ML, Huang O, James DBA, Horswill AR, Bayles KW, et al. *Staphylococcus aureus* Biofilms Induce Macrophage Dysfunction Through Leukocidin AB and Alpha-Toxin. mBio 2015. doi:10.1128/mBio.01021-15.

149. Badarau A, Rouha H, Malafa S, Battles MB, Walker L, Nielson N, et al. Context matters: The importance of dimerization-induced conformation of the LukGH leukocidin of *Staphylococcus aureus* for the generation of neutralizing antibodies. MAbs. 2016;8:1347–60. doi:10.1080/19420862.2016.1215791.

150. Thomsen IP, Sapparapu G, James DBA, Cassat JE, Nagarsheth M, Kose N, et al. Monoclonal Antibodies Against the *Staphylococcus aureus* Bicomponent Leukotoxin AB

Isolated Following Invasive Human Infection Reveal Diverse Binding and Modes of Action. J Infect Dis. 2017;215:1124–31. doi:10.1093/infdis/jix071.

151. Benjamin DK, Schelonka R, White R, Holley HP, Bifano E, Cummings J, et al. A blinded, randomized, multicenter study of an intravenous *Staphylococcus aureus* immune globulin. J Perinatol. 2006;26:290–5. doi:10.1038/sj.jp.7211496.

152. Rupp ME, Holley HP, Lutz J, Dicpinigaitis PV, Woods CW, Levine DP, et al. Phase II, Randomized, Multicenter, Double-Blind, Placebo-Controlled Trial of a Polyclonal Anti-*Staphylococcus aureus* Capsular Polysaccharide Immune Globulin in Treatment of *Staphylococcus aureus* Bacteremia▿. Antimicrob Agents Chemother. 2007;51:4249–54. doi:10.1128/AAC.00570-07.

153. Patel M, Kaufman DA. Anti-lipoteichoic acid monoclonal antibody (pagibaximab) studies for the prevention of staphylococcal bloodstream infections in preterm infants. Expert Opin Biol Ther. 2015;15:595–600. doi:10.1517/14712598.2015.1019857.

154. Fattom A, Matalon A, Buerkert J, Taylor K, Damaso S, Boutriau D. Efficacy profile of a bivalent *Staphylococcus aureus* glycoconjugated vaccine in adults on hemodialysis: Phase III randomized study. Hum Vaccin Immunother. 2015;11:632–41. doi:10.4161/hv.34414.

155. Hu J, Xu T, Zhu T, Lou Q, Wang X, Wu Y, et al. Monoclonal antibodies against accumulation-associated protein affect EPS biosynthesis and enhance bacterial accumulation of *Staphylococcus epidermidis*. PLoS ONE. 2011;6:e20918. doi:10.1371/journal.pone.0020918.

156. Salgado-Pabón W, Schlievert PM. Models matter: the search for an effective *Staphylococcus aureus* vaccine. Nat Rev Microbiol. 2014;12:585–91. doi:10.1038/nrmicro3308.

157. DeJonge M, Burchfield D, Bloom B, Duenas M, Walker W, Polak M, et al. Clinical trial of safety and efficacy of INH-A21 for the prevention of nosocomial staphylococcal bloodstream infection in premature infants. J Pediatr. 2007;151:260-5, 265.e1. doi:10.1016/j.jpeds.2007.04.060.

158. Rouha H, Badarau A, Visram ZC, Battles MB, Prinz B, Magyarics Z, et al. Five birds, one stone: Neutralization of α-hemolysin and 4 bi-component leukocidins of *Staphylococcus aureus* with a single human monoclonal antibody. MAbs. 2014;7:243–54. doi:10.4161/19420862.2014.985132.

159. Zhou C, Lehar S, Gutierrez J, Rosenberger CM, Ljumanovic N, Dinoso J, et al. Pharmacokinetics and pharmacodynamics of DSTA4637A: A novel THIOMAB™ antibody antibiotic conjugate against *Staphylococcus aureus* in mice. MAbs. 2016;8:1612–9. doi:10.1080/19420862.2016.1229722.

160. Wang-Lin SX, Zhou C, Kamath AV, Hong K, Koppada N, Saad OM, et al. Minimal physiologically-based pharmacokinetic modeling of DSTA4637A, A novel THIOMAB™ antibody antibiotic conjugate against *Staphylococcus aureus*, in a mouse model. MAbs. 2018;10:1131–43. doi:10.1080/19420862.2018.1494478.

161. Graf AC, Leonard A, Schäuble M, Rieckmann LM, Hoyer J, Maass S, et al. Virulence Factors Produced by *Staphylococcus aureus* Biofilms Have a Moonlighting Function Contributing to Biofilm Integrity. Mol Cell Proteomics. 2019;18:1036–53. doi:10.1074/mcp.RA118.001120.

162. Nordengrün M, Abdurrahman G, Treffon J, Wächter H, Kahl BC, Bröker BM. Allergic Reactions to Serine Protease-Like Proteins of *Staphylococcus aureus*. Front. Immunol. 2021. doi:10.3389/fimmu.2021.651060.

163. Wertheim HFL, Vos MC, Ott A, van Belkum A, Voss A, Kluytmans JA, et al. Risk and outcome of nosocomial *Staphylococcus aureus* bacteraemia in nasal carriers versus non-carriers. The Lancet. 2004;364:703–5. doi:10.1016/S0140-6736(04)16897-9.

164. Rindi S, Cicalini S, Pietrocola G, Venditti M, Festa A, Foster TJ, et al. Antibody response in patients with endocarditis caused by *Staphylococcus aureus*. Eur J Clin Invest. 2006;36:536–43.

165. Reed SB, Wesson CA, Liou LE, Trumble WR, Schlievert PM, Bohach GA, Bayles KW. Molecular Characterization of a Novel *Staphylococcus aureus* Serine Protease Operon. Infect Immun. 2001;69:1521–7. doi:10.1128/IAI.69.3.1521-1527.2001.

166. Baba T, Bae T, Schneewind O, Takeuchi F, Hiramatsu K. Genome sequence of *Staphylococcus aureus* strain Newman and comparative analysis of staphylococcal genomes: polymorphism and evolution of two major pathogenicity islands. J Bacteriol. 2008;190:300–10. doi:10.1128/JB.01000-07.

167. Zdzalik M, Karim AY, Wolski K, Buda P, Wojcik K, Brueggemann S, et al. Prevalence of genes encoding extracellular proteases in *Staphylococcus aureus* - important targets triggering immune response *in vivo*. FEMS Immunol Med Microbiol. 2012;66:220–9. doi:10.1111/j.1574-695X.2012.01005.x.

168. Bachert C, Zhang N. Chronic rhinosinusitis and asthma: novel understanding of the role of IgE 'above atopy'. J Intern Med. 2012;272:133–43. doi:10.1111/j.1365-2796.2012.02559.x.

169. Stentzel S, Teufelberger A, Nordengrün M, Kolata J, Schmidt F, van Crombruggen K, et al. Staphylococcal serine protease-like proteins are pacemakers of allergic airway reactions to *Staphylococcus aureus*. J Allergy Clin Immunol. 2017;139:492-500.e8. doi:10.1016/j.jaci.2016.03.045.

170. Nordengrün M, Michalik S, Völker U, Bröker BM, Gómez-Gascón L. The quest for bacterial allergens. Int J Med Microbiol. 2018;308:738–50. doi:10.1016/j.ijmm.2018.04.003.

171. Mootz JM, Malone CL, Shaw LN, Horswill AR. Staphopains Modulate *Staphylococcus aureus* Biofilm Integrity. Infect Immun. 2013;81:3227–38. doi:10.1128/IAI.00377-13.

172. Iwase T, Uehara Y, Shinji H, Tajima A, Seo H, Takada K, et al. *Staphylococcus epidermidis* Esp inhibits *Staphylococcus aureus* biofilm formation and nasal colonization. Nature. 2010;465:346–9. doi:10.1038/nature09074.

173. Boles BR, Horswill AR. Agr-mediated dispersal of *Staphylococcus aureus* biofilms. PLoS Pathog. 2008;4:e1000052. doi:10.1371/journal.ppat.1000052.

174. Lauderdale KJ, Boles BR, Cheung AL, Horswill AR. Interconnections between Sigma B, agr, and proteolytic activity in *Staphylococcus aureus* biofilm maturation. Infect Immun. 2009;77:1623–35. doi:10.1128/IAI.01036-08.

175. Si Y, Zhao F, Beesetty P, Weiskopf D, Li Z, Tian Q, et al. Inhibition of protective immunity against *Staphylococcus aureus* infection by MHC-restricted immunodominance is overcome by vaccination. Sci Adv. 2020;6:eaaw7713. doi:10.1126/sciadv.aaw7713.

176. McDevitt D, Francois P, Vaudaux P, Foster TJ. Identification of the ligand-binding domain of the surface-located fibrinogen receptor (clumping factor) of *Staphylococcus aureus*. Mol Microbiol. 1995;16:895–907. doi:10.1111/j.1365-2958.1995.tb02316.x.

177. Bayer AS, Sullam PM, Ramos M, Li C, Cheung AL, Yeaman MR. *Staphylococcus aureus* induces platelet aggregation via a fibrinogen-dependent mechanism which is independent of principal platelet glycoprotein IIb/IIIa fibrinogen-binding domains. Infect Immun. 1995;63:3634–41.

178. Colque-Navarro P, Palma M, Söderquist B, Flock JI, Möllby R. Antibody responses in patients with staphylococcal septicemia against two *Staphylococcus aureus* fibrinogen binding proteins: clumping factor and an extracellular fibrinogen binding protein. Clin Diagn Lab Immunol. 2000;7:14–20. doi:10.1128/cdli.7.1.14-20.2000.

179. Wolz C, Goerke C, Landmann R, Zimmerli W, Fluckiger U. Transcription of Clumping Factor A in Attached and Unattached *Staphylococcus aureus In vitro* and during Device-Related Infection. Infect Immun. 2002;70:2758–62. doi:10.1128/IAI.70.6.2758-2762.2002.

180. Moreillon P, Entenza JM, Francioli P, McDevitt D, Foster TJ, François P, Vaudaux P. Role of *Staphylococcus aureus* coagulase and clumping factor in pathogenesis of experimental endocarditis. Infect Immun. 1995;63:4738–43.

181. Que Y-A, Haefliger J-A, Francioli P, Moreillon P. Expression of *Staphylococcus aureus* Clumping Factor A in *Lactococcus lactis* subsp. cremoris Using a New Shuttle Vector. Infect Immun. 2000;68:3516–22.

182. Stutzmann Meier P, Entenza JM, Vaudaux P, Francioli P, Glauser MP, Moreillon P. Study of *Staphylococcus aureus* Pathogenic Genes by Transfer and Expression in the Less Virulent Organism *Streptococcus gordonii*. Infect Immun. 2001;69:657–64. doi:10.1128/IAI.69.2.657-664.2001.

183. Tkaczyk C, Kasturirangan S, Minola A, Jones-Nelson O, Gunter V, Shi YY, et al. Multimechanistic Monoclonal Antibodies (MAbs) Targeting *Staphylococcus aureus* Alpha-Toxin and Clumping Factor A: Activity and Efficacy Comparisons of a MAb Combination and an Engineered Bispecific Antibody Approach. Antimicrob Agents Chemother 2017. doi:10.1128/AAC.00629-17.

184. Ponnuraj K, Bowden MG, Davis S, Gurusiddappa S, Moore D, Choe D, et al. A "dock, lock, and latch" Structural Model for a Staphylococcal Adhesin Binding to Fibrinogen. Cell. 2003;115:217–28. doi:10.1016/S0092-8674(03)00809-2.

185. Ma J, Wei Y, Zhang L, Wang X, Di Yao, Liu D, et al. Identification of a novel linear B-cell epitope as a vaccine candidate in the N2N3 subdomain of *Staphylococcus aureus* fibronectin-binding protein A. J Med Microbiol. 2018;67:423–31. doi:10.1099/jmm.0.000633.

186. Provenza G, Provenzano M, Visai L, Burke FM, Geoghegan JA, Stravalaci M, et al. Functional analysis of a murine monoclonal antibody against the repetitive region of the fibronectin-binding adhesins fibronectin-binding protein A and fibronectin-binding protein B from *Staphylococcus aureus*. FEBS J. 2010;277:4490–505. doi:10.1111/j.1742-4658.2010.07835.x.

187. Rueden CT, Schindelin J, Hiner MC, DeZonia BE, Walter AE, Arena ET, Eliceiri KW. ImageJ2: ImageJ for the next generation of scientific image data. BMC Bioinformatics 2017. doi:10.1186/s12859-017-1934-z.

188. Giudicelli V, Brochet X, Lefranc M-P. IMGT/V-QUEST: IMGT Standardized Analysis of the Immunoglobulin (IG) and T Cell Receptor (TR) Nucleotide Sequences. Cold Spring Harbor Protocols. 2011;2011:pdb.prot5633-pdb.prot5633. doi:10.1101/pdb.prot5633.

189. Corpet F. Multiple sequence alignment with hierarchical clustering. Nucleic Acids Research. 1988;16:10881–90. doi:10.1093/nar/16.22.10881.

190. Artimo P, Jonnalagedda M, Arnold K, Baratin D, Csardi G, Castro E de, et al. ExPASy: SIB bioinformatics resource portal. Nucleic Acids Research. 2012;40:W597-W603. doi:10.1093/nar/gks400.

191. Bateman A, Martin M-J, Orchard S, Magrane M, Agivetova R, Ahmad S, et al. UniProt: the universal protein knowledgebase in 2021. Nucleic Acids Research. 2021;49:D480-D489. doi:10.1093/nar/gkaa1100.

192. Herbig M, Kräter M, Plak K, Müller P, Guck J, Otto O. Real-Time Deformability Cytometry: Label-Free Functional Characterization of Cells. In: Hawley TS, Hawley RG,

editors. Flow Cytometry Protocols. New York: Humana Press; 2017. p. 347–369. doi:10.1007/978-1-4939-7346-0_15.

193. Meyer TC, Schmidt F, Steinke J, Bröker BM, Völker U, Michalik S. Technical report: xMAPr - High-dynamic-range (HDR) quantification of antigen-specific antibody binding. J Proteomics. 2020;212:103577. doi:10.1016/j.jprot.2019.103577.

194. Wittmann N. Herstellung und Charakterisierung muriner monoklonaler Antikörper gegen *Staphylococcus aureus*-Proteine [Masters]: University Medicine Greifswald; 2018.

195. Frieder Schmiedeke. Charakterisierung von humanisierten monoklonalen Antikörpern gegen ausgewählte Biofilm-assoziierte *Staphylococcus aureus* Virulenzfaktoren: University Medicine Greifswald; 2019.

196. Meyer L, López T, Espinosa R, Arias CF, Vollmers C, DuBois RM. A simplified workflow for monoclonal antibody sequencing. PLoS ONE. 2019;14:e0218717. doi:10.1371/journal.pone.0218717.

197. Abdullah MR, Batuecas MT, Jennert F, Voß F, Westhoff P, Kohler TP, et al. Crystal Structure and Pathophysiological Role of the Pneumococcal Nucleoside-binding Protein PnrA. J Mol Biol. 2021;433:166723. doi:10.1016/j.jmb.2020.11.022.

198. Seidel SAI, Dijkman PM, Lea WA, van den Bogaart G, Jerabek-Willemsen M, Lazic A, et al. Microscale thermophoresis quantifies biomolecular interactions under previously challenging conditions. Methods. 2013;59:301–15. doi:10.1016/j.ymeth.2012.12.005.

199. Dubin G, Stec-Niemczyk J, Kisielewska M, Pustelny K, Popowicz GM, Bista M, et al. Enzymatic activity of the *Staphylococcus aureus* SplB serine protease is induced by substrates containing the sequence Trp-Glu-Leu-Gln. J Mol Biol. 2008;379:343–56. doi:10.1016/j.jmb.2008.03.059.

200. Khandoga AG, Khandoga A, Anders H-J, Krombach F. Postischemic Vascular Permeability Requires Both TLR-2 And TLR-4, But Only TLR-2 Mediates The Transendothelial Migration Of Leukocytes. Shock. 2009;31:593–9. doi:10.1097/SHK.0b013e318193c859.

201. Sproston NR, Ashworth JJ. Role of C-Reactive Protein at Sites of Inflammation and Infection. Front. Immunol. 2018. doi:10.3389/fimmu.2018.00754.

202. Mohanan S, Gopalan Nair R, Vellani H, C G S, George B, M N K. Baseline C-reactive protein levels and prognosis in patients with infective endocarditis: A prospective cohort study. Indian Heart J. 2018;70:S43-9. doi:10.1016/j.ihj.2018.05.001.

203. Dach E von, Albrich WC, Brunel A-S, Prendki V, Cuvelier C, Flury D, et al. Effect of C-Reactive Protein–Guided Antibiotic Treatment Duration, 7-Day Treatment, or 14-Day Treatment on 30-Day Clinical Failure Rate in Patients With Uncomplicated Gram-Negative Bacteremia. JAMA. 2020;323:2160. doi:10.1001/jama.2020.6348.

204. Benito N, Mur I, Ribera A, Soriano A, Rodríguez-Pardo D, Sorlí L, et al. The Different Microbial Etiology of Prosthetic Joint Infections according to Route of Acquisition and Time after Prosthesis Implantation, Including the Role of Multidrug-Resistant Organisms. J Clin Med 2019. doi:10.3390/jcm8050673.

205. Normann N, Tietz G, Kühn A, Fuchs C, Balau V, Schulz K, et al. Pathogen-specific antibody profiles in patients with severe systemic infections. Eur Cell Mater. 2020;39:171–82. doi:10.22203/eCM.v039a11.

206. Torres A, Cilloniz C, Niederman MS, Menéndez R, Chalmers JD, Wunderink RG, van der Poll T. Pneumonia. Nat Rev Dis Primers. 2021;7:25. doi:10.1038/s41572-021-00259-0.

207. Gomez de Agüero M, Ganal-Vonarburg SC, Fuhrer T, Rupp S, Uchimura Y, Li H, et al. The maternal microbiota drives early postnatal innate immune development. Science. 2016;351:1296–302. doi:10.1126/science.aad2571.

208. Sterlin D, Fadlallah J, Slack E, Gorochov G. The antibody/microbiota interface in health and disease. Mucosal Immunol. 2020;13:3–11. doi:10.1038/s41385-019-0192-y.

209. Martin RM, Brady JL, Am Lew. The need for IgG2c specific antiserum when isotyping antibodies from C57BL/6 and NOD mice. J Immunol Methods 1998. doi:10.1016/s0022-1759(98)00015-5.

210. Torres OB, Duval AJ, Sulima A, Antoline JFG, Jacobson AE, Rice KC, et al. A rapid solution-based method for determining the affinity of heroin hapten-induced antibodies to heroin, its metabolites, and other opioids. Anal Bioanal Chem. 2018;410:3885–903. doi:10.1007/s00216-018-1060-4.

211. Ganesan A, Ahmed M, Okoye I, Arutyunova E, Babu D, Turnbull WL, et al. Comprehensive *in vitro* characterization of PD-L1 small molecule inhibitors. Sci Rep. 2019;9:12392. doi:10.1038/s41598-019-48826-6.

212. Chandrabalan A, Thibeault PE, Deinhardt-Emmer S, Nordengrün M, Iqbal J, Mrochen DM, et al. *S. aureus* -serine protease-like protein B (SplB) activates PAR2 and induces endothelial barrier dysfunction; 2021.

213. Falati S, Gross P, Merrill-Skoloff G, Furie BC, Furie B. Real-time *in vivo* imaging of platelets, tissue factor and fibrin during arterial thrombus formation in the mouse. Nat Med. 2002;8:1175–81. doi:10.1038/nm782.

214. Friguet B, Djavadi-Ohaniance L, Goldberg ME. Some monoclonal antibodies raised with a native protein bind preferentially to the denatured antigen. Mol Immunol 1984. doi:10.1016/0161-5890(84)90053-1.

215. Rolain JM, Lecam C, Raoult D. Simplified Serological Diagnosis of Endocarditis Due to Coxiellaburnetii and *Bartonella*. Clin Diagn Lab Immunol. 2003;10:1147–8. doi:10.1128/CDLI.10.6.1147-1148.2003.

216. Nishiguchi S, Nishino K, Kitagawa I, Tokuda Y. Factors associated with delayed diagnosis of infective endocarditis: A retrospective cohort study in a teaching hospital in Japan. Medicine (Baltimore). 2020;99:e21418. doi:10.1097/MD.0000000000021418.

217. Dayer MJ, Jones S, Prendergast B, Baddour LM, Lockhart PB, Thornhill MH. Incidence of infective endocarditis in England, 2000–13: a secular trend, interrupted time-series analysis. The Lancet. 2015;385:1219–28. doi:10.1016/S0140-6736(14)62007-9.

218. Mackie AS, Liu W, Savu A, Marelli AJ, Kaul P. Infective Endocarditis Hospitalizations Before and After the 2007 American Heart Association Prophylaxis Guidelines. Can J Cardiol. 2016;32:942–8. doi:10.1016/j.cjca.2015.09.021.

219. Holland DJ, Simos PA, Yoon J, Sivabalan P, Ramnarain J, Runnegar NJ. Infective Endocarditis: A Contemporary Study of Microbiology, Echocardiography and Associated Clinical Outcomes at a Major Tertiary Referral Centre. Heart Lung Circ. 2020;29:840–50. doi:10.1016/j.hlc.2019.07.006.

220. Lamas CC, Fournier P-E, Zappa M, Brandão TJD, Januário-da-Silva CA, Correia MG, et al. Diagnosis of blood culture-negative endocarditis and clinical comparison between blood culture-negative and blood culture-positive cases. Infection. 2016;44:459–66. doi:10.1007/s15010-015-0863-x.

221. Garg P, Ko DT, Bray Jenkyn KM, Li L, Shariff SZ. Infective Endocarditis Hospitalizations and Antibiotic Prophylaxis Rates Before and After the 2007 American Heart Association Guideline Revision. Circulation. 2019;140:170–80. doi:10.1161/CIRCULATIONAHA.118.037657.

222. Østergaard L, Bruun NE, Voldstedlund M, Arpi M, Andersen CØ, Schønheyder HC, et al. Prevalence of infective endocarditis in patients with positive blood cultures: a Danish nationwide study. Eur Heart J. 2019;40:3237–44. doi:10.1093/eurheartj/ehz327.

223. Villiers MC de, Viljoen CA, Manning K, van der Westhuizen C, Seedat A, Rath M, et al. The changing landscape of infective endocarditis in South Africa. S Afr Med J. 2019;109:592–6. doi:10.7196/SAMJ.2019.v109i8.13888.

224. Erdem H, Puca E, Ruch Y, Santos L, Ghanem-Zoubi N, Argemi X, et al. Portraying infective endocarditis: results of multinational ID-IRI study. Eur J Clin Microbiol Infect Dis. 2019;38:1753–63. doi:10.1007/s10096-019-03607-x.

225. Cornelissen CG, Frechen DA, Schreiner K, Marx N, Krüger S. Inflammatory parameters and prediction of prognosis in infective endocarditis. BMC Infect Dis. 2013;13:272. doi:10.1186/1471-2334-13-272.

226. Verhagen DWM, Hermanides J, Korevaar JC, Bossuyt PMM, van den Brink RBA, Speelman P, van der Meer JTM. Prognostic value of serial C-reactive protein measurements in left-sided native valve endocarditis. Arch Intern Med. 2008;168:302–7. doi:10.1001/archinternmed.2007.73.

227. Cruse JM, Lewis RE. Atlas of immunology. 3rd ed. Boca Raton, FL: CRC Press/Taylor & Francis; 2010.

228. Harro JM, Peters BM, O'May GA, Archer N, Kerns P, Prabhakara R, Shirtliff ME. Vaccine development in *Staphylococcus aureus*: taking the biofilm phenotype into consideration. FEMS Immunol Med Microbiol. 2010;59:306–23. doi:10.1111/j.1574-695X.2010.00708.x.

229. Zimmermann K, Haas A, Oxenius A. Systemic antibody responses to gut microbes in health and disease. Gut Microbes. 2012;3:42–7. doi:10.4161/gmic.19344.

230. Christmann BS, Abrahamsson TR, Bernstein CN, Duck LW, Mannon PJ, Berg G, et al. Human seroreactivity to gut microbiota antigens. J Allergy Clin Immunol. 2015;136:1378-86.e1-5. doi:10.1016/j.jaci.2015.03.036.

231. Fadlallah J, Sterlin D, Fieschi C, Parizot C, Dorgham K, El Kafsi H, et al. Synergistic convergence of microbiota-specific systemic IgG and secretory IgA. J Allergy Clin Immunol. 2019;143:1575-1585.e4. doi:10.1016/j.jaci.2018.09.036.

232. Brown MM, Horswill AR. *Staphylococcus epidermidis*—Skin friend or foe? PLoS Pathog. 2020;16:e1009026. doi:10.1371/journal.ppat.1009026.

233. Gallo RL. Human Skin Is the Largest Epithelial Surface for Interaction with Microbes. Journal of Investigative Dermatology. 2017;137:1213–4. doi:10.1016/j.jid.2016.11.045.

234. Pasparakis M, Haase I, Nestle FO. Mechanisms regulating skin immunity and inflammation. Nat Rev Immunol. 2014;14:289–301. doi:10.1038/nri3646.

235. Kortekaas Krohn I, Aerts JL, Breckpot K, Goyvaerts C, Knol E, van Wijk F, Gutermuth J. T-cell subsets in the skin and their role in inflammatory skin disorders. Allergy 2021. doi:10.1111/all.15104.

236. Hudak S, Hagen M, Liu Y, Catron D, Oldham E, McEvoy LM, Bowman EP. Immune surveillance and effector functions of CCR10(+) skin homing T cells. J.I. 2002;169:1189–96. doi:10.4049/jimmunol.169.3.1189.

237. Janeway CA. Immunobiology 5: The immune system in health and disease / Charles A. Janeway … [et al.]. 5th ed. New York: Garland; Edinburgh : Churchill Livingstone; 2001.

238. Alangaden GJ. Nosocomial fungal infections: epidemiology, infection control, and prevention. Infect Dis Clin North Am. 2011;25:201–25. doi:10.1016/j.idc.2010.11.003.

239. Niemiec MJ, Kapitan M, Polke M, Jacobsen ID. Commensal to Pathogen Transition of *Candida albicans*. In: Reference Module in Life Sciences: Elsevier; 2017. p. 344. doi:10.1016/B978-0-12-809633-8.12077-1.

240. Macpherson AJ, Yilmaz B, Limenitakis JP, Ganal-Vonarburg SC. IgA Function in Relation to the Intestinal Microbiota. Annu Rev Immunol. 2018;36:359–81. doi:10.1146/annurev-immunol-042617-053238.

241. Mantis NJ, Rol N, Corthésy B. Secretory IgA's Complex Roles in Immunity and Mucosal Homeostasis in the Gut. Mucosal Immunol. 2011;4:603–11. doi:10.1038/mi.2011.41.

242. Macpherson A, Khoo UY, Forgacs I, Philpott-Howard J, Bjarnason I. Mucosal antibodies in inflammatory bowel disease are directed against intestinal bacteria. Gut. 1996;38:365–75. doi:10.1136/gut.38.3.365.

243. Kubinak JL, Round JL. Toll-like receptors promote mutually beneficial commensal-host interactions. PLoS Pathog. 2012;8:e1002785. doi:10.1371/journal.ppat.1002785.

244. Schommer NN, Gallo RL. Structure and function of the human skin microbiome. Trends Microbiol. 2013;21:660–8. doi:10.1016/j.tim.2013.10.001.

245. Beutler B. Pathogens, Commensals, and Immunity: From the Perspective of the Urinary Bladder. Pathogens. 2016;5:5. doi:10.3390/pathogens5010005.

246. Jenkins A, Diep B an, Mai TT, Vo NH, Warrener P, Suzich J, et al. Differential Expression and Roles of *Staphylococcus aureus* Virulence Determinants during Colonization and Disease. mBio 2015. doi:10.1128/mBio.02272-14.

247. Martínez JP, Gil ML, López-Ribot JL, Chaffin WL. Serologic response to cell wall mannoproteins and proteins of *Candida albicans*. Clin Microbiol Rev. 1998;11:121–41. doi:10.1128/CMR.11.1.121.

248. Pitarch A, Jiménez A, Nombela C, Gil C. Decoding serological response to Candida cell wall immunome into novel diagnostic, prognostic, and therapeutic candidates for systemic candidiasis by proteomic and bioinformatic analyses. Mol Cell Proteomics. 2006;5:79–96. doi:10.1074/mcp.M500243-MCP200.

249. Li F-q, Ma C-f, Shi L-n, Lu J-f, Wang Y, Huang M, Kong Q-q. Diagnostic value of immunoglobulin G antibodies against *Candida* enolase and fructose-bisphosphate aldolase for candidemia. BMC Infect Dis. 2013;13:253. doi:10.1186/1471-2334-13-253.

250. Mamtani S, Aljanabi NM, Gupta Rauniyar RP, Acharya A, Malik BH. *Candida* Endocarditis: A Review of the Pathogenesis, Morphology, Risk Factors, and Management of an Emerging and Serious Condition. Cureus. 2020;12:e6695. doi:10.7759/cureus.6695.

251. López-Ribot JL, Casanova M, Murgui A, Martínez JP. Antibody response to *Candida albicans* cell wall antigens. FEMS Immunol Med Microbiol. 2004;41:187–96. doi:10.1016/j.femsim.2004.03.012.

252. van der Kooi-Pol MM, Vogel CP de, Westerhout-Pluister GN, Veenstra-Kyuchukova YK, Duipmans JC, Glasner C, et al. High anti-staphylococcal antibody titers in patients

with epidermolysis bullosa relate to long-term colonization with alternating types of *Staphylococcus aureus*. J Invest Dermatol. 2013;133:847–50. doi:10.1038/jid.2012.347.

253. Feil EJ, Cooper JE, Grundmann H, Robinson DA, Enright MC, Berendt T, et al. How clonal is *Staphylococcus aureus*? J Bacteriol. 2003;185:3307–16. doi:10.1128/JB.185.11.3307-3316.2003.

254. Yang J-J, Chang T-W, Jiang Y, Kao H-J, Chiou B-H, Kao M-S, Huang C-M. Commensal *Staphylococcus aureus* Provokes Immunity to Protect against Skin Infection of Methicillin-Resistant *Staphylococcus aureus*. IJMS. 2018;19:1290. doi:10.3390/ijms19051290.

255. Meena DS, Kumar D. *Candida* Pneumonia: An Innocent Bystander or a Silent Killer? Med Princ Pract 2021. doi:10.1159/000520111.

256. Annavajhala MK, Gomez-Simmonds A, Uhlemann A-C. Multidrug-Resistant Enterobacter cloacae Complex Emerging as a Global, Diversifying Threat. Front Microbiol. 2019;10:44. doi:10.3389/fmicb.2019.00044.

257. Murray PR, Masur H. Current approaches to the diagnosis of bacterial and fungal bloodstream infections in the intensive care unit. Crit Care Med. 2012;40:3277–82. doi:10.1097/CCM.0b013e318270e771.

258. Aiello A, Farzaneh F, Candore G, Caruso C, Davinelli S, Gambino CM, et al. Immunosenescence and Its Hallmarks: How to Oppose Aging Strategically? A Review of Potential Options for Therapeutic Intervention. Front Immunol. 2019;10:2247. doi:10.3389/fimmu.2019.02247.

259. Goronzy JJ, Weyand CM. Understanding immunosenescence to improve responses to vaccines. Nat Immunol. 2013;14:428–36. doi:10.1038/ni.2588.

260. Salinas-Carmona MC, Perez LI, Galan K, Vazquez AV. Immunosuppressive drugs have different effect on B lymphocyte subsets and IgM antibody production in immunized BALB/c mice. Autoimmunity. 2009;42:537–44. doi:10.1080/08916930903019119.

261. Deepak P, Kim W, Paley MA, Yang M, Carvidi AB, Demissie EG, et al. Effect of Immunosuppression on the Immunogenicity of mRNA Vaccines to SARS-CoV-2 : A Prospective Cohort Study. Ann Intern Med. 2021;174:1572–85. doi:10.7326/M21-1757.

262. Carvalho MS, Trabulo M, Ribeiras R, Abecasis J, Leal da Costa F, Mendes M. A case of native valve infective endocarditis in an immunocompromised patient. Revista Portuguesa de Cardiologia (English Edition). 2012;31:35–8. doi:10.1016/j.repce.2011.11.015.

263. Fux CA, Shirtliff M, Stoodley P, Costerton JW. Can laboratory reference strains mirror 'real-world' pathogenesis? Trends Microbiol. 2005;13:58–63. doi:10.1016/j.tim.2004.11.001.

264. Head NE, Yu H. Cross-Sectional Analysis of Clinical and Environmental Isolates of *Pseudomonas aeruginosa* : Biofilm Formation, Virulence, and Genome Diversity. Infect Immun. 2004;72:133–44. doi:10.1128/IAI.72.1.133-144.2004.

265. Schweizer ML, Furuno JP, Sakoulas G, Johnson JK, Harris AD, Shardell MD, et al. Increased Mortality with Accessory Gene Regulator (agr) Dysfunction in *Staphylococcus aureus* among Bacteremic Patients. Antimicrob Agents Chemother. 2011;55:1082–7. doi:10.1128/AAC.00918-10.

266. Fournier P-E, Thuny F, Richet H, Lepidi H, Casalta J-P, Arzouni J-P, et al. Comprehensive Diagnostic Strategy for Blood Culture–Negative Endocarditis: A Prospective Study of 819 New Cases. Clin Infect Dis. 2010;51:131–40. doi:10.1086/653675.

267. Houpikian P, Raoult D. Blood culture-negative endocarditis in a reference center: etiologic diagnosis of 348 cases. Medicine (Baltimore). 2005;84:162–73. doi:10.1097/01.md.0000165658.82869.17.

268. Nakano Y, Kurano M, Morita Y, Shimura T, Yokoyama R, Qian C, et al. Time course of the sensitivity and specificity of anti-SARS-CoV-2 IgM and IgG antibodies for symptomatic COVID-19 in Japan. Sci Rep. 2021;11:2776. doi:10.1038/s41598-021-82428-5.

269. Hollander D, Kaunitz JD. The "Leaky Gut": Tight Junctions but Loose Associations? Dig Dis Sci. 2020;65:1277–87. doi:10.1007/s10620-019-05777-2.

270. Bala S, Marcos M, Gattu A, Catalano D, Szabo G. Acute binge drinking increases serum endotoxin and bacterial DNA levels in healthy individuals. PLoS ONE. 2014;9:e96864. doi:10.1371/journal.pone.0096864.

271. König J, Wells J, Cani PD, García-Ródenas CL, MacDonald T, Mercenier A, et al. Human Intestinal Barrier Function in Health and Disease. Clin Transl Gastroenterol. 2016;7:e196-. doi:10.1038/ctg.2016.54.

272. Obrenovich MEM. Leaky Gut, Leaky Brain? Microorganisms 2018. doi:10.3390/microorganisms6040107.

273. Haas A, Zimmermann K, Graw F, Slack E, Rusert P, Ledergerber B, et al. Systemic antibody responses to gut commensal bacteria during chronic HIV-1 infection. Gut. 2011;60:1506–19. doi:10.1136/gut.2010.224774.

274. Camilleri M. Leaky gut: mechanisms, measurement and clinical implications in humans. Gut. 2019;68:1516–26. doi:10.1136/gutjnl-2019-318427.

275. García-Granja PE, López J, Vilacosta I, Ortiz-Bautista C, Sevilla T, Olmos C, et al. Polymicrobial Infective Endocarditis: Clinical Features and Prognosis. Medicine (Baltimore) 2015. doi:10.1097/MD.0000000000002000.

276. Shah S, Shrestha N, Gordon S. Polymicrobial Infective Endocarditis. Open Forum Infect Dis 2015. doi:10.1093/ofid/ofv133.573.

277. Kiani D. The Increasing Importance of Polymicrobial Bacteremia. JAMA. 1979;242:1044. doi:10.1001/jama.1979.03300100022015.

278. Weinstein MP, Reller LB, Murphy JR. Clinical importance of polymicrobial bacteremia. Diagn Microbiol Infect Dis. 1986;5:185–96. doi:10.1016/0732-8893(86)90001-5.

279. Reyn CF von, Levy BS, Arbeit RD, Friedland G, Crumpacker CS. Infective endocarditis: an analysis based on strict case definitions. Ann Intern Med. 1981;94:505–18. doi:10.7326/0003-4819-94-4-505.

280. Sancho S, Artero A, Zaragoza R, Camarena JJ, González R, Nogueira JM. Impact of nosocomial polymicrobial bloodstream infections on the outcome in critically ill patients. Eur J Clin Microbiol Infect Dis. 2012;31:1791–6. doi:10.1007/s10096-011-1503-8.

281. Schiøtz PO, Høiby N, Hertz JB. Cross-reactions between *Staphylococcus aureus* and fifteen other bacterial species. Acta Pathol Microbiol Scand B. 1979;87:329–36. doi:10.1111/j.1699-0463.1979.tb02447.x.

282. Keasey SL, Schmid KE, Lee MS, Meegan J, Tomas P, Minto M, et al. Extensive Antibody Cross-reactivity among Infectious Gram-negative Bacteria Revealed by Proteome Microarray Analysis *. Mol Cell Proteomics. 2009;8:924–35. doi:10.1074/mcp.M800213-MCP200.

283. Méric G, Miragaia M, Been M de, Yahara K, Pascoe B, Mageiros L, et al. Ecological Overlap and Horizontal Gene Transfer in *Staphylococcus aureus* and *Staphylococcus epidermidis*. Genome Biol Evol. 2015;7:1313–28. doi:10.1093/gbe/evv066.

284. Blake JE, Metcalfe MA. A Shared Noncapsular Antigen Is Responsible for False-Positive Reactions by *Staphylococcus epidermidis* in Commercial Agglutination Tests for *Staphylococcus aureus*. J Clin Microbiol. 2001;39:544–50. doi:10.1128/JCM.39.2.544-550.2001.

285. Fournier JM, Bouvet A, Mathieu D, Nato F, Boutonnier A, Gerbal R, et al. New latex reagent using monoclonal antibodies to capsular polysaccharide for reliable identification of both oxacillin-susceptible and oxacillin-resistant *Staphylococcus aureus*. J Clin Microbiol. 1993;31:1342–4. doi:10.1128/jcm.31.5.1342-1344.1993.

286. Rollenske T, Szijarto V, Lukasiewicz J, Guachalla LM, Stojkovic K, Hartl K, et al. Cross-specificity of protective human antibodies against *Klebsiella pneumoniae* LPS O-antigen. Nat Immunol. 2018;19:617–24. doi:10.1038/s41590-018-0106-2.

287. Salomäki SP, Saraste A, Jalava-Karvinen P, Pirilä L, Hohenthal U. Prosthetic Valve Candida Endocarditis: A Case Report with 18F-FDG-PET/CT as Part of the Diagnostic Workup. Case Rep Cardiol. 2020;2020:4921380. doi:10.1155/2020/4921380.

288. Vojdani A, Rahimian P, Kalhor H, Mordechai E. Immunological cross reactivity between *Candida albicans* and human tissue. J Clin Lab Immunol. 1996;48:1–15.

289. Clancy CJ, Nguyen MH. Finding the "missing 50%" of invasive candidiasis: how nonculture diagnostics will improve understanding of disease spectrum and transform patient care. Clin Infect Dis. 2013;56:1284–92. doi:10.1093/cid/cit006.

290. Lalani T, Person AK, Hedayati SS, Moore L, Murdoch DR, Hoen B, et al. *Propionibacterium* endocarditis: a case series from the International Collaboration on Endocarditis Merged Database and Prospective Cohort Study. Scand J Infect Dis. 2007;39:840–8. doi:10.1080/00365540701367793.

291. Jakab E, Zbinden R, Gubler J, Ruef C, Graevenitz A von, Krause M. Severe infections caused by *Propionibacterium acnes*: an underestimated pathogen in late postoperative infections. Yale J Biol Med. 1996;69:477–82.

292. Banzon JM, Rehm SJ, Gordon SM, Hussain ST, Pettersson GB, Shrestha NK. *Propionibacterium acnes* endocarditis: a case series. Clin Microbiol Infect. 2017;23:396–9. doi:10.1016/j.cmi.2016.12.026.

293. Lodhi SH, Abbasi A, Ahmed T, Chan A. Acne on the Valve: Two Intriguing Cases of *Cutibacterium Acnes* Endocarditis. Cureus. 2020;12:e8532. doi:10.7759/cureus.8532.

294. Sohail MR, Gray AL, Baddour LM, Tleyjeh IM, Virk A. Infective endocarditis due to *Propionibacterium* species. Clin Microbiol Infect. 2009;15:387–94. doi:10.1111/j.1469-0691.2009.02703.x.

295. Bernard C, Renaudeau N, Mollichella M-L, Quellard N, Girardot M, Imbert C. Cutibacterium acnes protects *Candida albicans* from the effect of micafungin in biofilms. Int J Antimicrob Agents. 2018;52:942–6. doi:10.1016/j.ijantimicag.2018.08.009.

296. Bernard C, Lemoine V, Hoogenkamp MA, Girardot M, Krom BP, Imbert C. *Candida albicans* enhances initial biofilm growth of Cutibacterium acnes under aerobic conditions. Biofouling. 2019;35:350–60. doi:10.1080/08927014.2019.1608966.

297. Shirtliff ME, Peters BM, Jabra-Rizk MA. Cross-kingdom interactions: *Candida albicans* and bacteria. FEMS Microbiol Lett. 2009;299:1–8. doi:10.1111/j.1574-6968.2009.01668.x.

298. Oh I, Muthukrishnan G, Ninomiya MJ, Brodell JD, Smith BL, Lee CC, et al. Tracking Anti-*Staphylococcus aureus* Antibodies Produced *In Vivo* and *Ex Vivo* during Foot Salvage Therapy for Diabetic Foot Infections Reveals Prognostic Insights and Evidence of Diversified Humoral Immunity. Infect Immun 2018. doi:10.1128/IAI.00629-18.

299. Harro JM, Shirtliff ME, Arnold W, Kofonow JM, Dammling C, Achermann Y, et al. Development of a Novel and Rapid Antibody-based Diagnostic for Chronic *Staphylococcus aureus* Infections Based on Biofilm Antigens. J Clin Microbiol 2020. doi:10.1128/JCM.01414-19.

300. Mikulska M, Calandra T, Sanguinetti M, Poulain D, Viscoli C. The use of mannan antigen and anti-mannan antibodies in the diagnosis of invasive candidiasis: recommendations from the Third European Conference on Infections in Leukemia. Critical Care. 2010;14:R222. doi:10.1186/cc9365.

301. Parra-Sánchez M, Zakariya-Yousef Breval I, Castro Méndez C, García-Rey S, Loza Vazquez A, Úbeda Iglesias A, et al. *Candida albicans* Germ-Tube Antibody: Evaluation of a New Automatic Assay for Diagnosing Invasive Candidiasis in ICU Patients. Mycopathologia. 2017;182:645–52. doi:10.1007/s11046-017-0125-9.

302. Marmor S, Bauer T, Desplaces N, Heym B, Roux A-L, Sol O, et al. Multiplex Antibody Detection for Noninvasive Genus-Level Diagnosis of Prosthetic Joint Infection. J Clin Microbiol. 2016;54:1065–73. doi:10.1128/JCM.02885-15.

303. Lanzavecchia A, Bernasconi N, Traggiai E, Ruprecht CR, Corti D, Sallusto F. Understanding and making use of human memory B cells. Immunol Rev. 2006;211:303–9. doi:10.1111/j.0105-2896.2006.00403.x.

304. Jenul C, Horswill AR. Regulation of *Staphylococcus aureus* virulence. Microbiol Spectr 2018. doi:10.1128/microbiolspec.GPP3-0031-2018.

305. Miller LS, Fowler VG, Shukla SK, Rose WE, Proctor RA. Development of a vaccine against *Staphylococcus aureus* invasive infections: Evidence based on human immunity, genetics and bacterial evasion mechanisms. FEMS Microbiol Rev. 2020;44:123–53. doi:10.1093/femsre/fuz030.

306. Otto M. Molecular basis of *Staphylococcus epidermidis* infections. Semin Immunopathol 2012. doi:10.1007/s00281-011-0296-2.

307. Detrick B, Hamilton RG, Schmitz JL. Manual of molecular and clinical laboratory immunology. Washington, D.C.: ASM Press; 2016.

308. Tan K. Current protocols in immunology. John E. Coligan, Ada M. Kruisbeek David H. Margulies, Ethan M. Shevach and Warrren Strober (eds). John Wiley and Sons: New York US$240 (loose-leaf binder) (1991). Cell Biochem. Funct. 1991;9:295. doi:10.1002/cbf.290090416.

309. Amagai M, Matsuyoshi N, Wang ZH, Andl C, Stanley JR. Toxin in bullous impetigo and staphylococcal scalded-skin syndrome targets desmoglein 1. Nat Med. 2000;6:1275–7. doi:10.1038/81385.

310. Saida K, Kawasaki K, Hirabayashi K, Akazawa Y, Kubota S, Kasuga E, et al. Exfoliative toxin A staphylococcal scalded skin syndrome in preterm infants. Eur J Pediatr. 2015;174:551–5. doi:10.1007/s00431-014-2414-3.

311. Teufelberger AR, Nordengrün M, Braun H, Maes T, Grove K de, Holtappels G, et al. The IL-33/ST2 axis is crucial in type 2 airway responses induced by *Staphylococcus*

aureus-derived serine protease-like protein D. J Allergy Clin Immunol. 2018;141:549-559.e7. doi:10.1016/j.jaci.2017.05.004.

312. Kennedy AJ, Sundström L, Geschwindner S, Poon EKY, Jiang Y, Chen R, et al. Protease-activated receptor-2 ligands reveal orthosteric and allosteric mechanisms of receptor inhibition. Commun Biol. 2020;3:782. doi:10.1038/s42003-020-01504-0.

313. van Oss CJ. Hydrophobic, hydrophilic and other interactions in epitope-paratope binding. Mol Immunol. 1995;32:199–211. doi:10.1016/0161-5890(94)00124-j.

314. Boder ET, Midelfort KS, Wittrup KD. Directed evolution of antibody fragments with monovalent femtomolar antigen-binding affinity. Proc Natl Acad Sci U S A. 2000;97:10701–5. doi:10.1073/pnas.170297297.

315. Foote J, Eisen HN. Breaking the affinity ceiling for antibodies and T cell receptors. Proc Natl Acad Sci U S A. 2000;97:10679–81.

316. Acker MG, Auld DS. Considerations for the design and reporting of enzyme assays in high-throughput screening applications. Perspectives in Science. 2014;1:56–73. doi:10.1016/j.pisc.2013.12.001.

317. Rainard JM, Pandarakalam GC, McElroy SP. Using Microscale Thermophoresis to Characterize Hits from High-Throughput Screening: A European Lead Factory Perspective. SLAS Discov. 2018;23:225–41. doi:10.1177/2472555217744728.

318. Doria-Rose NA, Joyce MG. Strategies to guide the antibody affinity maturation process. Curr Opin Virol. 2015;11:137–47. doi:10.1016/j.coviro.2015.04.002.

319. Yaari G, Benichou JIC, Vander Heiden JA, Kleinstein SH, Louzoun Y. The mutation patterns in B-cell immunoglobulin receptors reflect the influence of selection acting at multiple time-scales. Phil. Trans. R. Soc. B. 2015;370:20140242. doi:10.1098/rstb.2014.0242.

320. Sok D, Laserson U, Laserson J, Liu Y, Vigneault F, Julien J-P, et al. The effects of somatic hypermutation on neutralization and binding in the PGT121 family of broadly neutralizing HIV antibodies. PLoS Pathog. 2013;9:e1003754. doi:10.1371/journal.ppat.1003754.

321. Pauli NT, Kim HK, Falugi F, Huang M, Dulac J, Henry Dunand C, et al. *Staphylococcus aureus* infection induces protein A-mediated immune evasion in humans. J Exp Med. 2014;211:2331–9. doi:10.1084/jem.20141404.

322. Kirik U, Persson H, Levander F, Greiff L, Ohlin M. Antibody Heavy Chain Variable Domains of Different Germline Gene Origins Diversify through Different Paths. Front Immunol. 2017;8:1433. doi:10.3389/fimmu.2017.01433.

323. Skamaki K, Emond S, Chodorge M, Andrews J, Rees DG, Cannon D, et al. *In vitro* evolution of antibody affinity via insertional scanning mutagenesis of an entire antibody

variable region. Proc Natl Acad Sci USA. 2020;117:27307–18. doi:10.1073/pnas.2002954117.

324. Pappas L, Foglierini M, Piccoli L, Kallewaard NL, Turrini F, Silacci C, et al. Rapid development of broadly influenza neutralizing antibodies through redundant mutations. Nature. 2014;516:418–22. doi:10.1038/nature13764.

325. Zhu X, Yu F, Wu Y, Ying T. Potent germline-like monoclonal antibodies: rapid identification of promising candidates for antibody-based antiviral therapy. Antib Ther. 2021;4:89–98. doi:10.1093/abt/tbab008.

326. Willis JR, Briney BS, DeLuca SL, Crowe JE, Meiler J. Human germline antibody gene segments encode polyspecific antibodies. PLoS Comput Biol. 2013;9:e1003045. doi:10.1371/journal.pcbi.1003045.

327. Haslinger-Löffler B, Kahl BC, Grundmeier M, Strangfeld K, Wagner B, Fischer U, et al. Multiple virulence factors are required for *Staphylococcus aureus*-induced apoptosis in endothelial cells. Cell Microbiol. 2005;7:1087–97. doi:10.1111/j.1462-5822.2005.00533.x.

328. Bien J, Sokolova O, Bozko P. Characterization of Virulence Factors of *Staphylococcus aureus*: Novel Function of Known Virulence Factors That Are Implicated in Activation of Airway Epithelial Proinflammatory Response. J Pathog 2011. doi:10.4061/2011/601905.

329. Karki P, Ke Y, Tian Y, Ohmura T, Sitikov A, Sarich N, et al. *Staphylococcus aureus*-induced endothelial permeability and inflammation are mediated by microtubule destabilization. J Biol Chem. 2019;294:3369–84. doi:10.1074/jbc.RA118.004030.

330. Pai AB, Patel H, Prokopienko AJ, Alsaffar H, Gertzberg N, Neumann P, et al. Lipoteichoic acid from *Staphylococcus aureus* induces lung endothelial cell barrier dysfunction: role of reactive oxygen and nitrogen species. PLoS ONE. 2012;7:e49209. doi:10.1371/journal.pone.0049209.

331. Kolar SL, Ibarra JA, Rivera FE, Mootz JM, Davenport JE, Stevens SM, et al. Extracellular proteases are key mediators of *Staphylococcus aureus* virulence via the global modulation of virulence-determinant stability. Microbiologyopen. 2013;2:18–34. doi:10.1002/mbo3.55.

332. Paharik AE, Salgado-Pabon W, Meyerholz DK, White MJ, Schlievert PM, Horswill AR. The Spl Serine Proteases Modulate *Staphylococcus aureus* Protein Production and Virulence in a Rabbit Model of Pneumonia. mSphere 2016. doi:10.1128/mSphere.00208-16.

333. McCormick JK, Tripp TJ, Dunny GM, Schlievert PM. Formation of Vegetations during Infective Endocarditis Excludes Binding of Bacterial-Specific Host Antibodies to Enterococcus faecalis. J Infect Dis. 2002;185:994–7. doi:10.1086/339604.

334. Thomas S, Liu W, Arora S, Ganesh V, Ko Y-P, Höök M. The Complex Fibrinogen Interactions of the *Staphylococcus aureus* Coagulases. Front. Cell. Infect. Microbiol. 2019. doi:10.3389/fcimb.2019.00106.

335. Martin DR, Witten JC, Tan CD, Rodriguez ER, Blackstone EH, Pettersson GB, et al. Proteomics identifies a convergent innate response to infective endocarditis and extensive proteolysis in vegetation components. JCI Insight 2020. doi:10.1172/jci.insight.135317.

336. Davidson CE, Asaduzzaman M, Arizmendi NG, Polley D, Wu Y, Gordon JR, et al. Proteinase-activated receptor-2 activation participates in allergic sensitization to house dust mite allergens in a murine model. Clin Exp Allergy. 2013;43:1274–85. doi:10.1111/cea.12185.

337. Asaduzzaman M, Nadeem A, Arizmendi N, Davidson C, Nichols HL, Abel M, et al. Functional inhibition of PAR 2 alleviates allergen-induced airway hyperresponsiveness and inflammation. Clin Exp Allergy. 2015;45:1844–55. doi:10.1111/cea.12628.

338. Hamilton JR, Frauman AG, Cocks TM. Increased Expression of Protease-Activated Receptor-2 (PAR2) and PAR4 in Human Coronary Artery by Inflammatory Stimuli Unveils Endothelium-Dependent Relaxations to PAR2 and PAR4 Agonists. Circulation Research. 2001;89:92–8. doi:10.1161/hh1301.092661.

339. Shoda T, Futamura K, Orihara K, Emi-Sugie M, Saito H, Matsumoto K, Matsuda A. Recent advances in understanding the roles of vascular endothelial cells in allergic inflammation. Allergology International. 2016;65:21–9. doi:10.1016/j.alit.2015.08.001.

340. Mrochen DM, Trübe P, Jorde I, Domanska G, van den Brandt C, Bröker BM. Immune Polarization Potential of the *S. aureus* Virulence Factors SplB and GlpQ and Modulation by Adjuvants. Front Immunol 2021. doi:10.3389/fimmu.2021.642802.

341. Vaudaux PE, François P, Proctor RA, McDevitt D, Foster TJ, Albrecht RM, et al. Use of adhesion-defective mutants of *Staphylococcus aureus* to define the role of specific plasma proteins in promoting bacterial adhesion to canine arteriovenous shunts. Infect Immun. 1995;63:585–90.

342. McDevitt D, Nanavaty T, House-Pompeo K, Bell E, Turner N, McIntire L, et al. Characterization of the interaction between the *Staphylococcus aureus* clumping factor (ClfA) and fibrinogen. Eur J Biochem. 1997;247:416–24. doi:10.1111/j.1432-1033.1997.00416.x.

343. Palmqvist N, Patti JM, Tarkowski A, Josefsson E. Expression of staphylococcal clumping factor A impedes macrophage phagocytosis. Microbes Infect. 2004;6:188–95. doi:10.1016/j.micinf.2003.11.005.

344. Higgins J, Loughman A, van Kessel KPM, van Strijp JAG, Foster TJ. Clumping factor A of *Staphylococcus aureus* inhibits phagocytosis by human polymorphonuclear

leucocytes. FEMS Microbiol Lett. 2006;258:290–6. doi:10.1111/j.1574-6968.2006.00229.x.

345. Hair PS, Echague CG, Sholl AM, Watkins JA, Geoghegan JA, Foster TJ, Cunnion KM. Clumping Factor A Interaction with Complement Factor I Increases C3b Cleavage on the Bacterial Surface of *Staphylococcus aureus* and Decreases Complement-Mediated Phagocytosis ▿. Infect Immun. 2010;78:1717–27. doi:10.1128/IAI.01065-09.

346. Harris RJ, Murnane AA, Utter SL, Wagner KL, Cox ET, Polastri GD, et al. Assessing Genetic Heterogeneity in Production Cell Lines: Detection by Peptide Mapping of a Low Level Tyr to Gln Sequence Variant in a Recombinant Antibody. Nat Biotechnol. 1993;11:1293–7. doi:10.1038/nbt1193-1293.

347. Wan M, Shiau FY, Gordon W, Wang GY. Variant antibody identification by peptide mapping. Biotechnology and bioengineering 1999. doi:10.1002/(sici)1097-0290(19990220)62:4<485::aid-bit12>3.0.co;2-e.

348. Yang Y, Strahan A, Li C, Shen A, Liu H, Ouyang J, et al. Detecting low level sequence variants in recombinant monoclonal antibodies. MAbs. 2010;2:285–98. doi:10.4161/mabs.2.3.11718.

349. Chen C, Roberts VA, Rittenberg MB. Generation and analysis of random point mutations in an antibody CDR2 sequence: many mutated antibodies lose their ability to bind antigen. Journal of Experimental Medicine. 1992;176:855–66. doi:10.1084/jem.176.3.855.

350. Petersen BM, Ulmer SA, Rhodes ER, Gutierrez-Gonzalez MF, Dekosky BJ, Sprenger KG, Whitehead TA. Regulatory Approved Monoclonal Antibodies Contain Framework Mutations Predicted From Human Antibody Repertoires. Front. Immunol. 2021. doi:10.3389/fimmu.2021.728694.

351. Wen D, Vecchi MM, Gu S, Su L, Dolnikova J, Huang Y-M, et al. Discovery and investigation of misincorporation of serine at asparagine positions in recombinant proteins expressed in Chinese hamster ovary cells. J Biol Chem. 2009;284:32686–94. doi:10.1074/jbc.M109.059360.

352. Thakur A, Nagpal R, Ghosh AK, Gadamshetty D, Nagapattinam S, Subbarao M, et al. Identification, characterization and control of a sequence variant in monoclonal antibody drug product: a case study. Sci Rep 2021. doi:10.1038/s41598-021-92338-1.

353. Carter P, Presta L, Gorman CM, Ridgway JB, Henner D, Wong WL, et al. Humanization of an anti-p185HER2 antibody for human cancer therapy. Proc Natl Acad Sci U S A. 1992;89:4285–9.

354. Jefferis R, Lefranc M-P. Human immunoglobulin allotypes: Possible implications for immunogenicity. MAbs. 2009;1:332–8.

355. Rabia LA, Desai AA, Jhajj HS, Tessier PM. Understanding and overcoming trade-offs between antibody affinity, specificity, stability and solubility. Biochemical Engineering Journal. 2018;137:365–74. doi:10.1016/j.bej.2018.06.003.

356. Li X, Wang X, Thompson CD, Park S, Park WB, Lee JC. Preclinical Efficacy of Clumping Factor A in Prevention of *Staphylococcus aureus* Infection. mBio. 2016;7:e02232-15. doi:10.1128/mBio.02232-15.

357. Bloom B, Schelonka R, Kueser T, Walker W, Jung E, Kaufman D, et al. Multicenter Study to Assess Safety and Efficacy of INH-A21, a Donor-Selected Human Staphylococcal Immunoglobulin, for Prevention of Nosocomial Infections in Very Low Birth Weight Infants. Pediatric Infectious Disease Journal. 2005;24:858–66. doi:10.1097/01.inf.0000180504.66437.1f.

358. Nanra JS, Timofeyeva Y, Buitrago SM, Sellman BR, Dilts DA, Fink P, et al. Heterogeneous *in vivo* expression of clumping factor A and capsular polysaccharide by *Staphylococcus aureus*: implications for vaccine design. Vaccine 2009. doi:10.1016/j.vaccine.2009.01.062.

359. Murphy E, Lin SL, Nunez L, Andrew L, Fink PS, Dilts DA, et al. Challenges for the evaluation of *Staphylococcus aureus* protein based vaccines: monitoring antigenic diversity. Hum Vaccin. 2011;7 Suppl:51–9. doi:10.4161/hv.7.0.14562.

360. Herman-Bausier P, El-Kirat-Chatel S, Foster TJ, Geoghegan JA, Dufrêne YF. *Staphylococcus aureus* Fibronectin-Binding Protein A Mediates Cell-Cell Adhesion through Low-Affinity Homophilic Bonds. mBio. 2015;6:e00413-15. doi:10.1128/mBio.00413-15.

361. Gries CM, Biddle T, Bose JL, Kielian T, Lo DD. *Staphylococcus aureus* Fibronectin Binding Protein A Mediates Biofilm Development and Infection. Infect Immun 2020. doi:10.1128/IAI.00859-19.

362. Zuo Q-F, Cai C-Z, Ding H-L, Wu Y, Yang L-Y, Feng Q, et al. Identification of the immunodominant regions of *Staphylococcus aureus* fibronectin-binding protein A. PLoS ONE. 2014;9:e95338. doi:10.1371/journal.pone.0095338.

363. Meenan NAG, Visai L, Valtulina V, Schwarz-Linek U, Norris NC, Gurusiddappa S, et al. The tandem beta-zipper model defines high affinity fibronectin-binding repeats within *Staphylococcus aureus* FnBPA. J Biol Chem. 2007;282:25893–902. doi:10.1074/jbc.M703063200.

364. Casolini F, Visai L, Joh D, Conaldi PG, Toniolo A, Höök M, Speziale P. Antibody Response to Fibronectin-Binding Adhesin FnbpA in Patients with *Staphylococcus aureus* Infections. Infect Immun. 1998;66:5433–42.

365. Ma J, Wei Y, Zhang L, Wang X, Di Yao, Liu D, et al. Identification of a novel linear B-cell epitope as a vaccine candidate in the N2N3 subdomain of *Staphylococcus aureus*

fibronectin-binding protein A. J Med Microbiol. 2018;67:423–31. doi:10.1099/jmm.0.000633.

366. Thibau A, Dichter AA, Vaca DJ, Linke D, Goldman A, Kempf VAJ. Immunogenicity of trimeric autotransporter adhesins and their potential as vaccine targets. Med Microbiol Immunol. 2020;209:243–63. doi:10.1007/s00430-019-00649-y.

367. Anderson AS, Miller AA, Donald RGK, Scully IL, Nanra JS, Cooper D, Jansen KU. Development of a multicomponent *Staphylococcus aureus* vaccine designed to counter multiple bacterial virulence factors. Hum Vaccin Immunother. 2012;8:1585–94. doi:10.4161/hv.21872.

368. Venkatasubramaniam A, Liao G, Cho E, Adhikari RP, Kort T, Holtsberg FW, et al. Safety and Immunogenicity of a 4-Component Toxoid-Based *Staphylococcus aureus* Vaccine in Rhesus Macaques. Front. Immunol. 2021. doi:10.3389/fimmu.2021.621754.

369. Clegg J, Soldaini E, McLoughlin RM, Rittenhouse S, Bagnoli F, Phogat S. *Staphylococcus aureus* Vaccine Research and Development: The Past, Present and Future, Including Novel Therapeutic Strategies. Front. Immunol. 2021. doi:10.3389/fimmu.2021.705360.

370. Forsgren A, Nordström K. Protein A from *Staphylococcus aureus*: the biological significance of its reaction with IgG. Ann N Y Acad Sci 1974. doi:10.1111/j.1749-6632.1974.tb41496.x.

371. Goodyear CS, Silverman GJ. Staphylococcal toxin induced preferential and prolonged *in vivo* deletion of innate-like B lymphocytes. Proc Natl Acad Sci U S A. 2004;101:11392–7. doi:10.1073/pnas.0404382101.

372. Begier E, Seiden DJ, Patton M, Zito E, Severs J, Cooper D, et al. SA4Ag, a 4-antigen *Staphylococcus aureus* vaccine, rapidly induces high levels of bacteria-killing antibodies. Vaccine. 2017;35:1132–9. doi:10.1016/j.vaccine.2017.01.024.

373. Klimka A, Mertins S, Nicolai AK, Rummler LM, Higgins PG, Günther SD, et al. Epitope-specific immunity against *Staphylococcus aureus* coproporphyrinogen III oxidase. NPJ Vaccines 2021. doi:10.1038/s41541-020-00268-2.

374. Adhikari RP, Karauzum H, Sarwar J, Abaandou L, Mahmoudieh M, Boroun AR, et al. Novel structurally designed vaccine for *S. aureus* α-hemolysin: protection against bacteremia and pneumonia. PLoS ONE. 2012;7:e38567. doi:10.1371/journal.pone.0038567.

375. Jefferies JMC, Macdonald E, Faust SN, Clarke SC. 13-valent pneumococcal conjugate vaccine (PCV13). Hum Vaccin. 2011;7:1012–8. doi:10.4161/hv.7.10.16794.

376. Agrawal A, Murphy TF. *Haemophilus influenzae* infections in the H. influenzae type b conjugate vaccine era. J Clin Microbiol. 2011;49:3728–32. doi:10.1128/JCM.05476-11.

377. Anderson AS, Jansen KU, Eiden J. New frontiers in meningococcal vaccines. Expert Rev Vaccines. 2011;10:617–34. doi:10.1586/erv.11.50.

378. Magyarics Z, Leslie F, Bartko J, Rouha H, Luperchio S, Schörgenhofer C, et al. Randomized, Double-Blind, Placebo-Controlled, Single-Ascending-Dose Study of the Penetration of a Monoclonal Antibody Combination (ASN100) Targeting *Staphylococcus aureus* Cytotoxins in the Lung Epithelial Lining Fluid of Healthy Volunteers. Antimicrob Agents Chemother 2019. doi:10.1128/AAC.00350-19.

379. Hilliard JJ, Datta V, Tkaczyk C, Hamilton M, Sadowska A, Jones-Nelson O, et al. Anti-Alpha-Toxin Monoclonal Antibody and Antibiotic Combination Therapy Improves Disease Outcome and Accelerates Healing in a *Staphylococcus aureus* Dermonecrosis Model. Antimicrob Agents Chemother. 2014;59:299–309. doi:10.1128/AAC.03918-14.

380. Domenech M, Sempere J, Miguel S de, Yuste J. Combination of Antibodies and Antibiotics as a Promising Strategy Against Multidrug-Resistant Pathogens of the Respiratory Tract. Front. Immunol. 2018. doi:10.3389/fimmu.2018.02700.

381. Lindsay JA, Moore CE, Day NP, Peacock SJ, Witney AA, Stabler RA, et al. Microarrays Reveal that Each of the Ten Dominant Lineages of *Staphylococcus aureus* Has a Unique Combination of Surface-Associated and Regulatory Genes†. J Bacteriol. 2006;188:669–76. doi:10.1128/JB.188.2.669-676.2006.

382. Loughman A, Sweeney T, Keane FM, Pietrocola G, Speziale P, Foster TJ. Sequence diversity in the A domain of *Staphylococcus aureus* fibronectin-binding protein A. BMC Microbiol. 2008;8:74. doi:10.1186/1471-2180-8-74.

383. Burke FM, McCormack N, Rindi S, Speziale P, Foster TJ. Fibronectin-binding protein B variation in *Staphylococcus aureus*. BMC Microbiol. 2010;10:160. doi:10.1186/1471-2180-10-160.

384. den Reijer PM, Sandker M, Snijders SV, Tavakol M, Hendrickx APA, van Wamel WJB. Combining *in vitro* protein detection and *in vivo* antibody detection identifies potential vaccine targets against *Staphylococcus aureus* during osteomyelitis. Med Microbiol Immunol. 2017;206:11–22. doi:10.1007/s00430-016-0476-8.

385. Bröker BM, Mrochen D, Péton V. The T Cell Response to *Staphylococcus aureus*. Pathogens. 2016;5:10.3390/pathogens5010031. doi:10.3390/pathogens5010031.

Supplementary figures

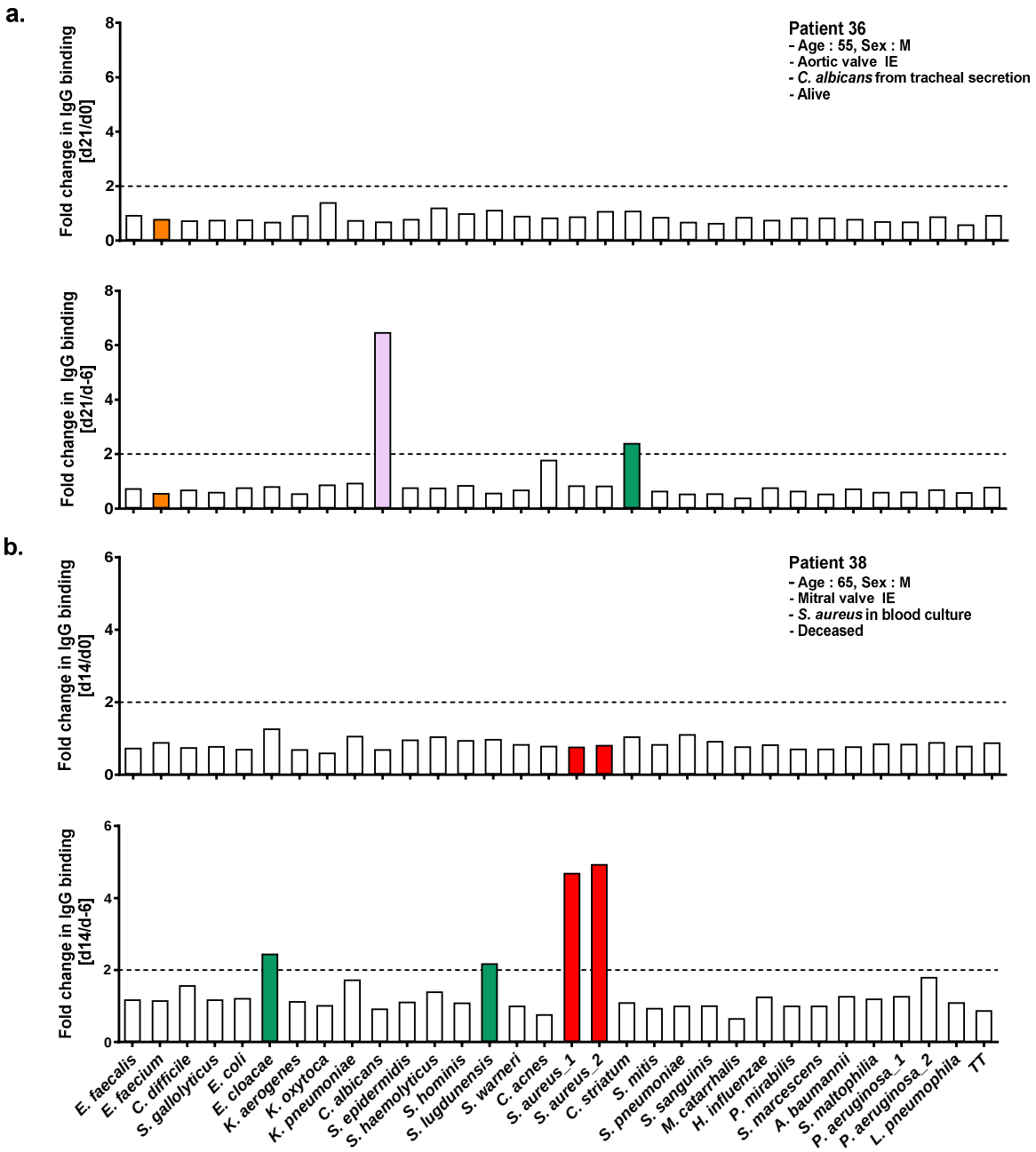

Figure S 1: Timing of sample collection matters. (a, and b) Fold-change was measured for the antibody response at various points at which the plasma samples were collected from the IE patients. The threshold for the significant increase was set to 2.0 (green bars), which is marked by a black dotted line. Fold-change was also calculated against the blood culture diagnosed pathogens (red bars) as well as swab-detected pathogens (orange bars). The fold-change against the swab-isolated pathogens that crosses the significance threshold are also shown (violet) (a) shows the fold change in IgG binding against the pathogens in patient 36 from d0 to d21 and d-6 and d21. (b) shows the fold change in IgG binding against the pathogens in patient 38 from d0 to d14 and d-6 and d14.

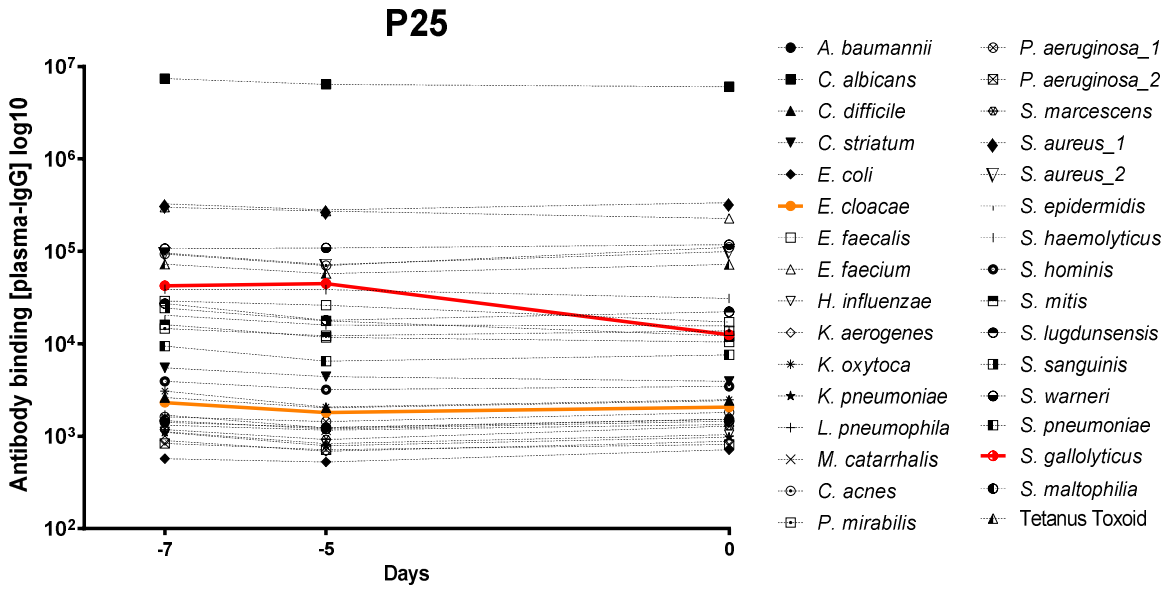

Figure S 2: Serology detects a reduction in antibodies titer. Antibody response value against the pathogens in the infection array was measured in consecutive plasma samples. The response values reflect the IgG binding and are plotted on a logarithmic scale on the y-axis against the timeline of sample collection. The red lines show the BC-diagnosed pathogens against which the decease in IgG titer was detected. The orange dotted lines show the pathogens diagnosed from other infection sites that did not cross the significance threshold (2.0).

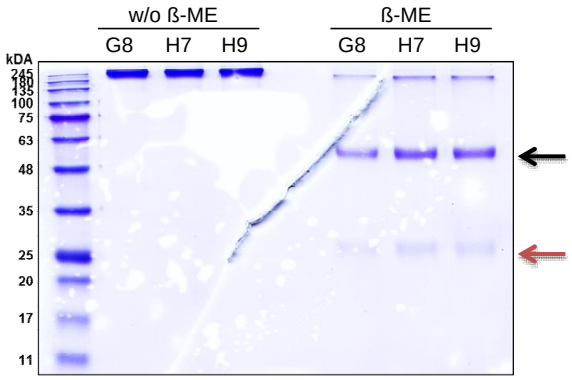

Figure S 3: All purified monoclonal antibodies show a high purity. For quality control, 1 µg each of anti-SplB G8, H7, and H9 mAbs and the protein marker VI prestained (M) were resolved on a 10% SDS gel and stained with Coomassie Blue staining. Both non-cleaved IgG antibodies (150 kDa) and the cleaved LCs and HCs of the antibodies (25 kDa (red arrow) and 50 kDa (black arrow), respectively) could be detected in all batches. No contaminating proteins were observed.

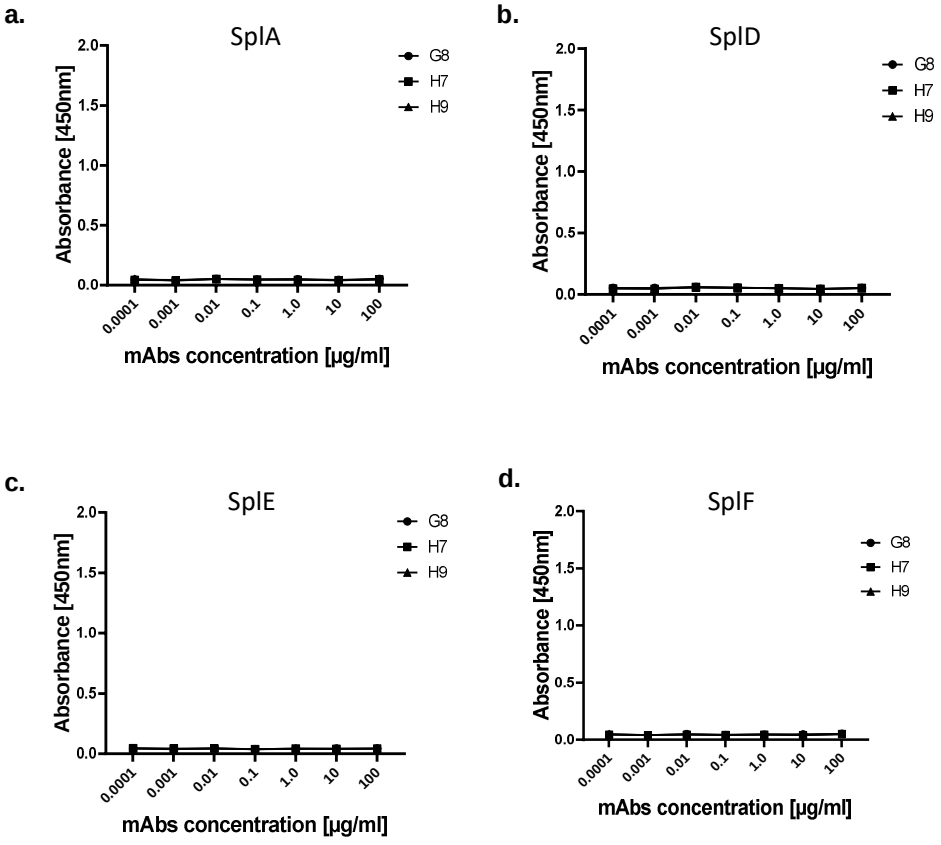

Figure S 4: Anti-SplB mAbs do not bind to other recombinant Spls. (a – d) The purified anti-SplB mAbs were tested for their ability to bind to other native recombinant Spls (SplA, SplD, SplE, and SplF). ELISA plates were coated with 1 µg/ml of each indicated Spl, blocked, and subsequently incubated with serially diluted anti-SplB mAbs. mAb binding was visualized using a goat α-mouse IgG-POD and TMB substrate. One of 2 similar experiments is depicted.

a. Light chains_G8, H7 and H9

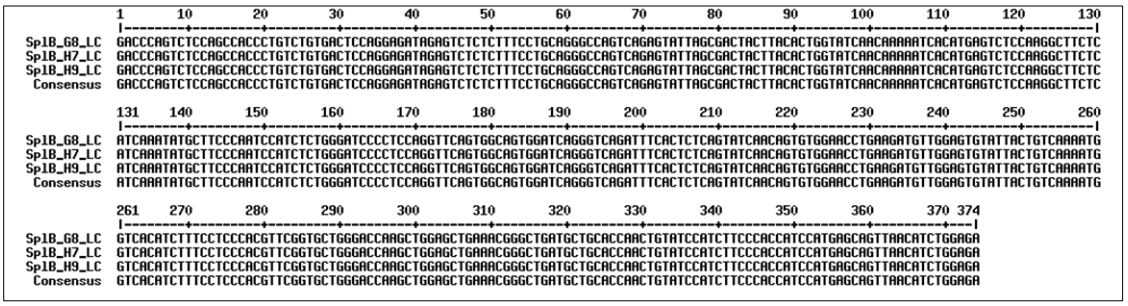

b. Heavy chains_G8, H7 and H9

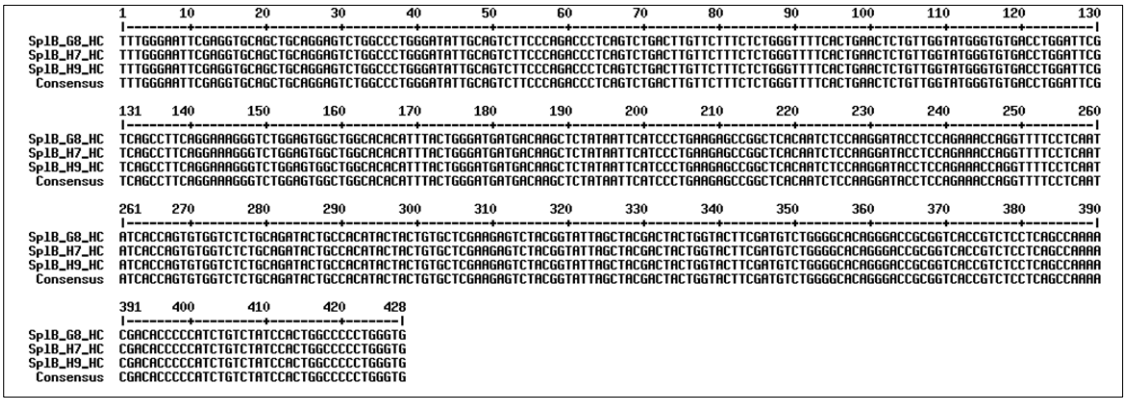

Figure S 5: Variable regions of the LCs and HCs of all three anti-SplB mAbs are identical. (a – b) Anti-SplB producing hybridomas were subjected to RNA isolation. RNA was reversed transcribed into cDNA, and variable gene regions of the LCs and HCs were amplified using PCR. After sequencing, the nucleotide sequences of LCs and HCs were aligned. All three anti-SplB mAbs are entirely identical.

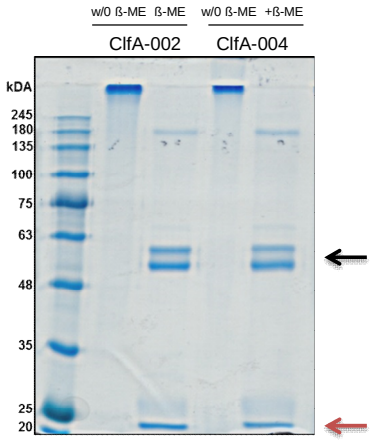

Figure S 6: ClfA-002 and ClfA-004 purified mAbs are of high purity. To analyze the purity of the mAbs, 1 µg each of ClfA-002 and ClfA-004 mAbs and the protein marker VI prestained (M) were run on a 10% SDS gel and stained with Coomassie. Under denaturing conditions, cleaved HCs and LCs (25 kDa (red arrow) and 50 kDa (black arrow), respectively) could be detected in all batches.

a. Light chains_ClfA (001-006)

```
                1       10        20        30        40        50        60        70        80        90       100       110       120       130
                |--------+---------+---------+---------+---------+---------+---------+---------+---------+---------+---------+---------+---------|
ClfA_LC_001     GTCATACTCACTTGTCGCTCAAGTACTGGGGCTGTTACAACTAGTAACTATGCCAACTGGGTCCAAGAAAAACCAGATCATTTATTCACTGGTCTAATAGGTGGTACCAGCAACCGAGCTCCAGGTGTTC
ClfA_LC_002     GTCATACTCACTTGTCGCTCAAGTACTGGGGCTGTTACAACTAGTAACTATGCCAACTGGGTCCAAGAAAAACCAGATCATTTATTCACTGGTCTAATAGGTGGTACCAGCAACCGAGCTCCAGGTGTTC
ClfA_LC_006     GTCATACTCACTTGTCGCTCAAGTACTGGGGCTGTTACAACTAGTAACTATGCCAACTGGGTCCAAGAAAAACCAGATCATTTATTCACTGGTCTAATAGGTGGTACCAGCAACCGAGCTCCAGGTGTTC
ClfA_LC_005     GTCATACTCACTTGTCGCTCAAGTACTGGGGCTGTTACAACTAGTAACTATGCCAACTGGGTCCAAGAAAAACCAGATCATTTATTCACTGGTCTAATAGGTGGTACCAGCAACCGAGCTCCAGGTGTTC
ClfA_LC_003     GTCATACTCACTTGTCGCTCAAGTACTGGGGCTGTTACAACTAGTAACTATGCCAACTGGGTCCAAGAAAAACCAGATCATTTATTCACTGGTCTAATAGGTGGTACCAGCAACCGAGCTCCAGGTGTTC
ClfA_LC_004     GTCATACTCACTTGTCGCTCAAGTACTGGGGCTGTTACAACTAGTAACTATGCCAACTGGGTCCAAGAAAAACCAGATCATTTATTCACTGGTCTAATAGGTGGTACCAGCAACCGAGCTCCAGGTGTTC
  Consensus     GTCATACTCACTTGTCGCTCAAGTACTGGGGCTGTTACAACTAGTAACTATGCCAACTGGGTCCAAGAAAAACCAGATCATTTATTCACTGGTCTAATAGGTGGTACCAGCAACCGAGCTCCAGGTGTTC

                131     140       150       160       170       180       190       200       210       220       230       240       250       260
                |--------+---------+---------+---------+---------+---------+---------+---------+---------+---------+---------+---------+---------|
ClfA_LC_001     CTGTCAGATTCTCAGGCTCCCTGATTGGAGACAAGGCTGCCCTCACCATCACAGGGGCACAGACTGAGGATGATGCAATGTATTTCTGTGCTCTATGGTACAGCACCCATTTTGTTTTCGGCGGTGGAAC
ClfA_LC_002     CTGTCAGATTCTCAGGCTCCCTGATTGGAGACAAGGCTGCCCTCACCATCACAGGGGCACAGACTGAGGATGATGCAATGTATTTCTGTGCTCTATGGTACAGCACCCATTTTGTTTTCGGCGGTGGAAC
ClfA_LC_006     CTGTCAGATTCTCAGGCTCCCTGATTGGAGACAAGGCTGCCCTCACCATCACAGGGGCACAGACTGAGGATGATGCAATGTATTTCTGTGCTCTATGGTACAGCACCCATTTTGTTTTCGGCGGTGGAAC
ClfA_LC_005     CTGTCAGATTCTCAGGCTCCCTGATTGGAGACAAGGCTGCCCTCACCATCACAGGGGCACAGACTGAGGATGATGCAATGTATTTCTGTGCTCTATGGTACAGCACCCATTTTGTTTTCGGCGGTGGAAC
ClfA_LC_003     CTGTCAGATTCTCAGGCTCCCTGATTGGAGACAAGGCTGCCCTCACCATCACAGGGGCACAGACTGAGGATGATGCAATGTATTTCTGTGCTCTATGGTACAGCACCCATTTTGTTTTCGGCGGTGGAAC
ClfA_LC_004     CTGTCAGATTCTCAGGCTCCCTGATTGGAGACAAGGCTGCCCTCACCATCACAGGGGCACAGACTGAGGATGATGCAATGTATTTCTGTGCTCTATGGTACAGCACCCATTRTGTTTTCGGCGGTGGAAC
  Consensus     CTGTCAGATTCTCAGGCTCCCTGATTGGAGACAAGGCTGCCCTCACCATCACAGGGGCACAGACTGAGGATGATGCAATGTATTTCTGTGCTCTATGGTACAGCACCCATTYTGTTTTCGGCGGTGGAAC

                261     270       280       290       300       310       321
                |--------+---------+---------+---------+---------+---------|
ClfA_LC_001     CAAGGTCACTGTCCTAGGTCAGCCCAAGTCCACTCCCACTCTCACCGTGTTTCCACCTTCC
ClfA_LC_002     CAAGGTCACTGTCCTAGGTCAGCCCAAGTCCACTCCCACTCTCACCGTGTTTCCACCTTCC
ClfA_LC_006     CAAGGTCACTGTCCTAGGTCAGCCCAAGTCCACTCCCACTCTCACCGTGTTTCCACCTTCC
ClfA_LC_005     CAAGGTCACTGTCCTAGGTCAGCCCAAGTCCACTCCCACTCTCACCGTGTTTCCACCTTCC
ClfA_LC_003     CAAGGTCACTGTCCTAGGTCAGCCCAAGTCCACTCCCACTCTCACCGTGTTTCCACCTTCC
ClfA_LC_004     CAAGGTCACTGTCCTAGGTCAGCCCAAGTCCACTCCCACTCTCACCGTGTTTCCACCTTCC
  Consensus     CAAGGTCACTGTCCTAGGTCAGCCCAAGTCCACTCCCACTCTCACCGTGTTTCCACCTTCC
```

b. Heavy chains_ClfA (001-006)

```
                1       10        20        30        40        50        60        70        80        90       100       110       120       130
                |--------+---------+---------+---------+---------+---------+---------+---------+---------+---------+---------+---------+---------|
ClfA_HC_001     GAGGTGCAGCTGCAGGAGTCTGGTGGAGGATTGGTGCAGCCTAAAGGGTCATTGAAACTCTCATGTGCAGCCTCTGGATTCAGTTTCAATACCTACGCCATGAACTGGGTCCGCCAGGCTCCAGGAAAGG
ClfA_HC_002     GAGGTGCAGCTGCAGGAGTCTGGTGGAGGATTGGTGCAGCCTAAAGGGTCATTGAAACTCTCATGTGCAGCCTCTGGATTCAGTTTCAATACCTACGCCATGAACTGGGTCCGCCAGGCTCCAGGAAAGG
ClfA_HC_006     GAGGTGCAGCTGCAGGAGTCTGGTGGAGGATTGGTGCAGCCTAAAGGGTCATTGAAACTCTCATGTGCAGCCTCTGGATTCAGTTTCAATACCTACGCCATGAACTGGGTCCGCCAGGCTCCAGGAAAGG
ClfA_HC_005     GAGGTGCAGCTGCAGGAGTCTGGTGGAGGATTGGTGCAGCCTAAAGGGTCATTGAAACTCTCATGTGCAGCCTCTGGATTCAGTTTCAATACCTACGCCATGAACTGGGTCCGCCAGGCTCCAGGAAAGG
ClfA_HC_004     GAGGTGCAGCTGCAGGAGTCTGGTGGAGGATTGGTGCAGCCTAAAGGGTCATTGAAACTCTCATGTGCAGCCTCTGGATTCAGTTTCAATACCTACGCCATGAACTGGGTCCGCCAGGCTCCAGGAAAGG
ClfA_HC_003     GAGGTGCAGCTGCAGGAGTCTGGTGGAGGATTGGTGCAGCCTAAAGGGTCATTGAAACTCTCATGTGCAGCCTCTGGATTCAGTTTCAATACCTACGCCATGAACTGGGTCCGCCAGGCTCCAGGAAAGG
  Consensus     GAGGTGCAGCTGCAGGAGTCTGGTGGAGGATTGGTGCAGCCTAAAGGGTCATTGAAACTCTCATGTGCAGCCTCTGGATTCAGTTTCAATACCTACGCCATGAACTGGGTCCGCCAGGCTCCAGGAAAGG

                131     140       150       160       170       180       190       200       210       220       230       240       250       260
                |--------+---------+---------+---------+---------+---------+---------+---------+---------+---------+---------+---------+---------|
ClfA_HC_001     GTTTGGAATGGGTTGCTCGCATAAGAAGTAAAAGTAATAATTATGCAACATATTATGCCGATTCAGTGAAAGACAGATTCACCATCTCCAGGGATGATTCAGAAAACATGCTCTATCTGCAAATGAACAA
ClfA_HC_002     GTTTGGAATGGGTTGCTCGCATAAGAAGTAAAAGTAATAATTATGCAACATATTATGCCGATTCAGTGAAAGACAGATTCACCATCTCCAGGGATGATTCAGAAAACATGCTCTATCTGCAAATGAACAA
ClfA_HC_006     GTTTGGAATGGGTTGCTCGCATAAGAAGTAAAAGTAATAATTATGCAACATATTATGCCGATTCAGTGAAAGACAGATTCACCATCTCCAGGGATGATTCAGAAAACATGCTCTATCTGCAAATGAACAA
ClfA_HC_005     GTTTGGAATGGGTTGCTCGCATAAGAAGTAAAAGTAATAATTATGCAACATATTATGCCGATTCAGTGAAAGACAGATTCACCATCTCCAGGGATGATTCAGAAAACATGCTCTATCTGCAAATGAACAA
ClfA_HC_004     GTTTGGAATGGGTTGCTCGCATAAGAAGTAAAAGTAATAATTATGCAACATATTATGCCGATTCAGTGAAAGACAGATTCACCATCTCCAGGGATGATTCAGAAAACATGCTCTATCTGCAAATGAACAA
ClfA_HC_003     GTTTGGAATGGGTTGCTCGCATAAGAAGTAAAAGTAATAATTATGCAACATATTATGCCGATTCAGTGAAAGACAGATTCACCATCTCCAGGGATGATTCAGAAAACATGCTCTATCTGCAAATGAACAA
  Consensus     GTTTGGAATGGGTTGCTCGCATAAGAAGTAAAAGTAATAATTATGCAACATATTATGCCGATTCAGTGAAAGACAGATTCACCATCTCCAGGGATGATTCAGAAAACATGCTCTATCTGCAAATGAACAA

                261     270       280       290       300       310       320       330       340       350       360       370       380       390
                |--------+---------+---------+---------+---------+---------+---------+---------+---------+---------+---------+---------+---------|
ClfA_HC_001     CTTGAAAACTGAGGACACAGCCATGTATTATTGTGTGAGACAATATCACTACGGTAGTTGGTCCGAACTTACTTACTGGGGCCAAGGGACTCTGGTCACTGTCTCTGCAGCCAAAACAACACCCCCATCA
ClfA_HC_002     CTTGAAAACTGAGGACACAGCCATGTATTATTGTGTGAGACAATATCACTACGGTAGTTGGTCCGAACTTACTTACTGGGGCCAAGGGACTCTGGTCACTGTCTCTGCAGCCAAAACAACACCCCCATCA
ClfA_HC_006     CTTGAAAACTGAGGACACAGCCATGTATTATTGTGTGAGACAATATCACTACGGTAGTTGGTCCGAACTTACTTACTGGGGCCAAGGGACTCTGGTCACTGTCTCTGCAGCCAAAACAACACCCCCATCA
ClfA_HC_005     CTTGAAAACTGAGGACACAGCCATGTATTATTGTGTGAGACAATATCACTACGGTAGTTGGTCCGAACTTACTTACTGGGGCCAAGGGACTCTGGTCACTGTCTCTGCAGCCAAAACAACACCCCCATCA
ClfA_HC_004     CTTGAAAACTGAGGACACAGCCATGTATTATTGTGTGAGACAATATCACTACGGTAGTTGGTCCGAACTTACTTACTGGGGCCAAGGGACTCTGGTCACTGTCTCTGCAGCCAAAACAACACCCCCATCA
ClfA_HC_003     CTTGAAAACTGAGGACACAGCCATGTATTATTGTGTGAGACAATATCACTACGGTAGTTGGTCCGAACTTACTTACTGGGGCCAAGGGACTCTGGTCACTGTCTCTGCAGCCAAAACAACACCCCCATCA
  Consensus     CTTGAAAACTGAGGACACAGCCATGTATTATTGTGTGAGACAATATCACTACGGTAGTTGGTCCGAACTTACTTACTGGGGCCAAGGGACTCTGGTCACTGTCTCTGCAGCCAAAACAACACCCCCATCA

                391     400       410       420       430       440       450       459
                |--------+---------+---------+---------+---------+---------+---------|
ClfA_HC_001     GTCTATCCACTGGCCCCTGGGTGTGGAGATACAACTGGTTCCTCTGTGACTCTGGGATGCCTGGTCAAA
ClfA_HC_002     GTCTATCCACTGGCCCCTGGGTGTGGAGATACAACTGGTTCCTCTGTGACTCTGGGATGCCTGGTCAAA
ClfA_HC_006     GTCTATCCACTGGCCCCTGGGTGTGGAGATACAACTGGTTCCTCTGTGACTCTGGGATGCCTGGTCAAA
ClfA_HC_005     GTCTATCCACTGGCCCCTGGGTGTGGAGATACAACTGGTTCCTCTGTGACTCTGGGATGCCTGGTCAAA
ClfA_HC_004     GTCTATCCACTGGCCCCTGGGTGTGGAGATACAACTGGTTCCTCTGTGACTCTGGGATGCCTGGTCAAA
ClfA_HC_003     GTCTATCCACTGGCCCCTGGGTGTGGAGATACAACTGGTTCCTCTGTGACTCTGGGATGCCTGGTCAAA
  Consensus     GTCTATCCACTGGCCCCTGGGTGTGGAGATACAACTGGTTCCTCTGTGACTCTGGGATGCCTGGTCAAA
```

Figure S 7: Variable regions of anti-ClfA mAbs LCs and HCs are identical for all mAbs except ClfA-004. (a – b) After generating cDNA from each hybridoma and sequencing it, the nucleotide sequences of LCs and HCs were aligned. The high consensus sequences are depicted in black color and the low consensus in red. The aligned nucleotide sequences showed that the ClfA 01, 002, 003, 005, and 006 mAbs were identical, while 004 differed from the other mAbs by one nucleotide, resulting in AA exchange from thyrosine (Tyr) to phenylalanine (Phe).

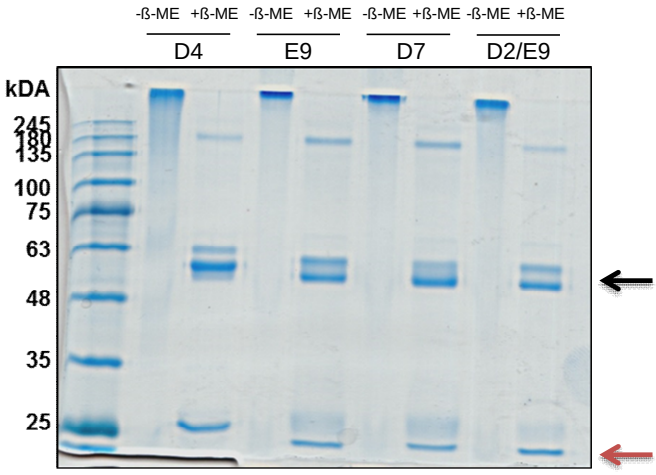

Figure S 8: The purified anti-FnBPA mAbs are of high purity. To check the purity of the purified mAbs, 1 µg each of mAb and the protein marker VI prestained (M) were run on a 10% SDS gel under native and denaturing conditions and stained with Coomassie. Cleaved LCs and HCs of the antibodies (25 kDa (red arrow) and 50 kDa (black arrow), respectively) could be detected in all batches.

a. Light chain_FnBPA (D4 and E9)

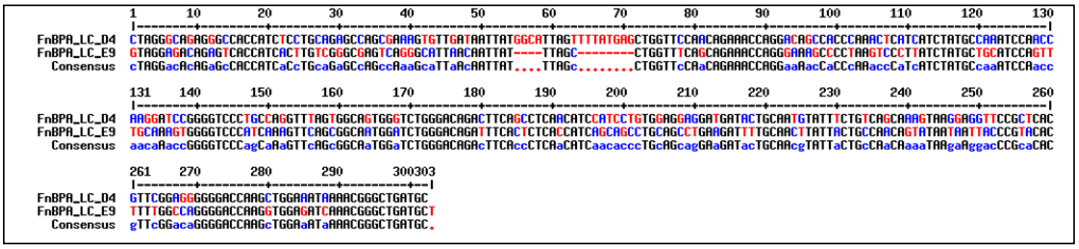

b. Heavy chain_FnBPA (D4 and E9)

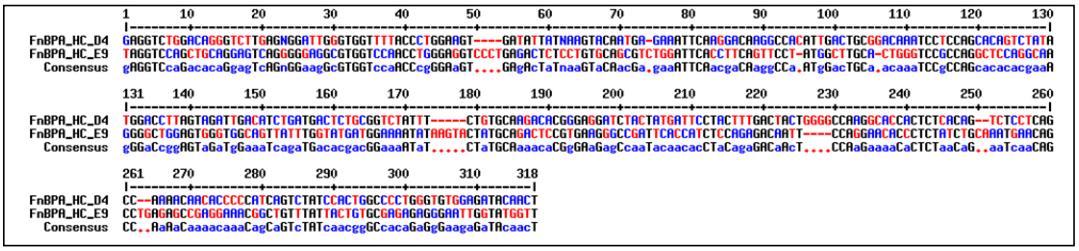

Figure S 9: The murine anti-FnBPA mAbs D4 and E9 strongly differ in their LCs and HCs sequences. RNA was isolated from the anti-FnBPA D4 and E9 hybridoma cultures, cDNA was generated, and the gene regions encoding variable regions of the LCs and HCs of each clone were amplified by PCR. After sequencing, the nucleotide sequences of LCs and HCs were aligned. The high consensus sequences are depicted in black color and the low consensus in red. The aligned nucleotide sequences show that the murine anti-FnBPA mAbs D4 and E9 are two different mAbs because of the numerous differences in the nucleotide sequences at various regions of the LCs and HCs.

Table S 1. Comparison of the variable region sequence of LCs and HCs of the generated monoclonal antibodies with the germline sequences.

Name	Germ line NCBI accession number	Regions	From	To	Length	Matches	Mismatches	Gaps	Identity (%)	Silent Mutations	Non-silent mutations	Amino acid changes
G8 HC	NC_000078.6	FR1	21	86	66	63	3	0	95.5	2	6	3
		CDR1	87	116	30	26	4	0	86.7	0	4	3
		FR2	117	167	51	50	1	0	98	0	1	1
		CDR2	168	188	21	21	0	0	100	0	0	0
		FR3	189	302	114	107	7	0	93.9	2	5	5
		CDR3	303	312	10	10	0	0	100	0	0	0
		Total			**292**	**277**	**15**	**0**	**94.9**	**4**	**16**	**12**
G8 LC	NC_000072.6	FR1	79	78	75	3	0	0	96.2	2	1	1
		CDR1	80	97	18	18	0	0	100	0	0	0
		FR2	98	148	51	51	0	0	100	0	0	0
		CDR2	149	157	9	9	0	0	100	0	0	0
		FR3	158	265	108	108	0	0	100	0	0	0
		CDR3	266	288	23	22	1	0	95.7	0	1	1
		Total			**287**	**283**	**4**	**0**	**98.6**	**2**	**2**	**2**
FnBPA D4 HC	NC_000078.6	FR1	75	74	68	6	0	0	91.9	3	4	3
		CDR1	76	99	24	22	2	0	91.7	0	2	2
		FR2	100	150	51	50	1	0	98	0	1	1
		CDR2	151	174	24	21	3	0	87.5	0	3	3
		FR3	175	288	114	112	2	0	98.2	0	2	2
		CDR3	289	298	10	10	0	0	100	0	0	0
		Total			**297**	**283**	**14**	**0**	**95.3**	**3**	**12**	**11**
FnBPA D4 LC	NC_000072.6	FR1	3	80	78	75	3	0	96.2	1	2	2
		CDR1	81	110	30	30	0	0	100	0	0	0
		FR2	111	161	51	49	2	0	96.1	0	2	2
		CDR2	162	170	9	6	3	0	66.7	1	2	1
		FR3	171	278	108	107	1	0	99.1	0	1	1
		CDR3	279	298	20	20	0	0	100	0	0	0
		Total			**296**	**287**	**9**	**0**	**97**	**2**	**7**	**6**
FnBPA E9 HC	NC_000078.6	FR1	2	75	74	61	13	0	82.4	5	9	6
		CDR1	76	99	24	20	4	0	83.3	2	2	1
		FR2	100	150	51	42	9	0	82.4	3	6	3
		CDR2	151	174	24	9	15	0	37.5	0	15	7
		FR3	175	288	114	98	16	0	86	4	12	8
		CDR3	289	293	5	4	1	0	80	1	0	0
		Total			**292**	**234**	**58**	**0**	**80.1**	**15**	**44**	**25**
FnBPA E9 LC	NC_000072.6	FR1	12	79	68	58	10	0	85.3	4	11	8
		CDR1	80	97	18	14	4	0	77.8	0	4	4
		FR2	98	148	51	44	7	0	86.3	3	4	2
		CDR2	149	157	9	6	3	0	66.7	2	1	1
		FR3	158	265	108	91	17	0	84.3	2	15	11
		CDR3	266	285	20	14	6	0	70	0	6	5
		Total			**274**	**227**	**47**	**0**	**82.8**	**11**	**41**	**31**
ClfA-002 and 004 HC	NC_000078.6	FR1	5	79	75	71	4	0	94.7	1	3	1
		CDR1	80	103	24	23	1	0	95.8	1	0	0
		FR2	104	154	51	51	0	0	100	0	0	0
		CDR2	155	184	30	30	0	0	100	0	0	0
		FR3	185	298	114	111	3	0	97.4	2	1	1
		CDR3	299	306	8	8	0	0	100	0	0	0
		Total			**302**	**294**	**8**	**0**	**97.4**	**4**	**4**	**2**
ClfA 002 LC	NC_000082.6	FR1	1	64	64	64	0	0	100	0	0	0
		CDR1	65	91	27	27	0	0	100	0	0	0
		FR2	92	142	51	51	0	0	100	0	0	0
		CDR2	143	151	9	9	0	0	100	0	0	0
		FR3	152	259	108	108	0	0	100	0	0	0
		CDR3	260	282	23	23	0	0	100	0	0	0
		Total			**282**	**282**	**0**	**0**	**100**	**0**	**0**	**0**
ClfA 004 LC	NC_000082.6	FR1	1	64	64	64	0	0	100	0	0	0
		CDR1	65	91	27	27	0	0	100	0	0	0
		FR2	92	142	51	51	0	0	100	0	0	0
		CDR2	143	151	9	9	0	0	100	0	0	0
		FR3	152	259	108	108	0	0	100	0	0	0
		CDR3	260	281	22	21	1	0	95.4	0	2	1
		Total			**281**	**280**	**1**	**0**	**99.6**	**0**	**2**	**1**

Eigenständigkeitserklärung

Hiermit erkläre ich, dass diese Arbeit bisher von mir weder an der Mathematisch-Naturwissenschaftlichen Fakultät der Universität Greifswald noch einer anderen wissenschaftlichen Einrichtung zum Zwecke der Promotion eingereicht wurde.

Ferner erkläre ich, dass ich diese Arbeit selbstständig verfasst und keine anderen als die darin angegebenen Hilfsmittel und Hilfen benutzt und keine Textabschnitte eines Dritten ohne Kennzeichnung übernommen habe.

_____

Jawad Iqbal

Curriculum Vitae

Jawad Iqbal

Ernst-Wulff-Weg 3, 17491, Greifswald, Germany

jawadiqbal1@msn.com

+49 1590 1631734

https://www.linkedin.com/in/jawad-iqbal-27b05a121/

Academic profile

2018-Present **Ph.D.; Immunology**
University Medicine Greifswald, Greifswald, Germany
Supervisors: Prof. Barbara Bröker and Dr. Silva Holtfreter
Dissertation topic: Pathogen-specific antibody response in infective endocarditis and characterization of anti-bacterial monoclonal antibodies

2011-2013 **Master of Philosophy (M.Phil.); Microbiology**
Quaid-i-Azam University; Islamabad, Pakistan
Thesis topic: Prevalence and Phylogenetic analysis of *Veillonella* spp. isolated from the tongue bio-film in healthy individuals

2006-2010 **Bachelor of Science (B.Sc.); Biotechnology**
Government College University; Lahore, Pakistan
Thesis topic: Identification of targeted sites in 3' UTRs of mRNAs by miRNAs in the genome of *C. briggsae*

Professional experience

2015-2017 **Research assistant**
Department of microbiology and molecular medicine, University of Geneva, Geneva, Switzerland

2014-2015 **Lecturer**
Department of Zoology, Abdul Wali Khan University, Mardan, Pakistan

Awards and recognitions

- DAAD STIBET Programme (2021)
- Card-ii-Omics (Ph.D. funding)
- Certificate of Merit; Quaid-i-Azam University (2013)
- Vice Chancellor's Medal (Distinction in M.Phil.); Quaid-i-Azam University (2013)

- Roll of Honor; (editor, The Gazette) Government College University (GCU) (2010)
- Certificate of Distinction; (co-editor, The Gazette) GCU (2010)

Publications

Chandrabalan A, Thibeault PE, Smiljanov B, Mittmann LA, Deinhardt-Emmer S, Nordengrün M, **Iqbal J**, Mrochen DM, Chamling B, Rauch BH, Reichel CA, Ramachandran R, Bröker BM, Darisipudi MN. *S. aureus*-serine protease-like protein B (SplB) activates PAR2 and induces endothelial barrier dysfunction. *bioRxiv*. 2020

Raafat D, Otto M, Reppschläger K, **Iqbal J**, Holtfreter S. Fighting *S. aureus* biofilms with monoclonal antibodies. *Trends in Microbiology*. 2019. S0966-842X(18)30285-3

Panasenko OO, Somasekharan SP, Villanyi Z, Zagatti M, Bezrukov F, Rashpa R, Cornut J, **Iqbal J**, Longis M, Carl SH, Peña C, Panse VG, Collart MA. Co-translational assembly of proteasome subunits in NOT-1 containing assemblysomes. *Nature Structural & Molecular Biology*. 2019. 26:110–120

Iqbal I, Aftab MN, Afzal M, Rehman AU, Aftab S, Zafar A, Din ZU, Khuharo AR, **Iqbal J**, Haq IU. Purification and characterization of cloned alkaline protease gene of *Geobacillus stearothermophilus*. *Journal of Basic Microbiology*. 2015. 55(2):160-71

Conferences, posters, and presentations

Darisipudi MN, Chandrabalan A, Thibeault PE, Smiljanov B, Mittmann LA, Deinhardt-Emmer S, Nordengrün M, **Iqbal J**, Mrochen DM, Chamling B, Rauch BH, Reichel CA, Ramachandran R, Bröker BM**.** *S. aureus*-serine protease-like protein B (SplB) activates PAR2 and induces endothelial barrier dysfunction. *World Immune Regulation Meeting-XV, 2021, Davos (CH), poster presentation.*

Iqbal J, Infection array - a new tool for diagnosing infective endocarditis (Greifswald study), Abschlusstreffen- Card-ii-Omics, *Universität Medicine Greifswald, 2021, Greifswald (DE), oral presentation.*

Raafat D, **Iqbal J**, Holtfreter S. Using serology as a diagnostic tool in infective endocarditis. *Mikrobiologisches Kolloquium der Universität Greifswald, 2021, Greifswald (DE), oral presenatation.*

Holtfreter S, **Iqbal J**, Raafat D. *Monoclonal antibodies against Staphylococcus aureus. Mikrobiologisches Kolloquium der Universität Greifswald, 2021, Greifswald (DE), oral presentation.*

Iqbal J, Michalik S, Hentschker C, Surmann K, Salazar MG, Busch L, Meyer T, Ruotsalainen E, Kontinen VP, Bröker BM, Völker U, Holtfreter S: Proteomics and immunoproteomics

provide insights into bacterial and host factors contributing to the outcome of *S. aureus* infective endocarditis. *II Joint Meeting of the German Society for Immunology (DGfI) and the Italian Society of Immunology, Clinical Immunology and Allergology (SIICA), 10–13 September 2019, Munich (DE), poster presentation.*

Iqbal J, Michalik S, Hentschker C, Surmann K, Salazar MG, Busch L, Meyer T, Ruotsalainen E, Kontinen VP, Bröker BM, Völker U, Holtfreter S: Proteomics and immunoproteomics provide insights into bacterial and host factors contributing to the outcome of *S. aureus* infective endocarditis. *DGFI Autumn School Immunology, 2018, Merseburg (DE), poster presentation.*

Certifications

- Good Manufacturing Practice (GMP) course (GMP Academy, 2021, DE)
- Clinical Research Training for Junior Clinical Research Associate (ECCRT, 2021, BE)
- Foundational ICH-Good Clinical Practice (GCP) Training, (ECCRT, 2020, BE)
- Local Clinical Trial Legislation in Germany (ECCRT, 2020, BE)

Languages

- English (C1) (Full Professional Proficiency)
- German (B1) (Intermediate Proficiency)
- Pashto (C2) (Native/Bilingual Proficiency)
- Urdu (C2) (Native/Bilingual Proficiency)

Acknowledgment

I would like to express my sincere gratitude and appreciation for Prof. Barbara Bröker, whose guidance, support, and encouragement have been invaluable throughout my Ph.D. journey. She has created an environment that is conducive to critical thinking and scientific exploration, and I am grateful for the opportunity to work in such a research group.

I would like to give special thanks to my direct supervisor, Dr. Silva Holtfreter. Without her assistance and dedicated involvement in my Ph.D. research, this work would have never been possible. I am incredibly thankful and indebted to her for sharing her expertise and valuable guidance to steer me in the right direction whenever she thought I needed it. I would also like to thank my co-supervisor, Dr. Dina Raafat, for her support in the experimental work as well as for providing valuable comments and suggestions for polishing my writing skills. My supervisor's immense knowledge, motivation, and patience have given me the confidence and power to excel in conducting academic research.

The research funding for my Ph.D. was provided by the European Social Fund, Card-ii- omics, ESF/14-BMA55-0037/16. Because of the necessary support from the funding agency, I was able to finish my experimental work successfully. Moreover, Card-ii-Omics generously provided funding to actively participate in different conferences, courses, and events that polished my scientific as well as soft skills.

I would like to thank the Card-ii-Omics team for arranging, collecting, and providing the sample material for the GIES and RIES studies. From the Card-ii-Omics team at the Institute of Immunology, I thank Juan, Fawaz, Erika, Susanne, and Sabine. I would also like to thank Dr. Raila Busch, Dr. Irina Müller-Kozarez and Dr. Anne Strohbach from the Department of Internal Medicine B, Prof. Matthias Nauck and Katja Levin from the Institute of Clinical Chemistry and Laboratory Medicine, and Prof. Karsten Becker and Dr. Christian Kohler from the Friedrich Loeffler Institute for Medical Microbiology.

I would also like to thank our external cooperation partners for their support in conducting crucial experiments. With the scientific and technical support of Dr. Thomas P. Kohler at the Department of Molecular Genetics and Infection Biology, Universität Greifswald, I conducted the microscale thermophoresis assay for the antibody-protein experiment. I would also like to thank Prof. Christoph Reichel and Bojan Smiljanov at the Walter-Brendel-Zentrum für Experimentelle Medizin, LMU München, for his collaboration in the *in vivo* mouse model experiments.

I also wish to thank Daniel Mrochen for performing the critical preliminary work for producing SplB hybridomas. Similarly, ClfA and FnBPA hybridomas were generated by Dr. Dina Raafat, which greatly facilitated the project, and I am thankful for that.

I have thoroughly enjoyed working with my colleagues and appreciate their support during the past 3.5 years. I would like to thank Juan, Nicole, Goran, Liliane, and Frieder for helping me during my Ph.D. journey. I would like to extend my gratitude to Dr. VSN Murthy Darisipudi

for his kind support and encouragement in the scientific area as well as personal growth. I am grateful to Erika, Susi, and Fawaz for their constant support in my experimental work. Furthermore, I would like to thank Carmelina and Maja for their help in organizing the paperwork and documentation.

In the end, I am grateful to my parents and siblings, whose moral support encouraged and motivated me. Finally, I would like to thank Oliver, Mursal, and Abubakar, who supported me and believed in me throughout my scientific career. This work would not have been possible without all the support, and I thank everyone for that.

Jawad Iqbal